

Vadose Hydrology at Jinapsan Cave, Northern Guam

Kaylyn K. Bautista

John W. Jenson

Mark Lander

Timothy Righetti

Technical Report #163

April 2018



WERI

**WATER AND ENVIRONMENTAL RESEARCH INSTITUTE
OF THE WESTERN PACIFIC
UNIVERSITY OF GUAM**

ACKNOWLEDGMENTS

This work was funded by the National Science Foundation (Grant #1451595), Strategic Environmental Research and Development Program (G14AC00103), the Pacific Islands Climate Science Center (G12A003), the United States Geologic Survey (G16 AP0048), and administered through the Water and Environmental Research Institute of the Western Pacific.

ABSTRACT

Eight years of monthly data (2008-2016) were analyzed from an active tropical limestone cave in Guam, the southernmost of the Mariana Islands, in the western Pacific Ocean. The purpose of this study was to characterize fast and slow vadose processes of aquifer recharge in the Plio-Pleistocene Mariana Limestone, which occupies about 75% of the surface of the Northern Guam Lens Aquifer (NGLA). Accurate understanding of aquifer recharge in the NGLA is important because the aquifer supplies 90% of the island's drinking water. This hydrogeologic study was conducted concurrent with paleoclimate research, in which correlative data on CO₂ and other cave meteorological parameters were also collected. For this study, a ground survey grid was established on the surface above the cave, a vegetated talus slope beneath the >150-m cliff in the Mariana Limestone behind the cave. Cave and vadose zone 3-D models were constructed from the surface survey and a cave interior survey. Cross sections display talus slope (33°) features, inferred epikarst and vadose layer dimensions, cave floor slope (-34°), and structural and geomorphic features of the cave, including a brackish water-table pool at the cave bottom. GIS products include georeferenced cave boundary and cave room shapefiles. A plan-view map displays significant boulder talus and limestone-forest trees, cave entrance location, and the underlying cave boundary and fractures mapped on the cave ceiling. Thicknesses of the talus and vadose bedrock sections range from 1.3 to 17.0 meters and 1.7 to 46.4 meters, respectively. Drip rate and discharge rate data from 7 cave stations are presented in graphs showing varying responses between percolation and changes in rainfall during wet (Jun-Nov) and dry (Dec-May) seasons. Six stations (Trinity, Flatman, Station 1, Station 2, Stumpy, and Stumpy's Brother) exhibited seasonal drip responses to wet-dry rainfall cycles. Amidala, the slowest drip, displayed mostly perennial dripping, with several overflow occurrences. Average drip rate, plotted on a log scale, divided stations based on order of magnitude into inferred hydrologic preferential pathway categories: *fracture flow* (fast; 10³-10⁴ drips/hr), *fracture-fissure* (fast; 10²-10³ drips/hr), *small fissure flow* (medium; 10¹-10² drips/hr), and *matrix flow* (slow; <10¹ drips/hr). Trinity is characterized as fracture flow; Flatman as a fissure-fracture flow; Station 1, Station 2, and Stumpy's Brother as small fissure flow; and Stumpy and Amidala as matrix flow.

TABLE OF CONTENTS

LIST OF TABLES	v
LIST OF FIGURES	v
CHAPTER	
I.	INTRODUCTION
1.1	Introduction.....1
1.2	Purpose.....1
1.3	The Northern Guam Lens Aquifer and Its Geologic Setting1
1.4	Hydrologic zones in carbonate island karst aquifers3
1.5	Porosity in carbonate island karst aquifers5
1.6	Previous Studies.....5
II.	SETTING: JINAPSAN CAVE
2.1	Location and Geologic setting7
2.2	Cave Description.....9
2.2.1	Navigating the Cave.....12
III.	METHODS
3.1	Previous Work29
3.1.1	Sampling Stations36
3.2	Drip-count database43
3.3	Cave survey.....46
IV.	RESULTS
4.1	Map of Jinapsan Cave surface plan and cross sections.....52
4.2	Drip-water Data56
4.3	Drip rate magnitude and variability60
4.3.1	Trinity.....66
4.3.2	Flatman68
4.3.3	Station 1.....71
4.3.4	Station 2.....75
4.3.5	Stumpy's Brother78
4.3.6	Stumpy.....81
4.3.7	Amidala84
4.4	Drip rate variability.....87
V.	DISCUSSION
5.1	Percolation Categorization.....89
5.2	Fast Percolation.....89
5.2.1	Trinity89
5.2.2	Flatman91
5.2.3	Station 192
5.2.4	Station 293
5.2.5	Stumpy's Brother93
5.3	Slow Percolation94
5.3.1	Stumpy94
5.3.2	Amidala.....95
5.4	Relationship to the NGLA96

VI.	SUMMARY and CONCLUSION	
6.1	Summary	99
6.2	Conclusion	99
	REFERENCES	100
	APPENDICES	
	A.1 – Jinapsan Cave Ground Surface and Cave Surveys	104
	A.2 – Previous Jinapsan Ground Surface and Cave Surveys.....	117
	B – Jinapsan Cave drip-count database	122

LIST OF TABLES

2.1	Summary of Jinapsan Cave approximate room area and volume, and corresponding figures in this section	13
3.1	Summary of equations used to calculate observed and inferred values for drip rate (drips/hr) and dripwater flux (mL/day)	45
4.1	Ceiling and floor distances between cave stations, respective estimated limestone bedrock and talus layer thicknesses, and hypothesized hydrologic pathway of each station.....	56
4.2	Summary for entire record (wet and dry seasons) drip rate descriptive statistics (drips/hour) per station for 8-year record 2008-2016	56
4.3	Summary for entire record of dripwater flux descriptive statistics (milliliters/day) per station.....	57
4.4	Summary of wet season drip rate descriptive statistics per station.....	59
4.5	Summary of dry season drip rate descriptive statistics per station	59
4.6	Summary of storms on time series graphs	62
4.7	Summary of days between drip response and rainfall events for all stations	67
5.1	Cave drip stations characterized by discharge types.....	90

LIST OF FIGURES

1.1	Map of Guam in the western Pacific, the northern limestone and southern volcanic areas divided by the Pago-Adelup Fault.....	2
1.2	USEPA Map of the Northern Guam Sole Source Aquifer boundary	2
1.3	Schematic of a composite island from the CIKM.....	3
1.4	Lens geometry and zones of the NGLA	4
1.5	Conceptual model of the NGLA: Recharge, storage, transfer, and discharge	4
1.6	Triple porosity model.....	5
2.1	a) Geographic locations of Jinapsan Cave and Jinapsan Overlook station.....	7
	b) Aerial view of northern coastline east of Jinapsan cave site	8
	c) View of Jinapsan Cave area from Jinapsan Overlook, AAFB Fanihi Station.....	8

2.2	Geologic location of Jinapsan Cave boundary and entrance via GPS coordinates	9
2.3	Plan and profile views of Jinapsan Cave	10
2.4	a) Plan view of Jinapsan Cave	10
	b) Cross-section A-A' of Jinapsan Cave and Section K as in 2.4c below	11
	c) Jinapsan Cave cross sections B through K	11
2.5	Map created on <i>ArcMap 10.2.2</i> of Jinapsan Cave boundary, site landmark (boulder) and cave entrance, cave areas (rooms), current cave stations and route to navigate to them.....	12
2.6	a) Jinapsan Cave entrance on talus slope.....	14
	b) Close-up of cave entrance.....	14
2.7	Steep vertical passage from Entrance room to The Slide	15
2.8	Initial passage looking to entrance floor (cross-section B) from Anteroom top level (cross-section C).....	15
2.9	Anteroom looking to passage as in Figure 2.4c cross-section I.....	16
2.10	Anteroom looking down to upper part of The Slide, which curves left	16
2.11	On rope, Midslide, looking up to The Slide curve.....	17
2.12	Midslide platform.....	17
2.13	On rope, Midslide, looking toward Elbow Room.....	18
2.14	On rope, Midslide, looking to passage to Junction which leads to Shakey and Stumpy Rooms.....	18
2.15	a) Looking to passage leading to Elbow Room from Junction room	19
	b) Boulder-size cave rubble of floor of upper part of Junction room	19
2.16	Looking from the Junction into the Canyon	20
2.17	Looking toward passage leading to Shakey Room from the Junction.....	20
2.18	Looking into Shakey Room	21
2.19	Caver descending into Stumpy Room from Shakey Room	21
2.20	Looking into Stumpy Room from the hole in Shakey Room occupied by caver in previous photo.....	22
2.21	Stumpy Room's sloped ceiling	22
2.22	Flowstone covering northeastern wall and floor in Stumpy Room	23
2.23	Caver, on rope, ascending to The Slide from Elbow Room	23
2.24	Bottom of the middle tier looking up to the Midslide platform.....	24
2.25	Top tiers, mostly of flowstone	24
2.26	Smallest of the traversable openings into Big Room from bottom tier	25
2.27	Looking from Big Room to the descent from middle tier, behind cave in orange	25
2.28	Looking into Big Room from main opening.....	26
2.29	Stalactite network on ceiling of Big Room.....	27
2.30	Black stain clearly follows fractures that form a network of stalactite intersections	27
2.31	Looking at the Pool, cross-section J of Figure 2.4c	28
3.1	Field and laboratory tasks for monthly sampling as of September 2016.....	30
3.2	Surface slope survey stations, and surface logger and gas sampling sites.....	31
3.3	a) Lower soil gas well	32

	b) Close up at Lower soil gas well.....	32
3.4	a) View of Mergagan and Pati Points from Top of the Rock rain collection station.....	33
	b) Rain gauge and collector on Top of the Rock site.....	33
3.5	Rain collector site outside House 5, Dean's Circle at the University of Guam...	34
3.6	Map of cave temperature and pressure logger and CO ₂ sampling sites.....	34
3.7	October 22, 2013 photo of fresh glass plate deployed at Amidala station for calcite precipitate collection	35
3.8	a) Decanting drip-water into aliquots for $\delta^{18}\text{O}$, Sr/Ca, alkalinity, anions, and δD analyses	35
	b) Collecting Pool samples for analysis.....	36
3.9	Ceiling features above Flatman station.....	37
3.10	a) Flatman station tripod and stalagmite.....	37
	b) Close up of Flatman stalagmite	37
3.11	August 16, 2008 photo of Flatman stalagmite, freshly cored	38
3.12	June 10, 2009 photo of Station 1 stalagmite, freshly cut	38
3.13	Station 1 stalactite	38
3.14	April 22, 2005 photo of Shakey at Station 2.....	39
3.15	Station 2 stalactite	39
3.16	Longitudinal slab from Shakey, Station 2 stalagmite	39
3.17	Stumpy location (left) and Stumpy's Brother (right) stations	40
3.18	Longitudinal slice through Stumpy's stalagmite used for dating by Sinclair et al (2012).....	40
3.19	Amidala station	41
3.20	a) August 6, 2008 photo of cutting Trinity stalagmite.....	41
	b) Trinity collection station mounting above stalagmite base	41
3.21	a) Topside of Trinity stalagmite.....	42
	b) Bottom of Trinity stalagmite	42
3.22	Trinity drip collection bottle at station and overhead stalactite	42
3.23	a) Counting drip rate for Stumpy (left) and Stumpy's Brother (right) stalactites	43
	b) Counting drips at Trinity station.....	44
3.24	2D <i>Compass</i> cave survey plot.....	46
3.25	2D cave (C#) and surface (V#) survey plan plot	47
3.26	a) Plan view of 3-D model of Jinapsan Cave passages on <i>Compass CaveXO</i> cave-modeling software	48
	b) 3D profile passage model of Jinapsan Cave on <i>Compass CaveXO</i> cave-modeling software with transparency set to 50%	48
3.27	Map created in <i>ArcMap 10.2.2</i> of cave survey stations at Jinapsan Cave	49
3.28	a) Looking ~SE to ground surface above Trinity (surface station V52).....	50
	b) Looking upslope (~NW) to Trinity ground surface.....	51
3.29	Roadside excavation in Mariana Limestone (Qtm) epikarst on AAFB	51
4.1	a) Plan of Jinapsan Cave showing ground surface boulder and vegetation landmarks, cave entrance and underlying cave boundary, cave-ceiling fracture traces (concealed on surface slope), and transects of cross-sections A-A' and B-B'	52

	b) Cross section of A-A' transect	53
	c) Cross section of B-B' transect.....	54
	d) Simplified positions of Jinapsan Cave drip stations and estimated talus layer and bedrock layer thicknesses	55
4.2	Logs of entire record mean drip rates (drips/hr) for each station, which are assigned by orders of magnitude into hypothesized hydrologic pathway: fracture, fracture-fissure, fissure, and matrix	58
4.3	Logs of entire record mean dripwater flux (mL/day) for each station, which are assigned by orders of magnitude into hypothesized hydrologic pathway: fracture, fracture-fissure, fissure, and matrix	58
4.4	Trinity drip rate (drips per hour, purple) and dripwater flux (milliliters per day, black) versus AAFB rainfall (inches)	61
4.5	Total rainfall (inches) and respective estimated maximum surface winds (knots) for storms that passed over Guam between September 2008 through September 2016.....	63
4.6	Percent of drip rate for the entire record (colored by station), wet season (light blue), and dry season (light yellow) found within ± 1 standard deviation (σ) from each station's entire record drip rate mean, wet season mean, and dry season mean for frequency histograms within $\pm 0.5 \sigma$ intervals	64
4.7	Frequency histograms of Trinity's a) drip rates for the entire record, b) wet season drip rates, and c) dry season drip rates $\pm 2 \sigma$ from respective means at $\pm 0.5 \sigma$ intervals	65
4.8	Flatman drip rate (drips per hour, orange) and dripwater flux (milliliters per day, black) versus AAFB rainfall (inches)	69
4.9	Frequency histograms of Flatman's a) drip rates for the entire record, b) wet season drip rates, and c) dry season drip rates $\pm 2 \sigma$ from respective means at $\pm 0.5 \sigma$ intervals	70
4.10	Station 1 drip rate (drips per hour, green) and dripwater flux (milliliters per day, black) versus AAFB rainfall (inches)	73
4.11	Frequency histograms of Station 1 a) drip rates for the entire record, b) wet season drip rates, and c) dry season drip rates $\pm 2 \sigma$ from respective means at $\pm 0.5 \sigma$ intervals	74
4.12	Station 2 drip rate (drips per hour, light green) and dripwater flux (milliliters per day, black) versus AAFB rainfall (inches)	76
4.13	Frequency histograms of Station 2 a) drip rates for the entire record, b) wet season drip rates, and c) dry season drip rates $\pm 2 \sigma$ from respective means at $\pm 0.5 \sigma$ intervals	77
4.14	Stumpy's Brother drip rate (drips per hour, light blue) and dripwater flux (milliliters per day, black) versus AAFB rainfall (inches)	79
4.15	Frequency histograms of Stumpy's Brother a) drip rates for the entire record, b) wet season drip rates, and c) dry season drip rates $\pm 2 \sigma$ from respective means at $\pm 0.5 \sigma$ intervals	80
4.16	Stumpy drip rate (drips per hour, blue) and dripwater flux (milliliters per day, black) versus AAFB rainfall (inches)	82

4.17	Frequency histograms of Stumpy's a) drip rates for the entire record, b) wet season drip rates, and c) dry season drip rates $\pm 2 \sigma$ from respective means at $\pm 0.5 \sigma$ intervals	83
4.18	Amidala drip rate (drips per hour, pink) and dripwater flux (milliliters per day, black) versus AAFB rainfall (inches)	85
4.19	Frequency histograms of Amidala's a) drip rates for the entire record, b) wet season drip rates, and c) dry season drip rates $\pm 2 \sigma$ from respective means at $\pm 0.5 \sigma$ intervals	86
4.20	Semi-log plots of a) entire record mean drip rate (μ) versus entire record relative standard deviation (σ/μ), b) wet season mean drip rate versus wet season relative standard deviation, c) dry season mean drip rate versus dry season relative standard deviation	88
5.1	Conceptual model of vadose percolation	98

INTRODUCTION

1.1 Introduction

It is universally acknowledged that fresh water is essential to life and human prosperity. On tropical islands, the accessibility, quantity, and quality of fresh water vary according to each island's geologic characteristics and climate. On tropical limestone islands, an important source of fresh water is aquifers (Jones and Banner 2003), natural bodies of rock capable of capturing, storing, and transmitting economically significant quantities of groundwater (Ford and Williams 2007). Island aquifers are typically small, unconfined, and respond quickly to natural and anthropogenic processes (UNESCO 1991). Understanding local aquifer behavior is vital to the sustainable management of island water resources (Dillon 1997; Gingerich 2003; Tribble 2008).

1.2 Purpose

Vadose caves, where accessible, provide a uniquely useful means of observing and studying vadose processes in karst aquifers (Osborne 2002; Mahmud et al 2016). Previous studies on Guam have located and mapped most of Guam's accessible caves (Taboroši 2004). In 2008, WERI researchers at the University of Guam selected Jinapsan Cave on the northern tip of Guam for a long-term study of groundwater and paleo-climate processes. Previous work by Partin et al. (2012) has produced insights into the pre-instrumental climate (wet-dry) of Guam. The purpose of the thesis research reported here is to take advantage of the eight-year record of vadose hydrology that has been collected thus far to gain new insights into the processes of vadose percolation, which exert fundamental control on the rates, volume, and distribution of recharge and storage in the Northern Guam Lens Aquifer (NGLA) in particular, and island karst aquifers in general.

1.3 The Northern Guam Lens Aquifer and Its Geologic Setting

The island of Guam is the largest and southernmost island of the Mariana Island chain in the Western Pacific (Figure 1.1). It is on the Mariana Ridge, 110 km northwest of the Mariana Trench. At 549 km² in area, the island is elongate in shape, ~48 km long, and ranges from 6.4 to 17.7 km wide (Taboroši 2006). The major physiographic provinces of limestone terrain in the north and volcanic terrain in the south are divided at the island's median by the Pago-Adelup Fault. The NGLA is designated by USEPA as a sole source aquifer for the island, because it supplies over 90% of the island's potable water supply, more than 50% of the community's drinking water (USEPA 2000). It yields about 35 million gallons per day (mgd), tapped by about 120 production wells (GWA 2014). It is comprised of the limestone bedrock north of the Pago-Adelup fault. The NGLA (Figure 1.2) contains an unconfined fresh groundwater lens in highly permeable limestone bedrock that is underlain by a practically impermeable volcanic basement unit (Mink and Vacher 1997). Formed in the limestone plateau of northern Guam, the NGLA is thus classified as a carbonate island karst aquifer (Jenson et al 2006).

The geologic core of Guam is the Eocene Facpi Formation, a submarine basaltic pillow-dike complex. It is overlain by the Oligocene Alutom Formation, a deformed pyroclastic volcanic unit that forms the surface in the northern portion of southern Guam, and comprises the basement beneath the limestone bedrock aquifer of northern Guam.

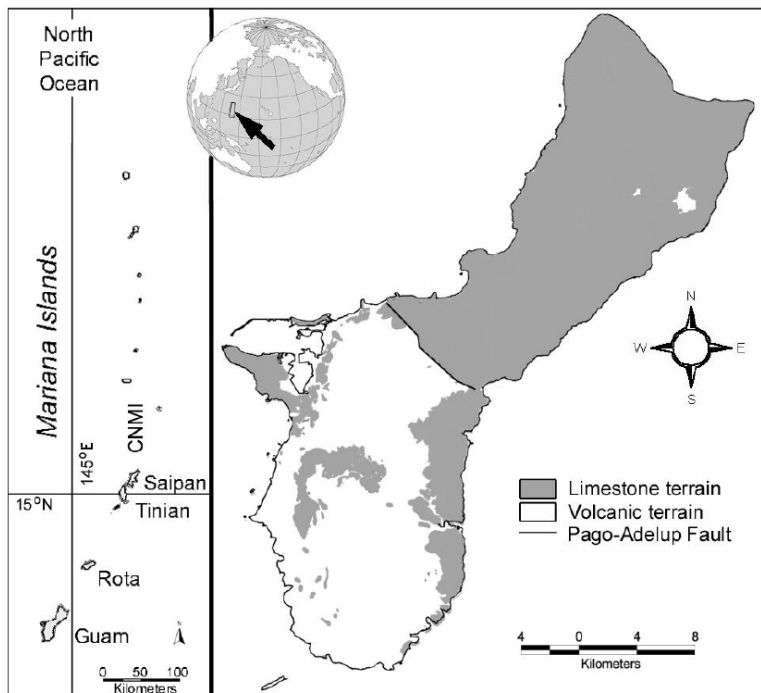
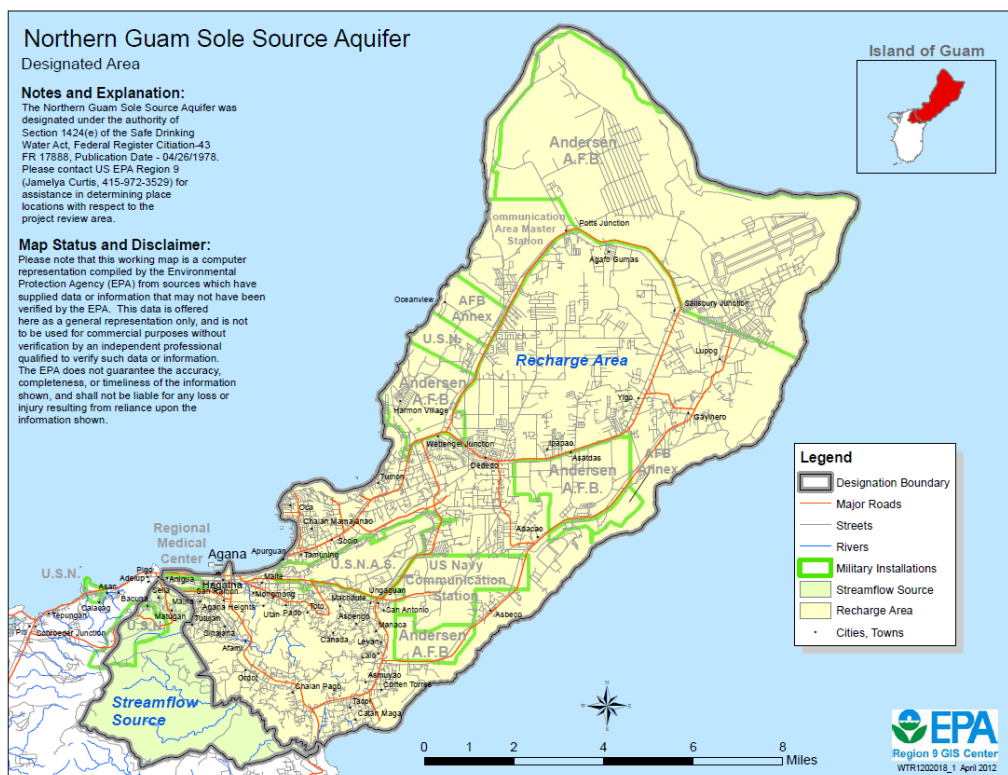


Figure 1.1
Map of Guam in the western Pacific, the northern limestone and southern volcanic areas divided by the Pago-Adelup Fault (Taboroši et al 2004).

The limestone unit that comprises the core of the NGLA is the Miocene-Pliocene Barrigada Limestone, a thick detrital foraminiferal limestone deposited on the submerged edifice that was generally rising as the depositional mantle thickened (Schlanger 1964; Tracey et al 1964). The Barrigada Limestone is mostly covered, and is entirely surrounded by

the Plio-Pleistocene Mariana Limestone, comprised of the reef and lagoon deposits that formed up until the emergence of the plateau, probably about 2,000,000 years ago. Grooves and terraces on the cliff faces of the northern plateau mark sea-level still-stands of unknown dates and durations.



**Figure 1.2
USEPA
Map of the
Northern
Guam Sole
Source
Aquifer
boundary.**

Karst on Guam has been described in terms of the Carbonate Island Karst Model (CIKM) (Mylroie et al 2001): 1) the carbonate rocks are young and have never been buried; 2) freshwater-saltwater mixing occurs at lens boundaries; 3) glacio-eustasy has vertically moved the lens up and down; and 4) local tectonic movement can overprint effects of glacio-eustasy. Carbonate islands can be divided into four categories based on bedrock-basement-sea level relationships: 1) simple, 2) carbonate-covered, 3) composite, and 4) complex (Mylroie et al 2001; Jenson et al 2006). Northern Guam can be characterized under the CIKM as a composite island (Figure 1.3): carbonate and non-carbonate (volcanic) rocks are exposed on the plateau, providing both autogenic and allogenic, the lens is partitioned, and conduit cave systems can develop, particularly at the contact of carbonate and volcanic rocks (Mylroie and Mylroie 2007).

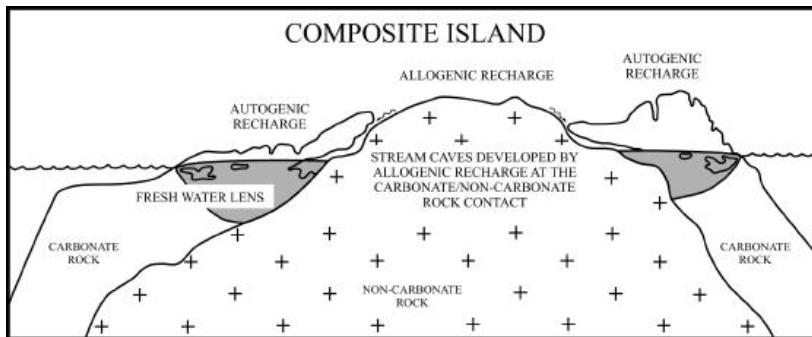


Figure 1.3
Schematic of a composite island from the CIKM (Keel, Mylroie and Jenson 2005).

1.4 Hydrologic zones in carbonate island karst aquifers

Unconfined carbonate island karst aquifers such as the NGLA contain four vertically-distributed hydrologic zones: 1) the vadose zone, 2) freshwater phreatic zone, 3) the mixing zone, and 4) the marine phreatic zone (Figures 1.4 and 1.5) (Ford and Williams 2007). The vadose zone extends beneath the land surface to the water table, where voids in the rock are only partially filled by percolating water. It includes the soil layer (if present), the epikarst, or subcutaneous zone, and the transmission zone (Williams 2008). The epikarst is a highly porous weathered limestone zone typically partially filled with sediment from the overlying soil layer and root systems of surface vegetation. It is distinguished from the underlying vadose body by its high porosity, and typically exhibits high storage capacity, variable void distribution, and pervasive macro-porosity, including soil pipes, dissolutional vugs, and dissolution-widened fractures (Ford and Williams 2007).

Below the vadose zone is the phreatic zone, which begins at the water table. Voids in this area are completely filled with freshwater moving horizontally in the direction of the local hydraulic gradient. The mixing zone is in the phreatic zone where fresh and salt waters meet and create a corrosive mixture. Ongoing work by Gulley et al. (2015) has indicated porosity may be enhanced at the water table, and possibly at the halocline by the production of carbon dioxide from organic material that is trapped by the density gradients at the water table and halocline.

Meteoric water that infiltrates at the ground surface and descends to the water table can arrive by vadose percolation, vadose fast flow, or a combination of both (Mylroie et al. 1999). Freshwater recharge to the NGLA includes mostly autogenic recharge from rainwater descending initially through the soil and epikarst layers to the transmission zone (Jocson et al 2002). Oxygen isotope concentrations in dripwater samples analyzed from Jinapsan Cave by

Partin et al. (2012) showed that little rain makes it to the vadose zone during dry season conditions. Allogenic recharge occurs locally at the flanks of Mount Santa Rosa and Mataguac Hill as storm water runoff converges on solution dolines and descends through caves that form along the limestone-volcanic contacts and descend to the water table. Vadose fast-flow contribution to recharge is uncertain, but seems unlikely to be substantial during intense rainfall events (Contractor and Jenson 2000).

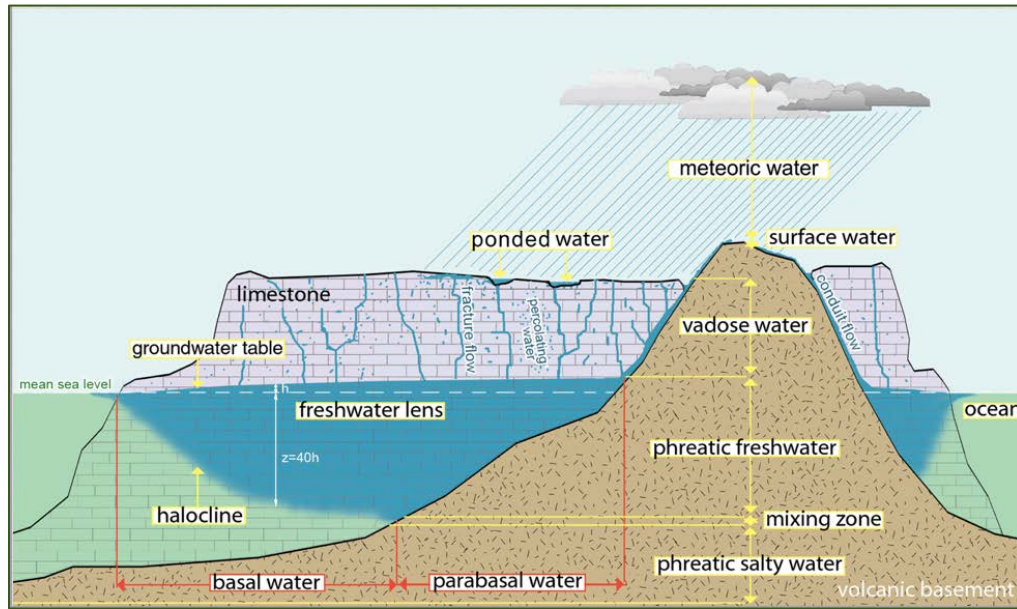


Figure 1.4 Lens geometry and zones of the NGLA. Not to scale (Adapted from <http://north.hydroguam.net/illustr/hydrology-geometry2-large.png>).

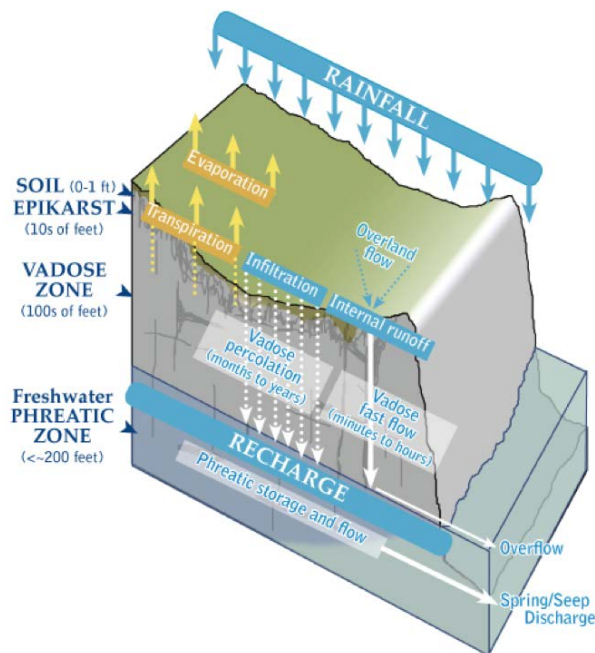


Figure 1.5
Conceptual model of the NGLA: Recharge, storage, transfer, and discharge (Adapted from <http://north.hydroguam.net>).

Percolation through the vadose zone must escape capture by roots in the epikarst and can take months to years to reach the water table as water descends by gravity (Lander et al 2001). Vadose fast flow, however, can only take minutes to hours via natural fractures and shafts and solution sinkholes (Contractor and Jenson 2000; Jocson et al 2002). At the phreatic zone, water can also move at slow or fast rates. At either rate, slow, pore to pore, or rapid, through cave-like network of conduits, aquifer discharge occurs along the coast, which constitutes the

outer boundary of the aquifer (Jenson et al 2006).

1.5 Porosity in carbonate island karst aquifers

Karst aquifers in general can have three types of porosity (Worthington, 1999) (Figure 1.6). The small-scale, typically inter-particle, primary porosity of the bulk material, or matrix, is called matrix porosity. Carbonate island karst aquifers form originally in fresh marine deposits composed largely of the mineral aragonite, which is more soluble than calcite. As groundwater passes through the pores, the fresh water dissolves the aragonite and precipitates calcite, changing the porous deposited rocks into a harder rock of generally larger, but fewer pores, i.e., voids. Eustatic sea level fluctuations and tectonic uplift and subsidence can cause this transformation to occur repeatedly, as the fresh-water lens moves up and down through the carbonate section (Palmer 2007).

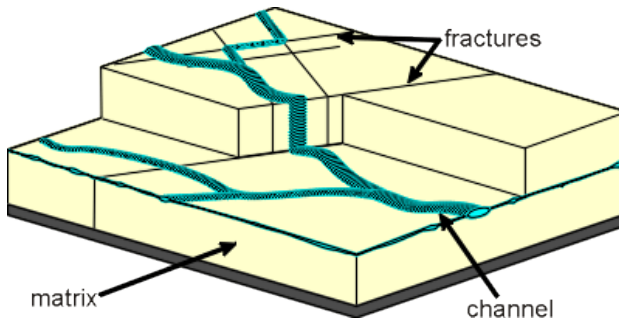


Figure 1.6
Triple porosity model
(<http://www.worthingtongroundwater.com>)

Fractures and fissures through the matrix unit are defined as secondary porosity, and can form an inter-connected network in which flow converges on dissolution-widened trunk routes. Conduits, channels, and caves are dissolution-enlarged flow paths, which typically develop along certain secondary routes, and are defined as tertiary porosity (Ford and Williams 2007, Sheffer et al 2011).

Conduit network systems can form in three places relative to the water table – above, at, or below it (Fetter 2001). Vadose caves form above the water table in the vadose zone, water-table caves form at the water table, where vadose and phreatic waters meet, and phreatic caves develop below the water table. Vadose and phreatic processes result in distinctive types of voids and secondary and tertiary pathways in karst aquifers. Speleothems (stalactites and stalagmites), for example, form only in the vadose environment, and can be subsequently dissolved in a phreatic environment if the cave becomes submerged in fresh water. In island karst aquifers, changes in the water-table elevation driven by changes in relative sea-level can result in complex over-printing of vadose and phreatic type pathways.

1.6 Previous Studies

Cave drip studies in tropical cave environments have been scarcely conducted and published. Drip rate studies are labor-intensive. Research is found mostly of caves in continental karst. Access to cave sites and updated technology may be more readily available, compared to those in tropical cave environments, especially on islands. The analyses and interpretations of the data collected in this study are informed by drip rate results from five relevant drip studies.

McCann (2013 unpublished) conducted a five-month study at Jinapsan Cave of cave meteorological factors that affect speleothem development. Cave temperature hovered around ~26 °C, with no apparent influences except mean annual temperature. Humidity values were observed over 90%. High fidelity was found between outside and internal air pressures, an indication of no pressure differences. A mild correlation was found between a cave speleothem's drip rate and outside pressure. The cave's tidal pool showed a 1-2 hour

lag and amplitude dampening when compared to oceanic tides. The pool temperature was 25.7 °C, signifying no main transfer of waters occurred.

Sheffer et al. (2011) conducted high-resolution rainfall and water percolation measurements at Sif Cave, Israel from December 2006 through October 2007. PVC sheets and barrels with pressure transducers allowed drip rate and volume to be recorded from three different areas. Surface rain gauges, rainfall-simulating sprinklers, and tracer dye injections allowed for artificial irrigation and preferential flow path experimentation. The study identified three distinct types of flow regimes: ‘quick flow’ preferential flow paths (large fractures and conduits), ‘intermediate flow’ through secondary crack system, and ‘slow flow’ through the matrix. Drip rates at one site were an order of magnitude higher than the other two, and was categorized under the ‘quick flow’ regime.

Arbel et al. (2010) studied local precipitation, nine cave drips, drip water salinity, surface soil moisture, electrical conductivity, and tracers during a three-year study at Orenin Cave in Mount Carmel, Israel. From this study, they posited four hydrological types of drips: perennial, seasonal, post-storm, and overflow. Perennial drips discharge throughout the year, have low discharge and long recession. Seasonal drips are dry during the summer and dripping depends on seasonal rainfall distribution and soil profile wetness. These drips had higher discharge rates and fluctuations. Post-storm drips occurred after significant rainstorms (few hours), reached maximum drip rates within 1-2 days, and decayed after 2-3 weeks. Overflow drips occurred late in the season (Feb-Mar) when perennial or seasonal drip discharges were exceeded and epikarst storage was filled completely and overflowed.

Baker and Brundson’s (2003) high resolution drip rate study at Stump Cross Caverns, Northern England, found differing responses of rapid-to-slow drip discharge between drip sites. Variability increased with mean drip rate. A White test (for non-linearity) showed strong evidence of that many of the drip sequences are non-linear. They concluded there was a non-linear input (weather) at the drip sites along with non-linearities within their karst system, leading to non-linear dripping, independent of drip rate.

Fernandez-Cortes et al. (2008) studied dripwater discharge from a single stalactite in the Cueva del Agua, Southern Spain, with a precipitation monitoring station above the cave. They found the drip regime not seasonal, but linked to slow infiltration. Sudden changes in the drip regime were attributed to infiltration along preferential pathways and draining of the microfissure system within the vadose zone. When dripping was constant, a chaotic drip flow was also discovered to be linked to barometric oscillation of air inside the cave (10 ± 3.7 mbar), which caused a mean oscillation in drip rate (0.5 ± 0.2 mm/h).

SETTING: JINAPSAN CAVE

2.1 Location and Geologic setting

Jinapsan Cave is located at 13° 38' 24.232" N, 144° 52' 42.032" E on the coastal terrace at a cliff base 2.3 km northwest of Mergagan Point (Taboroši 2004), ~ about 460 meters inland from the northern Guam coastline (Figure 2.1a). It is surrounded by a secondary limestone forest (Figure 2.1b, 2.1c) (Taboroši 2013) and lies within the portion of Andersen Air Force Base (AAFB) that is managed as wildlife habitat (in the “overlay” zone) by the Guam National Wildlife Refuge (GNWR). The cave has been called Castro's Cave (Taboroši 2004), as members of the Castro family, local owners of the adjacent private property northwest of Tarague Beach, were among the first to aid in giving directions to the cave site. The cave is now referred to as Jinapsan Cave. There are two hiking routes by which to reach Jinapsan Cave: 1) from the GNWR on the west, or 2) through the AAFB and the Castro's private beach property, on the east. Access to the cave site through the GNWR is provided by a permit issued to the Water and Environmental Research Institute at the University of Guam. Access through the private beach property requires access to the trailhead at Tarague Beach on AAFB and prior permission from the Castro family for transit through their property. An overlook of Jinapsan Beach, and the general view of the Jinapsan Cave area (Figure 2.1b, c), can be accessed with permit at an AAFB Fanihi (bat) observation station, atop the Jinapsan Cliffside within AAFB property. The station is a 20-minute hike from a parking area by an AAFB ungulate fence, through a secondary limestone forest, to the Jinapsan Cliffside.

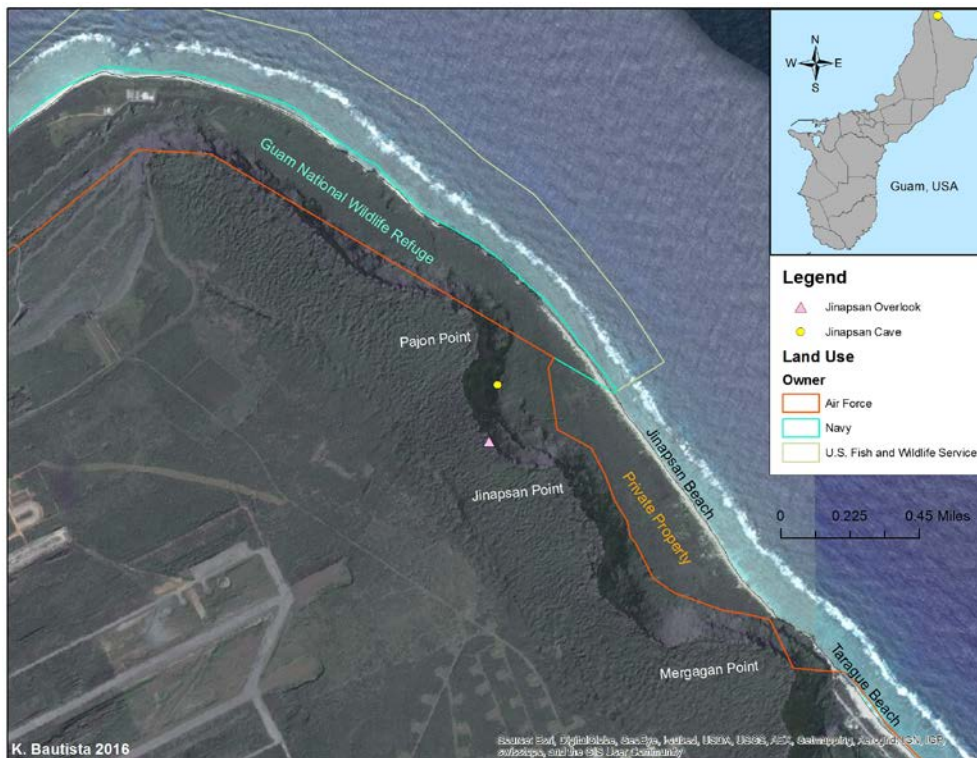


Figure 2.1a
Geographic
locations of
Jinapsan Cave
and Jinapsan
Overlook
station.
Legend shows
land
ownership.
The cave lies
closer to
Pajon Point
than Jinapsan
Point, but was
named
Jinapsan Cave
since it was
originally
accessed
mostly by way
of Jinapsan
Beach.



Figure 2.1b Aerial view of northern coastline east of Jinapsan Cave site. Jinapsan Cave lies on the opposite side of Pajon Point. (<http://north.hydroguam.net/photo-aerials/004.jpg>)

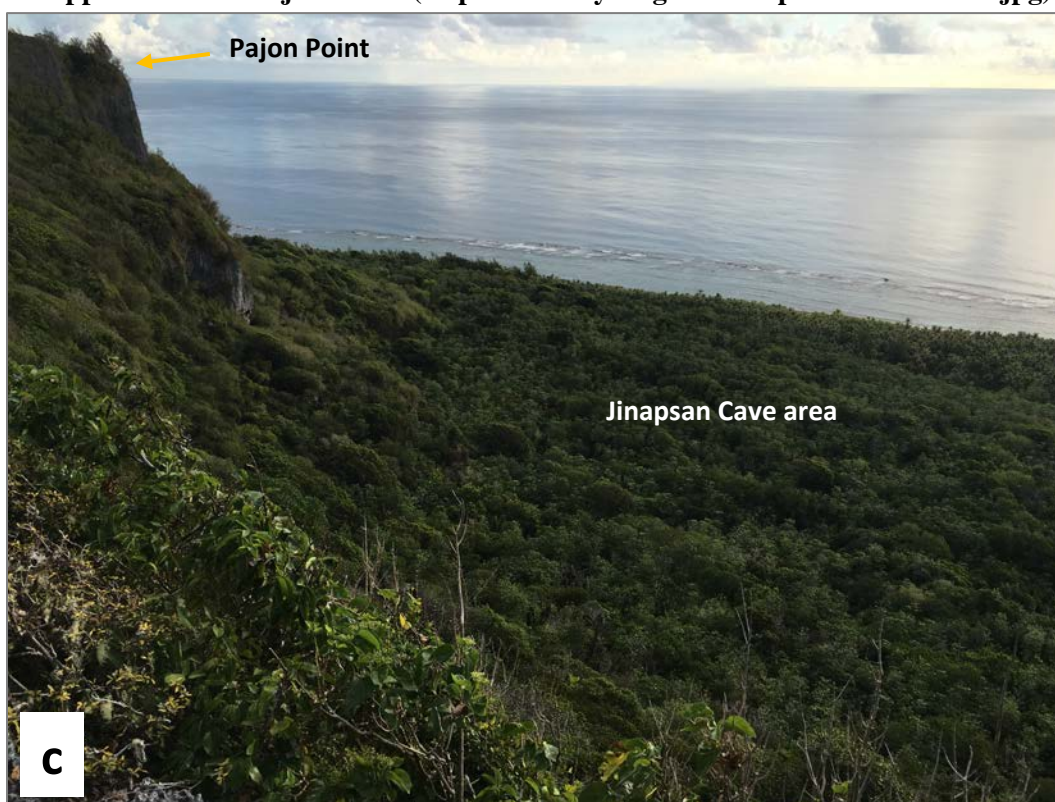


Figure 2.1c View of Jinapsan Cave area from Jinapsan Overlook, AAFB Fanihi Station. The general direction of the cave from this overlook is $\sim 20^\circ$ east from N.

Jinapsan Cave is formed in Pliocene-Pleistocene Mariana Limestone (Figure 2.2) approximately 1.8 Ma to 2.0 Ma in age (Randall and Siegrist 2000). The entrance of the cave lies at the base of a talus slope beneath the cliff that stands behind it. The direction of descent into the cave extends toward the cliff.

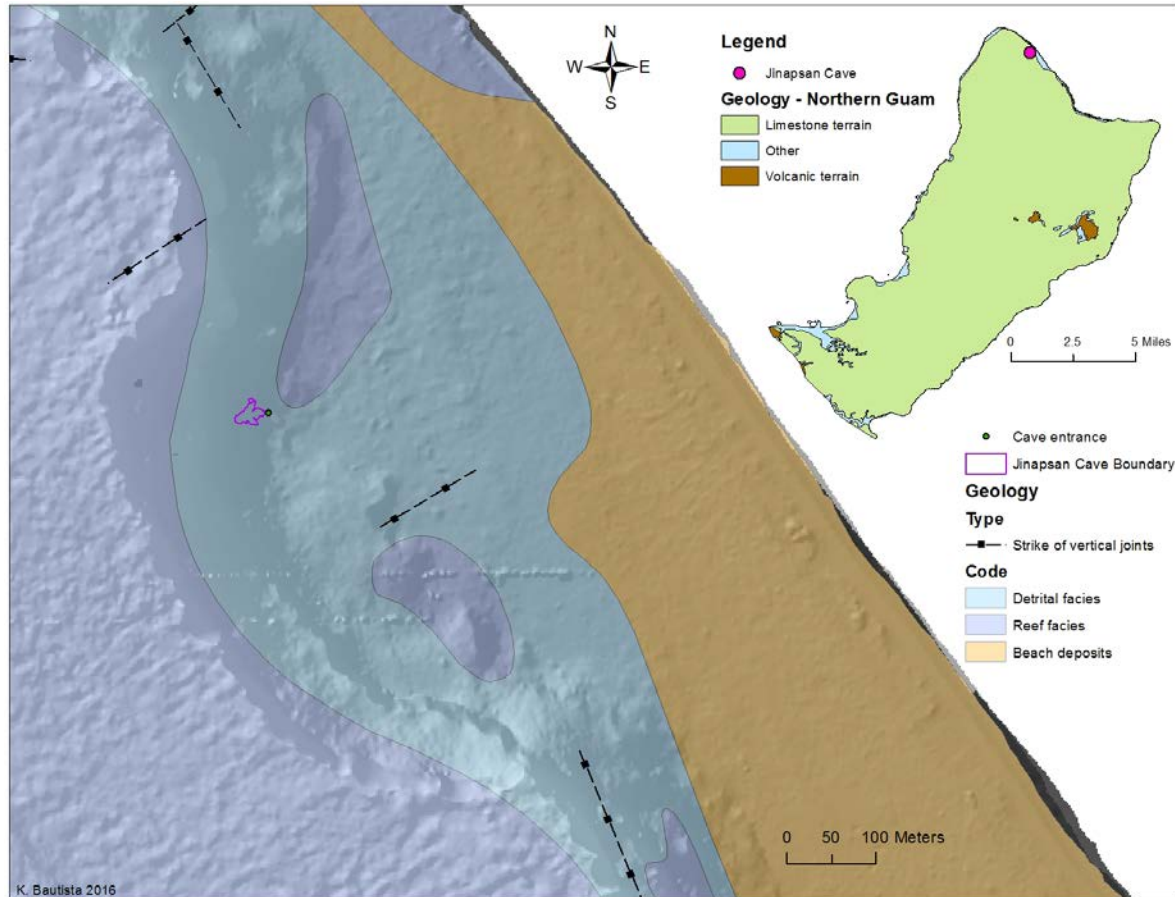


Figure 2.2 Geologic location of Jinapsan Cave boundary and entrance via GPS coordinates.

2.2 Cave Description

Jinapsan Cave is interpreted by Mylroie and Mylroie (2012) and Miklavič (2011) as a cave that has undergone progradational collapse (i.e., a *breakdown cave*) from dissolutional voids that originated at some depth now below modern sea level. It is an inclined, roughly prolately spheroidal, single-chamber cave, partitioned by flowstone walls and large stalagmites, and columns, which make the cave seem multi-chambered (Figures 2.3 and 2.4a, b, c). It contains actively growing speleothems, thus fitting the speleological category of *live cave* (US EPA 2002). The entrance, which faces east, is the single opening and highest point of the cave. The cave descends through varying-sized vadose passages to four rooms. A freshwater pool at the bottom is the lowest point of the cave, ~25 m vertically from the entrance and ~35 m horizontally. The pool water is brackish (on average 4,000 $\mu\text{S}/\text{cm}$). Rubble present in it shows no signs of dissolution, indicating the pool maintains calcite saturation. Taboroši (2006) inspected the room of the pool underwater and reported the floor in the pool is covered with rubble deposits, with no apparent phreatic passages. Two maps are shown in this report: 1) a simplified plan view of Jinapsan cave's entrance, passages,

“rooms,” drip stations, and the freshwater pool, and a profile view of major cave walls and entrance’s vertical distance above the water table (Taboroši et al 2008) and 2) Mylroie’s et al (2012) plan and cross section views showing cave floor and major cave deposit details.

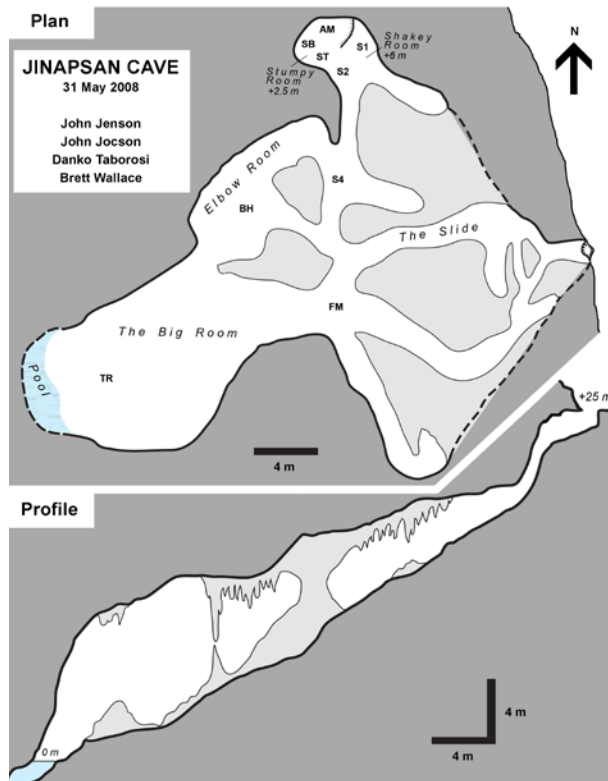


Figure 2.3 Plan and profile views of Jinapsan Cave. Named areas and 7 previously monitored sites are marked. Data collection stations (discussed below) are shown: Flatman (FM), Station 1 (S1), Station 2 (S2), Stumpy (ST), Stumpy’s Brother (SB), Amidala (AM), Trinity (TR), Pool (Taboroši et al 2008).

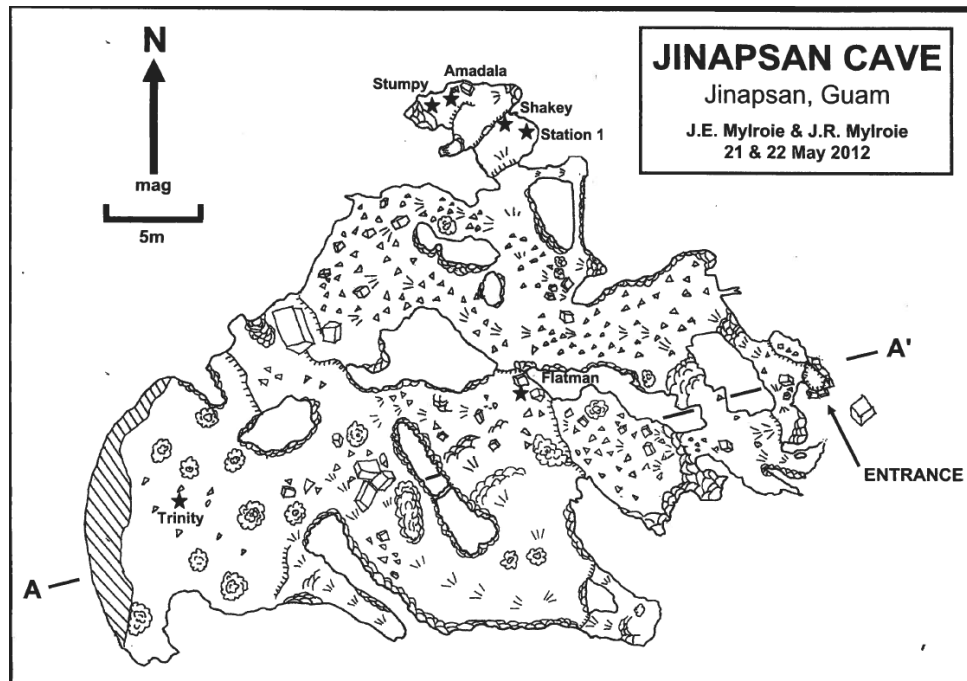


Figure 2.4a Plan view of Jinapsan Cave (Mylroie, J. E. et al. 2012 unpublished).

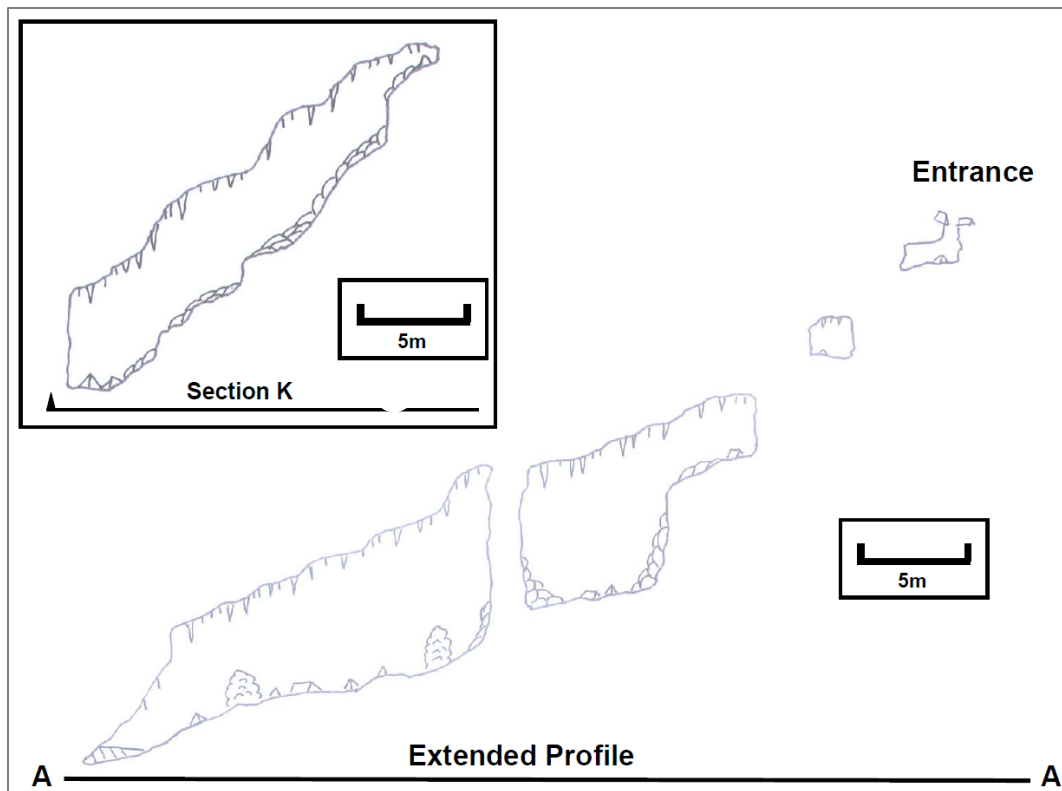


Figure 2.4b Cross-section A-A' of Jinapsan Cave and Section K as in 2.4c below.

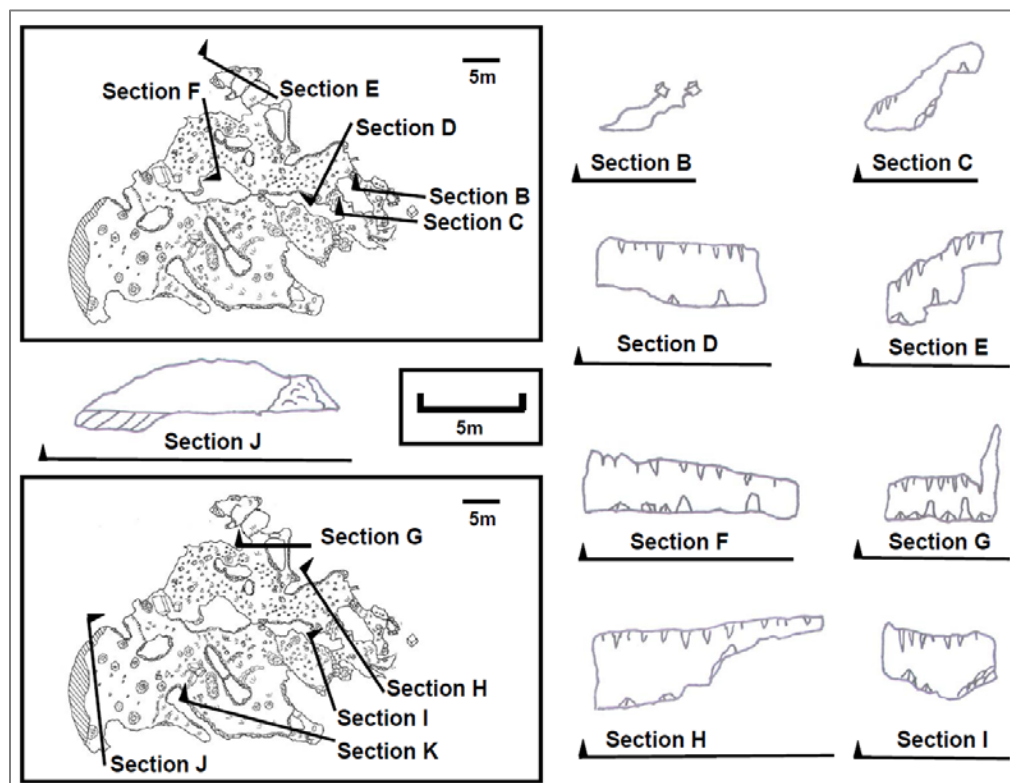


Figure 2.4c Jinapsan Cave cross sections B through K.

2.2.1 Navigating the cave

Figure 2.5 shows names give the rooms and the main routes through the cave. Table 1 summarizes the dimensions of the rooms and key for the photos. The entrance is an eastward-facing circular void created by ceiling collapse of the bedrock surface, exposed at the foot of the talus slope (Figure 2.6a, b). The initial passage is 0.8 m wide by 1.2 m and 1.06 m deep (Figure 2.4c cross-section B), with an area of 11 m² and volume of 13 m³ (Table 1.1). It is the only opening to the cave. From the entrance, there are two routes to the interior. One is a short vertical drop into the Slide (Figure 2.7). The other passage leads to the Anteroom (Figure 2.4c cross-section C and Figure 2.8). The Anteroom is oblong shaped, 2.48 m by 4.08 m, and 14 m² in area and 36 m³ in volume. It has a low ceiling, 2.47 m high, with some large stalactites. The Anteroom floor is covered with medium-grained loose sediment that most likely has blown in from the outside and gravel-sized limestone clasts.

From the Anteroom are two possible descent routes. One route (Figure 2.4c Section I and 2.9) is through a steep slope of flowstone and large boulder-sized rubble down to the top of a tiered platform. Another follows an opening to the Slide (Figures 2.4c cross-section D and 2.10), which halfway down, meets at the same tiered platform. This area is called Midslide since it can also be reached by traversing halfway down the Slide (Figure 2.11). The platform at Midslide (Figure 2.12) is centrally located among the data-collection stations. The ceiling is 4-5m high, mostly bare from breakdown, with few stalactites. The floor is covered with dirt and gravel-sized cave rubble.

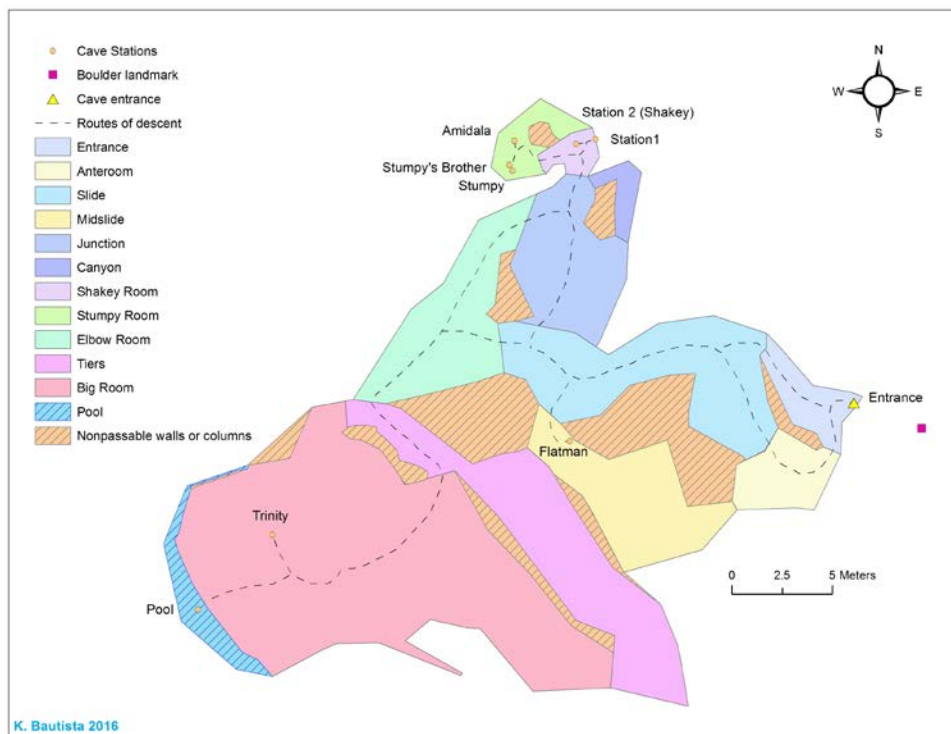


Figure 2.5
Map created
on ArcMap
10.2.2 of
Jinapsan cave
boundary, site
landmark
(boulder) and
cave entrance,
cave areas
(rooms),
current cave
stations and
route to
navigate to
them.

Cave Room	Approximate Area (m ²)	Approximate Volume (m ³)	Figures
Cave Entrance	-	-	2.6a, b
Entrance (room)	11	13	2.7, 2.8
Anteroom	14	36	2.9, 2.10
The Slide	53	63	2.10, 2.11
Midslide	35	188	2.12 – 2.14, 2.24
Junction	32	64	2.15a, b
The Canyon	5	11	2.16
Shakey Room	5	11	2.18, 2.19
Stumpy Room	9	16	2.20 – 2.22
Elbow Room	37	90	2.23
The Tiers	60	372	2.24 – 2.26
Big Room	161	650	2.27 – 2.30
Pool	9	-	2.31
Nonpassable walls/columns	71	-	-

Table 2.1 Summary of Jinapsan Cave approximate room area and volume, and corresponding figures in this section.



Figure 2.6a Jinapsan Cave entrance on talus slope. Machete for scale, circled in yellow.



Figure 2.6b Close-up of cave entrance. Cave helmet for scale. (Photos: J. Jenson)



Figure 2.7 (left) Steep vertical passage from Entrance room to The Slide (yellow arrow). Note tree root protruding from ceiling, wrapping around wall in upper right of photo. Bag for scale. (Photo: J. J. Bautista)

Figure 2.8 (right) Initial passage looking to entrance floor (cross-section B) from Anteroom top level (cross-section C). (Photo: J. Jenson)



Figure 2.9 Anteroom looking to passage as in Figure 2.4c cross-section I.



Figure 2.10 Anteroom looking down to upper part of The Slide, which curves left (yellow arrow) (Photos: J. J. Bautista)



Figure 2.11 On rope, Midslide, looking up to The Slide curve. (Photo: J. J. Bautista)



Figure 2.12
Midslide platform. Yellow arrow indicates
direction toward Anteroom opening in Figure
2.9. Site with collection bottle is Flatman.

Opposite the platform, also at Midslide, are two routes leading to two cave boundary areas. One is by a steep descent on a rope into the southern end of the Elbow Room (Figure 2.4c cross-section F, and Figure 2.13). The other is through a passage leading to the Junction (Figure 2.14), a 2.8 m wide by 5.31 m long room, with an area of $\sim 32 \text{ m}^2$ and volume of $\sim 64 \text{ m}^3$. The ceiling is low and decorated with actively dripping soda-straw stalactites. The room floor is composed of separate areas of large boulder-size breakdown rubble, flowstone, and small, gravel-sized cave rubble (Figures 2.15a, b). The Junction is at the intersection between the Elbow Room, the Canyon (Figure 2.16), and

the entrance to the Shakey Room (Figure 2.17).



Figure 2.13 On rope, Midslide, looking toward Elbow Room. Cavers and flashlight for scale. (Photo: J. Jenson)



Figure 2.14 On rope, Midslide, looking to passage (arrow) to Junction which leads to Shakey and Stumpy Rooms. Caver for scale. (Photo: J. J. Bautista)



Figure 2.15a Looking to passage (yellow arrow) leading to Elbow Room from Junction Room. Caver and bag for scale. (Photo: K. Bautista)



Figure 2.15b
Boulder-size cave rubble of floor of upper part of Junction Room. Bag and flashlight for scale.
 (Photo: J. J. Bautista)

The Canyon is behind a large section of cave wall (6.5 m long, 2.2 m high) that fractured and slipped forward from its original position. The area between the fractured and current wall is less than 2 m wide, and is only traversable along the top of the boulder. The room area is $\sim 5 \text{ m}^2$ and volume is $\sim 11 \text{ m}^3$. The ceiling is $\sim 4 \text{ m}$ above the northern end, the ground 1.75 m below. At the fracture site flowstone covers the wall entirely.



Figure 2.16 (left) Looking from the Junction into the Canyon. Caver in upper middle of photo is on a 2-m high section of cave wall that fractured and slipped off.
Figure 2.17 (right) Looking toward passage leading to Shakey Room from the Junction.
 (Photos: J. J. Bautista)

The Shakey Room (Figure 2.18) is 3.5 m long and 2.03 m wide, with an area of $\sim 5 \text{ m}^2$ and volume of $\sim 11 \text{ m}^3$. It has a steeply sloped ceiling with small stalactites, and the highest ceiling point is approximately 2 m. The floor is partly covered by flowstone, with the remainder covered with sediment and small, gravel-sized cave rubble.



Figure 2.18
Looking into Shakey Room.
(Photo: J. Jenson)

A traversable hole opens to the Stumpy Room (Figure 2.19), which is 20.6 m vertically deep from the entrance and 35.6 m from the surface. The room is C-shaped (Figures 2.6 and 2.20), 6.04 m long by 2.69 m wide (Figure 2.4c cross-section E), and 1.63 m high with a steeply-sloped ceiling (Figure 2.21). Flowstone covers most of the wall and

floor (Figures 2.22). The room area is $\sim 9 \text{ m}^2$ and room volume is $\sim 16 \text{ m}^3$.



Figure 2.19 Caver descending into Stumpy Room from Shakey Room.



Figure 2.20 Looking into Stumpy Room from the hole in Shakey Room occupied by caver in previous photo. (Photos: J. J. Bautista)



Figure 2.21 Stumpy Room's sloped ceiling. (Photos: J. Jenson)



Figure 2.22
Flowstone covering
northeastern wall and
floor in Stumpy Room.

At the bottom of the Slide is the Elbow Room (Figure 2.4c cross-section F and 2.23). As the name suggests, it is an L-shaped room, $\sim 37 \text{ m}^2$ in area, 90 m^3 in volume (Figure 2.6), and 12.6 m long and 6.7 m at the widest point. The ceiling is steeply-sloped and decorated with

small soda straw stalactites. The floor is littered with coarse, boulder-size cave rubble. This room connects the end of the Slide to a set of tiers that further descend to the Big Room.



Figure 2.23
Caver, on rope,
ascending to The Slide
from Elbow Room.
Yellow arrow points NE
to upward passage
leading to Shakey and
Stumpy Rooms. White
arrow leads SW to the
Tiers and then to Big
Room. (Photo: J.
Jenson)

The area called the Tiers occupies a separate junction connecting the Midslide platform (Figure 2.24) to three openings into

Big Room: one at the top (Figure 2.25), and two at the end (Figures 2.26 and 2.27). It is 19.7 m long by 4.46 m wide, $\sim 60 \text{ m}^2$ in area, and $\sim 372 \text{ m}^3$ in volume. The center (middle tier) is 27.1 m from the ground surface. The ceiling height is 4.16 m at the center of the room, and has small stalactites. The floor of the top tiers has smooth flowstone, while the floor descending from the middle to the bottom set of tiers changes from small gravel-sized cave rubble to large boulders.



Figure 2.24 (left) Bottom of the middle tier looking up to the Midslide platform. Tripod at Flatman station for scale. Yellow arrow shows direction from Midslide platform to Anteroom.



Figure 2.25 (right) Top tiers, mostly of flowstone. One opening to Big Room is behind bag. Bag and flashlight for scale.



Figure 2.26
Smallest of the traversable openings into Big Room from the bottom tier. Elbow Room direction marked by yellow arrow. Bag and flashlight for scale.
(Photos: J. J. Bautista)



Figure 2.27 Looking from Big Room to the descent from the middle tier, behind caver in orange. Note black sediment on room walls and floor rubble. (Photo: J. Jensen)

The bottom tier leads to the Big Room, the largest chamber, which occupies the lowest portion of Jinapsan Cave (Figure 2.28). Excluding the pool, the floor is 10 m wide and 12 m long, with a ceiling elevation about 2.1 m high at the center of the room. The room area is $\sim 161 \text{ m}^2$, and volume $\sim 650 \text{ m}^3$. The floor is littered with boulder-sized cave rubble and dripstone stalagmite mounds. Numerous stalactites have detached from the soft limestone ceiling. The number of ceiling stalactites is fewer than the stalagmite mounds directly below. Black stains on the ceiling follow along the network of small stalactites, with several clusters of larger stalactites (Figures 2.29 and 2.30). Most large stalactites are broken and form boulder-size rubble on the floor, and few have connected with corresponding stalagmites and formed columns. The Pool, sits at the lowest point of Big Room, and the terminus of the traversable cave (Figure 2.31). Changes in pool water level and temperature display tidal-influenced patterns.



Figure 2.28 Looking into Big Room from main opening. Yellow arrow points to Trinity station.



Figure 2.29 Stalactite network on ceiling of Big Room. (Photos: J. Jenson)



Figure 2.30 Black stain clearly follows fractures that form a network of stalactite intersections. (Photos: J. Jenson)



Figure 2.31 Looking at the Pool, cross-section J of Figure 2.4c.

METHODS

3.1 Previous Work

From August 2008 through September 2016, a research team made monthly (generally 4-5 weeks apart) two-day visits to Jinapsan Cave. Protocols (Figure 3.1) have varied somewhat over the years, as technology, techniques, and objectives have evolved, but Day-1 protocol as of September 2016 included recording surface ambient CO₂ measurements and collecting soil gas at two locations (upper and lower) on the talus slope (Figures 3.2 and 3.3a, b). On a boulder on the talus slope, 49 m asl (above sea level), a rain gauge was installed in 2011 (Figures 3.4a and b). Rainwater was collected for $\delta^{18}\text{O}$ analysis at the same site starting October 2012 and was discontinued in 2015 after $\delta^{18}\text{O}$ concentrations were found to be identical with samples collected at UOG (Figure 3.5). In the cave, CO₂ measurements were recorded monthly in Anteroom, Midslide, Shakey Room, and Big Room, and samples of cave air gas were collected in Shakey Room and Big Room (Figure 3.6). Air temperature and pressure have been measured by loggers similarly placed inside the cave, as well as on the slope outside of the cave. Drip water was collected overnight at each of the seven stations by a bottle set out on the first day of each visit: Flatman, Station 1, Station 2, Stumpy, Stumpy's Brother, Amidala, and Trinity. Stalactite drip counts have been recorded at five of the seven stations (where drip intervals are generally <5 minutes): Flatman, Station 1, Station 2, Stumpy's Brother, and Trinity (Appendix B). A tipping bucket rain gauge has been installed at Station 2 (Shakey) (Figure 2.22), at which one of the stalagmites (Shakey) from which data was collected in 2005 for paleoclimate studies (Partin et al. 2012; Sinclair et al. 2012). For Day 2, overnight collection bottles were collected, and a glass plate placed under each drip to collect monthly to bi-monthly samples of calcite precipitate (Figure 3.7). Drip-water bottles were weighed, and water decanted into smaller vials for $\delta^{18}\text{O}$, Sr/Ca, alkalinity, anions, and δD analyses (Figures 3.8a). Pool water is collected for the same analyses (Figure 3.8b). If enough water was available, Ultrameter® measurements were recorded for conductivity, total dissolved solids, pH, temperature, and oxygen reduction potential. From May 2015 to September 2016 stalactite drips and pool water were collected in situ for $\delta^{13}\text{C}$ analysis.

Day 1

Trailhead

- Ambient CO₂ measurement

Outside Cave

- Ambient CO₂ measurement
- Soil gas sampling - Upper & Lower sites
- Pressure & temperature logger swap
- Retrieve rain gauge - Top of the Rock (TOTR)
- Rainwater collection - TOTR [*discontinued 5/2015*]

Inside Cave

- Room CO₂ measurement
 - Anteroom, Midslide, Shakey & Big Rooms
- Cave air gas sampling - Shakey & Big Rooms
- Retrieve pressure and temperature loggers
 - Shakey Room
 - Big Room atmospheric (1) & Pool (1)
- Retrieve monthly calcite collection plates
- Station drip counts
- Deploy overnight drip-water collection bottles
- Retrieve rain gauge - Station 2 (Shakey)
- Swap monthly CO₂ logger - Stumpy Room

WERI

- Dry plates overnight
- Download data

Day 2

Inside Cave

- Retrieve, weigh and decant drip-water into vials
 - *Amidala discontinued 5/2015*
- Trinity 20-minute water collection, weigh, & decant
- Collect Pool water
- Capture immediate stalactite drip
 - Flatman, Stations 1 & 2, Trinity and Pool
- Deploy pressure and temperature loggers
- Deploy rain gauge at Station 2
- Deploy fresh calcite collection plates
 - *Trinity discontinued 1/2016*
- Ultrameter measurements on leftover drip water

WERI

- Upload data report
- Alkalinity tests & ship water and plates to UT-A

Figure 3.1 Field and laboratory tasks for monthly sampling as of September 2016.

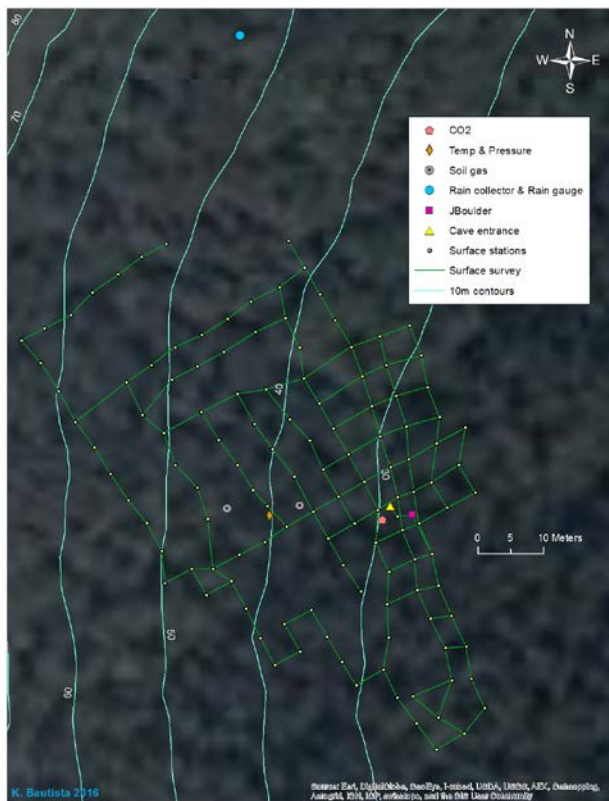


Figure 3.2
Surface slope survey stations, and surface logger and gas sampling sites.



Figure 3.3a Lower soil gas well (blue arrow). Surface temperature and pressure logger site under boulder (yellow arrow).



Figure 3.3b Close up at Lower soil gas well. Bag of exetainers for scale.



Figure 3.4a View of Mergagan and Pati Points from Top of the Rock rain collection station.



Figure 3.4b Rain gauge and collector on Top of the Rock site. Machete for scale. (Photo: J. Jenson)



Figure 3.5
Rain collector site outside House 5, Dean's Circle at the University of Guam.

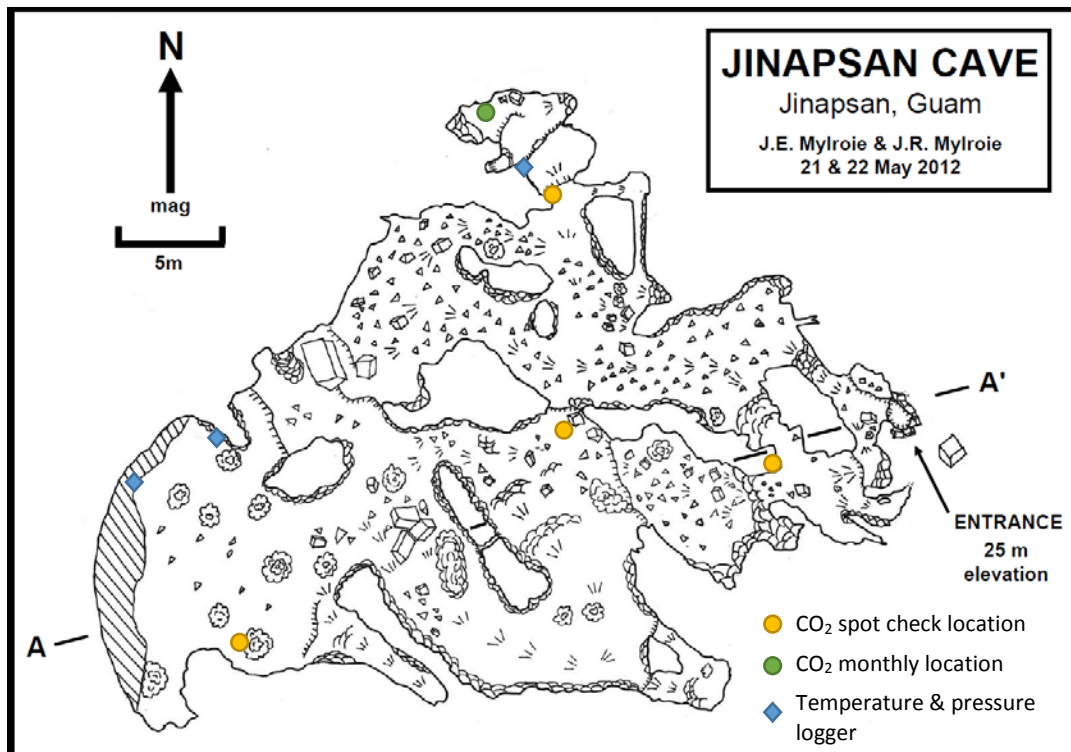


Figure 3.6 Map of cave temperature and pressure logger and CO₂ sampling sites. (Based on Mylroie and Mylroie, 2012, unpublished map)



Figure 3.7 October 22, 2013 photo of fresh glass plate deployed at Amidala station for calcite precipitate collection. Top is sanded to create rough surface calcite will cling to. Plate number in top corner is oriented NE and dip direction is recorded. (Photo: J. Jenson)



Figure 3.8a Decanting drip-water into aliquots for $\delta^{18}\text{O}$, Sr/Ca, alkalinity, anions, and δD analyses. (Photo: J. J. Bautista)



Figure 3.8b Collecting pool samples for analysis. (Photo: J. J. Bautista)

3.1.1 Sampling Stations

Since 2008 nine stalagmites with actively dripping stalactites overhead and the pool were established as monitoring stations in Jinapsan Cave. From June 2009, Borehole in Elbow Room, and Station 4 in the Junction were discontinued, reducing the number of stations to eight. Flatman (Figure 2.12), Stumpy, Stumpy's Brother (Figure 3.17), and Stumpy Amidala (Figure 3.19) stations are each equipped with a Plexiglas® board fused to a tripod. Trinity is anchored onto its dripstone mound (Figure 3.20b). Station 1 is marked by a Plexiglas® board mounted onto a plastic flower pot perched against a cave wall (Figure 3.13). The rain gauge at Station 2 is stabilized with a stack of fallen speleothems (Figure 2.18). Each site has a short piece of PVC pipe on which to locate and stabilize drip water collection bottles overnight under respective stalactites. Placement of the PVC sections on the Plexiglas® platforms is marked with white nail polish to help maintain alignment under the respective drip. During the month-long intervals between drip-water collection, sanded glass plates, etched with a number, are placed in notches filed in the tops of the PVC sections to collect calcite precipitate from respective stalactite drips (Figure 3.7).

At the Midslide platform, Flatman is the sole station (Figure 2.12). The feeder stalactite is small and ~4 m above the floor, and thus can be difficult to find among the surrounding cluster of active small stalactites (Figure 3.9). The rest of the ceiling is mostly bare from breakdown, with few stalactites varying in size from large ones to small soda straws. The Flatman station (tripod) (Figure 3.10a) is 0.64 m above the base of its stalagmite (Figure 3.10b), and 4.04 m below its stalactite. The stalagmite was cored in August 2008 (Figure 3.11) and brought to the Jackson School of Geosciences at the University of Texas at Austin for analysis.



Figure 3.9
Ceiling
features above
Flatman
station.
Yellow arrow
points to
Flatman's
feeder
stalactite.



Figure 3.10a Flatman station tripod and stalagmite. Equipment for scale.
Figure 3.10b Close up of Flatman stalagmite (front). Pen for scale.



Figure 3.11
August 16, 2008 photo of Flatman stalagmite,
freshly cored.

In the Shakey Room, Stations 1 and 2 are the next set of stations vertically deep from the cave entrance. Station 1 is situated on a flowstone wall on the eastern side of the room. Its stalagmite was cut at the base in June 2009 (Figure 3.12). The station is 0.17 m above the stalagmite base, and 0.70 m below the stalactite. Station 1's feeder stalactite is among a cluster of actively dripping stalactites, some which are connected to respective stalagmites on the flowstone wall (Figure 3.13).



Figure 3.12
June 10, 2009 photo of Station 1 stalagmite,
freshly cut.
(Photo: J. Jenson)



Figure 3.13
Station 1 stalactite (yellow arrow).
Stalagmite was removed from its base
under flower pot in June 2009.

Station 2, from which the stalagmite Shakey was collected (Partin et al. 2012; Sinclair et al. 2012), is 1.04 m from Station 1. Shakey was removed at its base in April 2005 (Sinclair et al. 2012) (Figure 3.14). The current stalactite (Figure 3.15), on the sloped section of the ceiling, is ~1 inch (2.5mm). Shakey's cut length measures 26.5 inches (0.67 m), and is reported having a smooth exterior (Figure 3.16). The ceiling height above Station 2 is 0.81 m.



Figure 3.14
April 22, 2005 photo of Shakey at Station 2.
Note length of soda straw on feeder stalactite.
(Photo: J. Jenson)



Figure 3.15 (above)
Station 2 stalactite. Yellow arrow indicates end of stalactite.



Figure 3.16 (right)
Longitudinal slab from Shakey, Station 2 stalagmite.
Samples were drilled for dating and stable oxygen and carbon analyses. (Photo: S. Hsia)

In the Stumpy Room, Stumpy, Stumpy's Brother, and Amidala stations are the next set of stations vertically deep from the cave entrance. The Stumpy station (tripod) is 0.48 m directly above the floor, and 1.68 m below the room ceiling (Figure 3.17 left). Stumpy was cut at its base also in April 2005, for analysis by Sinclair et al. (2012). It is 13.64 inches (0.35 m) in length, and is reported having a smooth exterior (Figure 3.18). Stumpy's stalactite is small and is 1.68 m above the station tripod. Stumpy's Brother station (Figure 3.17 right) is between Stumpy and Amidala (Figure 3.19), 0.4 m and 1.2 m, respectively. The station is 1.52 m below the ceiling, and 0.35 m above the floor, directly over Stumpy Brother's stalagmite. Stumpy's Brother is still in place and its overhead stalactite is ~2 cm longer than Stumpy.



Figure 3.17
Stumpy location (left) and
Stumpy's Brother (right) stations.
(Photo: J. Jenson)

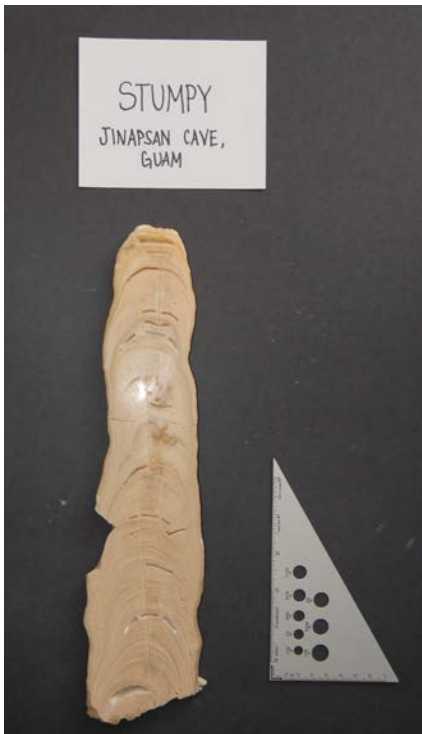


Figure 3.18
Longitudinal slice through Stumpy's stalagmite used for
dating by Sinclair et al. (2012). (Photo: S. Hsia)

Amidala station is directly over the Amidala stalagmite, 0.68m above the room floor. Its feeder stalactite hangs 0.62 m above the station (tripod). The stalagmite is irregularly shaped, and may be so from calcite deposition of neighboring actively dripping stalactites.



Figure 3.19
Amidala station. Lid for scale. Purple arrow marks stalactite. (Photo: J. Jenson)

Trinity, at the eastern end of Big Room, is the furthest speleothem from the cave entrance both vertically and horizontally (Figure 2.5). The station is mounted 0.75 m above the side of a dripstone mound, from which the Trinity stalagmite was cut in August 2008 (Figures 3.20a, b; Figures 3.21a, b). The small stalactite, 1.20 m above the station, is along a line of small active stalactites (Figure 3.22).



Figure 3.20a
August 6, 2008 photo of cutting Trinity stalagmite. Pen for scale. (Photo: J. Jenson)



Figure 3.20b
Trinity collection station mounting above stalagmite base. (Photo: J. Jenson)

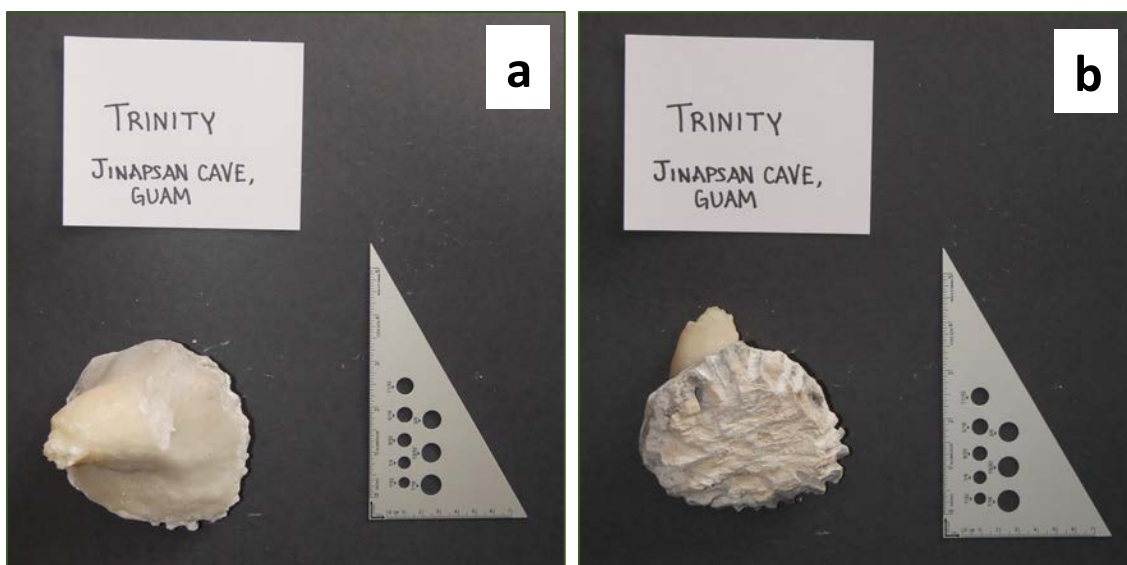


Figure 3.21a Topside of Trinity stalagmite.

Figure 3.21b Bottom of Trinity stalagmite. (Photos: S. Hsia)

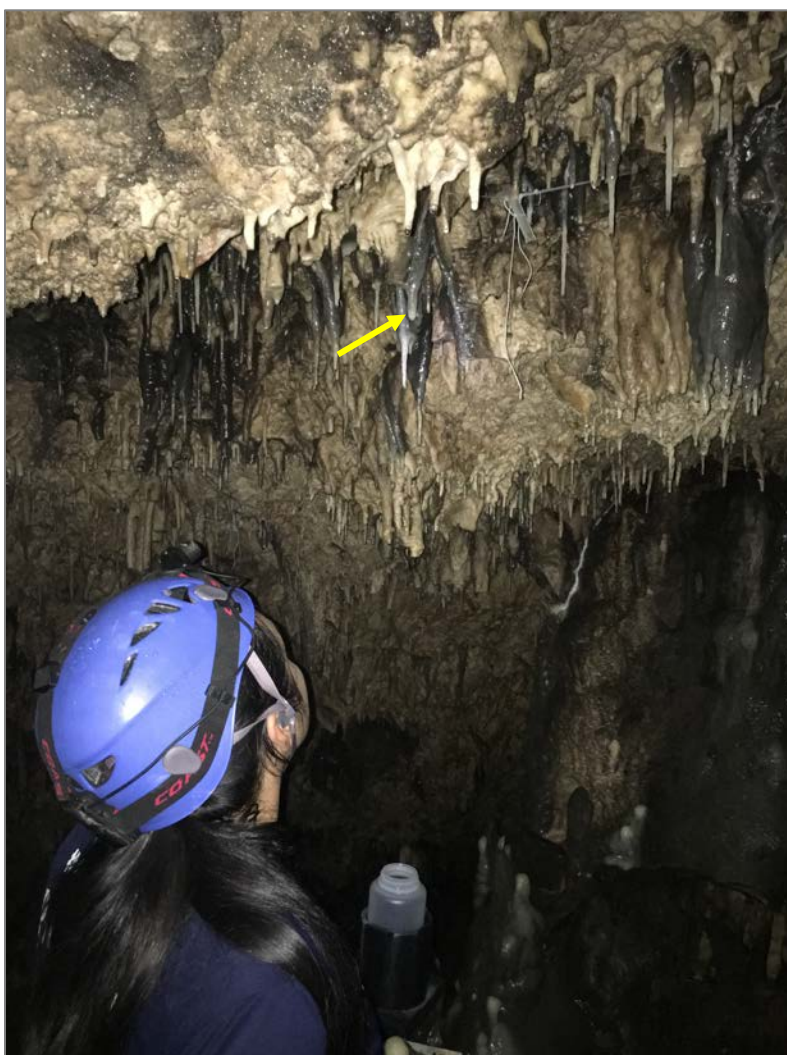


Figure 3.22

Trinity drip collection bottle at station and overhead stalactite (yellow arrow). Note black staining along fracture network. (Photo: K. Bautista)

3.2 Drip-count database

Drip counts (in seconds) were recorded on both days of monthly field trips from September 2008 until May 2015, when drip counting was reduced to only one day of each monthly visit, generally the first. Two drip-count methods were used: 1) a slow drip method for drip intervals on the order of 10 seconds or more and 2) a fast drip method for drip intervals on the order of seconds. The slow drip method uses a stopwatch or timer to count seconds between each of three drips from a station stalactite. A starting drip, drip zero, is used to begin count after it hits the bottle or plate. As drip one hits the bottle or plate, the time is recorded. The timer continues until up to the third drip. The slow drip method is used for stations Flatman, Station 1, Station 2, Stumpy, Stumpy's Brother, and Stumpy Amidala (Figure 3.23a). If a station drip interval exceeds five minutes, it is noted in the field records, and a drip count is not taken. On occasional visits, however, if field time allowed, or out of interest, the slow drip method was conducted at a station with an observed drip rate greater than five minutes.

The fast drip method uses a stopwatch or timer to count the number of stalactite drips in a three-minute period (Figure 3.23b). When a starting drip, drip zero, hits the bottle or plate, the timer is started. Drips are counted until the timer reaches three minutes. The fast drip method is used for the Trinity station.



Figure 3.23a Counting drip rate for Stumpy (left) and Stumpy's Brother (right) stalactites. (Photo: J. Jenson)



Figure 3.23b Counting drips at Trinity station. Note line of stalactites along dark stained fracture above the station. (Photo: J. Jenson)

Drip count records from September 2008 to December 2014 were input into an Excel® database. Monthly Day 1 and Day 2 drip counts were averaged for each station, and also input into the same database as each month's drip rate in drips/hour. Table 3.1 summarizes the treatment of drip-rate data. On two occasions, February 2010 and July 2014, cave teams did not make trips to collect data. In February 2010, a team member was injured at home on the morning of the scheduled visit, which precluded visiting the cave until the next month. In July 2014, the island was continuously on watch for three consecutive major storms, which precluded the cave visit for the month.

Formula	Equation	
$\frac{\text{Observed drips}}{\text{hr}} = \left(\frac{1 \text{ drip}}{\text{average seconds}} \right) \left(\frac{3600 \text{ seconds}}{1 \text{ hr}} \right)$	1	Calculated drip rates (drips/hr) from recorded data.
$\frac{\text{Observed mL}}{\text{drip}} = \left(\frac{\text{dripwater weight mL}}{\text{bottle time mins}} \right) \left(\frac{\text{average seconds}}{\text{drip}} \right) \left(\frac{1 \text{ min}}{60 \text{ seconds}} \right)$	2	Calculated dripwater flux (milliliters/day) from recorded data.
$\frac{\text{Observed mL}}{\text{day}} = \left(\frac{\text{drips}}{\text{hr}} \right) \left(\frac{\text{mL}}{\text{drip}} \right) \left(\frac{24 \text{ hrs}}{1 \text{ day}} \right)$	3	
$\frac{\text{Estimated mL}}{\text{day}} = \left(\frac{\text{water collected g}}{\text{bottle time mins}} \right) \left(\frac{1400 \text{ mins}}{\text{day}} \right) \left(\frac{1 \text{ mL}}{1 \text{ g}} \right)$	4	Calculated estimated drip rates (drips/hr) for drip counts recorded as > 5 minutes.
$\frac{\text{Estimated drips}}{\text{hr}} = \left(\frac{\text{water collected g}}{\text{bottle time mins}} \right) \left(\frac{60 \text{ mins}}{1 \text{ hr}} \right) \left(\frac{\text{drip}}{\text{exp. mL}} \right) \left(\frac{1 \text{ mL}}{1 \text{ g}} \right)$	5	Estimated dripwater flux (mL/day) calculated from overnight dripwater collection amounts (g) and deployment times (mins) Eq. 4.
$\frac{\text{Estimated mL}}{\text{day}} = \left(\frac{\text{drips}}{\text{hr}} \right) \left(\frac{\text{exp. mL}}{\text{drip}} \right) \left(\frac{24 \text{ hrs}}{1 \text{ day}} \right)$	6	Experimental water-drop volume values (mL/drip) were used in Eqs. 5 and 6 to estimate dripwater flux (mL/day) and drip rate (drips/hr) from recorded overnight dripwater collection amounts (g) and deployment times (mins).
$\frac{\text{Estimated seconds}}{\text{drip}} = \left(\frac{3600 \text{ seconds}}{1 \text{ hr}} \right) \left(\frac{\text{hr}}{\text{estimated drips}} \right)$	7	Estimated drip rates (drips/hr) were input into Eq. 7 to calculate drip rates in seconds per drip.

Table 3.1 Summary of equations used to calculate observed and estimated values for drip rate (drips/hr) and dripwater flux (mL/day). Exp. refers to ‘experimental.’

3.3 Cave Survey

In addition to comprehensive surveys by Taboroši (2008) and Mylroie and Mylroie (2012) several more limited or focused surveys were conducted at Jinapsan Cave at various times using cave surveying techniques from Dasher (1994). Metric tape was used to measure station distances on the ground surface. Bosch laser range finders were used to measure station distances and ceiling and floor heights in the cave. A Suunto duo compass and clinometer were used to measure azimuth and inclination. Separate ground surface surveys were conducted from May 2012 and April 2014 and from June to September 2014, and interior cave surveys from September 2015 through February 2016. Survey data input into *Compass Project Manager* and *CaveXO* produced 2-dimensional survey plots (Figure 3.24) and 3-dimensional cave plots (Figures 3.25), respectively. A GPS waypoint marking a boulder landmark by the cave entrance georeferenced surveys with respect to elevation above sea level, ~29 m (Figure 3.26a, b). Surveys were exported as 2D line and point shapefiles, and projected as layers over satellite imagery on GIS software, ArcMap 10.2 (Figure 3.27). A model of cave rooms and non-passage polygons was delineated from survey shapefiles, and room floor areas (sq. m) and room volumes (cu. m) were calculated (Section 2, Figure 2.5, Table 2.1).

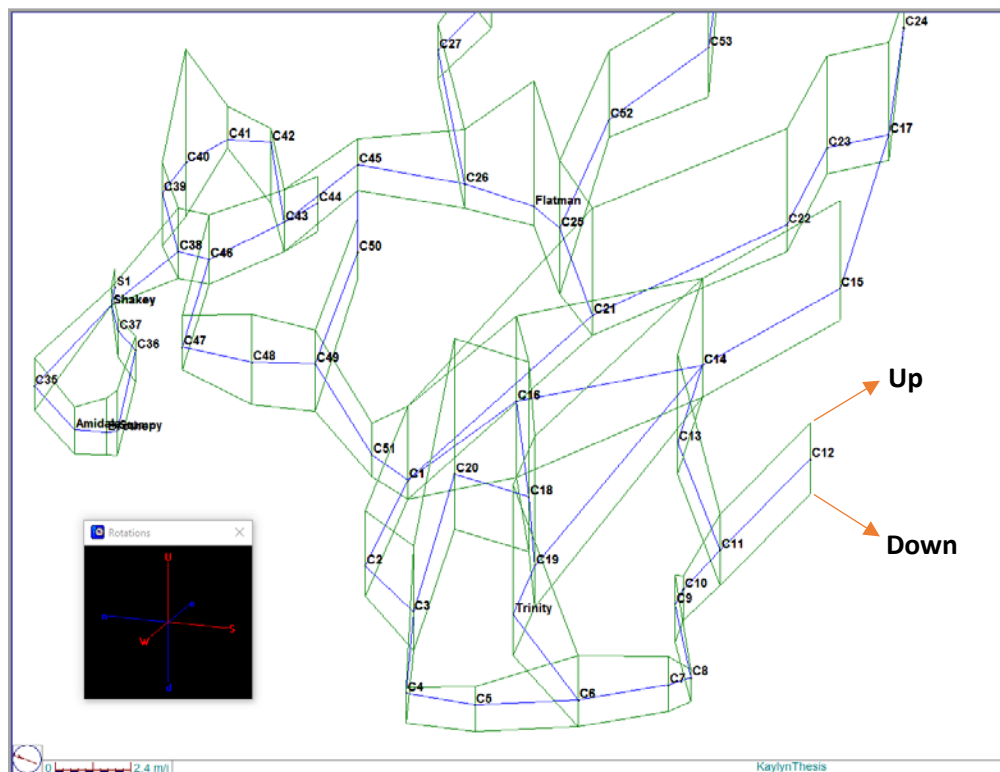


Figure 3.24 2D *Compass* cave survey plot

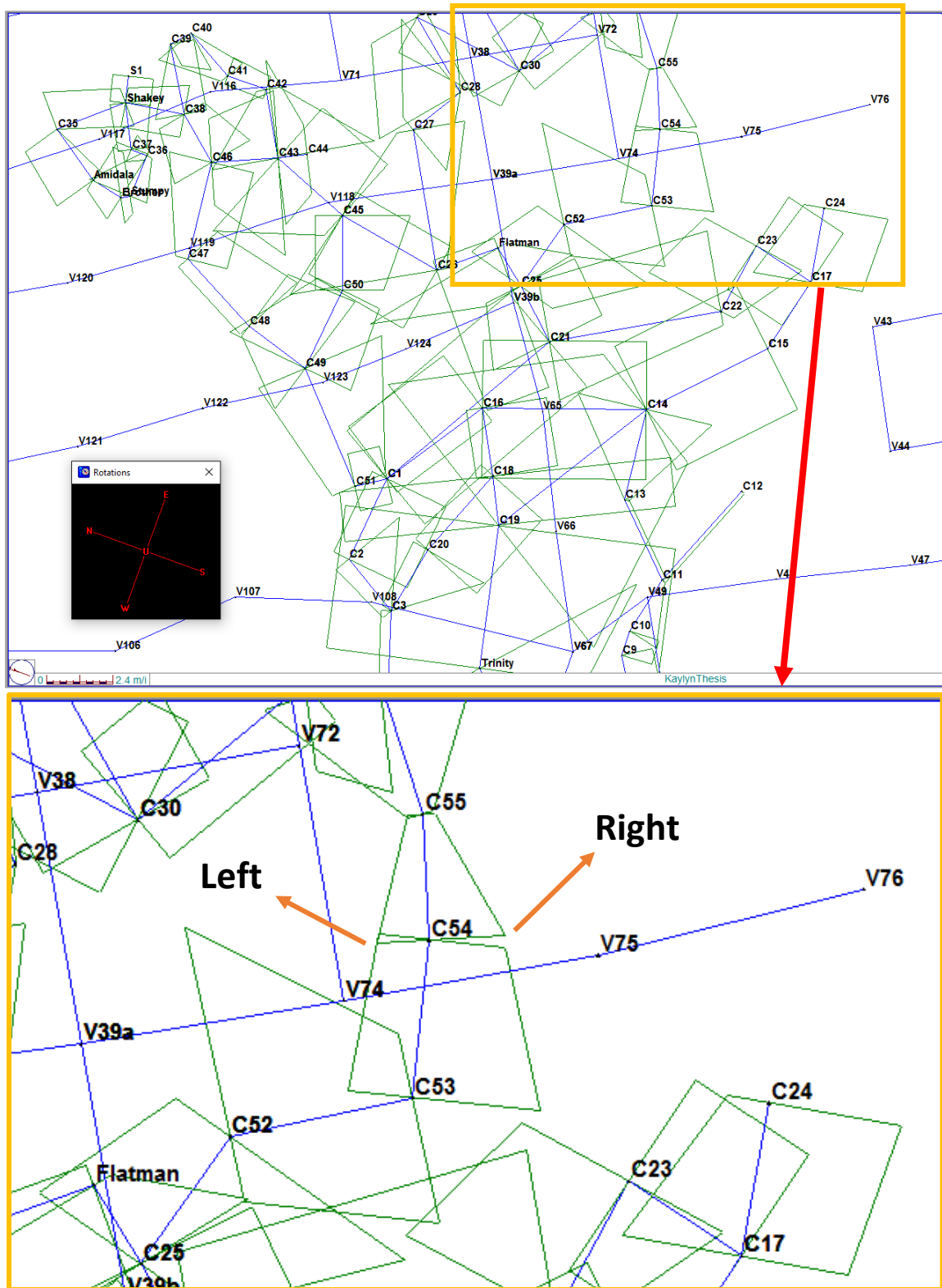


Figure 3.25 2D cave (C#) and surface (V#) survey plan plot. Compass in smaller window shows N. Insert (yellow box) shows left and right distances (cave walls) in green. Left and right labeling is dependent on direction of survey shot, from station # to station #). Survey direction is from C54 (from station) to C55 (to station).

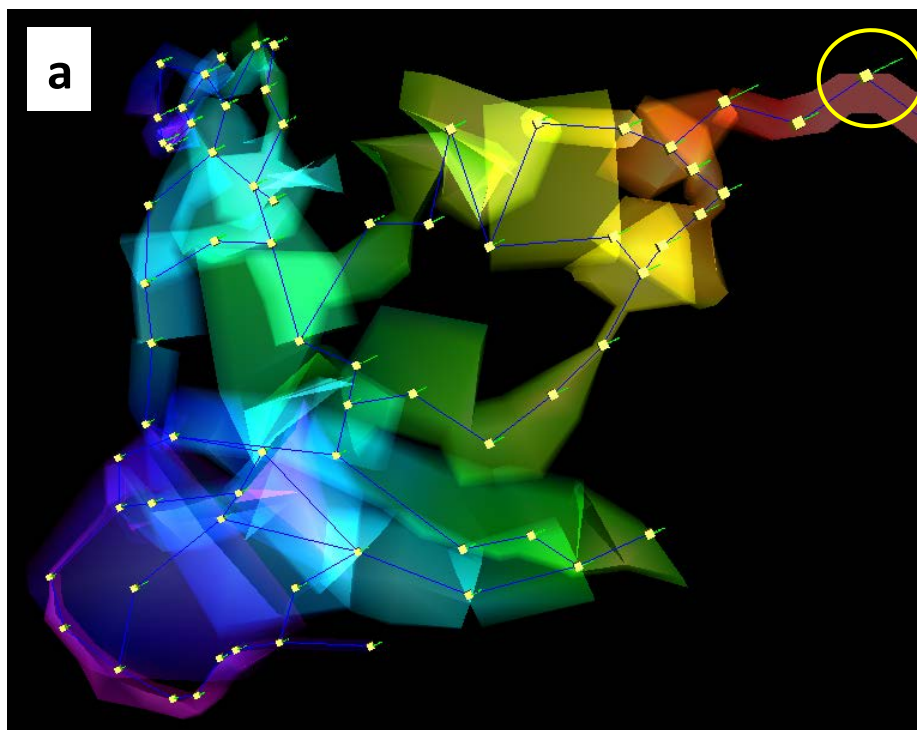


Figure 3.26a
Plan view of 3-D
model of Jinapsan
Cave passages on
Compass CaveXO
cave-modeling
software.
Transparency set at
50%. Color gradient
shows elevation as
interpreted from a
GPS reference
point, Boulder
landmark, (yellow
circle) outside the
cave by the
entrance.

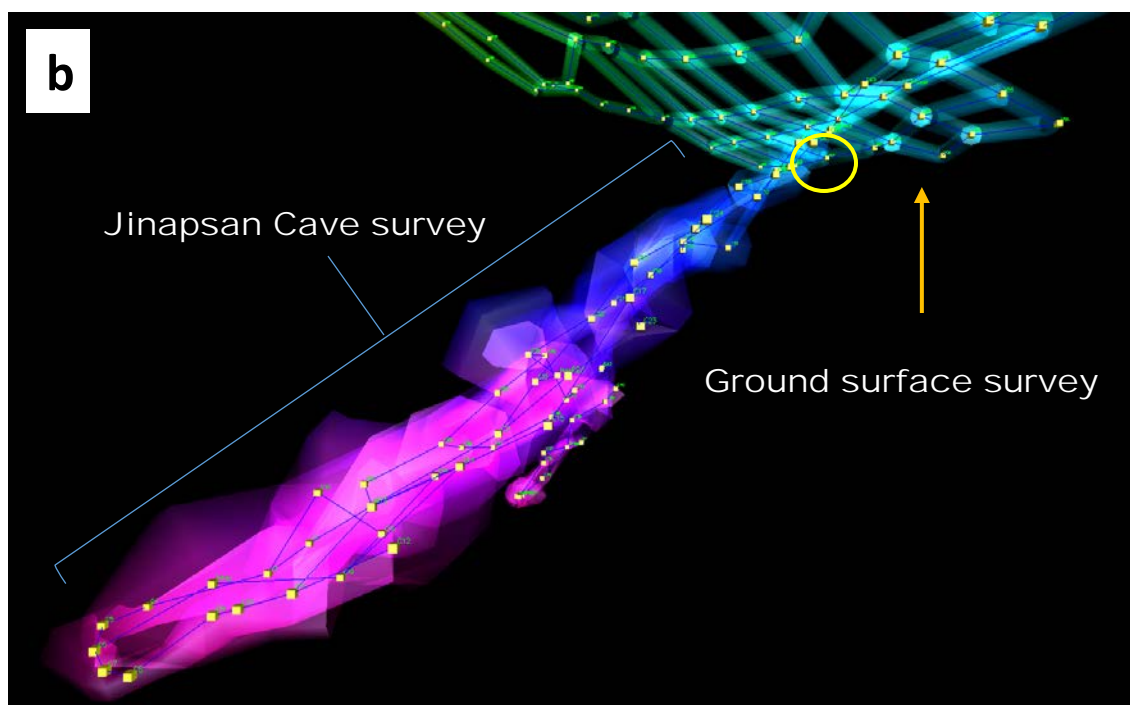


Figure 3.26b 3D profile passage model of Jinapsan Cave on *Compass Cave XO* cave modeling software with transparency set to 50%. Color gradient shows elevation as interpreted from a GPS referenced boulder landmark (yellow circle) outside the cave entrance.

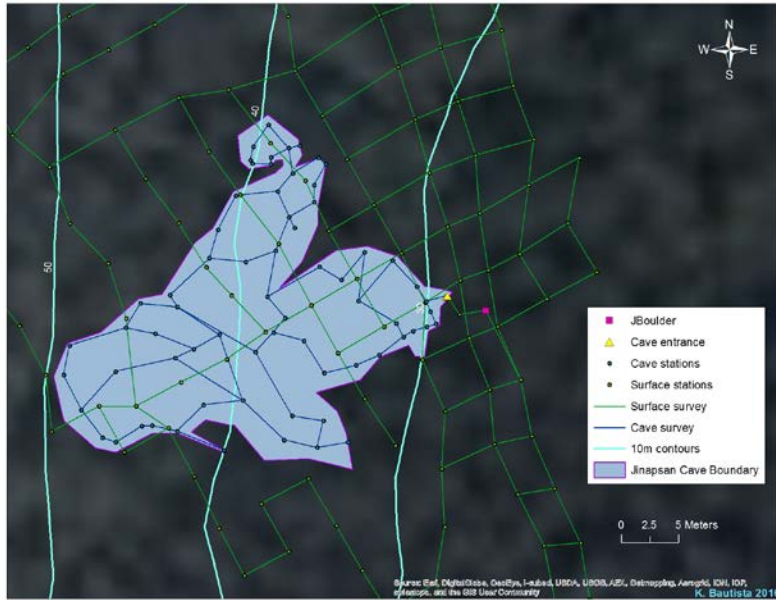


Figure 3.27
Map created in *ArcMap 10.2.2* of cave survey stations at Jinapsan Cave. Surface survey is green mesh with green circles. Cave survey is blue with orange circles. Yellow triangle marks cave entrance. Coordinates at the pink square are a georeferenced waypoint that ties the surveys together.

A cross section (Transect A-A') (Figure 4.1b) of the cave entrance to the pool was drawn from printed 2-D survey profile

plots with a scale of 5 meters per inch. Ceiling and floor distances of cave survey stations were marked from corresponding up and down passage data, respectively. Cave sediment characteristics (stalactites, stalagmites, rubble, flowstone, etc.) were sketched from survey notes. The ground surface points directly above cave survey points were marked using surface survey stations and a straight edge ruler. Ground surface characteristics (boulders and trees) were drawn from survey observations (Figures 3.28a and b). Cave and surface slopes were measured from the entrance to the pool, and to V52, respectively, on *Compass* cave-modeling software. A second cross-section of the Shakey and Stumpy Rooms (Transect B-B') was drawn from printed 2-D profile survey plots with a scale of 4 meters per inch (Figure 4.1c). A southward transect view was the best direction to draw cave room detail from the printed *Compass* plots.

Notational grain size and sorting of talus slope material was inferred and drawn from studies and information conducted by Sanders et al (2009; 2010) and Luckman (2013). Ancient epikarst height above sea level is interpreted from Mariana Limestone epikarst pits and pinnacles exposed at a roadside exaction on AAFB (Figures 3.29). Pits were drawn ~1m deep, 10 m apart from the cave entrance extending toward the cliff, under the talus slope. Images were drawn to scale and sized to best show details; Transect A-A' was set to 11" by 17" and Transect B-B' was set to 8.5" by 11". Markings were digitized using text and pen tools on *Pixelmator* graphic design software. Final cross sections were saved in JPEG and PDF formats.

Figure 3.28a
Looking ~SE to ground surface above Trinity (Surface station V52).





Figure 3.28b Looking upslope (~NW) to Trinity ground surface. Bag for scale.



Figure 3.29 Roadside excavation in Mariana Limestone (Qtm) epikarst on AAFB. Ladder for scale.

RESULTS

4.1 Map of Jinapsan Cave surface plan and cross sections

A plan of the Jinapsan Cave site (Figure 4.1a) displays the ground surface boulder and vegetation landmarks, cave entrance and underlying cave boundary, fracture traces observed concave, concealed on surface slope, and transects A-A' and B-B'. A cross-section along the A-A' transect (Figure 4.1b) displays calculated thickness of the overlying Mariana limestone bedrock and talus slope. The slope of the line from cave entrance to cave bottom (behind pool), measured from the *Compass* program, is -34.3° . The transect runs from the cave entrance to the Anteroom and top of The Slide, then from Flatman, Big Room entrance, Trinity, and the Pool. From the cave entrance to the highest surface survey point (V52, directly above pool) the slope is $+33.0^\circ$. A cross-section, along transect B-B' (Figure 4.1c), displays the Shakey and Stumpy Rooms and the thickness estimates of the overlying limestone bedrock and talus slope. Observations from 2012 and 2014 surface survey show outcropping ledges, and boulders indicate a thinner talus slope of less than 8 meters above the Shakey and Stumpy Rooms, possibly only a few meters deep. A summary of estimated limestone bedrock and talus layer thicknesses above each data-collection station is presented in Figure 4.1d and Table 4.1. Hypothesize hydrologic pathway for each data-collection station inside the cave is discussed below.

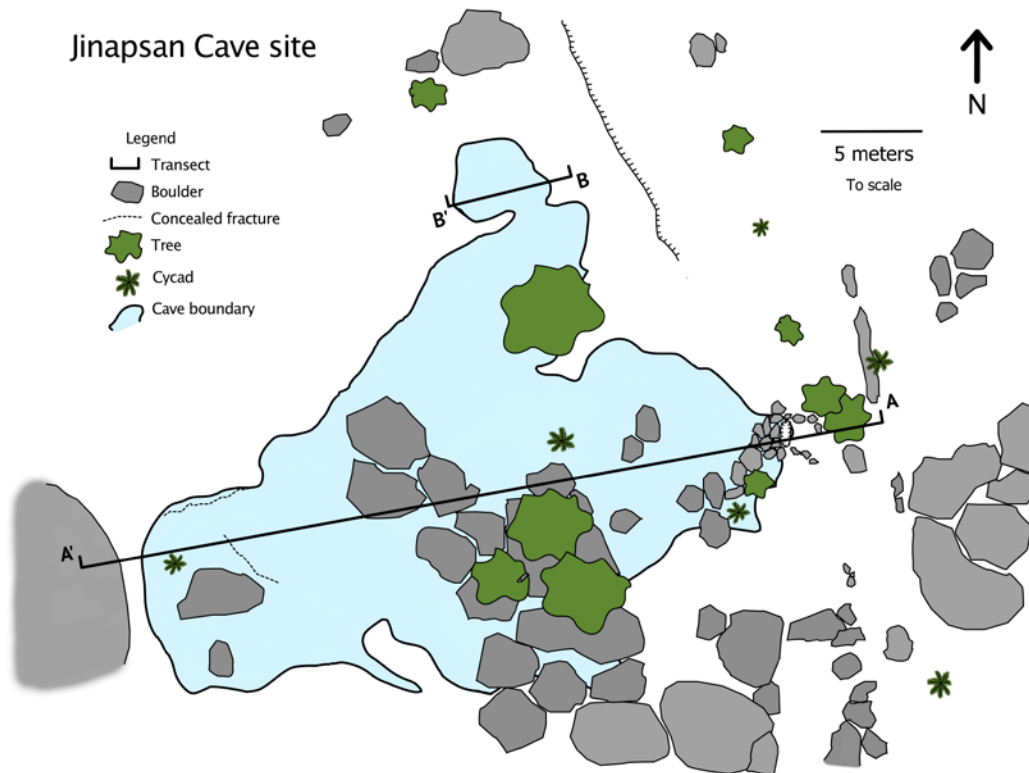


Figure 4.1a Plan of Jinapsan Cave showing ground surface boulder and vegetation landmarks, cave entrance and underlying cave boundary, cave-ceiling fracture traces (concealed on surface slope), and transects of cross-sections A-A' and B-B'. Cross-section A-A' follows an azimuth direction between 260° and 265° (SW)

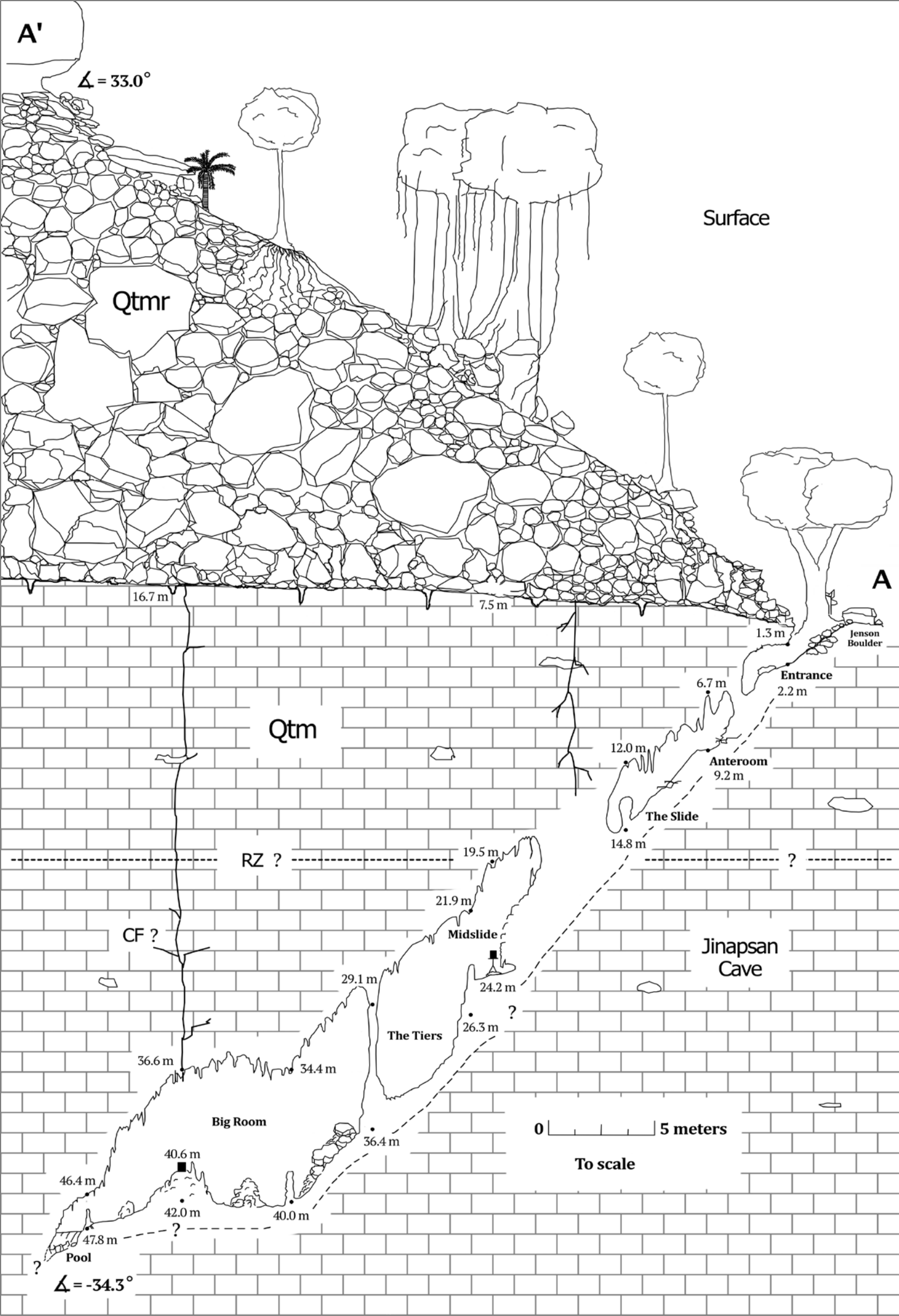


Figure 4.1b Cross section of A-A' transect. Distances are vertical depths from ground surface. Surrounding limestone bedrock is Mariana Limestone and the talus slope is reef facies debris from uplifted Mariana Limestone cliffs. Intersected cave rooms are labeled. Estimated bottom of root zone (RZ) displayed as horizontal dashed line based on root observations on floors of the Anteroom and The Slide. Observed fracture above Trinity station (black square) is displayed, but upward reach is unknown (CF for concealed fracture). Bottom of cave boundary (curving dashed line) is unknown based on extensive amount of flowstone or breakdown debris. Scale of view is 5m. Drawn to scale.

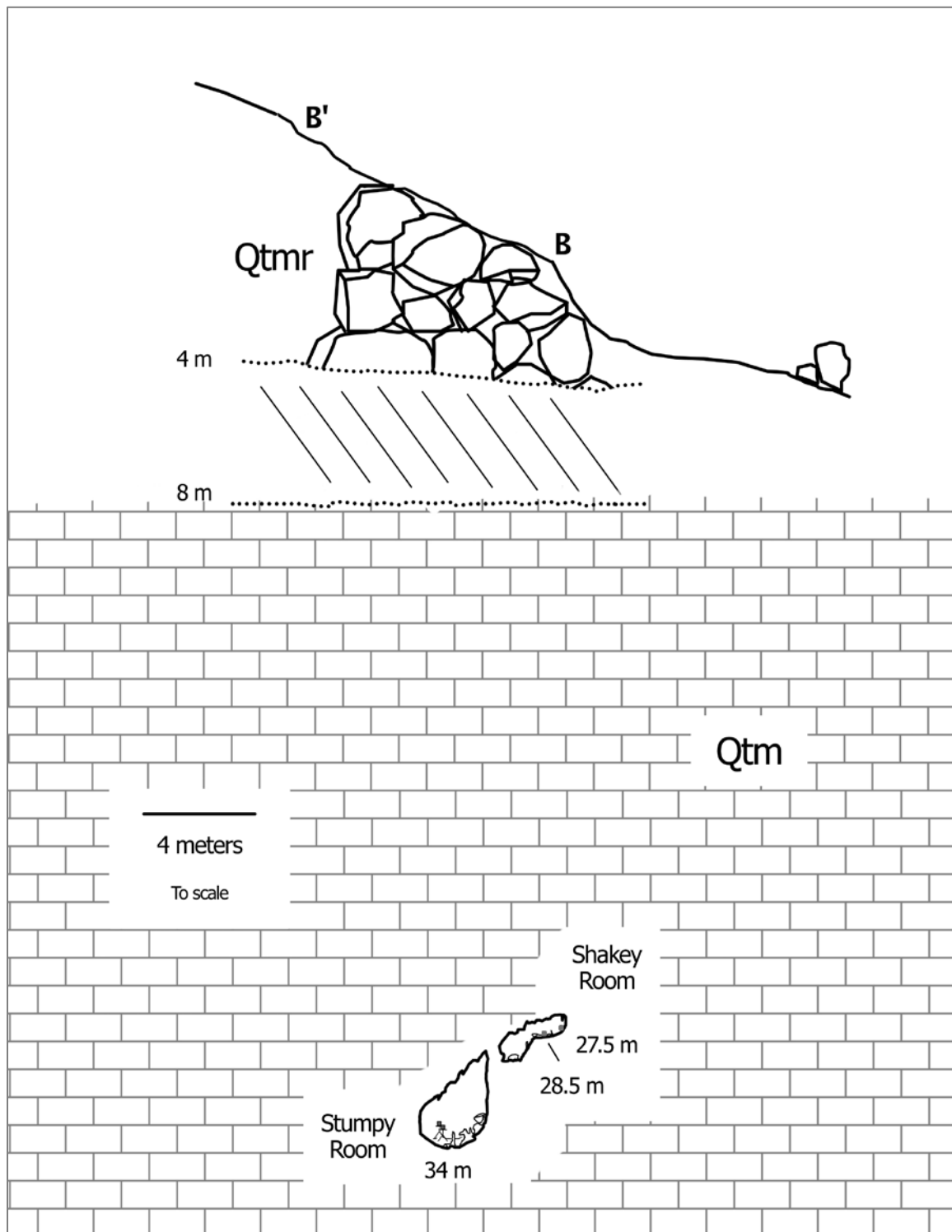


Figure 4.1c Cross section of B-B' transect. Distances are vertical depths from the ground surface. Estimated talus depth, at least 4 m to no more than 8 m, is indicated by between the dotted lines. A 2-m escarpment is downslope from transect B-B'.

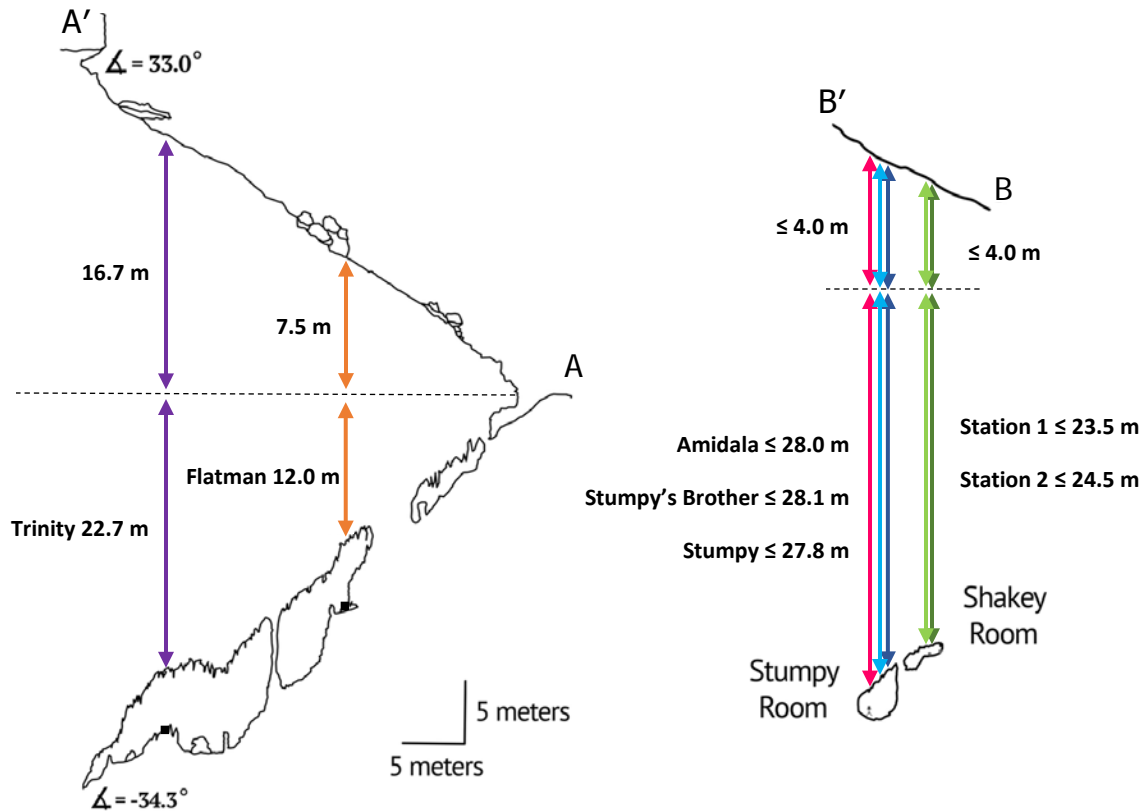


Figure 4.1d Simplified positions of Jinapsan Cave drip stations and estimated talus layer and bedrock layer thicknesses. Dashed line represents estimated epikarst location. Stumpy and Shakey Room overlying bedrock thicknesses are based on the assumption that talus layer is ≤ 4 m. Solid lines are color coded by station: Trinity (purple), Flatman (orange), Station 1 (light green), Station 2 (dark green), Stumpy's Brother (light blue), Stumpy (dark blue), Amidala (pink).

Station Name	Station to stalagmite base (m)	Station to ceiling (m)	Estimated limestone bedrock thickness (m)	Estimated talus layer thickness (m)	Hypothesized Hydrologic Pathway
Trinity	0.75	1.20	22.70	16.7	Fracture
Flatman	0.64	4.04	12.02	7.5	Fracture-Fissure
Station 1	0.17	0.70	23.5 – 19.5	4.0 – 8.0	Fissure
Station 2	0.0, i.e. stalagmite removed	0.81	24.5 – 20.5	4.0 – 8.0	Fissure
Stumpy's Brother	0.35	1.52	28.1 – 24.1	4.0 – 8.0	Fissure
Stumpy	0.48, stalagmite removed	1.68	27.8 – 23.8	4.0 – 8.0	Matrix
Amidala	0.68	0.62	28.0 – 24.0	4.0 – 8.0	Matrix

Table 4.1 Ceiling and floor distances between cave stations, respective estimated limestone bedrock and talus layer thicknesses, and hypothesized hydrologic pathway of each station, which will be discussed in the next section.

4.2 Drip-water Data

Physical parameters and descriptive statistics for each station and the associated drip rates and dripwater flux are summarized in Tables 4.2 and 4.3. Mean drip rates (μ), standard deviation (σ), normalized standard deviation (σ/μ) (i.e. coefficient of variation), minimum, maximum, normalized minimum (minimum/ σ), normalized maximum (maximum/ σ), and range were calculated for each station (number of measurements, N). Number of measurements (drip counts) (N) is the total number of non-suspect and non-spurious monthly data for each station, whether observed, inferred (calculated), or a combination. The cave was not visited in 3 out of the 97 collection months between September 2008 and September 2016.

Entire Record	Trinity	Flatman	Station 1	Station 2	Stumpy's Brother	Stumpy	Amidala
Drip counts (N)	94	94	93	94	86	87	68
Mean (drips/hr) (μ)	2613	244.5	46.9	43.8	41.3	7.7	6.0
Std. deviation (σ)	1052	72.3	35.0	16.7	4.1	4.5	10.3
Relative s.d. (σ/μ)	0.40	0.30	0.75	0.38	0.10	0.58	1.73
Min	1160	103.8	0.03	26.0	33.0	0.15	0.73
Max	5840	366.1	184.6	122.0	50.7	25.7	49.0
Normalized min (min/ σ)	1.1	1.4	0.00084	1.6	8.0	0.033	0.071
Normalized max (max/ σ)	5.6	5.1	5.3	7.3	12.2	5.7	4.7
Range	4680	262.3	184.6	96.0	17.7	25.6	48.2

Table 4.2 Summary for entire record (wet and dry seasons) drip rate descriptive statistics (drips/hour) per station for 8-year record 2008-2016.

Entire Record	Trinity	Flatman	Station 1	Station 2	Stumpy's Brother	Stumpy	Amidala
Dripwater fluxes (N)	92	71	90	83	69	83	68
Mean (mL/day) (μ)	4971	364.4	87.0	75.6	71.5	13.7	11.0
Std. deviation (σ)	2180	110.3	62.4	28.3	7.6	7.3	18.7
Min	2081	139.2	0.11	43.5	57.9	0.32	1.3
Max	13075	532.6	310.2	202.6	88.8	37.1	86.9
Normalized min (min/ σ)	0.95	1.3	0.0017	1.5	7.7	0.044	0.070
Normalized max (max/ σ)	6.0	4.8	5.0	7.2	11.8	5.1	4.6
Range	10994	393.4	310.0	159.1	30.9	36.7	85.6

Table 4.3 Summary for entire record of dripwater flux descriptive statistics (milliliters/day) per station. Flux rates are based on overnight collection of dripwater from each station (1 per month).

Trinity has a total of 94 drip rate counts – 1 is inferred from overnight dripwater weight, and 92 dripwater fluxes – 64 are observed, 28 are inferred from drip counts, and 2 are suspect for error. Flatman has 94 observed drip rate counts and 94 fluxes – 66 are observed, 5 are inferred from drip counts (N = 71), 14 are suspect and 9 are spurious for error. Station 1 has 93 drip rate counts because 1 drip count was not taken. Station 1 has 93 fluxes – 84 are observed, 6 are inferred from drip counts (N = 90), and 3 are suspect for error. Station 2 has 94 observed drip rates, and 94 dripwater fluxes – 79 are observed, 4 are inferred (N = 83), 6 are suspect and 5 are spurious for error. Stumpy's Brother has 86 drip counts – 85 are observed and 1 is inferred from overnight dripwater weight. Stumpy's Brother has 69 fluxes – 63 are observed, 6 are inferred from drip counts (N = 69), 13 are suspect and 4 are spurious for error. Stumpy has 87 drip counts – 15 are observed, 72 are inferred, and there is 1 month without a drip count. Stumpy has 88 fluxes – 82 are observed, 1 is inferred from drip counts (N = 83), 4 are suspect and 1 is spurious for error. Amidala has 68 drip counts – 63 are observed, 5 are inferred, and there are 2 visits without a drip count. Amidala has 68 fluxes – 67 are observed, 1 is inferred, and the same 2 visits without drip counts also do not have overnight dripwater weights.

Mean drip rates and dripwater flux values from Tables 4.2 and 4.3 are plotted on a \log_{10} scale in Figures 4.2 and 4.3. Mean drip rates in this study spanned three orders of magnitude (10^1 to 10^3), similar to Sheffer et al. (2010). For this study, stations were also categorized into hypothesized hydrologic pathways based on order of magnitude: (A) fracture, (B) fracture-fissure, (C) fissure, or (D) matrix, following the model in Sheffer et al. (2010). Trinity, with the fastest drip rate and dripwater magnitude of 10^3 is tentatively assigned to fracture flow (A). The next fastest station is Flatman, with a drip rate and dripwater flux magnitude of 10^2 , is assigned to fracture-fissure flow (B). Station 1, Station 2, and Stumpy's Brother are assigned to fissure flow (C), with orders of magnitude between 10^2 and 10^1 . Stumpy and Amidala stations are assigned to matrix flow (D), and have the lowest drip rate and dripwater flux magnitude of $\sim 10^1$.

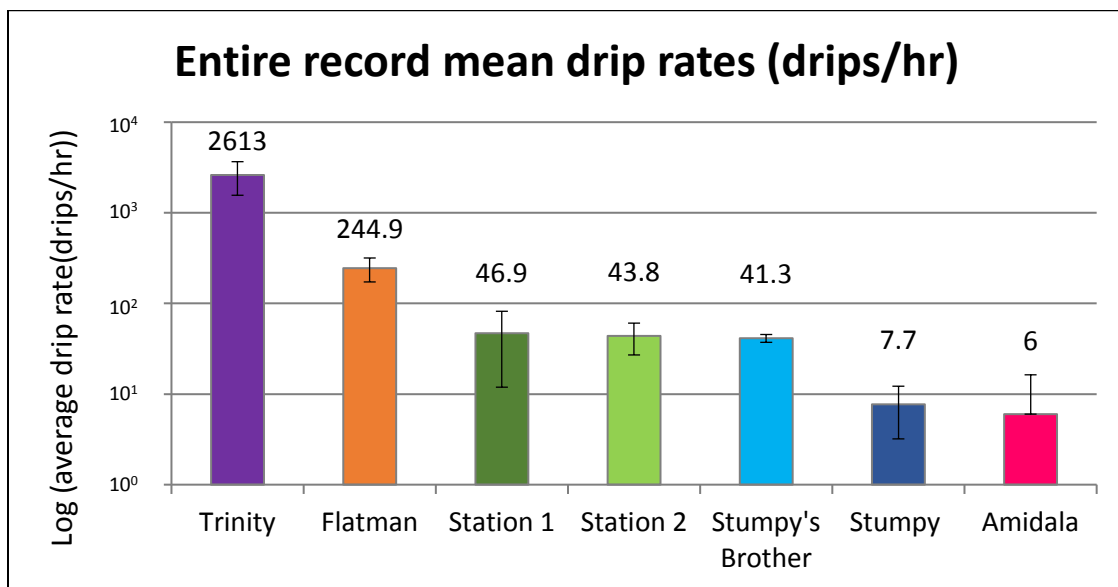


Figure 4.2 Logs of entire record mean drip rate (drips/hr) for each station, which are assigned by orders of magnitude into hypothesized hydrological pathway: fracture, fracture-fissure, fissure, and matrix, which will be discussed in the next section.

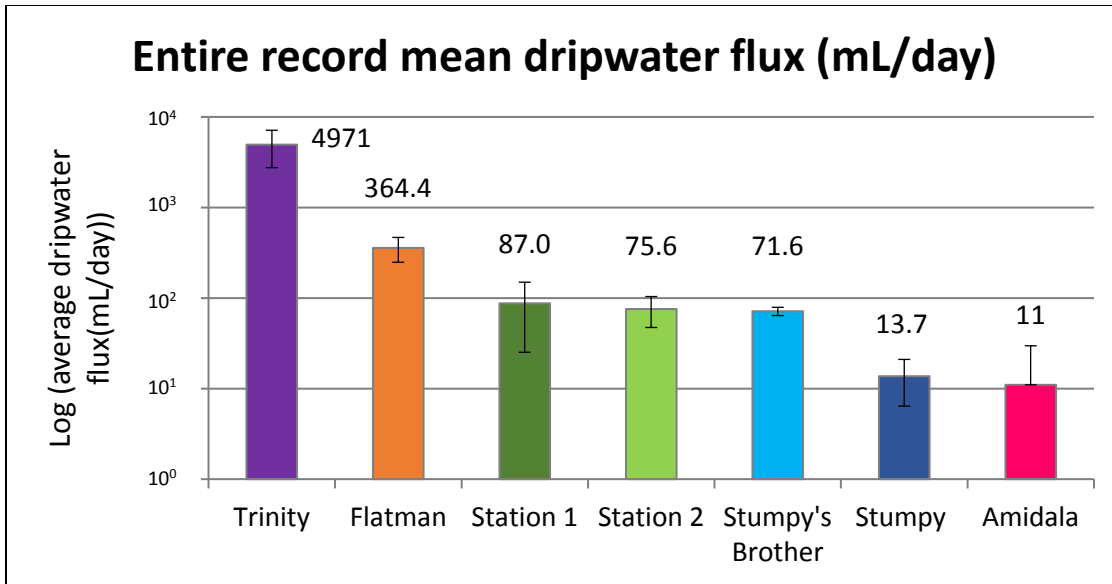


Figure 4.3 Logs of entire record mean dripwater flux (mL/day) for each station, which are assigned by orders of magnitude into hypothesized hydrological pathway: fracture, fracture-fissure, fissure, and matrix, which will be discussed in the next section.

Descriptive statistics (population size, N ; mean, μ ; standard deviation, σ ; normalized standard deviation, σ/μ , i.e. coefficient of variation; minimum, maximum, normalized minimum and maximum, and range) of each station's wet season and dry season drip rate (drips/hour) data are presented in Tables 4.4 and 4.5. Mean values for both wet and dry seasons follow the order of magnitude pattern as respective total drip rate datasets: 10^3 (Trinity), 10^2 (Flatman), 10^1 (Station 1, Station 2, and Stumpy's Brother), and 10^0 (Stumpy and Amidala).

Wet Season	Trinity	Flatman	Station 1	Station 2	Stumpy's Brother	Stumpy	Amidala
Drip counts (N)	48	48	48	48	45	44	33
Mean (drips/hr) (μ)	2647	248.9	55.2	45.3	41.3	7.5	3.8
Std. deviation (σ)	1299	84.9	37.8	19.9	4.5	3.8	4.6
Relative s.d. (σ/μ)	0.49	0.34	0.69	0.44	0.11	0.50	1.20
Min	1160	103.8	0.03	26.0	33.0	0.35	0.73
Max	5840	366.1	184.6	122.0	50.7	13.8	25.0
Normalized min (min/ σ)	0.89	1.2	0.00078	1.3	7.4	0.093	0.16
Normalized max (max/ σ)	4.5	4.3	4.9	6.1	11.3	3.7	5.5
Range	4680	262.3	184.6	96.0	17.7	13.4	24.3

Table 4.4 Summary of wet season drip rate descriptive statistics per station.

Dry Season	Trinity	Flatman	Station 1	Station 2	Stumpy's Brother	Stumpy	Amidala
Drip counts (N)	46	46	45	46	41	43	35
Mean (drips/hr) (μ)	2577	240.7	38.1	42.3	41.3	7.8	8.0
Std. deviation (σ)	722	56.8	29.7	12.7	3.8	5.0	13.5
Relative s.d (σ/μ)	0.28	0.24	0.78	0.30	0.09	0.64	1.68
Min	1210	140.3	0.21	26.7	33.5	0.15	0.84
Max	4630	327.3	113.7	82.8	48.3	25.7	49.0
Normalized min (min/ σ)	1.7	2.5	0.0070	2.1	8.9	0.029	0.063
Normalized max (max/ σ)	6.4	5.8	3.8	6.5	12.8	5.1	3.6
Range	3420	187.0	113.5	56.1	14.8	25.6	48.1

Table 4.5 Summary of dry season drip rate descriptive statistics per station.

4.3 Drip rate magnitude and variability

In this section, I show the monthly time series for the drip rates from September 2008 through September 2016 for each of the 7 collection stations (Figures 4.4, 4.8, 4.10, 4.12, 4.14, 4.16, and 4.18). The results for the seven stations are described in order of decreasing drip rates (Figure 4.2, left to right). The symbols and notations for the graphs are described here, for Trinity, the first of the series. Each graph shows drip rates (drips/hour). Solid circles on the plots are measured values. See Figure 4.4 For Trinity station. Hollow circles are inferred values – Equation 5 for inferred drip rates, and Equation 6 for inferred dripwater fluxes. Events of interest are labeled with a capital letter and discussed in the next section. Data points regarded as irregular are circled and labeled according to the following categories: 1) suspect – might be true, but uncertain of error or, 2) spurious – based on false assumption, wrong. Missing data (i.e. disrupted collection such as fallen drip bottle) are marked. No cave visits (i.e. missed cave trips in February 2010, July 2014, and June 2016) are marked with grey hollow circles. All time-series reflect that during a Day 2 cave visit on August 13, 2014, a ~5.0 magnitude earthquake occurred NW of Ritidian Beach, causing data collection to be postponed until August 18, 2014, 6 days post-earthquake.

Daily rainfall (inches), obtained from an AAFB rain gauge installed at the flight line runway tower are shown as blue bars on the top of each time series. Daily rainfall of 4 inches and greater is associated with storm passages or large rainfall events. Names of storms that passed within $\pm 3^\circ$ latitude of Guam are included on station graphs. A summary of storms is presented in Table 4.6 and Figure 4.5 (JTWC 2009, 2011, 2012, 2013, 2014, Hong Kong Observatory 2016). One non-tropical cyclone rainfall event, labeled Non-TC, is included in each time series.

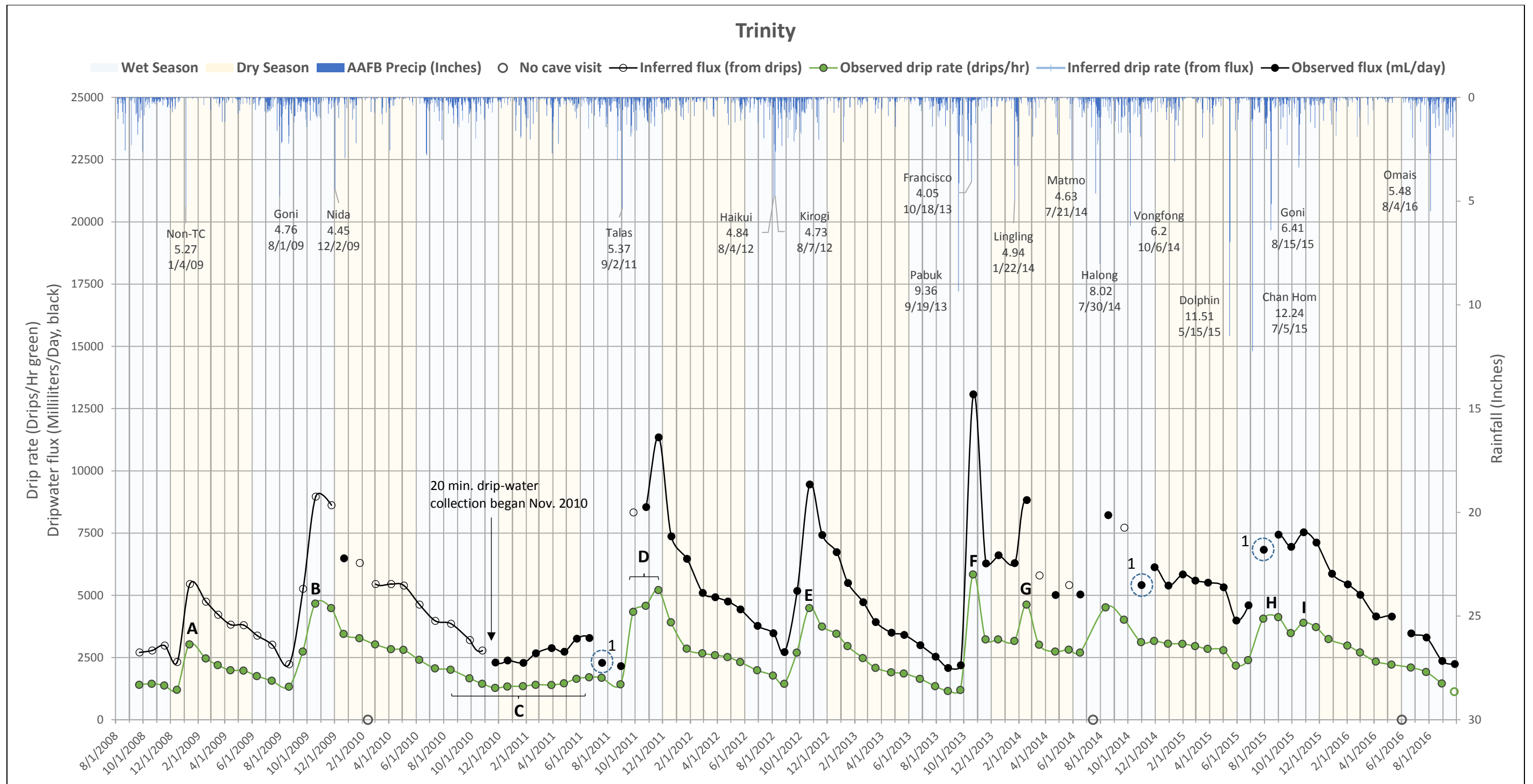


Figure 4.4 Trinity drip rate (drips per hour, purple) and dripwater flux (millimeters per day, black) versus AAFB rainfall (inches). Wet (Jun-Nov) and dry (Dec-May) seasons indicated with pale blue and pale yellow shading, respectively. Observed data is plotted as solid circles. Inferred data is plotted as hollow circles. Events of interest are marked by a letter and will be discussed in the next section. Data regarded as suspect (1) and spurious (2) were plotted and circled. No cave visits are marked with grey hollow circles.

Storm	Name	Duration	Est Max Sfc Winds (kts)	Guam Date	Rainfall (Inch)	Rain band/ Eye Passage	Developed	Passed Direction
TS 08W	Goni	28 JUL – 08 AUG 2009	45	01 AUG	4.76	Rain band	NW	-
ST 26W	Nida	22 NOV - 03 DEC 2009	150	02 DEC	4.45	Eye	SE	S
TS 15W	Talas	25 AUG - 04 SEP 2011	55	02 SEP	5.37	Rain band	NW	-
Ty 12W	Haikui	02 - 08 AUG 2012	65	04 AUG	4.84	Rain band	N	NW
TS 13W	Kirogi	02 – 09 AUG 2012	45	07 AUG	4.73	Rain band	N	N
Ty 19W	Pabuk	18 - 26 SEP 2013	90	19 SEP	9.36	Rain band	E	N – NW
ST 26W	Francisco	15 - 25 OCT 2013	140	18 OCT	4.05	Eye	E	SW – NW
TD 01W	Lingling	18 - 19 JAN 2014	30	22 JAN	4.94	Rain band	SW	-
Ty 10W	Matmo	17 - 23 JUL 2014	85	21 JUL	4.63	Rain band	SW	-
ST 11W	Halong	28 JUL - 10 AUG 2014	140	30 JUL	8.02	Eye	E	N – NW
ST 19W	Vongfong	01 – 14 OCT 2014	155	6 OCT	6.2	Eye	SE	N – NW
ST 07W	Dolphin	06 – 20 MAY 2015	100	15 MAY	11.51	Eye	SE	N – NW
Ty 10W	Chan Hom	29 JUN – 13 JUL 2015	90	5 JUL	12.24	Eye	E	N – NW
Ty 16W	Goni	13 – 25 AUG 2015	100	15 AUG	6.41	Eye	E	N – NW
TS 07W	Omais	02 – 09 AUG 2016	60	4 AUG	5.48	Rain band	N	N

Table 4.6 Summary of storms on time series graphs. Est Max Sfc Winds = Estimated Max Surface Winds.

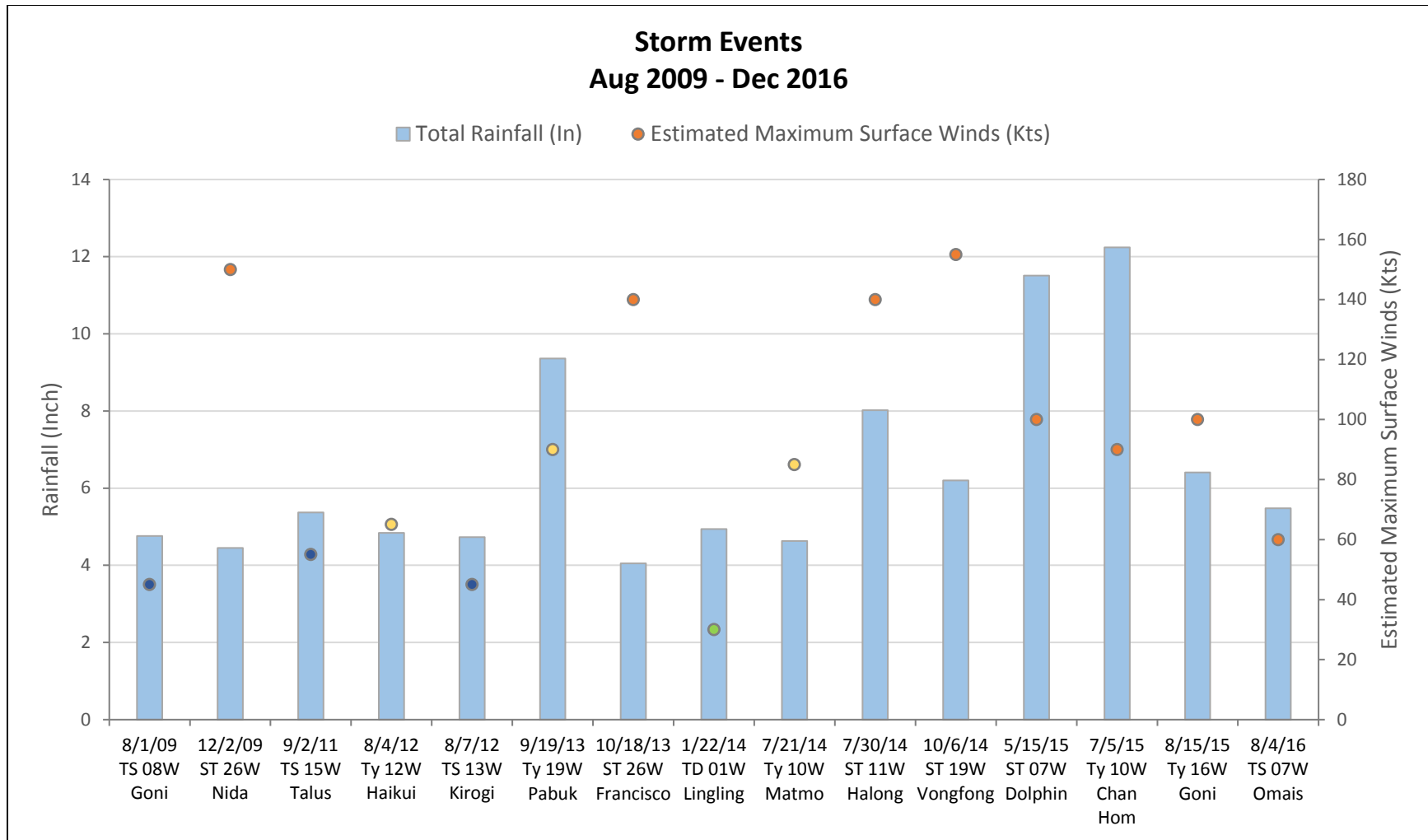


Figure 4.5 Total rainfall (inches) and respective estimated maximum surface winds (knots) for storms that passed over Guam between September 2008 through September 2016. Tropical Cyclones are first issued in alphanumeric codes by chronological appearance (#W for Western North Pacific Ocean) then designated a general name (i.e. Goni). Estimated maximum surface winds (knots) are categorized by strength: green – tropical depression, blue – tropical storm, yellow – typhoon, and orange – super typhoon.

For a preliminary assessment of drip rate variability, I plotted the percent of drip rates within $\pm 1 \sigma$ for each station (Figure 4.6). Percentage of entire record drip rate data (8 years; 2008-2016) within $\pm 1 \sigma$: Trinity is ~63%, Flatman is ~54%, Station 1 is ~66%, Station 2 is ~79%, Stumpy's Brother is ~62%, Stumpy is ~76%, and Amidala is the largest at ~91%. And to test for variability for each time series, I have plotted histograms to show the variability of the drip rate: for the entire record, for the wet season, and for the dry season record at intervals of 0.5σ (Figures 4.7, 4.9, 4.11, 4.13, 4.15, 4.17, and 4.19).

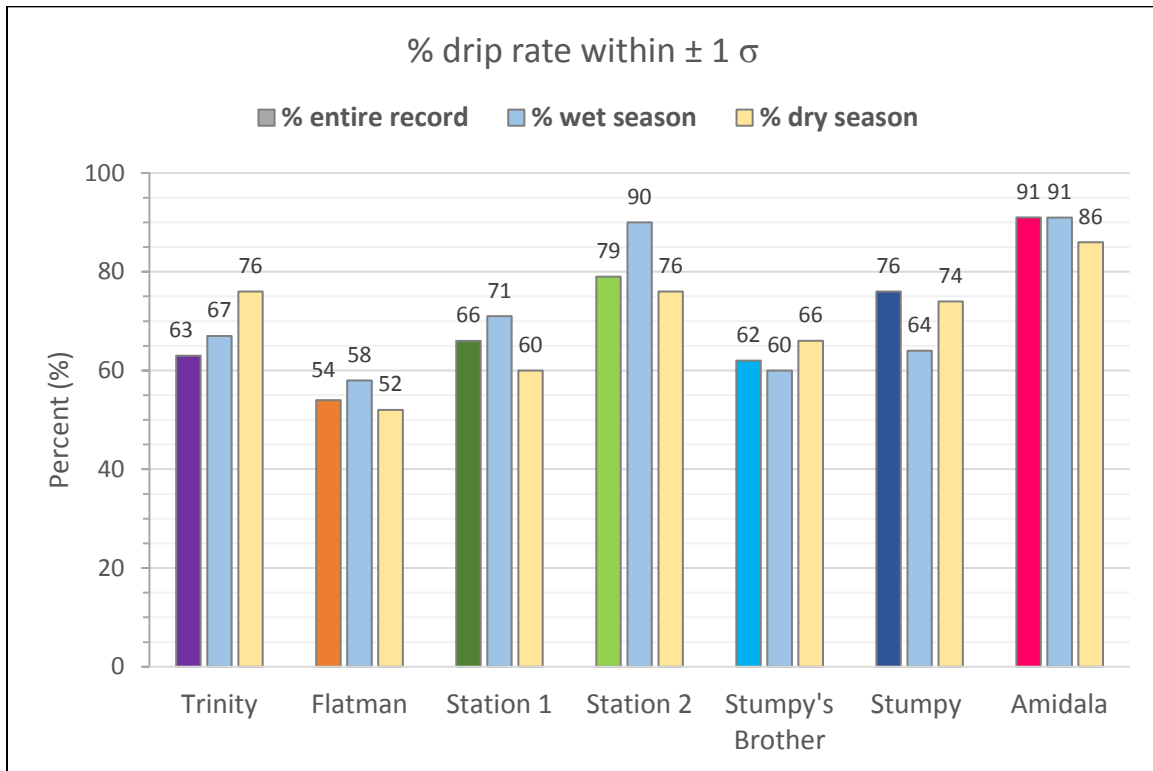


Figure 4.6 Percent of drip rate for entire record (colored by station), wet season (light blue), and dry season (light yellow) found within ± 1 standard deviation (σ) from each station's entire record drip rate mean, wet season mean, and dry season mean for frequency histograms with $\pm 0.5 \sigma$ intervals.

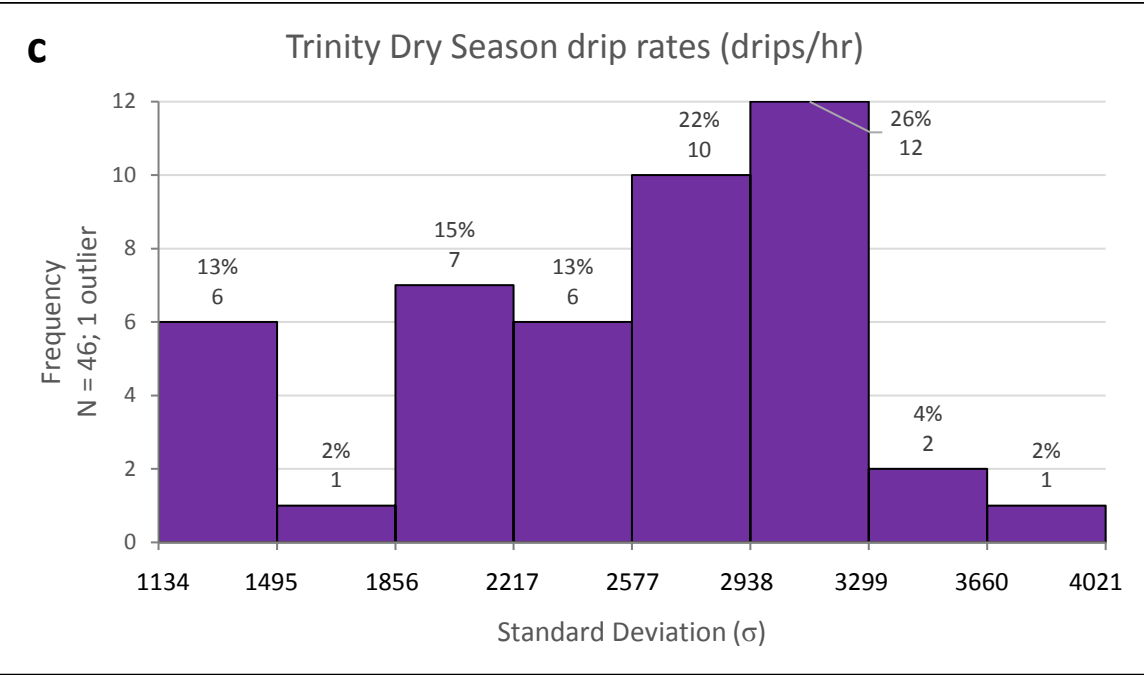
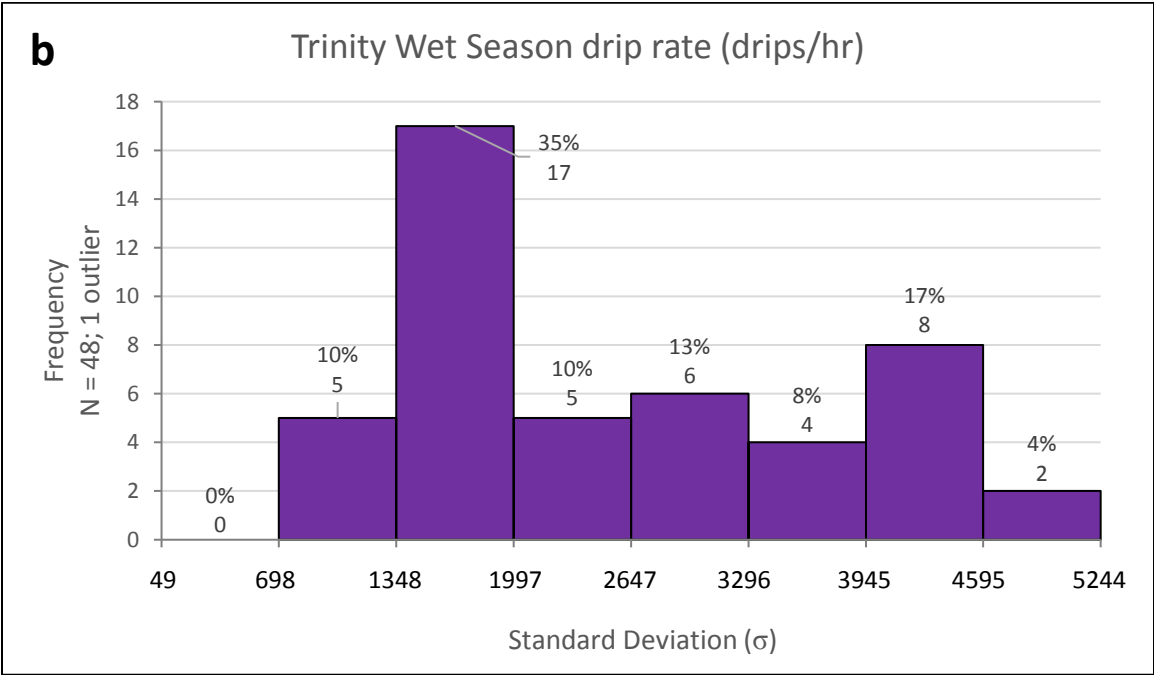
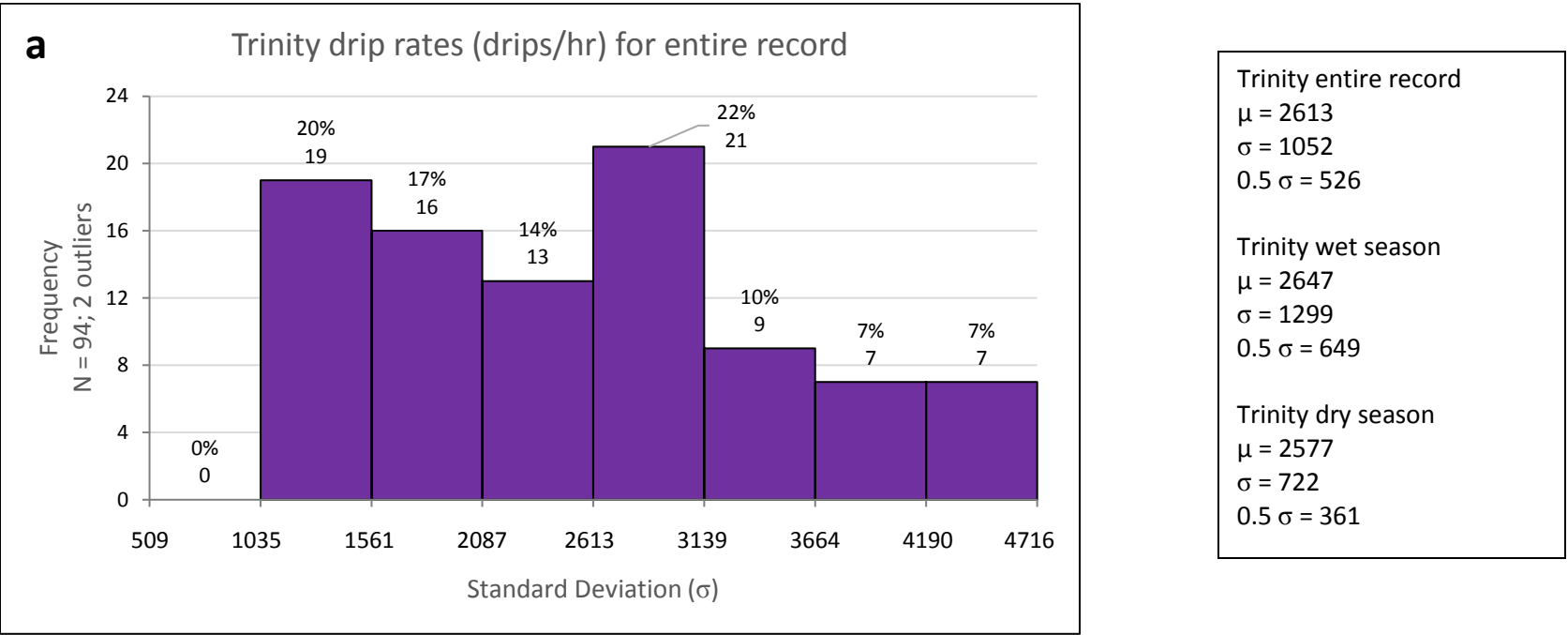


Figure 4.7 Frequency histograms of Trinity's a) drip rates for entire record, b) wet season drip rates, and c) dry season drip rates within $\pm 2 \sigma$ from respective means at $\pm 0.5 \sigma$ intervals.

4.3.1 Trinity

This station's stalactite has an average entire record drip rate of 2,613 drips per hour with a standard deviation of 1,052 drips per hour (Table 4.2), and dripwater flux of 4.971 milliliters per day with a standard deviation of 2,180 milliliters per day (Table 4.3). Average drip volume (mL/drip) is 0.079 (Appendix B). Of 94 drip rates and 91 dripwater flux values respectively, the fastest drip and discharge rates were 5,840 drips/hr and 13,075 mL/day in October 2013, and slowest drip and discharge rates were 1,160 drips/hr and 2,081 mL/day respectively, in August 2013. Drip rates peak near the ends of the wet seasons, and gradually decrease through the dry seasons. Another indicator of a pattern of strong input response is by a drip rate peak following between ~8 to 81 days after rainfall input (Table 4.7). A gradual decrease in discharge rate was also observed through both wet and dry cycles in 2009 and 2010.

Data suspect for error (footnoted 1) occur in July 2011, October 2014, and July 2015 (Figure 4.4). There is 1 inferred drip rate, on September 2016. Inferred dripwater fluxes from overnight dripwater bottle overflow ($n = 24$) are September 2008 to November 2009 and January to October 2010. From November 2010 to the end of the dataset, protocol was changed to collect dripwater volume for 20 minutes on Day 2 at this site. Inferred dripwater fluxes calculated from drip rate ($n = 4$) are September 2011 and March, May, and September 2014.

In Trinity's time series, events of interest are listed in Table 4.7. Event "A" is the first drip rate increase (peak response), 8 days after rainfall from a non-tropical cyclone event in January 2009. Event "B" in October 2009 is drip rate increase (peak response) 79 days after tropical storm Goni. Event "C" is a flatline in drip rate (trough; unresponsive) between June 2010 and June 2011, the driest (least rainfall events) of the wet-dry season cycles in the dataset (Lander, personal communication, 2017). Event "D" in November 2011 is a drip rate increase (peak response) 80 days post tropical storm Talas (Sept. 2011). Event "E" is another drip rate increase 79 and 76 days after 2 storms, typhoon Haikui and tropical storm Kirogi (Aug. 2012) respectively. Event "F" is another peak, 32 days after typhoon Pabuk (Sept. 2013). In the same wet-dry cycle, Event "G," the peak response, occurred 27 days after tropical depression Lingling, in January 2014. Event "H" was 75 days after super typhoon Dolphin and 24 days after typhoon Chan Hom. Event "I" was 73 days after typhoon Goni.

The frequency distributions of the entire record for Trinity is skewed downward to the right (Figures 4.7a). The highest frequency (22%) is between the mean, 0 and 0.5σ (2613 to 3139 drips/hr). The second highest begins between -1.5 and 1σ and gradually decreases to $+2 \sigma$ (4716 drips/hr) above the mean. The wet season histogram (Figure 4.7b) shows one-third of the drip rates (35%) at its highest frequency, between -1 and -0.5σ (1348 to 1997 drips/hr), and is also skewed downward to the right. The highest frequency in the dry season histogram (Figure 4.7c) is 26%, between 0.5 and 1σ (2938 to 3299 drips/hr) and is slightly skewed downward in the opposite direction, to -2σ (1134 drips/hr). For the entire record drip rate, and more often the wet season drip rates, Trinity drips at slower rates, since more than half of total frequencies are below each respective mean, 51% (entire) and 55% (wet). The dry season is the opposite (54%), and drips faster.

Rainfall Event	Trinity	Flatman		Station 1		Station 2	Stumpy's Brother		Stumpy		Amidala
Non-TC 1/4/09	A ; 8 1/12/09	A ; 8 1/12/09		A ; 72 3/16/09		-	N/A		A ; 129 5/13/09		N/A
TS Goni 8/1/09	B ; 79 10/19/09	B ; 20 8/21/09		B ; 52 9/22/09		A ; 52 9/22/09	A ; 52 9/22/09		B ; 52 9/22/09		-
ST Nida 12/2/09	-	-		C ; 20 12/22/09		-	-		-		-
Unnamed 6/1/10-6/1/11	C unresponsive 8/16/10 – 6/20/11	C 11/23/10	D 5/23/11	D 11/22/10 – 6/20/11		B 8/16/10 – 1/24/11	B 11/10 – 5/11	C 8/29/11	C 8/17/2010	D 2/22/11	A 6/21/11
TS Talas 9/2/11	D ; 80 9/27 – 11/21/11	E ; 80 11/21/11		E ; 25 9/26/11	F ; 108 12/19/11	C ; 25 9/27/11	D ; 80 11/22/11		E ; 25 9/27/11	F ; 109 12/20/11	B ; 109 12/20/11
Ty Haikui 8/4/12	E ; 79 10/22/12	F ; 79 10/22 – 11/20/12		G ; 24 8/28/12		D ; 79 10/23/12	E ; 108 11/20/12		G ; 24 8/28/12		C ; 140 12/22/12
TS Kirogi 8/7/12	E ; 76 10/22/12	F ; 76 10/22 – 11/20/12		G ; 21 8/28/12		D ; 76 10/23/12	E ; 105 11/20/12		G ; 21 8/28/12		C ; 137 12/22/12
Ty Pabuk 9/19/13	F ; 32 10/21/13	G ; 32 10/21/13		H ; 32 10/21/13		-	F ; 32 10/21/13		H ; 32 10/21/13		-
ST Francisco 10/18/13	-	-		-		E ; 32 11/19/13	-		-		-
TD Lingling 1/22/14	G ; 27 2/18/14	H ; 54 3/17/14		I ; 27 2/18/14		F ; 27 2/18/14	-		I ; 55 3/18/14		-
Ty Matmo 7/21/14	-	-		-		-	-		-		-
ST Halong 7/30/14	-	-		J ; 24 10/30/14		-	-		-		-
ST Vongfong 10/6/14	-	I ; 53 11/28/14		K ; 116 1/30/15		G ; 106 1/30/15	G ; 116 1/30/15		J ; 207 5/1/15		-
ST Dolphin 5/15/15	H ; 75 7/29 – 8/30/15	J ; 14 5/29/15		L ; 14 5/29/15		H ; 15 5/29/15	H ; 14 5/29/15		-		N/A
Ty Chan Hom 7/5/15	H ; 24 7/29 – 8/30/15	K ; 142 11/24/15		M ; 24 7/29/15		-	I ; 24 7/29/15		K ; 25 7/30/15		N/A
Ty Goni 8/15/15	I ; 73 10/27/15	K ; 101 11/24/15		N ; 44 9/28/15	O ; 128 12/21/15	I ; 44 9/28/15	J ; 101 11/24/15		-		N/A
TS Omais 8/4/16	-	-		-		-	-		-		N/A

Table 4.7 Summary of days between drip response and rainfall events for all stations. Dashes indicate no significant drip rate response. Stumpy's Brother and Amidala did not begin drip counting observations prior to May 2010. Amidala's drip rate measurements ended April 2015.

Trinity station is 40.6 m from the surface (Figure 4.1b), the deepest of the 7 stations. The estimated thicknesses of limestone bedrock and talus layers are 22.7 m and 16.7 m respectively (Table 4.1 and Figures 4.1d). The ground surface, at the end of transect A-A', is coarse, boulder-size talus debris, with one very large boulder upslope (Figures 3.28a, b). This area is also directly upslope from the boulder patch above the Flatman station. Limestone forest trees (*Cycas sp.*, *Neisosperma sp.*, *Ochrosia sp.*, and *Aglaia sp.*) are nearby, however the area is devoid of shade from tree canopy.

4.3.2 Flatman

Flatman's average drip rate (Table 4.2) is 244.9 drips/hr with a standard deviation of 72.3. Its average dripwater flux is 364.4 milliliters/day with a standard deviation of 110.3 (Table 4.3). Average drip size is 0.063 milliliters per drip. Of 94 drip rate data values, the fastest drip rate (drips/hr) was 366.1 and the slowest drip rate was 103.8, observed in August 2009 and August 2013, respectively. Of 71 dripwater flux values, the most drip water collected overnight was 532.6 mL/day in August 2009, and the least, 139.2 mL/day, in August 2013.

Dates of data determined to be suspect for error (labeled '1') (Figure 4.8) are July 2010, May 2011, September 2011, October 2012, March and October 2013, and March 2014. Dates of spurious data (labeled '2') are November to December 2009, January and June 2010, June 2011, and November 2012. One missing data point is on August 2014, when an earthquake during the trip caused the team to abandon Day 1 protocol. The weighing scale was left behind in the cave and final drip-water weight was not able to be recorded. Dates of no data are in February 2010 and July 2014, since cave visit did not occur. Flatman's drip rate is the second fastest, through an order of magnitude slower than Trinity's. It peaks in the mid- to late- wet season, and drips rapidly after the onset of the dry season.

Events of interest are listed in Table 4.7. Event A is a drip rate increase (response) 8 days after the non-tropical cyclone rainfall event in January 2009. Event B is a drip rate increase (peak response) 20 days after Goni (Aug. 2009). Event C and D are drip rate responses during the driest wet-dry season, June 2010 through June 2011. Event E is a drip rate increase 80 after Talas. Event F is another drip rate peak increase, 79 and 76 days after Haikui and Kirogi. Event G is another increase response, 32 days after Pabuk. In the same wet-dry season, Event H occurred 54 days after Lingling. Event I is a drip rate increase (response) of this dataset, 53 days after Vongfong. Event J occurred 14 days after super typhoon Dolphin. Event K occurred 142 days after Chan Hom and 101 days after Goni.

Flatman's full-record histogram (Figures 4.9a) is slightly skewed to the left. The largest frequency (20%) is 1 to 1.5 σ above the mean, between 317 and 353 drips/hr ($\mu = 245$ drips/hr). A gradual decrease is seen to -2, with an interruption between -1.5 to 1 σ (136 to 173 drips/hr). Bimodality is distinct in the wet season histogram (Figure 4.9b), with 42% and 31% of the drip rate closer to the extremes, between 291 and 334 drips/hr (0.5 to 1 σ) and 122 to 164 drips/hr (-1.5 to -1 σ), respectively ($\mu = 249$ drips/hr). Flatman's dry season histogram's (Figure 4.9c) highest frequency is 22%, between 1 and 1.5 σ (298 to 326 drips/hr) above the mean, 241 drips/hr. Its gradually decreases to -2 σ , with a pattern disruption between 0.5 and 1 σ (frequency = 7%).

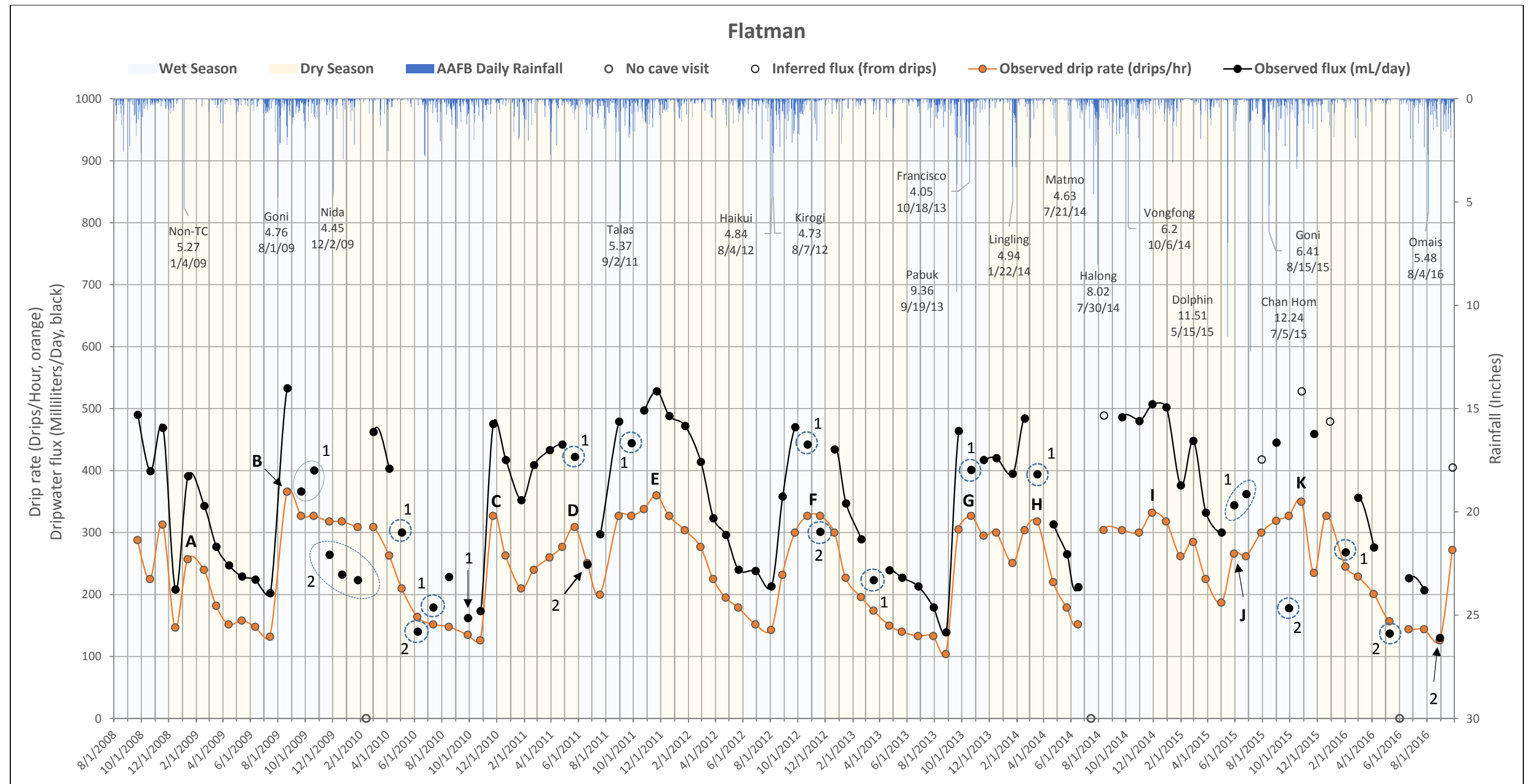
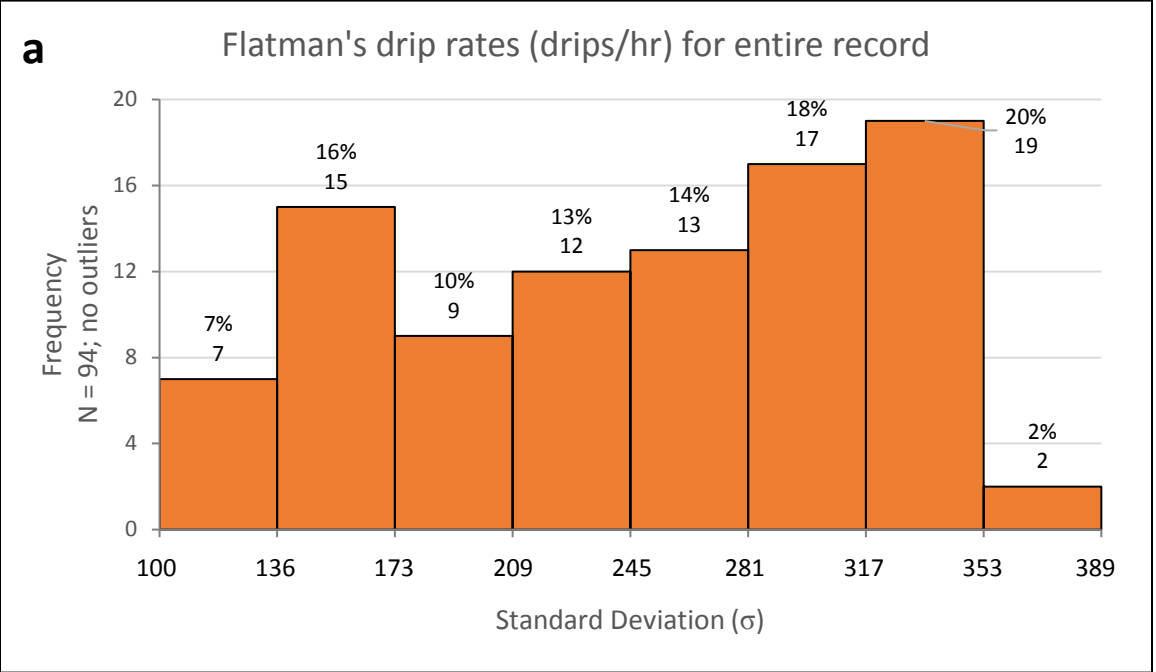


Figure 4.8 Flatman drip rate (drips per hour, orange) and dripwater flux (milliliters per day, black) versus AAFB rainfall (inches). Wet (Jun-Nov) and dry (Dec-May) seasons indicated with pale blue and pale yellow shading, respectively. Observed data is plotted as solid circles. Inferred data is plotted as hollow circles. Events of interest are marked by a letter and will be discussed in the next section. Data regarded as suspect (1) and spurious (2) were also plotted and circled. No cave visits are marked with grey hollow circles.



Flatman entire record

$\mu = 245$

$\sigma = 72.3$

$0.5 \sigma = 36.1$

Flatman wet season

$\mu = 249$

$\sigma = 84.9$

$0.5 \sigma = 42.5$

Flatman dry season

$\mu = 240.7$

$\sigma = 56.8$

$0.5 \sigma = 28.4$

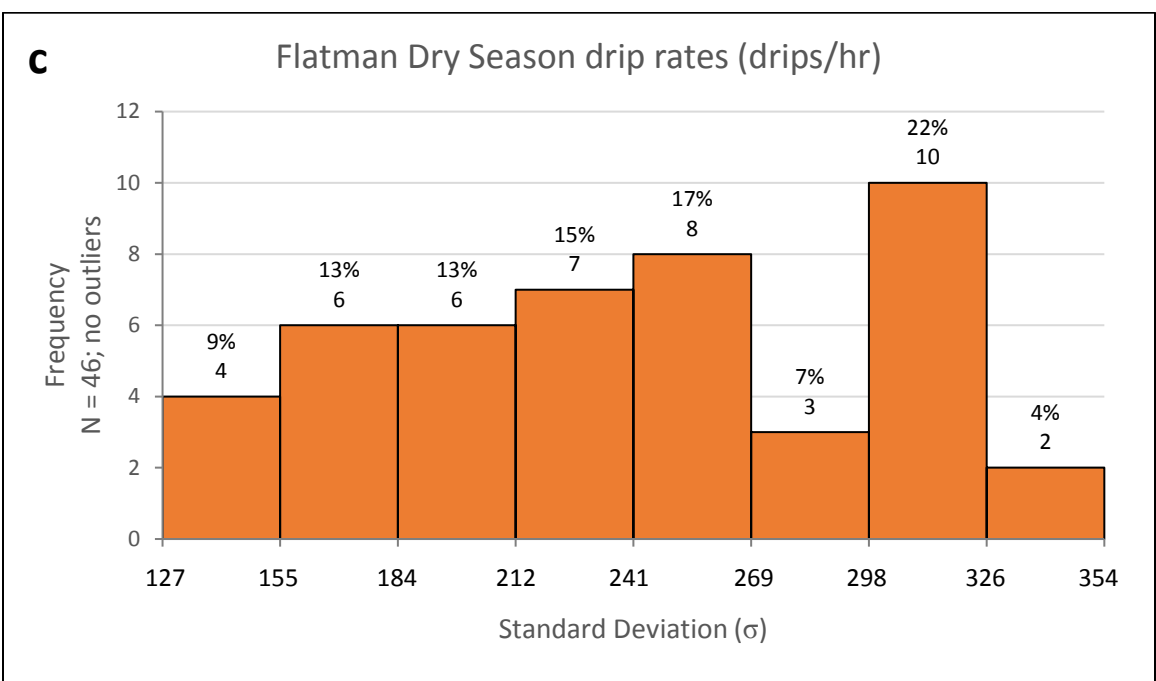
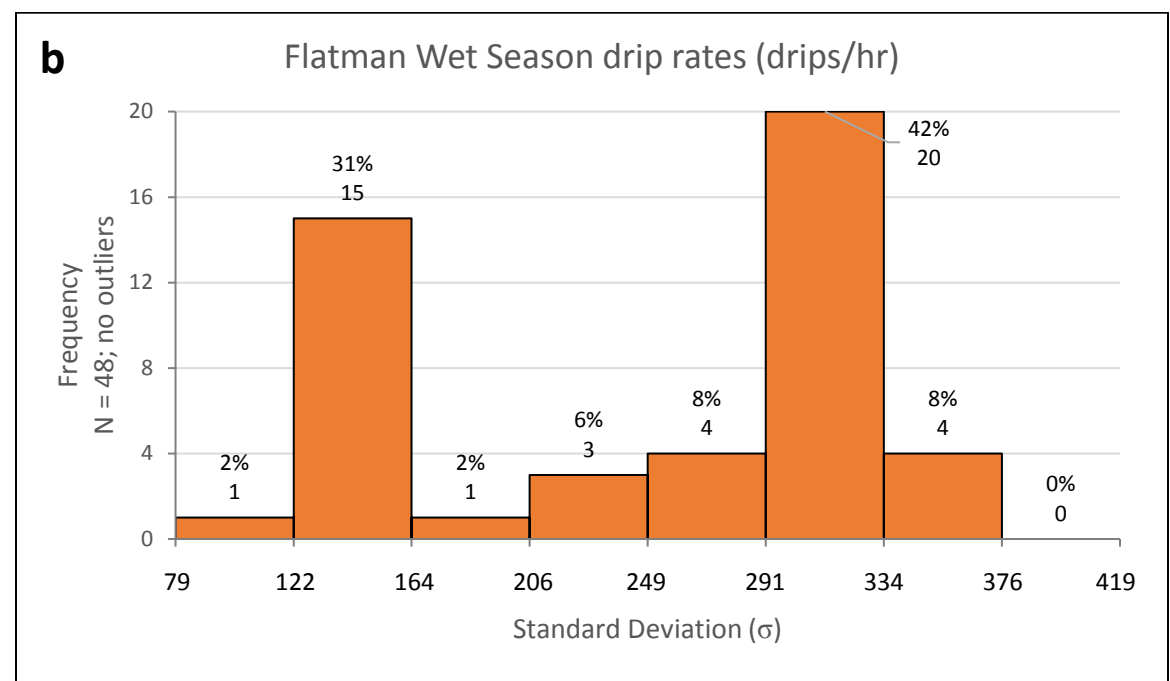


Figure 4.9 Frequency histograms of Flatman's a) drip rates for entire record, b) wet season drip rates, and c) dry season drip rates $\pm 2 \sigma$ from respective means at $\pm 0.5 \sigma$ intervals.

Flatman's stalactite and stalagmite base below the ground surface is 19.5 m and 24.2 m, respectively (Figure 4.1b). The station is 23.6 m below the ground surface. The limestone bedrock has an estimate thickness of 12 m, and the overlying talus an estimate thickness of 7.5 m (Table 4.1 and Figure 4.1d). The ground surface directly above the Flatman stalactite is a 'staircase' feature of cemented boulders (~1 to 2 m each in height). This 'staircase' is part of a ~12 x 12-m patch of large angular and subangular boulders (the largest ~4m high). Subaerial and aerial roots anchor a cluster of 3-4 banyan trees (*Ficus prolixa*) atop the largest boulders.

4.3.3 Station 1

This station has an average drip rate of 46.9 drips per hour with a standard deviation of 35.0 drips per hour (Table 4.2) for its entire record. The average entire record dripwater flux is 87.0 milliliters per day with a standard deviation of 62.4.2 (Table 4.3). Average drip volume is 0.083 milliliters per drip. Of 93 drip-rate measurements, the fastest was 184.6 drips/hr in September 2011, observed 23 days after Tropical Storm Talus (5.37 in rainfall) (Table 4.7 and Figure 4.10). The slowest observed drip rate was 4.0 drips/hr, in March 2012. The highest overnight discharge rate was 223.3 mL/day, and the least was 13.9 mL/day, in August 2011 and March 2012, respectively.

In Station 1's dataset, observed drips rates (<5 mins) are shown as filled circles (Figure 4.10). Dates of inferred drip rates (when drip rate >5 min) are February 2009, April to August 2010, January through August 2013, May and June 2014, and May to July 2016. Dates for not visiting the cave are February 2010, July 2014, and June 2016. October 2012, January 2014, and April 2016 were determined to be suspect (1) for error. Dates of inferred discharge rates for: fallen bottle - March 2009; overflow - October 2009, September 2011, and August 2014; vandalism - July 2015; and forgotten weight record - December 2015.

Drip rate maxima and minima were observed mid- to end of the wet season (Aug-Dec) and mid-dry season to mid-wet season, except between February to May 2011 and May to November 2015. In the mid-wet to mid-dry seasons of March 2012 through December 2014, drip rates gradually decreased alongside precipitation amounts. The opposite is observed from mid-dry to mid-wet seasons. Drip rates were significantly slower (> 5 minutes) in the dry season, and increased in the wet season, especially after storm events.

Events of interest are listed in Table 4.7. Event A is a drip rate maximum in March 2009, 79 days after a non-tropical cyclone event. Event B in September 2009 occurred 52 days after Goni. Event C is another maximum, 20 days after Nida. Event D, from November 2010 to March 2011 is a period of drip rate responses of small amounts of rainfall infiltration. In September 2011, a drip rate increase occurred 25 days after Talas, Event E. Event F occurred 108 days after Talas, Event G in August 2012 is another maximum, 24 and 21 days after Haikui and Kirogi. Event H in October 2013 is another maximum, 32 days after Pabuk. Event I in February 2014 is an intra-seasonal maximum, 27 days after Lingling. Event J is a drip rate maximum, in October 2014, 24 days after Vongfong. Events K (Jan 2015) and L (May 2015) are intra-seasonal responses 116 days after Vongfong, then 14 days after Dolphin. Event M in July 2015 is a drip rate maximum, 24 days after Chan Hom. Events N (Sept 2015) and O (Dec 2015) occurred 44, then 128 days after Goni.

Station 1's drip rates for the entire record ($\pm 0.5 \sigma$ intervals) (Figure 4.11a) is skewed to the right, with its largest frequency (20%) between -0.5 and 0σ (29.4 to 46.9 drips/hr).

The wet season drip rate histogram (Figure 4.11b) is also skewed to the right. Its largest frequency (21%) is from -1 to -0.5 σ (17.4 to 36.3 drips/hr). The dry season (Figure 4.11c) is also skewed to the right. Its largest frequency is 24%, between -1.5 to -1 σ (-6.4 to 8.5 drips/hr).

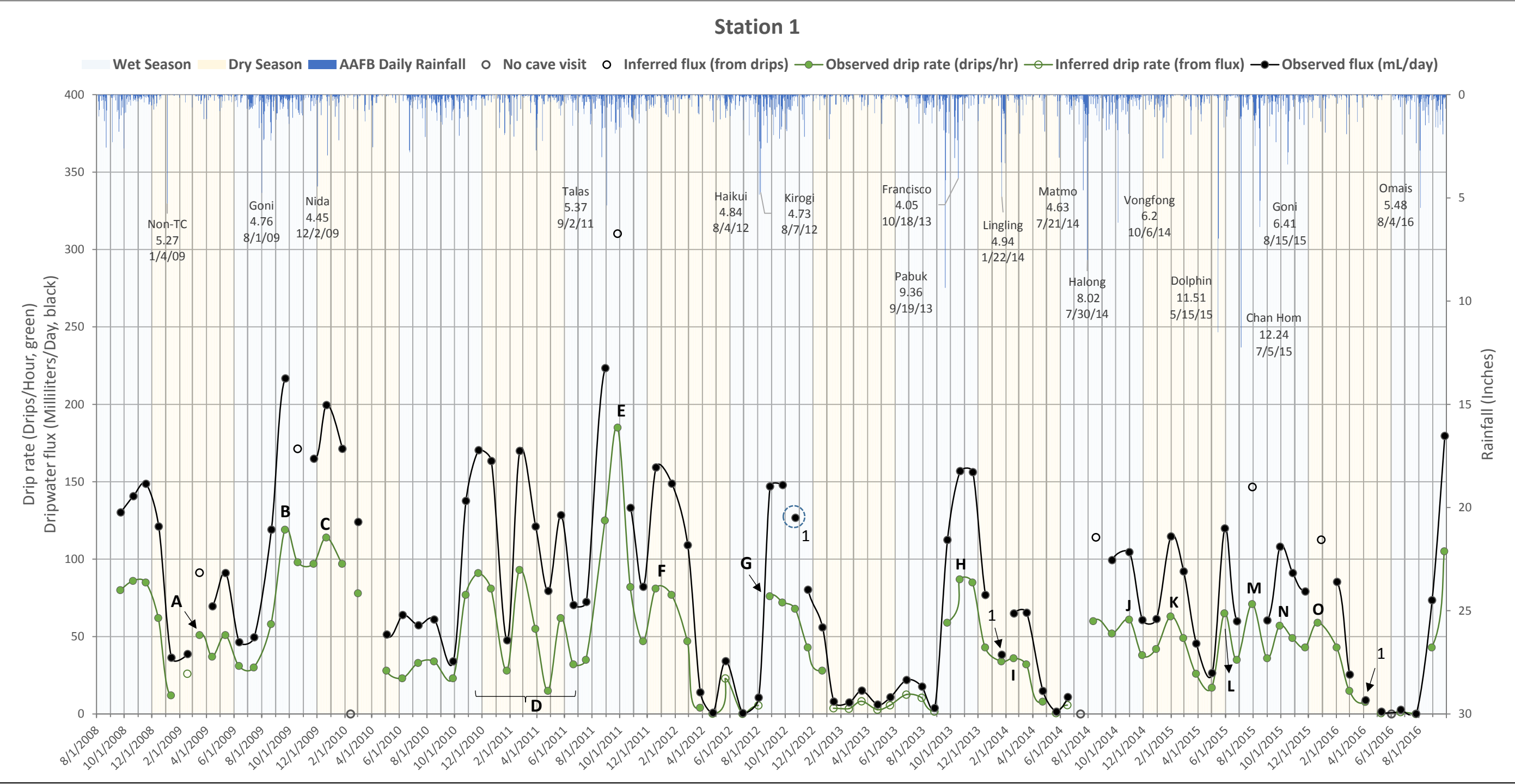
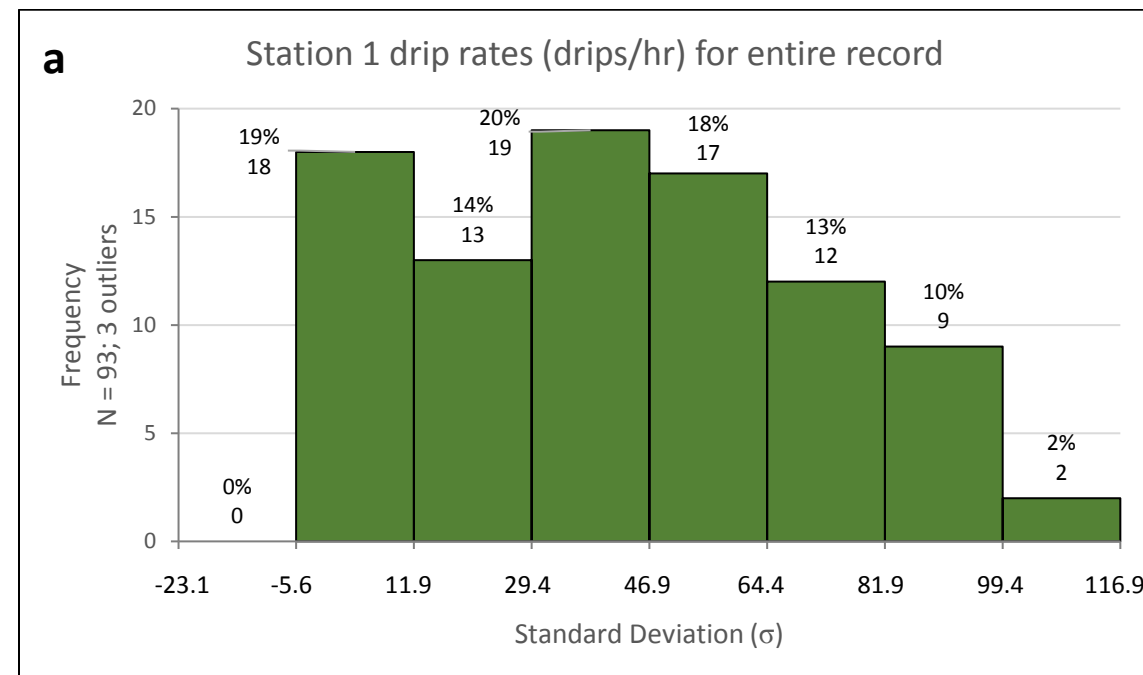


Figure 4.10 Station 1 drip rate (drips per hour, green) and dripwater flux (millimeters per day, black) versus AAFB rainfall (inches). Wet (Jun-Nov) and dry (Dec-May) seasons indicated with pale blue and pale yellow shading, respectively. Observed data is plotted as solid circles. Inferred data is plotted as hollow circles. Events of interest are marked by a letter and discussed in the next section. Data regarded as suspect (1) and spurious (2) were plotted and circled. No cave visits are marked with grey hollow circles.



Station 1 entire record

$\mu = 46.9$

$\sigma = 35.0$

$0.5 \sigma = 17.5$

Station 1 wet season

$\mu = 55.2$

$\sigma = 37.8$

$0.5 \sigma = 18.9$

Station 1 dry season

$\mu = 38.1$

$\sigma = 29.7$

$0.5 \sigma = 14.8$

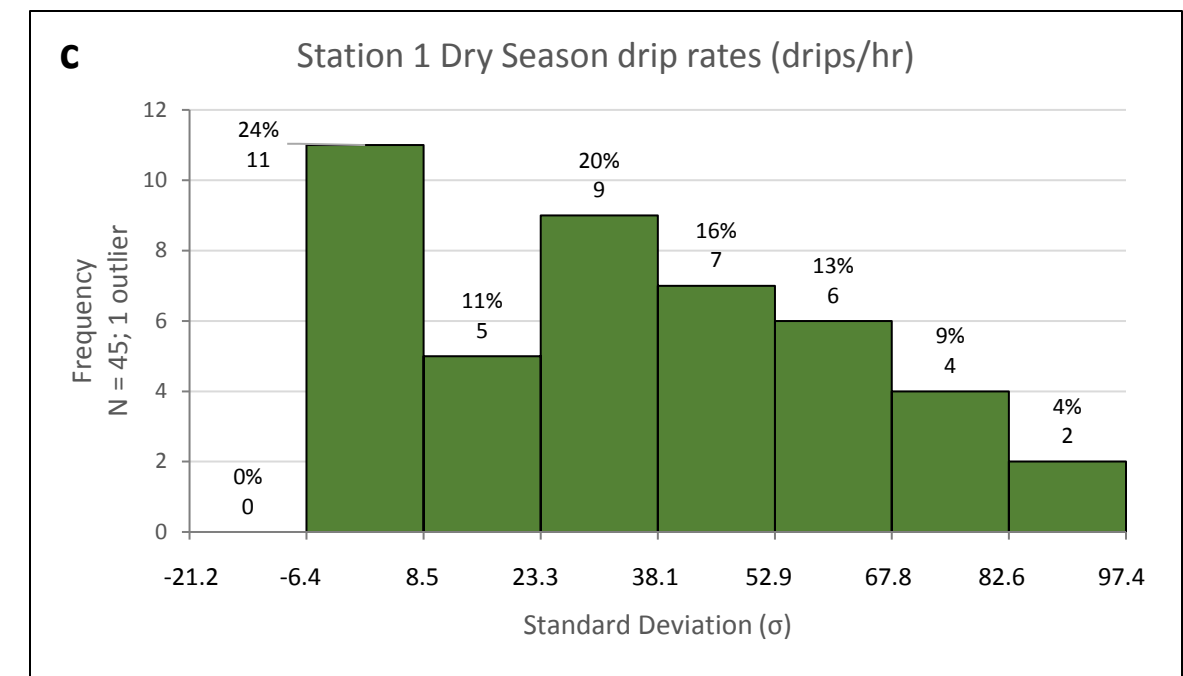
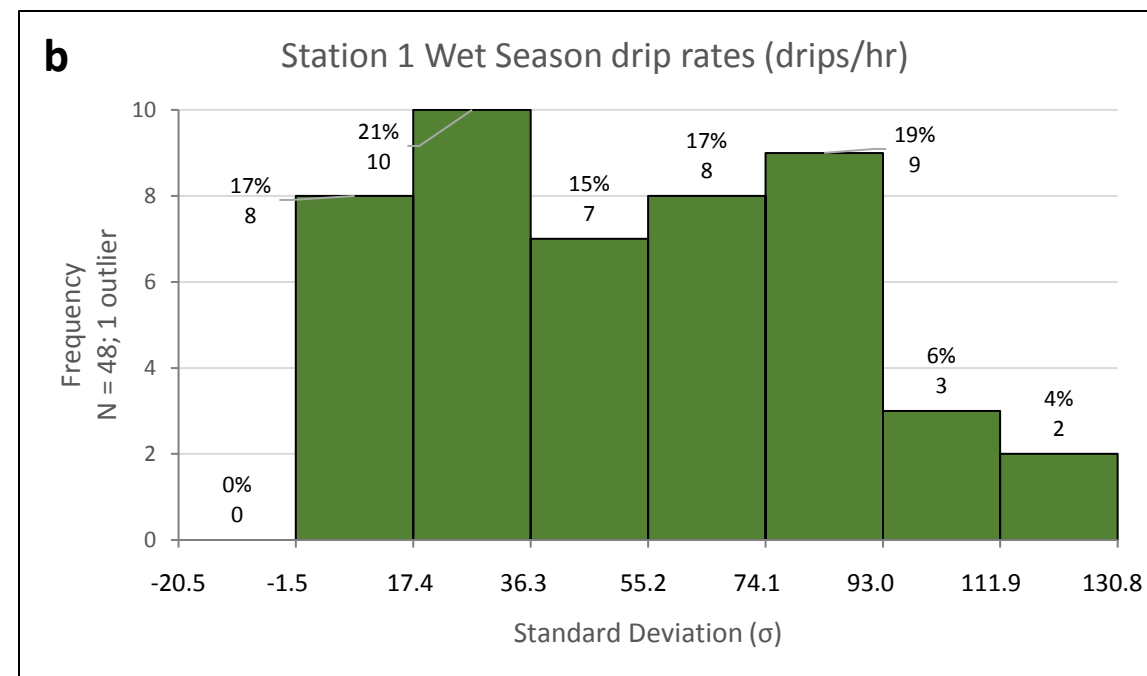


Figure 4.11 Frequency histograms of Station 1 a) drip rates for entire record, b) wet season drip rates, and c) dry season drip rates $\pm 2 \sigma$ from respective means at $\pm 0.5 \sigma$ intervals.

Station 1's stalactite, at its origin, is 26.9 m below the ground surface (Figure 4.1c). The limestone bedrock is an estimated thickness ranges 23.5 to no less than 19.5m (Table 4.1 and Figure 4.1d), and the overlying talus thickness ranges 4 to 8m. The ground surface has a ~26° slope of patches of cobble-size talus. It is upslope from a drop-off, ranging between 2-3 m from the ground below. No large boulders or trees sit directly above the station. However, one large limestone tree (dbh > ~100 cm) and several small understory limestone trees (dbh < 50 cm) surround the ground above the station.

4.3.4 Station 2

Station 2's stalactite has an average entire record drip rate of 43.8 drips per hour with a standard deviation of 16.7 drips per hour (Table 4.2). Its average dripwater flux for the entire record is 75.6 milliliters per day with a standard deviation of 28.3 milliliters per day (Table 4.3). Average drip volume is 0.072 milliliters per drip. Of 94 drip-rate values, the fastest observed was 122.0 drips/hr, in September 2008, the first record for this dataset. Correspondingly the largest overnight discharge was 202.6 mL, also in September 2008. The slowest recorded drip-rate was 26.0 drips/hr, July 2016. However, the smallest dripwater volume collected was in June 2016, 43.5 mL.

Data determined to be suspect (1) for error are in August 2009 (Figure 4.12), April 2011, May and June 2014, Mar 2015, and July 2016. Spurious (2) data are January 2010, October and November 2011, March 2014, and September 2015.

Station 2's drip-rate displays a clear response to seasonal rainfall input. Drip-rate maxima are at mid- to late- wet season months, which gradually decrease to drip-rate minima in the following dry season. The next peak marks the onset of the next wet season. A decreasing drip-rate trend for this station is also visible for this dataset. From December 2011 to the end of the dataset (September 2016), drip rate oscillates between 25 and 50 drips/hr with respect to seasonal rainfall input.

Events of interest are listed in Table 4.7. Event A in September 2009 is the dataset's first drip-rate maxima, and occurred 52 days after Goni. Event B, between August 2010 and January 2011, is a drip-rate response during the driest wet-dry cycle of the eight-year dataset, similarly as Station 1. Event C, in September 2011, is the next drip-rate response, 25 days after Talas. Event D is another drip-rate maximum, 79 and 76 days after Haikui and Kirogi. Event E, in November 2013, is a drip-rate response, 32 days after Francisco. Event F is an intra-seasonal drip-rate response, 27 days after Lingling. Event G in January 2015 occurred 106 days after Vongfong. Event H occurred 15 days after Dolphin in May 2015. The last event, I, in September 2015, occurred 44 days after Goni.

Station 2's histogram for its entire drip-rate record ($\pm 0.5 \sigma$ intervals) (Figure 4.13a) has a single mode (32%) between 35.5 and 43.8 drips/hr (-0.5 to 0σ), below the mean. The wet season (Figure 4.13b) histogram also exhibits its single mode (48%) below the mean, between 35.4 and 45.3 drips/hr (-0.5 to 0σ). The dry season (Figure 4.13c) has two equally large modes (24%), one below, -1 to -0.5σ (29.6 to 35.9 drips/hr), and the other above, 0 to 0.5σ , the mean – between 31.7 and 38.2 drips/hr, then between 42.3 to 48.6 drips/hr. All three histograms have majority of their drip rates close to the mean and are skewed to the right, with tails extending to $+2 \sigma$ – entire: ~79%, wet: ~90%, and dry: ~76% (Figure 4.6).

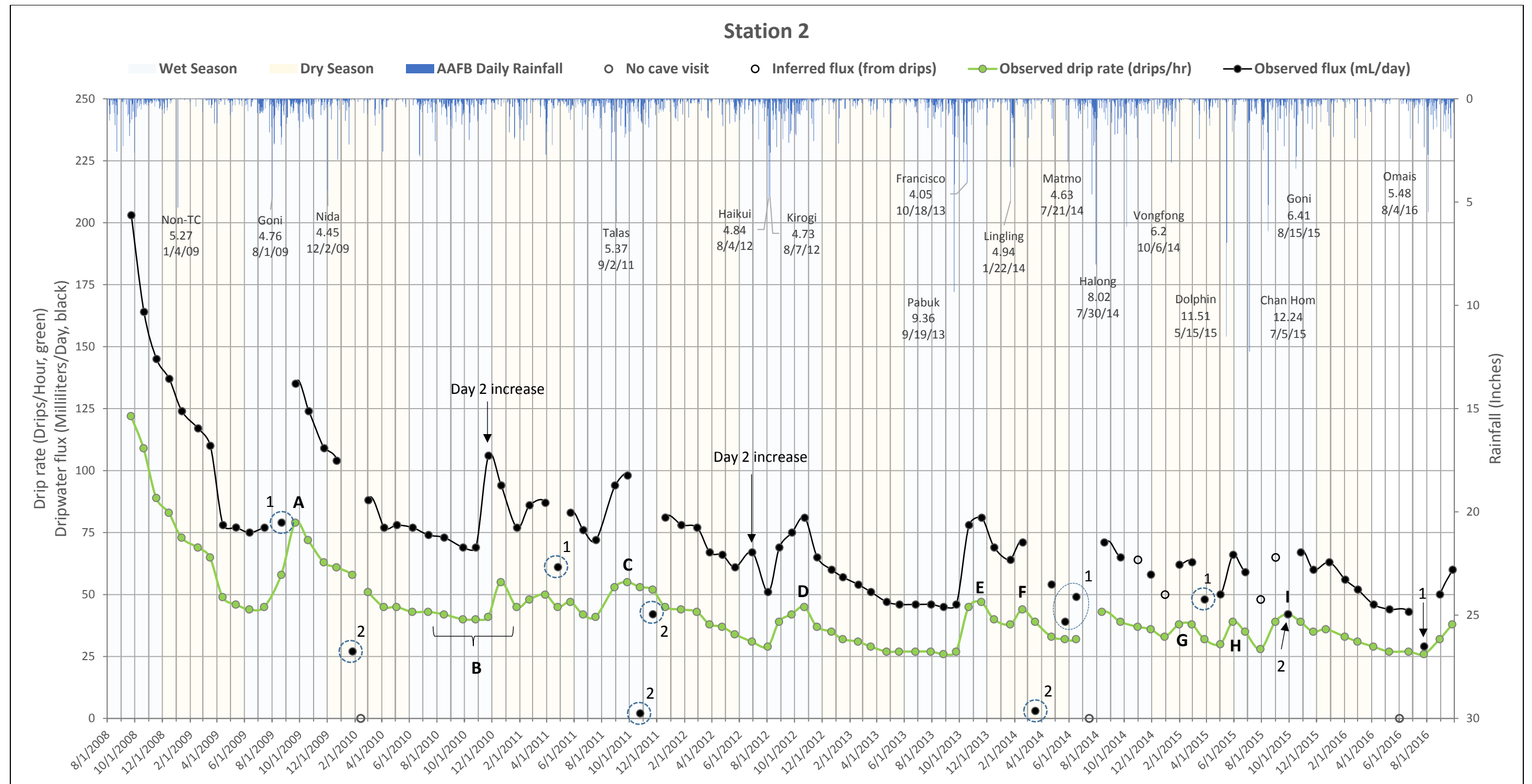


Figure 4.12 Station 2 drip rate (drips per hour, light green) and dripwater flux (millimeters per day, black) versus AAFB rainfall (inches). Wet (Jun-Nov) and dry (Dec-May) seasons indicated with pale blue and pale yellow shading, respectively. Observed data is plotted as solid circles. Inferred data is plotted as hollow circles. Events of interest are marked by a letter and discussed in the next section. Data regarded as suspect (1) and spurious (2) were plotted and circled. No cave visits are marked with grey hollow circles.

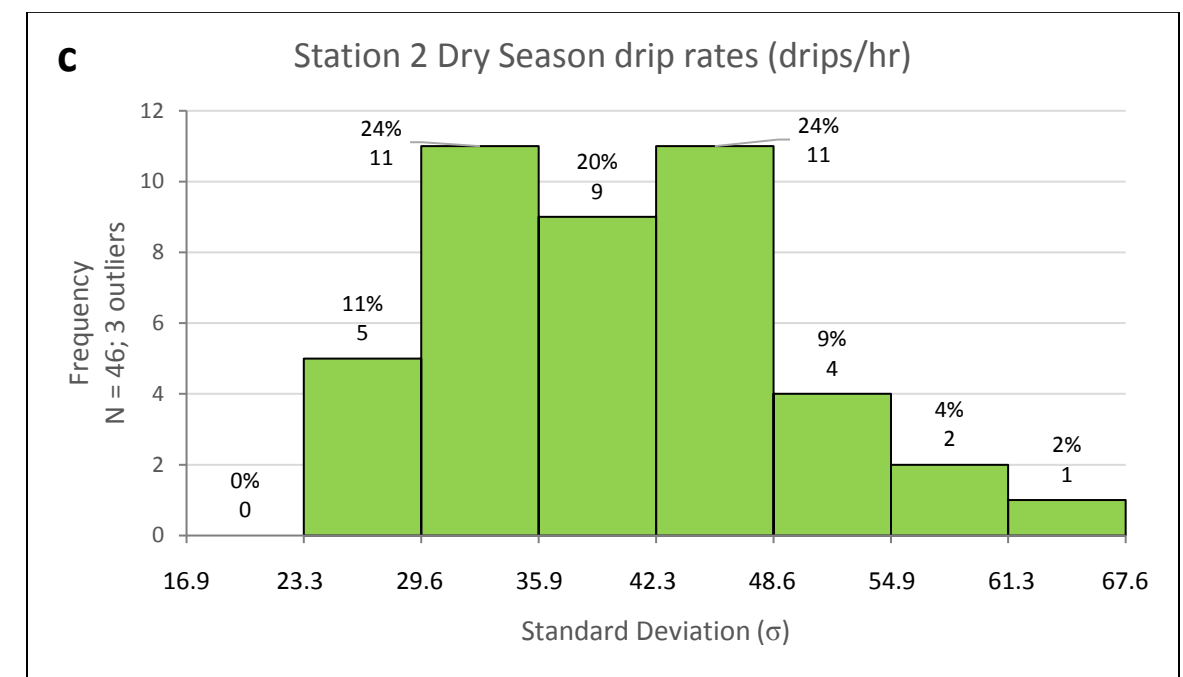
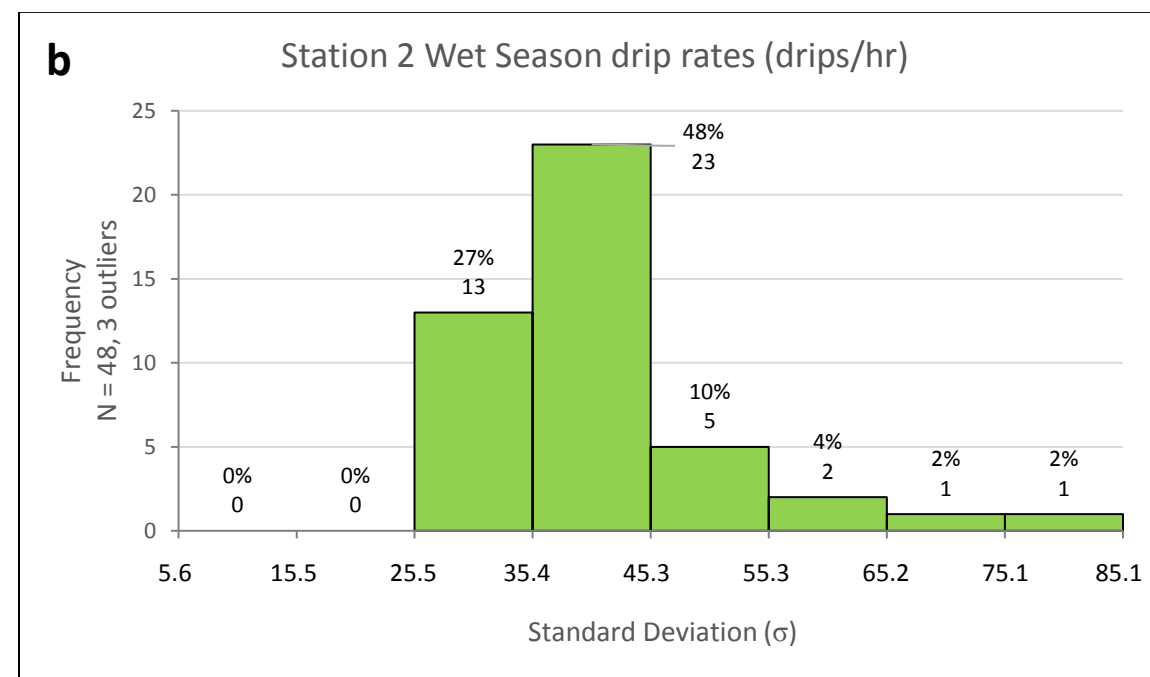
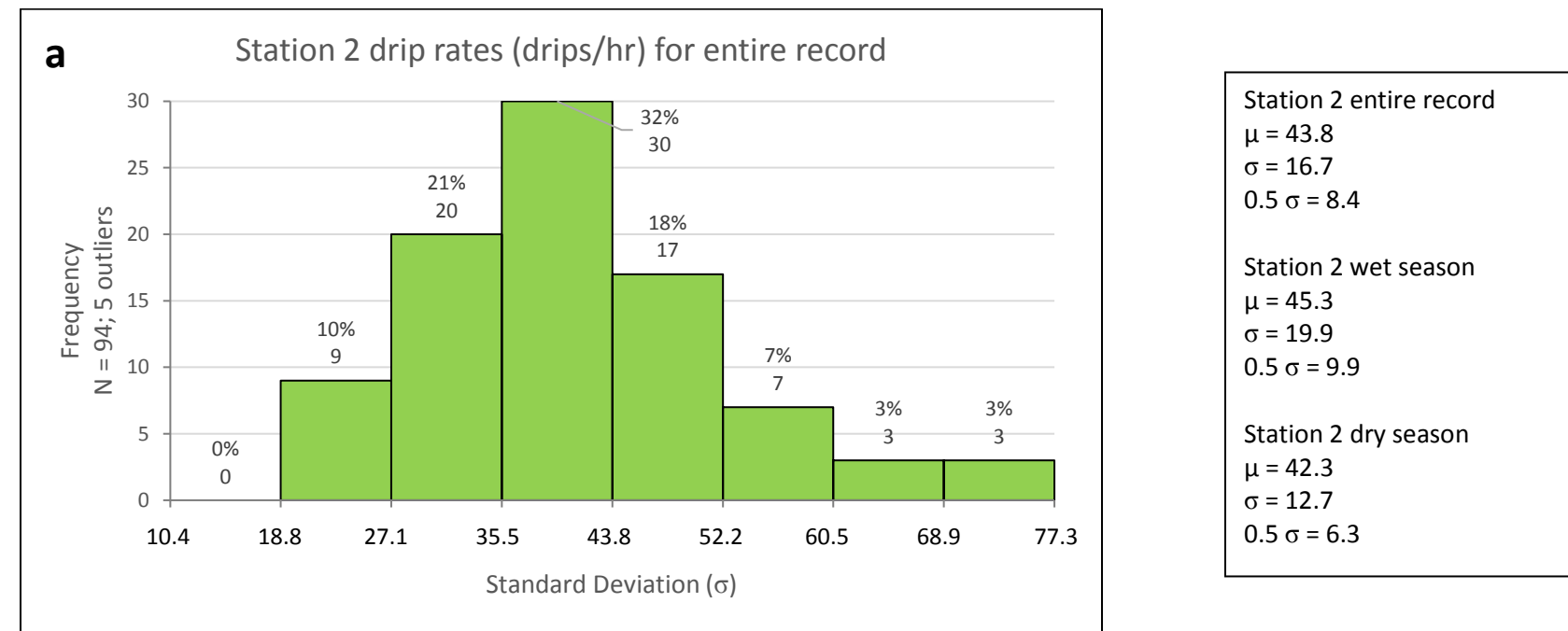


Figure 4.13 Frequency histograms of Station 2 a) drip rates for entire record, b) wet season drip rates, and c) dry season drip rates $\pm 2 \sigma$ from respective means at $\pm 0.5 \sigma$ intervals.

Station 2's stalagmite at its base is 28.5 m below the ground surface (Figure 4.1c). The overlying layers of limestone bedrock and talus thicknesses range from 24.5 to no less than 20.5 m, and 4 m to 8 m, respectively (Table 4.1 and Figure 4.1d). Station 2, 1.04 m from Station 1, shares similar ground surface features and vegetation: the area is of course cobble-size talus debris, has a slope of 26°, and is near one large limestone forest tree and few small limestone forest trees (*Triphasia trifolia* and *Guamia* sp.)

4.3.5 Stumpy's Brother

This station's stalactite has an average drip rate of 41.3 drips per hour with a standard deviation of 4.1 drips per hour, and an average drip-water flux of 71.5 milliliters per day with a standard deviation of 7.6 milliliters per day (Tables 4.2 and 4.3). Average drip volume is 0.072 milliliters per drop. The fastest drip rate was 50.7 drips/hr, observed in September 2009. The slowest drip rate was 33.0 drips/hr, observed in June 2016. The most and least water discharged was 88.8 mL/day in September 2009, and 57.9 mL/day in September 2013.

Data determined to be suspect (1) (Figure 4.14) are in April, August, October, and November 2010, September 2011, August and November 2012, January and February 2013, January, August, and October 2014, and July 2016. Data determined to be spurious (2) are October 2009, July and October 2011, and March 2012. There is one inferred drip rate date, June 2015, when a drip count was not taken. Inferred flux data dates are: July and November 2009 (bottle fell), June 2012 (uncentered bottle), June, July and December 2015 (unrecorded deployment time).

Stumpy Brother's drip displays a monotonic seasonal trend. From the mid-dry season to beginning of the wet season, the drip-rate gradually decreases. Then from mid-wet season, the drip-rate peaks and then gradually decreases following the next dry season. From November 2010 to May 2011 and January 2015 however, an occurrence of intra-seasonal variability is observed.

Events of interest are listed in Table 4.7. Event A, in September 2009, is the first drip rate response, 52 days after Goni. Events B (Nov 2010 – May 2011) and C (Aug 2011) are intra-seasonal variabilities in drip rate responses during a non-storm period in the dataset. Event D in November 2011 is a drip rate response, 80 days after Talas. The next drip rate maximum is Event E in November 2012, 108 and 105 days after Haikui and Kirogi. Event F occurred in October 2013, 32 days after Pabuk. Event G in January 2015 occurred 116 days after Vongfong, and is another intra-seasonal variability. Event H occurred 14 days (May 2015) after typhoon Dolphin. Event I in July 2015 occurred 24 days after Chan Hom. Event J occurred 101 days (Nov 2015) after Goni.

Stumpy Brother's histogram for the entire record ($\pm 0.5 \sigma$ intervals) (Figure 4.15a) shows its highest frequency (24%) between -0.5 to 0σ (41.3 to 43.4 drips/hr). The wet season histogram (Figure 4.15b) has equal frequencies (22%) close to the mean, -0.5 to 0.5σ (39.0 to 43.5 drips/hr). The dry season histogram's (Figure 4.15c) highest frequency (24%) is from 0 to 0.5σ (41.3 to 43.2 drips/hr). Skew directions for the entire and wet season histograms are to the right. The dry season has equal frequencies approaching both tails.

Stumpy's Brother is ~34 m from the ground surface. The estimated limestone bedrock and talus thicknesses range 28.1 to 24.1 m and 4 to 8 m, respectively (Table 4.1 and Figure 4.1c and d). The ground surface, upslope from Stations 1 and 2, also shares cobble-size talus debris and is near a large limestone forest tree and few smaller limestone forest trees (*Triphasia trifolia* and *Guamia* sp.).

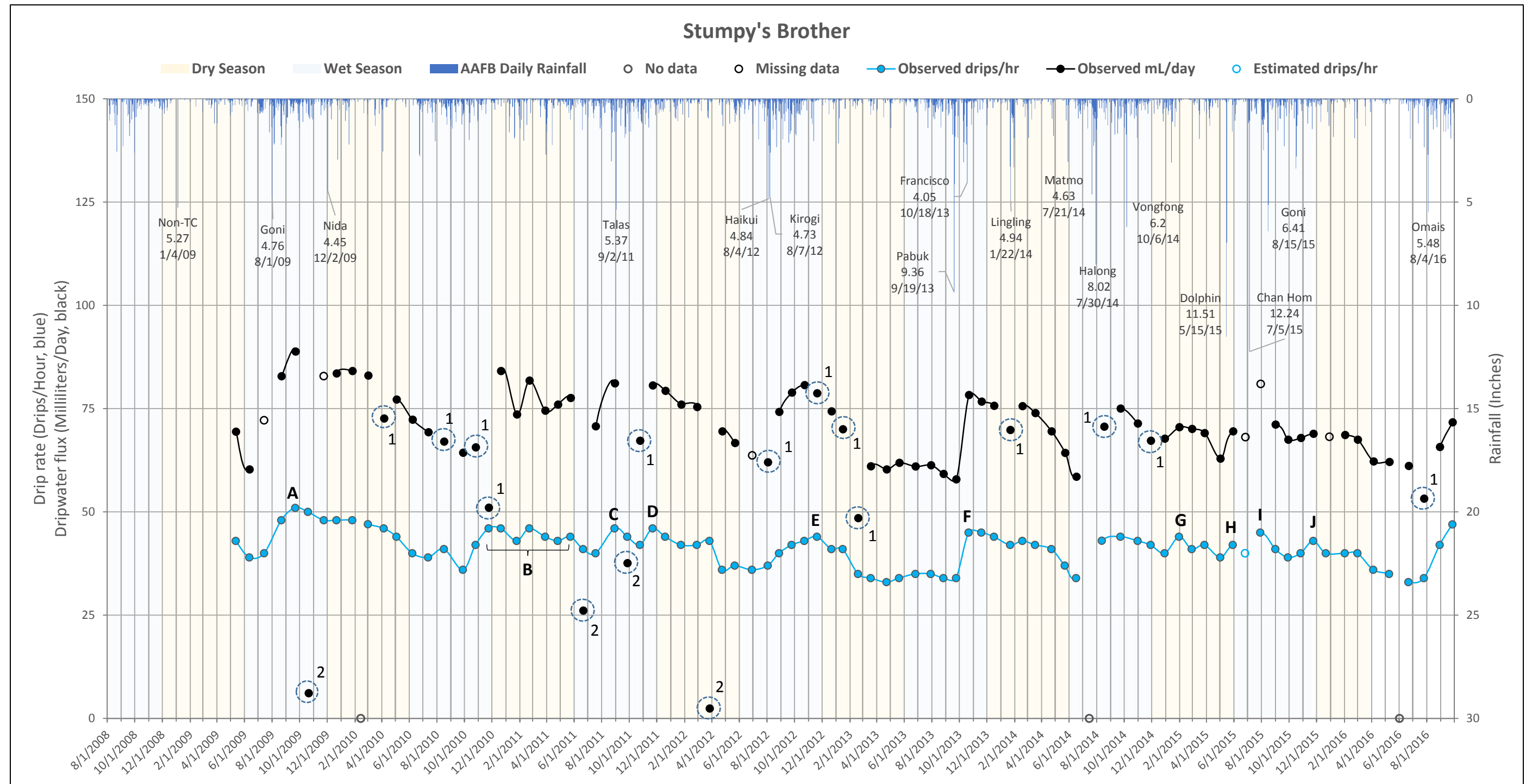
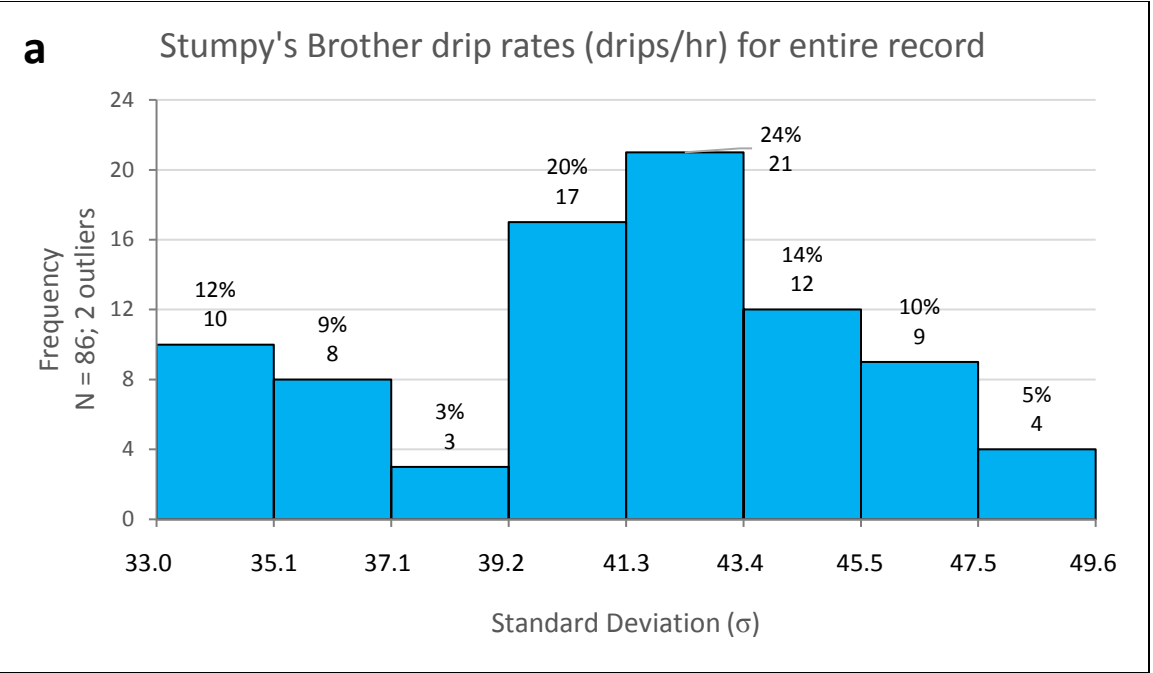


Figure 4.14 Stumpy's Brother drip rate (drips per hour, light blue) and dripwater flux (millimeters per day, black) versus AAFB rainfall (inches). Wet (Jun-Nov) and dry (Dec-May) seasons indicated with pale blue and pale yellow shading, respectively. Observed data plotted as solid circles. Inferred data is plotted as hollow circles. Events of interest are marked by a letter and discussed in the next section. Data regarded as suspect (1) and spurious (2) were plotted and circled. No cave visits are marked with grey hollow circles.



Stumpy's Brother entire record
 $\mu = 41.3$
 $\sigma = 4.1$
 $0.5 \sigma = 2.1$

Stumpy's Brother wet season
 $\mu = 41.3$
 $\sigma = 4.5$
 $0.5 \sigma = 2.2$

Stumpy's Brother dry season
 $\mu = 41.3$
 $\sigma = 3.8$
 $0.5 \sigma = 1.9$

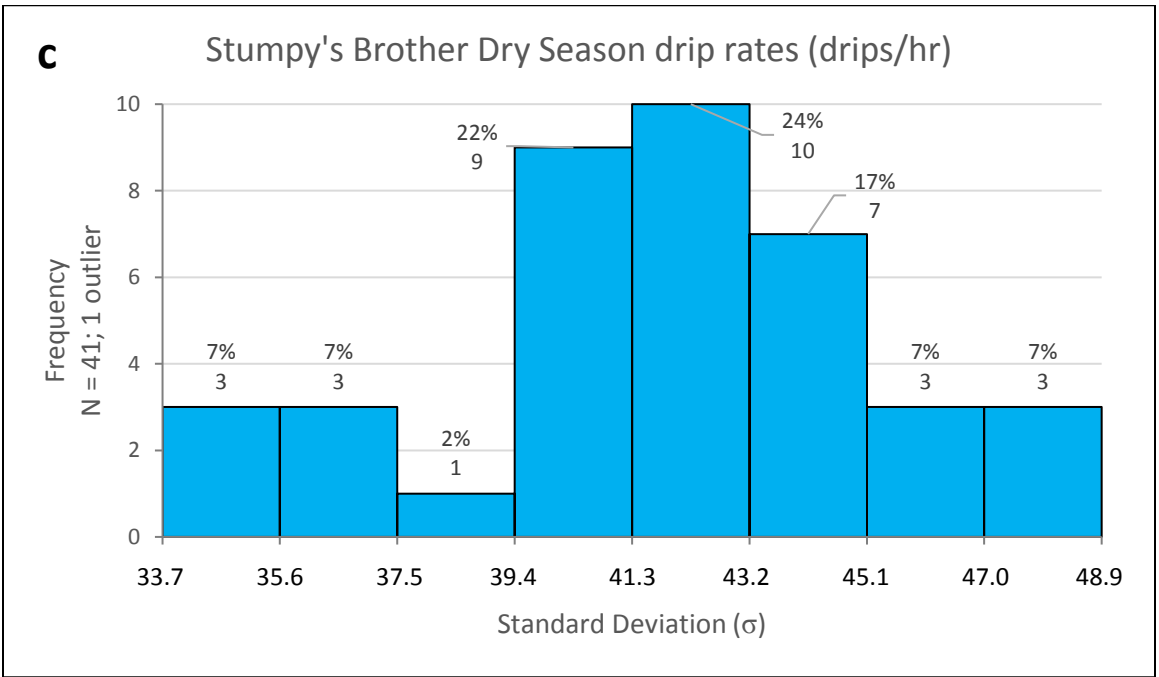
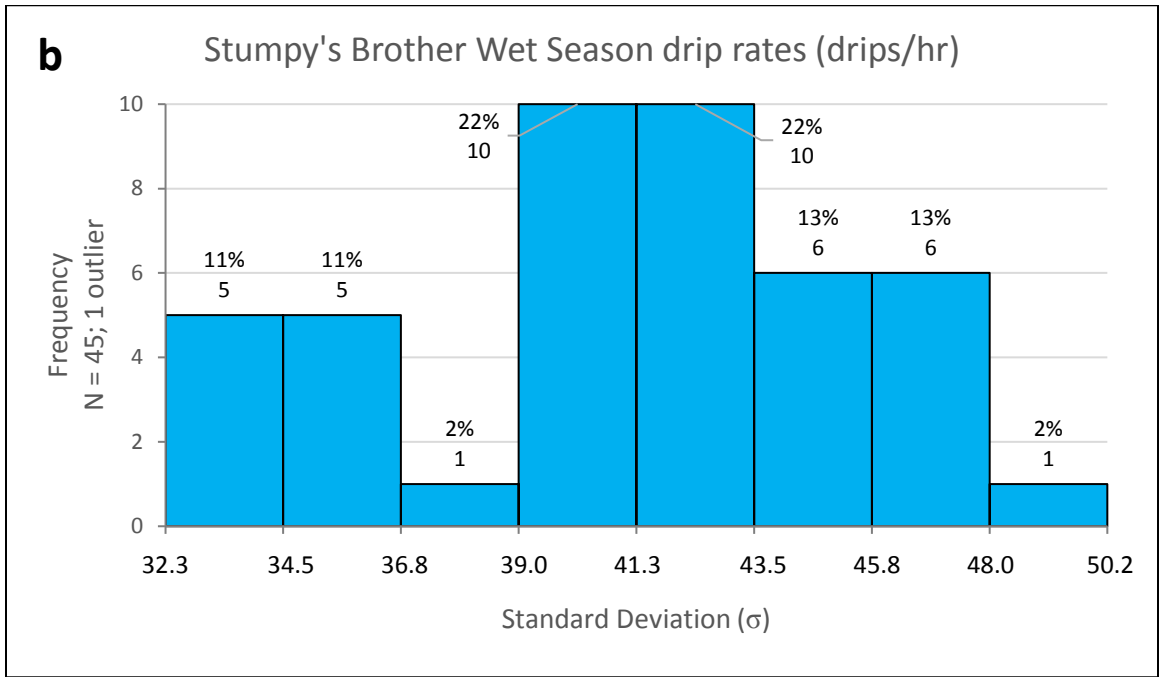


Figure 4.15 Frequency histograms of Stumpy's Brother a) drip rates for entire record, b) wet season drip rates, and c) dry season drip rates $\pm 2 \sigma$ from respective means at $\pm 0.5 \sigma$ intervals.

4.3.6 Stumpy

This station's stalactite has an average estimated drip rate of 7.7 drips per hour with a standard deviation of 4.4 drips per hour for the entire record (Table 4.2). Estimated drip-water flux was averaged to 13.7 milliliters per day with a standard deviation of 7.3 milliliters per day (Table 4.3). Average drip volume is 0.079 milliliters per drip. Of 87 observed and calculated drip-rate values, the fastest was 25.7 drips/hr, observed in May 2009. The slowest was 0.15 drips/hr, observed in January 2012. Correspondingly, the most water collected overnight was 37.1 mL/day in May 2009, and the least was 0.32 mL/day, in January 2012.

In the eight-year dataset, Stumpy has 15 recorded drip counts - November 2011, February to April 2015, June 2015, October 2015 to May 2016, and June to August 2016 (Figure 4.16). All other dates ("drip rate > 5 minutes") are estimates calculated using Equations 4 through 6 (Table 3.1) and monthly overnight drip weights. Dates of suspect data are March and April 2015, and April and July 2016. January 2013 is the only date of spurious data, when collection bottle was found not centered under drip and barely any sample water was collected. There is no drip rate or flux rate for November 2010 as barely any water was collected from the bottle being uncentered under the drip.

Stumpy's drip-rate displays seasonal responses, as well as multiple intra-seasonal variabilities. From April to August 2011 the drip-rate and discharge rates are constant and the low in value, which corresponds little rainfall in the dry season. Between September 2011 to April 2012, the drip-rate resumes another intra-seasonal drip trend. Intra-seasonal variabilities are December 2009 to March 2010, December 2010 to March 2011, December 2011 to April 2012, February 2013, February to March 2014, and December 2014 to April 2015.

Events of interest are listed in Table 4.7. Event A, in May 2009, is the first drip-rate response, 129 days after a non-tropical cyclone event. Event B, in September 2009, is another drip-rate maximum, 52 days after Goni. In August 2010 and February 2011, events C, and D, occurred during the driest period (lack of storm events) in this eight-year dataset. Two events, E (Sept 2011) and F (Dec 2011), occurred 25, then 109, days after Talas. Event G, in August 2012, is another drip-rate maximum, 24 days after Haikui, and 21 days after Kirogi. Event H, in October 2013, occurred 32 days after Pabuk. Event I (Mar 2014) occurred 55 days after Lingling. Event J (May 2015) occurred 207 days after Vongfong. Event K, in July 2015, occurred 25 days after Chan Hom.

Stumpy's histogram for the entire record ($\pm 0.5 \sigma$ intervals) (Figure 4.17a) has its highest frequency (32%) between 7.7 and 9.9 drips/hr (0 to 0.5 σ), above the mean. The data is also skewed to the left. The wet season histogram (Figure 4.17b) has its highest frequency (25%), also above the mean, between 9.4 and 11.3 drips/hr (0.5 to 1 σ). The dry season histogram's (Figure 4.17c) highest frequency (40%) is also above the mean, between 7.8 and 10.4 drips/hr (0 to 0.5 σ). The data is close to the mean, starting from 1 σ , with a skew to the left.

The base of Stumpy's stalagmite is ~34m from the ground surface (Figures 4.1c and d). The overlying limestone bedrock layer ranges 27.8 to 23.8m thick, and the talus layer ranges 4 to 8m thick (Table 4.1). The Stumpy Room ground surface, ~3.5m upslope from the Shakey Room, is of similar cobble-size talus debris with nearby small limestone forest trees and the same large limestone forest tree <10m away.

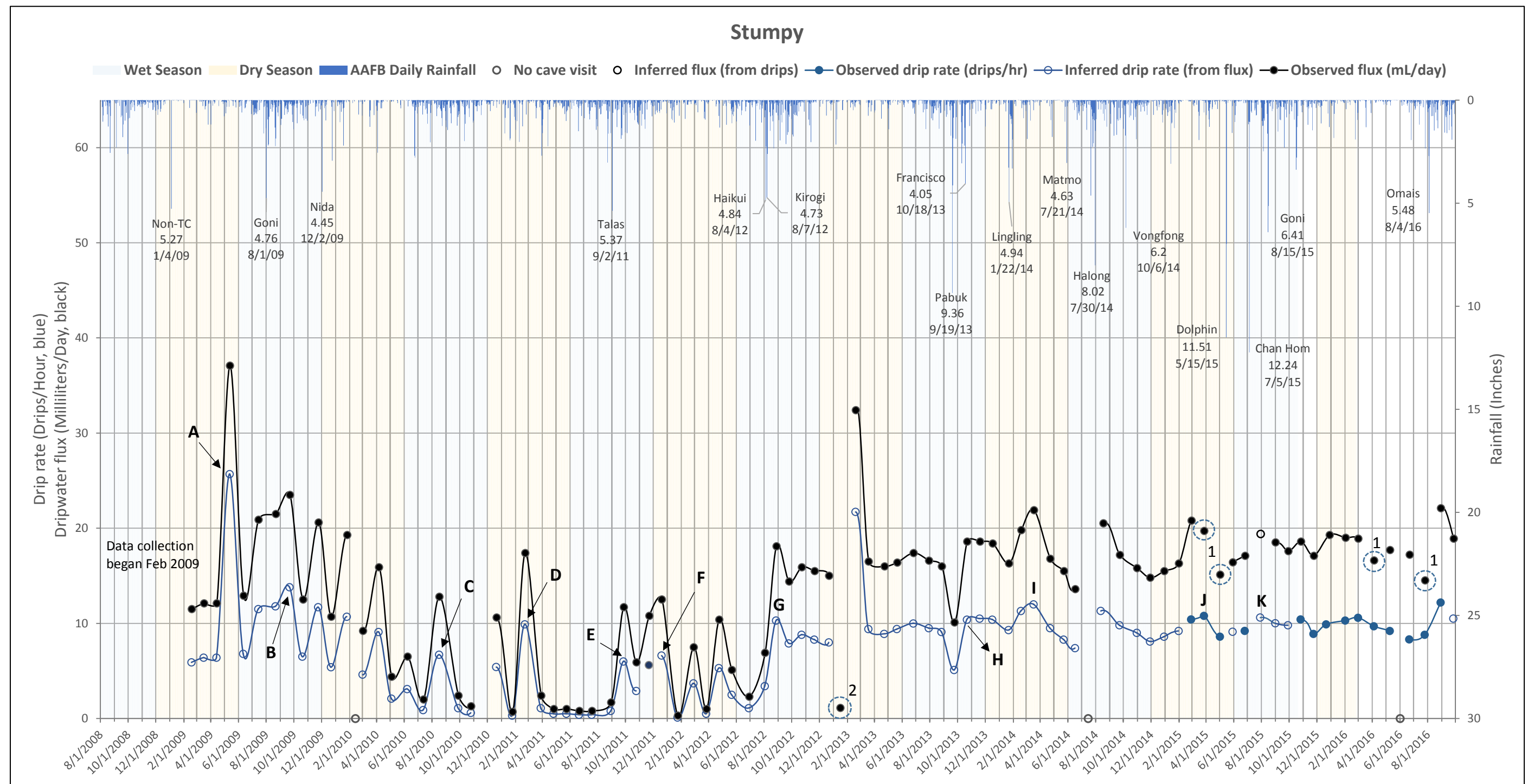
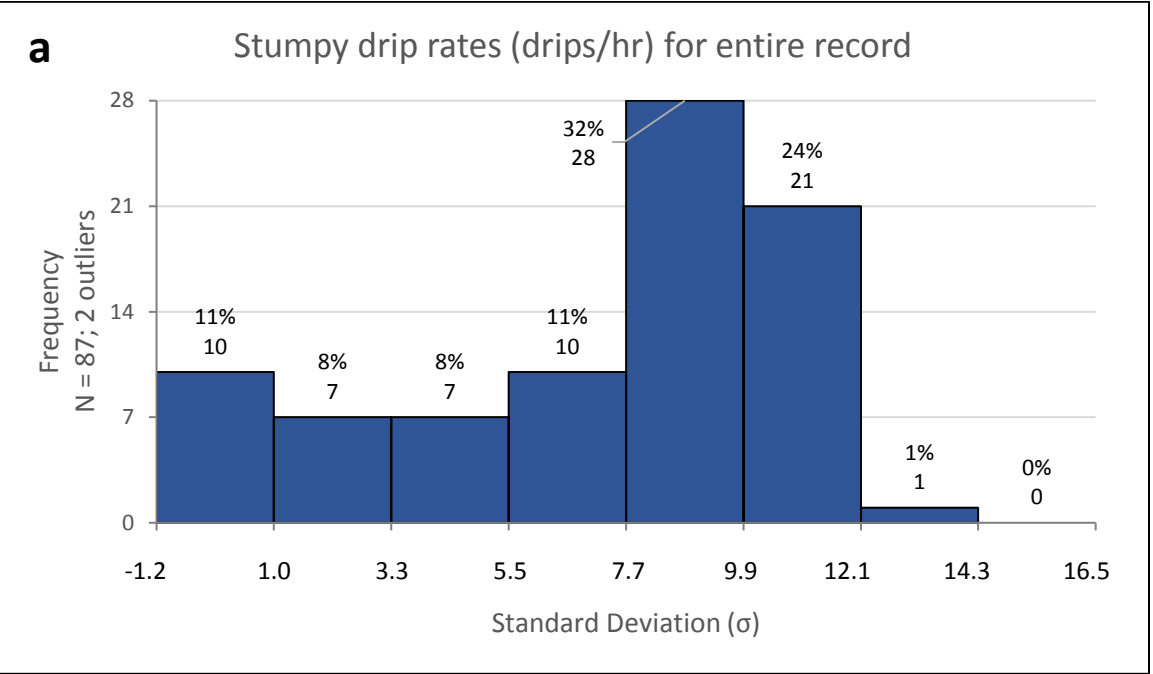


Figure 4.16 Stumpy drip rate (drips per hour, blue) and dripwater flux (millimeters per day, black) versus AAFB rainfall (inches). Wet (Jun-Nov) and dry (Dec-May) seasons indicated with pale blue and pale yellow shading, respectively. Observed data is plotted as solid circles. Inferred data is plotted as hollow circles. Events of interest are marked by a letter and discussed in the next section. Data regarded as suspect (1) and spurious (2) were plotted and circled. No cave visits are marked with grey hollow circles.



Stumpy entire record
 $\mu = 7.7$
 $\sigma = 4.4$
 $0.5 \sigma = 2.2$

Stumpy wet season
 $\mu = 7.5$
 $\sigma = 3.8$
 $0.5 \sigma = 1.9$

Stumpy dry season
 $\mu = 7.8$
 $\sigma = 5.0$
 $0.5 \sigma = 2.5$

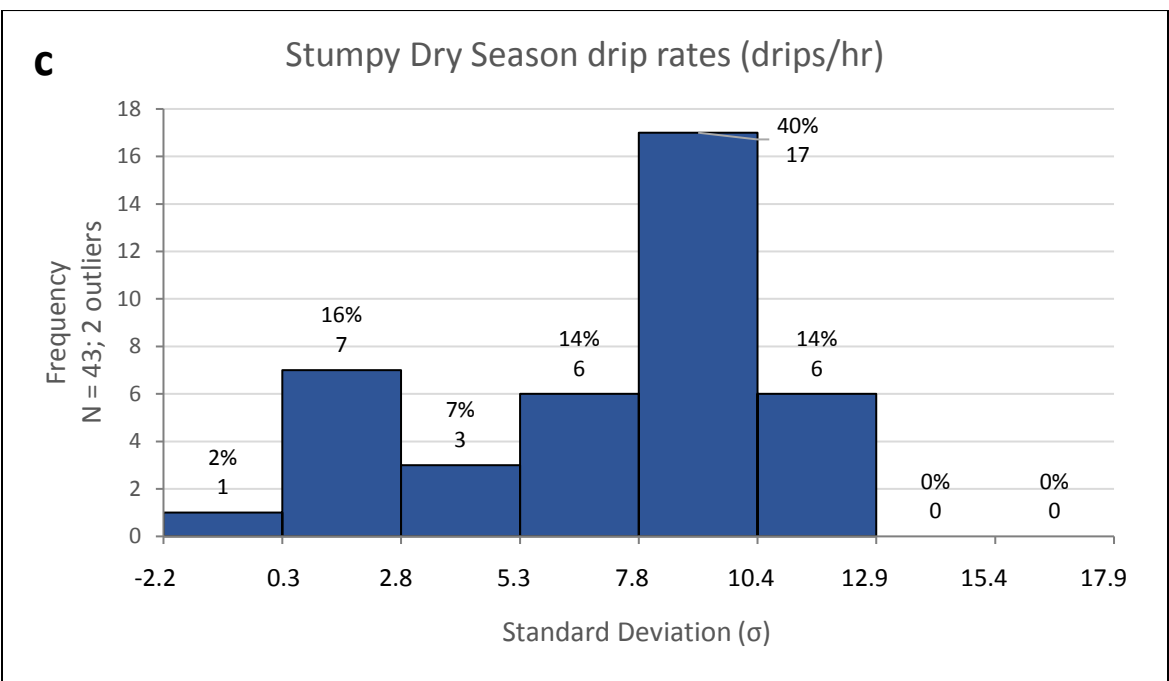
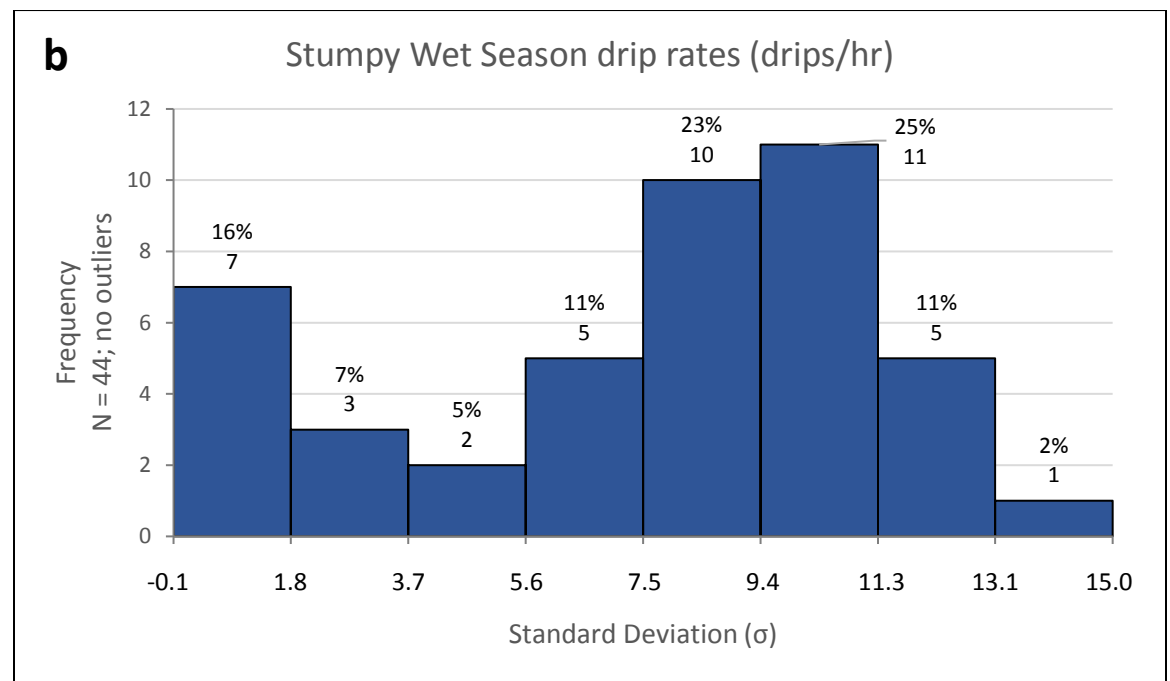


Figure 4.17 Frequency histograms of Stumpy's a) drip rates for the entire record, b) wet season drip rates, and c) dry season drip rates $\pm 2 \sigma$ from respective means at $\pm 0.5 \sigma$ intervals.

4.3.7 Amidala

Amidala's stalactite has an average estimated drip rate of 6.0 drips per hour with a standard deviation of 10.3 drips per hour for its entire record (Table 4.2). The average drip-water flux for the entire record is 11.0 milliliters per day with a standard deviation of 18.7 milliliters per day (Table 4.3). Average drip volume (mL/drip) is 0.076. Of 68 drip count measurements, December 2012 had the fastest drip rate, and largest drip-water flux, 49.0 drips/hr and 86.9 mL/day respectively (Figure 4.18). The slowest drip rate, and smallest dripwater flux, was estimated to be 0.73 drips/hr, with an observed 1.3 mL/day in June 2014. The collection bottle fell on August and November 2009. No water was collected, and no drip count was inferred for those months. Data collection ended in May 2015.

Amidala's station, 1.2m from Stumpy's Brother, and 1.6m from Stumpy, displays relatively flat (low response) trend compared to rainfall infiltration from 2009 through 2011 and 2013 to 2015. Between 2011 and 2013, intra-seasonal maxima occurred at the beginning of the dry seasons. After the peaks, the drip-rate returned to flat, uniform mode.

Events of interest are in June 2011 (A) (Table 4.7), December 2011 (B), and December 2012 (C). Event "A," in June 2011 is thought to be an intra-seasonal occurrence following the wet-dry season of 2010-2011. Event "B" in December 2011 is a drip-rate response, 109 days after storm Talas. Event "C" in December 2012 is another drip-rate response, 140 and 137 days after storms Haikui and Kirogi. There were no further notable responses following Event C, despite varying rainfall amounts associated with storms that passed Guam.

Amidala's drip rate histogram for the entire record ($\pm 0.5 \sigma$ intervals) (Figure 4.19a) has its highest drip-rate frequency (79%) between 0.8 and 6.0 drips/hr (-0.5 to 0σ). The histogram shape is skewed to the right. In the wet season histogram (Figure 4.19b) three prominent frequencies are clustered around the mean, with the highest (42%) between 1.5 and 3.8 drips/hr (-0.5 to 0σ). This histogram also has a right skew. The dry season histogram (Figure 4.19c) has its prominent frequencies below the mean. The highest, 71%, is between 1.3 and 8.0 drips/hr (-0.5 to 0σ), and the histogram shape is also skewed to the right. All three histograms have $>63\%$ of data within $\pm 1 \sigma$ from the mean: entire – 91%, wet season – 91%, and dry season – 86%.

Amidala's station, ~35m from the surface, shares similar cobble-sized talus debris as Stumpy and Stumpy's Brother stations, and is also near the same large limestone forest tree and few *Triphasia* and *Guamia* trees. The limestone bedrock layer is estimated to range 28 to 24m thick, while the talus layer is estimated to range 4 to 8m thick (Figure 4.1c and Table 4.1).

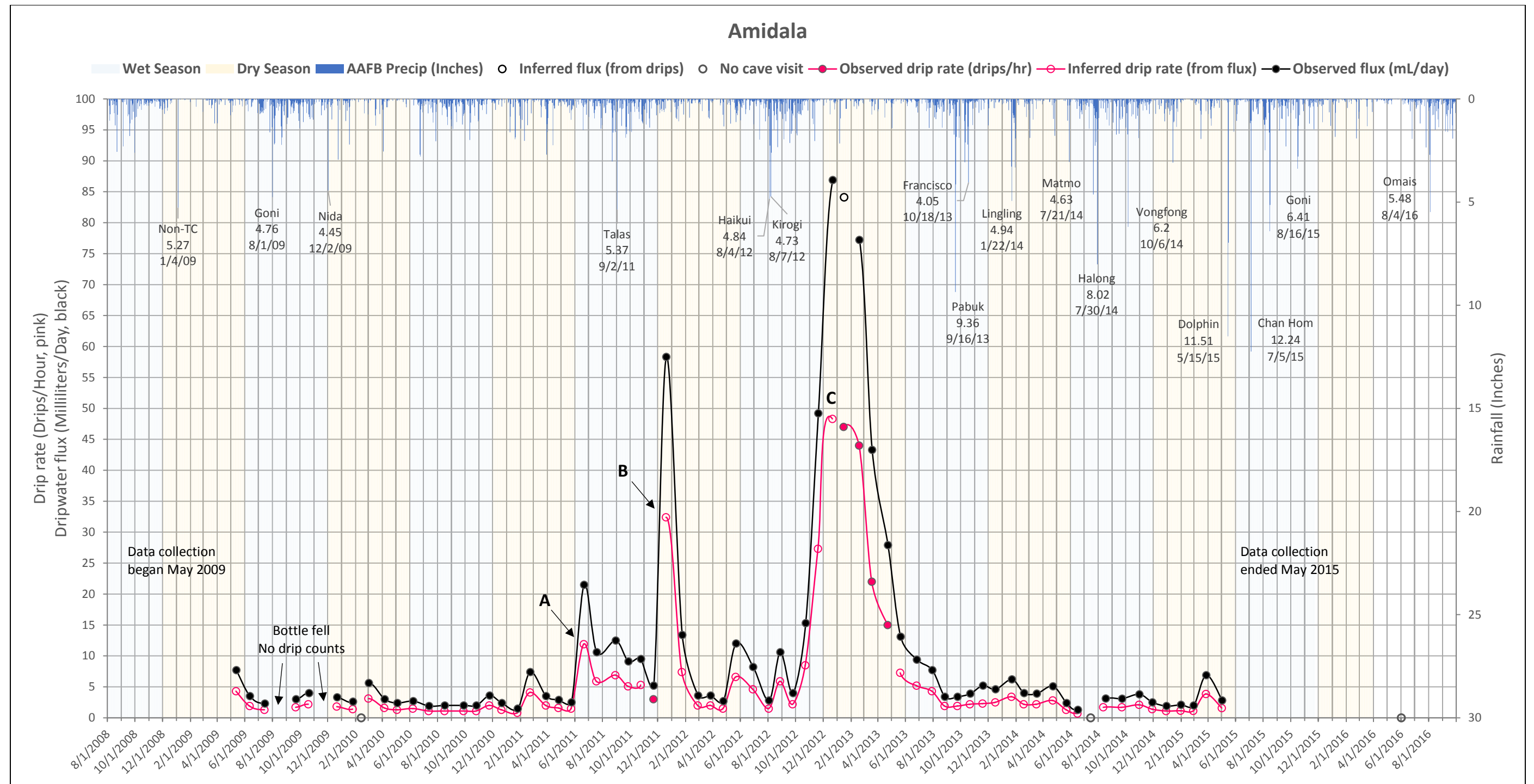
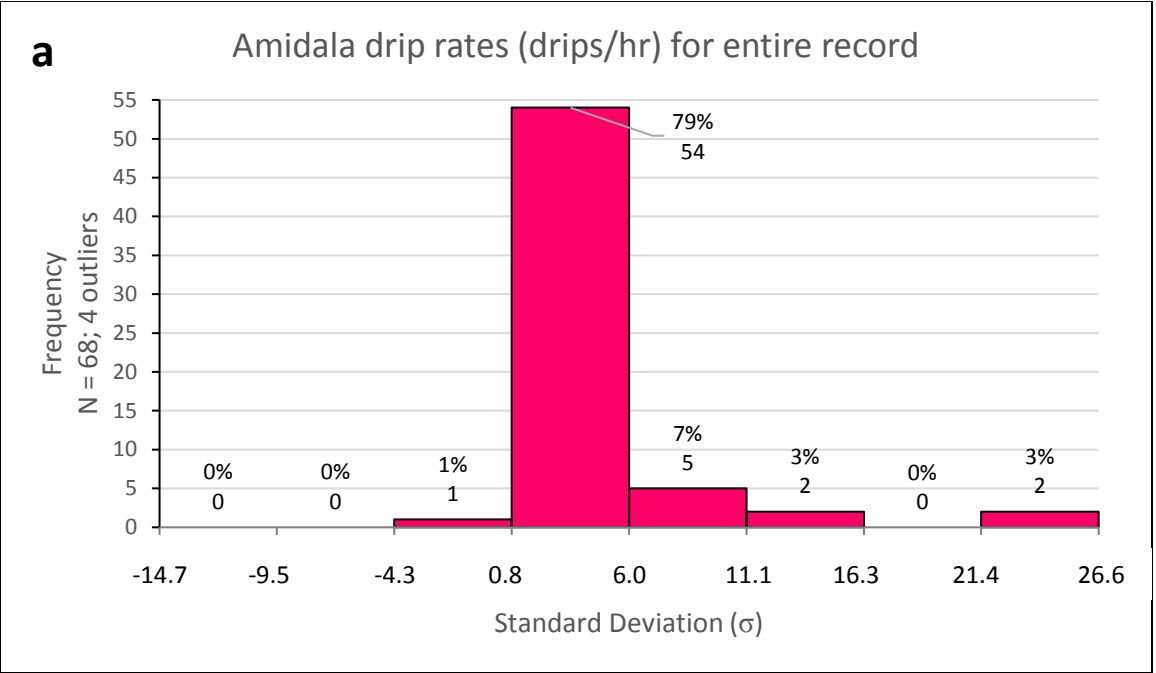


Figure 4.18 Amidala drip rate (drips per hour, pink) and dripwater flux (millimeters per day, black) versus AAFB rainfall (inches). Wet (Jun-Nov) and dry (Dec-May) seasons indicated with pale blue and pale yellow shading, respectively. Observed data plotted as solid circles. Inferred data is plotted as hollow circles. Events of interest are marked by a letter and discussed in the next section. Data regarded as suspect (1) and spurious (2) were plotted and circled. No cave visits are marked with grey hollow circles.



Amidala entire record
 $\mu = 6.0$
 $\sigma = 10.3$
 $0.5 \sigma = 5.2$

Amidala wet season
 $\mu = 3.8$
 $\sigma = 4.6$
 $0.5 \sigma = 2.3$

Amidala dry season
 $\mu = 8.0$
 $\sigma = 13.5$
 $0.5 \sigma = 6.7$

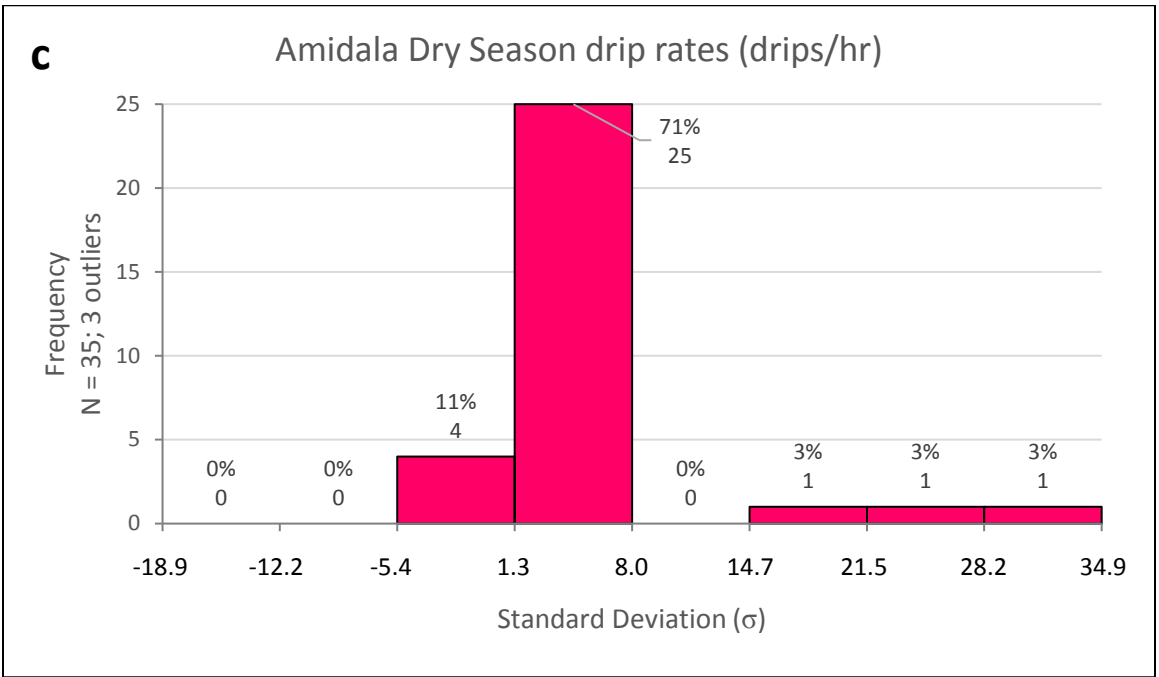
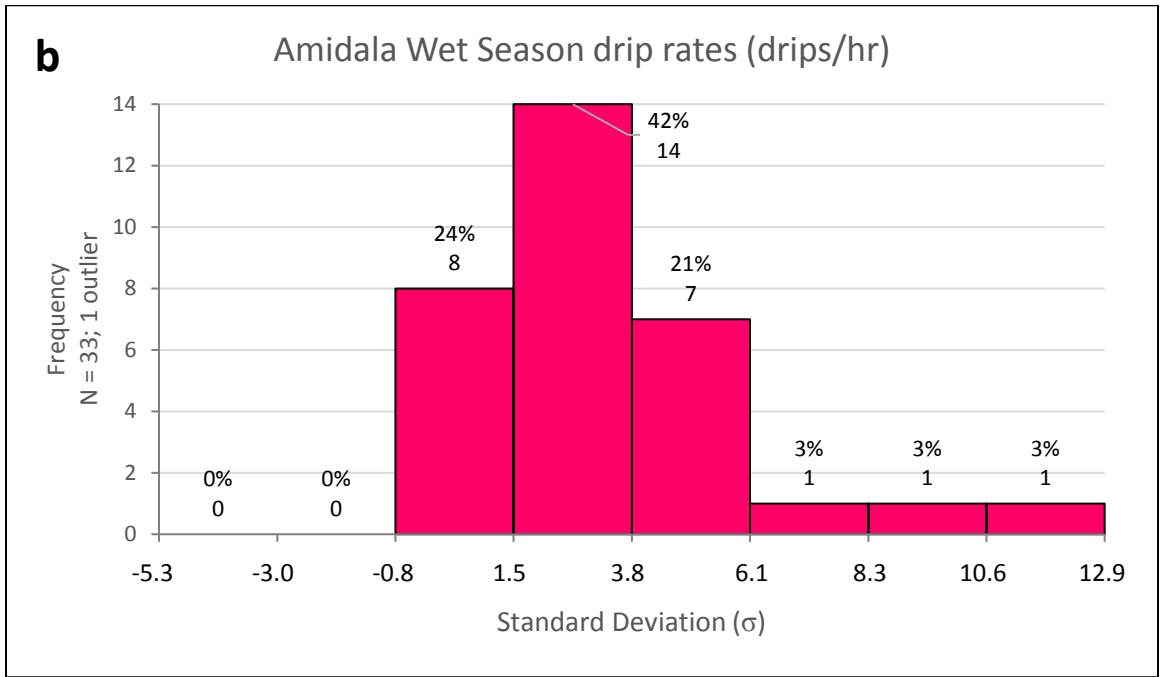


Figure 4.19 Frequency histograms of Amidala's a) drip rates for the entire record, b) wet season drip rates, and c) dry season drip rates $\pm 2 \sigma$ from respective means at $\pm 0.5 \sigma$ intervals.

4.4 Drip rate variability

Finally, to characterize the relative variability of drip rates between stations, I plotted relative (or normalized) standard deviation (coefficient of variation, $C_v = \sigma/\mu$) of the drip rate against the drip rate for each station. Figure 4.20 shows the plots for the entire record, wet seasons, and dry seasons. Relative standard deviation is plotted on the y-axis on a linear scale. Drip rate is plotted on the x-axis on a \log_{10} scale. (See Tables 4.2, 4.4, 4.5). Each graph is divided into four quadrants: (I) fast drip rate, high variability; (II) fast drip rate, low variability; (III) slow drip rate, low variability; and (IV) slow drip rate, high variability. The middle five stations (Figures 4.2, 4.3) – Flatman, Station 1, Station 2, Stumpy’s Brother, and Stumpy – are seen clustered together, spanning quadrants II and III. Flatman, plots in quadrant II, between 10^2 and 10^3 average drips/hr. Stumpy’s Brother, Station 1, and Station 2 plot in quadrant III between 10^1 and 10^2 average drips/hr. Note that Station 1, Station 2, and Stumpy’s Brother have similar drip rates, but variability ranges from ~0.1 to 0.8. Stumpy plots in quadrant II, but between 10^0 and 10^1 average drips/hr. Amidala and Trinity are outliers of this cluster. Amidala plots in quadrant IV (slow drip rate, high variability) between 10^0 and 10^1 average drips/hr, and ~1.7 relative standard deviation for the 2008-2016 record and dry season, and ~1.20 for the wet season. Trinity plots in quadrant II (fast drip rate, low variability), between 10^3 and 10^4 average drips/hr, with 0.4 relative standard deviation for the 2008-2016 record, 0.5 for the wet season, and 0.3 for the dry season.

By analyzing the differences or trends among graphed station drip-rates and rainfall (Figures 4.4, 4.8, 4.10, 4.12, 4.14, 4.16, and 4.18), frequency histograms by $\pm 0.5 \sigma$ intervals (Figures 4.7, 4.9, 4.11, 4.13, 4.15, 4.17, and 4.19), semi-log plots (Figures 4.28a, b, and c), field observations and records (all surface photos and Appendices A and B), and cave maps (Figures 4.1a, b, c, and d), inferences of each drip station’s dripwater discharge type (Table 5.1) and hydrologic pathways (Table 4.1) can be made.

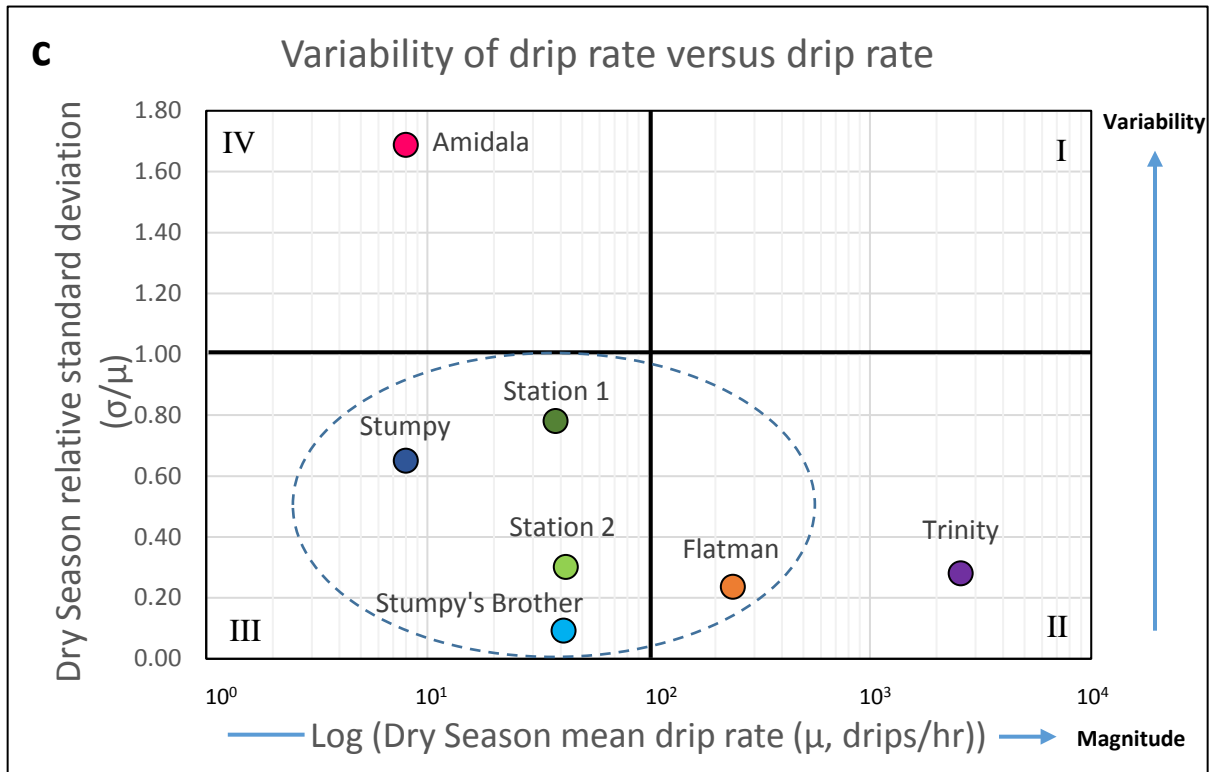
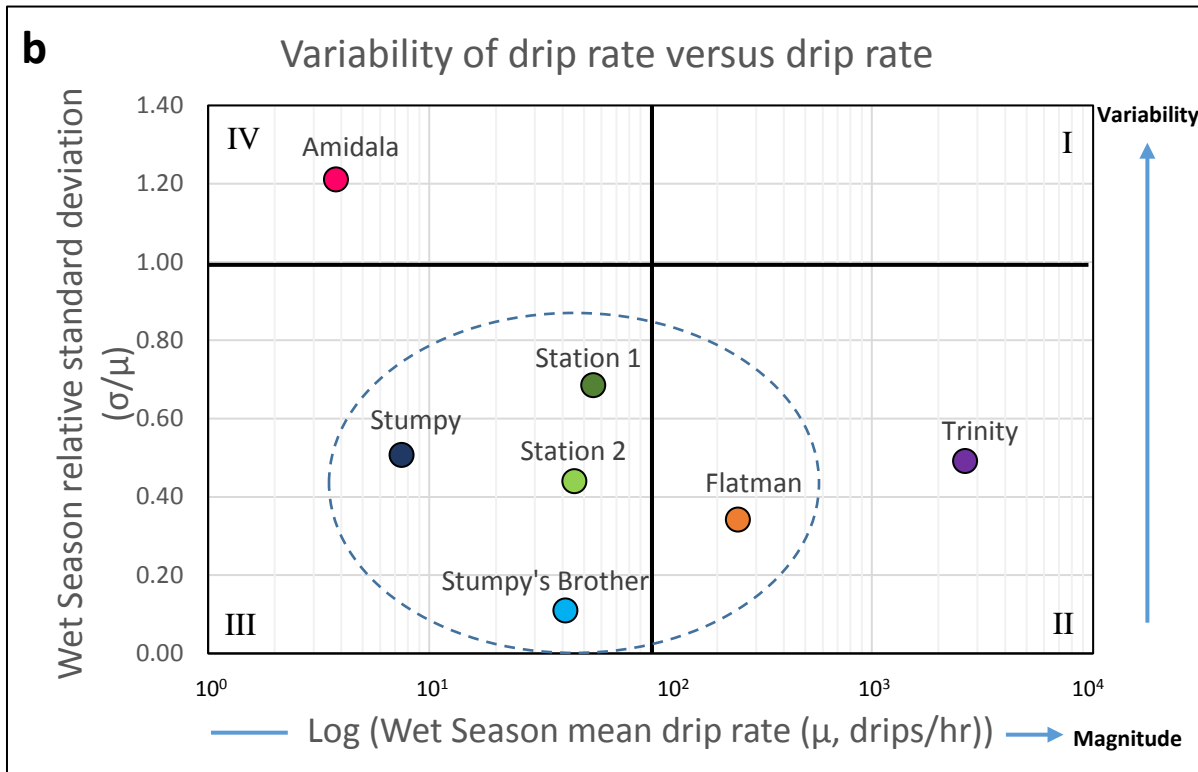
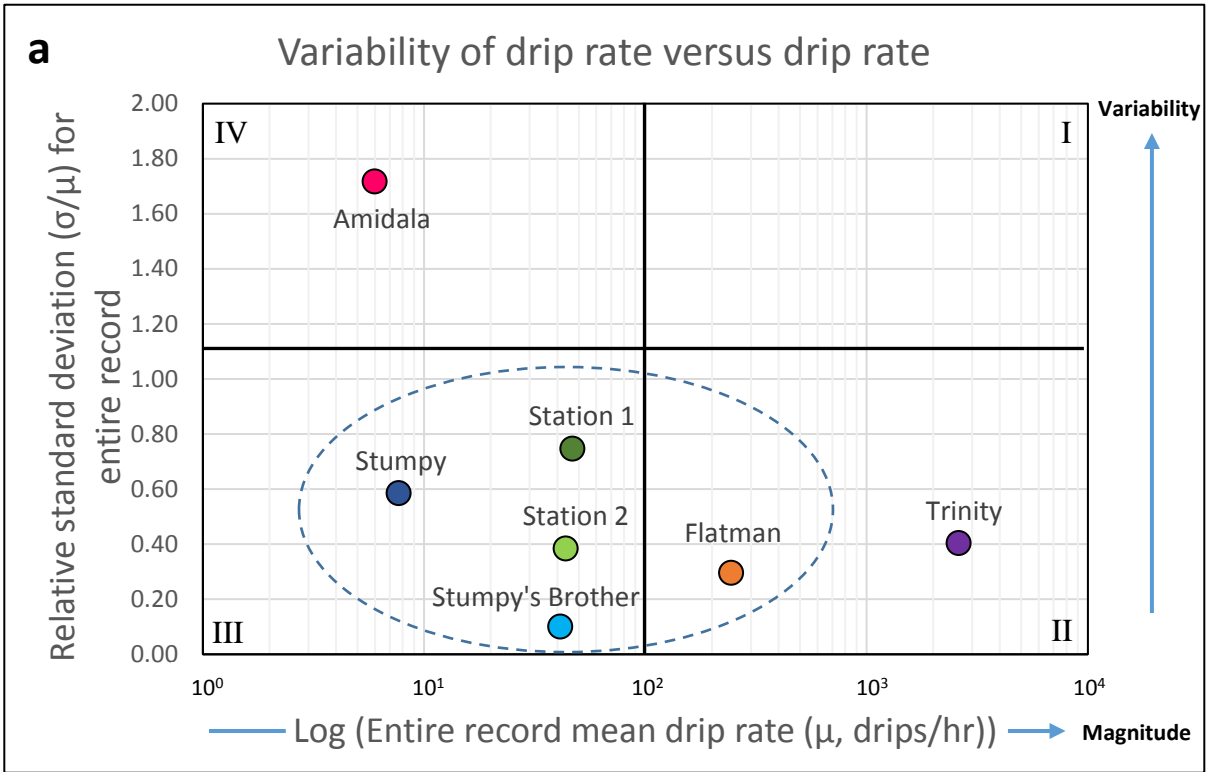


Figure 4.20 Semi-log plots of a) entire record mean drip rate (μ) versus entire record standard deviation (σ/μ), b) wet season mean drip rate versus wet season relative standard deviation, c) dry season mean drip rate versus dry season relative standard deviation.

DISCUSSION

5.1 Percolation Categorization

Previous high-resolution drip rate studies (e.g. Baker, Genty and Fairchild, 2000; Baker and Brundson, 2003; Tooth and Fairchild, 2003; Arbel et al., 2008, 2010; Matthey and Collister, 2008; Fernandez-Cortes, Calaforra and Sánchez-Martos, 2008; Miorandi et al., 2010; Sheffer et al., 2011; and Mahmud et al., 2015) have proposed general drip categories to infer percolation hydrologies based on drip rate, dripwater chemistry characteristics, or both. I've used three schemes to classify Jinapsan Cave drips taking into consideration the drip rates and vadose zone thickness (Figure 4.1d): (1) fast versus slow percolation (this study); (2) quick, intermediate, and slow flows (Sheffer et al. 2011); and (3) post-storm, overflow, seasonal, and perennial (Arbel et al. 2010) (Table 5.1).

For the first scheme, fast percolation is associated with high drip rates ($>10^2$ drips/hr). Drip rates with intervals greater than 5 minutes (or <10 drips/hr) are associated with slow percolation. For the second scheme (Sheffer et al. 2011), quick flow follows through preferred flow paths such as conduits (or enlarged fractures). Intermediate flow is through the fissure system. Slow flow percolates through the matrix. For the third scheme (Arbel et al. 2010), post-storm and overflow occurrences are high dripping rates and viewed initially as fast percolation, which gradually switch to either seasonal or perennial dripping. Seasonal drips have alternating fast and slow percolation based on seasonal rainfall input. Perennial drips are constant, and slow, regardless of seasonal rainfall input.

5.2 Fast percolation

5.2.1 Trinity

Trinity exhibits the fastest drip rate, with order of magnitude 10^3 . The drip rates show monotonic seasonality, generally rising rapidly near the end of the wet season (Figure 4.4). The drip forms along one of the major fractures in the ceiling of the Big Room (Figures 3.22, 4.1a). It is notable that there is no late-wet-season peak during the relatively dry wet season of 2010 (Event C). There are several notable responses (Events D to F), however, beginning with the wet season of 2011, when each wet season had one or more heavy rainfalls associated with storm passages (Table 4.7). These drip events suggest that the drip rate increases when infiltration is sufficient to fill fracture storage. The drip rate decreases as fracture storage is emptied. The minimum drip rates are probably produced from matrix storage that enters the fractures after fracture storage is exhausted.

Large stalagmites hang above, and columns occur by, a large dripstone mound present under this fracture. Trinity's stalagmite, however, is short. With an average of 10^3 drip rate and dripwater flux magnitude for the entire record (and 10^3 wet and dry season drip rate magnitude) (Figures 4.2 and 4.3), calcite doesn't precipitate well onto the stalagmite, as shown by its small size (Figures 3.20a, 3.21a and b).

Category			Diagnostic Characteristics	Station
This study	Sheffer et al. (2011)	Arbel et al. (2010)		
Fast Percolation Drip rate >10 ² drips/hr	Quick Flow	Post-storm	<ul style="list-style-type: none"> • Drips start a few hours after significant rainstorms • Reach maximum drip rates within 1-2 days, then decay after 2-3 weeks 	-
		Overflow	<ul style="list-style-type: none"> • Drips occur when perennial or season drip discharge capacities are exceeded and epikarst storage is completely filled and overflow 	Amidala
Slow Percolation <10 ² drips/hr	Intermediate Flow	Seasonal	<ul style="list-style-type: none"> • Dry during dry season • Dripping onset occurs after seasonal rainfall • Higher discharge rates and fluctuations than perennial drips • Longer recession • Drips continue between rain events 	Trinity Flatman Station 1 Station 2 Stumpy's Brother
		Perennial	<ul style="list-style-type: none"> • Drips discharge throughout year • Drip rates increase after season threshold • Low discharge • Long recession 	Amidala

Fastest
↑
↓
Slowest

Stumpy?

Table 5.1 Cave drip stations characterized by discharge types.

Trinity's wet and dry season frequency histograms also display the non-constant drip rate attributed to seasonal infiltration (Arbel et al. 2010) (Figures 4.7b and c). The wet season drip rates concentrated between -0.5 to -1σ below the mean (Figure 4.7b) are indicators of the previous dry season dripping: low drips/hr. The next, higher frequencies between 1 to 1.5σ above the mean (increasing drip rates) are most likely from the onset into wet season dripping after respective increasing rainfall infiltration. The left skew of the dry season histogram (Figure 4.7c) displays Trinity's low drip rates, which mostly come from gradual drawdown of water, if any, left over from the previous wet season.

On all three graphs of variability vs. drip rate (Figures 4.20a-c) Trinity plotted in quadrant II: fast magnitude-low relative variability. Infiltrating water may be distributed through an overlying fissure network feeding this fracture, producing large drip rates as water consistently flushes through this pathway. The opposite would be exhibited by a drip fed by a matrix pathway, where water gradually stored in overlying voids is drawn down faster as wet season or storm rainfall infiltrates through the pore spaces, and variations to potentially consistent data would be then observed by possible overflow occurrences (Amidala). Fracturing above the station could be an effect of possible (1) overlying bedrock fracturing from weight of fallen cliff talus (Figures 3.28a and b) and overlying boulder patch, (2) stress from ceiling breakdown in the Big Room (Figures 2.28 through 2.30), and (3) deep tree rooting from nearby *Ficus* trees above Flatman (Figure 4.1b).

Trinity's drip rate pattern of high drip rates during the wet season and low drip rates in the dry season is characteristic of a seasonal drip rate type (Arbel et al. 2010) (Table 5.1). The 10^3 order of magnitude for average drip rate (Figure 4.2), and quadrant II position, are indicative of fast percolation (quick flow, Sheffer et al. 2011). The station's observed situation among a fracture network indicates that hydrologic pathway is fracture-based (Table 4.1).

5.2.2 Flatman

Flatman's drip rate is an order of magnitude slower than Trinity's (10^2 vs. 10^3), but shows a stronger and more consistent season response (Events B, C, E, F, G, I, and K). There are some intra-seasonal fluctuations (A, D, H, and J, particularly during the dry seasons of 2011 (Event D) and 2014 (Event H), and 2015 (Event J) (Table 4.7 and Figure 4.8). The Flatman drip rate may be more sensitive to high-intensity rainfall events, particularly during the dry seasons.

The bimodality of Flatman's wet season histogram displays the dry season dripping into months of the wet season cycle (Figure 4.9b). One frequency peak, occurring below the mean, between -1 to -1.5σ , is this dry season low drip rates. The drip rate spike from wet season rainfall infiltration for half of this data occurs between 0.5 and 1σ , above the mean. The uniformity, with a slight left skew, of the dry season histogram until the highest frequency between 1 and 1.5σ is the typical dripping rate decrease into well below the dry season mean (Figure 4.9c). On all three graphs of relative variability vs drip rate Flatman plotted in quadrant II: high magnitude-low variability (Figures 4.20a-c).

A factor to the drip rate pattern relative to rainfall input could be fracturing in the limestone bedrock overlying Flatman's drip. The section (7.5 m) of overlying talus boulders on the slope surface above Flatman's stalactite is a potential influence (Figure 4.1b). Stress from the initial laying down of the boulders, and continued compaction after that, could have created fractures and fissure networks in the overlying bedrock. Seasonal and storm rainfall

would be drawn through this network quickly, as posited at Trinity's station. A closer observance of Flatman's stalactite and its surrounding area though is not possible given its ceiling height >4 m above the platform (Figure 3.10). From what can be seen, its situation among a stalactite cluster is an indicator it is, or has been, fed readily by some preferential pathway.

Flatman's pattern of low dripping in the dry season and gradual increase in the wet season, and responses to storm water infiltration, is characteristic of a seasonal drip type. Its position in quadrant II on the semi-log graphs, and 10^3 average drips/hr (Figure 4.2) for average dripping rate, proposes Flatman's inferred hydrologic pathway is categorized as fracture-fissure (Table 4.1), between fracture ($<10^4$) and fissure ($>10^2$), and percolation is considered as fast flow (Table 5.1).

5.2.3 Station 1

Station 1's drip rate is an order of magnitude slower than Flatman's (10^1 vs 10^2). This station shows remarkable intra-seasonal variability (Events D, F, I, K, and O) and shows occasional peaks of order of magnitude 10^2 (Events B and E), especially in the dry and wet seasons of 2011 (Table 4.7 and Figure 4.10). In the dry seasons of 2012, 2013, and 2016, the drip rate shuts down to $<10^1$ drips/hr. At the onset of the wet season, and seasonal rainfall infiltration increases, drip rate also increases.

Station 1's wet season histogram (Figure 4.11b) displays frequencies clustered close to the mean, which represents the faster drip rates associated with the larger volumes of rainfall infiltrated in the wet season. The dry season's histogram displays the highest frequency peak between -1 and -0.5 σ , and has a tail that extends above the mean to 2 σ (Figure 4.11c), consistent with the dry season dripping (low drip rates, and shut off drip mode). The dry season storm response events would be found in the tail, closer to +2 σ . These differences between wet and dry drip rates could be associated with the fracture network Station 1 is in. Wet season responses will be relative to rainfall infiltration amounts, which would produce varying drip rate magnitudes, dispersed into multiple frequency intervals. Dry season responses would be the opposite, with at least one major frequency below the mean, as drip rate significantly decreases relative to little rainfall infiltration. On all three graphs of relative variability vs drip rate, Station 1 plotted in quadrant III (Figures 4.20a-c).

Seasonality may partly be explained by the stalactite's association among an observed fracture system, with flowstone covering the east Shakey Room wall and part of the floor (Figure 3.13). Tree roots extending deep through the talus and limestone layers may also be attributed to opening preferential pathways, or, if large enough, as from a large limestone forest tree, possibly cause conduits to enlarge. Surface bedrock ledge observations of the ground directly above the Shakey Room (Appendix A.2) suggest a thin talus layer, possibly with large spaces between boulders, and a thicker bedrock layer influenced by sediment drawn down through vadose pathways by heavy rainfall events. This situation may also apply above the Stumpy Room, with the room center less than 3.5m upslope (eastward) of the Shakey Room (Figure 4.1a and c).

Station 1's drip rate pattern is seasonal since it exhibits slow drip rates in the dry season and faster drip rates in the wet season (Arbel et al. 2010). A 10^1 average drip rate (Figure 4.2) and position in quadrant III categorize Station 1's drip as medium flow (Table

5.1, Sheffer et al. 2011), with an inferred hydrologic pathway associated with a fissure network (Table 4.1), between fracture (fast flow) and matrix (slow flow) porosities.

5.2.4 Station 2

Station 2's drip rate began at an order of magnitude of 10^1 drips/hr at the start of the record, and shows steady decline thereafter, with the μ of 43.8 drips/hr for the period of the record. The drip rate pattern displays monotonic seasonal fluctuations throughout (Events A, C, D, E, and I), with some intra-seasonal fluctuations in the dry seasons of 2011 (Event B), 2014 (Event F), and 2015 (Events G and H) (Table 4.7 and Figure 4.12). It is possible this pattern is influenced by the fracture network associated with Station 1, however there is no observed connection to said network (Figures 3.14 and 3.15). Fractures (or enlarged fissures) closer to Station 1 seem to be the preferential pathways for percolating vadose water, and may be claiming water from Station 2's drip network, which could potentially explain the decreasing magnitudes of event drip rates (125 drips/hr and gradually decreases in range) regardless of storm rainfall amounts. At the ground surface, a thin talus layer of mostly boulder ledges with more spaces could allow heavy rain events to draw down high influxes of smaller sediment past the buried epikarst, potentially clogging fast flow pits into smaller fissure networks. If enough rerouting occurred, a muted seasonal response to rainfall input would happen. Such is observed after two storm events, Haikui (4.84 in) and Kirogi (4.73 in), which deposited storm rainfall in consecutive days. The drip rate's range reduces to ~35 drips/hr after these storms, and continues to plateau to a range of ~25 drips/hr until the end of the dataset, 2016.

Station 2's wet season histogram's (Figure 4.13b) highest frequency (48%) between right below the mean (-0.5 and 0σ), contains drip rates of transition between the dry season and the next wet season: from slow drips to fast drips, which are usually the maxima (peaks) indicating the transition. The 3 highest (24, 20, 24%) frequencies in the dry season histogram (Figure 4.13c), between -1 to 0.5σ contain the opposite: from fast wet season drips transitioning gradually to slower dry season drips. On all three semi-log graphs (Figures 4.20a-c), Station 2 plotted in quadrant III: low magnitude-low variability. Station 2's wet season variability (Figure 4.20b) is ~0.45, whereas the dry season's (Figure 4.20c) is ~0.3. This difference may be an effect of more varying wet season rainfall infiltration (and storm rainfall amounts) in contrast to the dry season's sparse rainfall (and storm passages).

Station 2's drip rate pattern is characteristic of seasonal drips (Arbel et al. 2010): slower (drier) drip rates during the dry season and faster (wetter) rates in the wet season (Table 5.1). Since this station's drip rate range has been ~25 drips/hr from late 2011 to the end of the dataset, its flow is considered intermediate (Sheffer et al. 2011). A 10^1 average drip rate, dripping slower than that influenced by a fracture but faster than those fed by the matrix (Figure 4.2), and the position in quadrant III, infer Station 2's hydrologic pathway as small fissure-fed (Table 4.1). Percolation is thus categorized as medium (Table 5.1) based on the station's lower order of drip rate magnitude, low variability, and decreasing drip rate trend.

5.2.5 Stumpy's Brother

Stumpy's Brother drip rate is the third station with an average drip rate at an order magnitude of 10^1 drips/hr (Figure 4.2). Its drip pattern is monotonic seasonal (Events A, C, E, F, I, and J) with some intra-seasonal variability in the 2010 wet season through 2011 dry

season (Event B) (Table 4.7 and Figure 4.14) and 2014 and 2015 dry seasons (G and H). The fluctuations between wet and dry season drip rates is not a stark contrast as previous seasonal stations: Trinity, Flatman, and Stations 1 and 2. There is a slight steady decrease in drip rate from ~12 drips/hr to ~10 drips/hr across the period of record.

Drip rate maxima in the wet season do not exceed a magnitude of 10^1 drips/hr despite varying amounts of rainfall. The average number of days of drip rate maxima following a storm event is 51, with the shortest ~14 days (Event H), and at most ~116 days (Event G). The intra-seasonal event, “B” has a drip rate range which varies between 6 and 10 drips/hr. Interestingly it occurs during the driest of the wet-dry seasons in the data record, where we would expect to see a consecutive slow drip rates.

Stumpy Brother’s wet season histogram (Figure 4.15b) has two pronounced clusters of frequencies, 11% (-1 to -1 σ) and 22% (-0.5 and 0.5 σ). The 11% frequency contains the drip rates from the end of the dry season. The other end contains the fastest drip rate responses. For this season, majority of the drip rates linger close to the mean, 41.3 drips/hr. The dry season (Figure 4.10c) displays the contrast: majority of the dry season drip rates are clumped between -0.5 and 1 σ . The intra-seasonal peaks occur at the upper end of the histogram, closer to 2 σ . On all three semi-log graphs (Figures 4.20a-c) Stumpy’s Brother is in quadrant III: low magnitude (10^1 drips/hr)-low variability (~0.1), the smallest drip rate variation among the seven stations.

Stumpy’s Brother has a drip rate pattern characteristic of a seasonal drip rate (Arbel et al. 2010) – slow during the dry season and faster dripping after seasonal rainfall infiltration in the wet season (Table 5.1). With an average drip rate of 10^2 (Figure 4.2) and position in quadrant III, this station’s flow is considered intermediate flow (Sheffer et al. 2011). Percolation is considered medium, and inferred hydrologic pathway by small fissures.

5.3 Slow Percolation

5.3.1 Stumpy

Stumpy is the next slowest drip rate, an order of magnitude less than Stumpy’s Brother (10^0 vs 10^1) (Figure 4.2). It displays a remarkably irregular drip rate pattern over the eight-year record. The first half of the dataset has drip rate variations up to 2012, then changes to a seasonal pattern in the second half, to 2016. Events B, E, G, H, and K are distinctly seasonal drip rate maxima, each occurring after a storm passage during the wet season (Table 4.7 and Figure 4.16). They are ~ 10^1 drip rate magnitude, and average ~35 days for drip rate response. Between Events B and C, C to D, and F to G, a pattern of monthly alternating peaks and troughs that steadily decrease are observed, with a drip rate range that also decreased from ~7 to ~5 drips/hr. This occurrence between B and C, and C to D, may be lag responses drawn into the following dry season caused by Typhoon Nida rainfall infiltration. The 2011 dry season slow drip rates are what is expected during a dry to wet season transition, where there is a response lag into the wet season, before a response from wet season infiltration. The occurrence between Events F and G is a second drip rate pattern of monthly alternating peaks and troughs. It begins ~3 months after Tropical Storm Talas, and may also be a lag response drawn into the dry season. Event I is an intra-seasonal drip response to Tropical Depression Lingling, which occurred in the dry season of 2014. Event J is another intra-seasonal response, to Vongfong.

Stumpy’s wet season histogram (Figure 4.17b) exhibits a frequency cluster between -0.5 and 1.5 σ . This cluster shows the wet season peaks at the right end, then majority of the

season drip rates right above the mean. A second cluster is at the left side of the histogram, which represent the amount of drip rates close to shut off mode (<10 drips/hr). In the dry season (Figure 4.17c) half of the drip rates (50%) are within $+0.5\sigma$ of the μ , with the rest in the tail that skews to -2σ . This single mode represents drip rates from the second half of the dataset (2012 to 2016), which has a smaller range. Stumpy plots in quadrant III of the variability vs rate graphs (Figure 4.20 a-c): slow drip rate (10^0 drips/hr)-low variability (between ~ 0.5 to ~ 0.65).

Stumpy shares a similar boulder ledge surface and thin talus and thick bedrock layers as the Shakey Room stations (Appendix A.2), however its irregular drip pattern makes it difficult to accurately associate the station into specific drip rate, and flow, types. Events B, E, G, H, and K can be associated with seasonal dripping (Arbel et al. 2010) (Figure 5.1), and given the slow drip rate magnitude (10^0 drips/hr), flow types for these events would be associated with slow flow (Sheffer et al. 2011). By the station's position on the variability vs rate graphs, percolation could be associated as slow, with an inferred hydrologic pathway of small fissures. The three volatile drip rate variations however, are patterns that have yet to be identified into drip and flow types. Therefore, the Stumpy station cannot accurately be associated with the drip and flow types in Figure 5.1.

5.3.2 Amidala

Amidala is the last and slowest of the drip stations, with an order of magnitude $<10^0$ drips/hr (Figure 4.2). Its drip data is remarkably slow and steady despite intensity between the wet and dry seasons (range >8 drips/hr) (Figure 4.18). Events A, B, and C are three drip rate responses an order of magnitude larger than the rest of the dataset, increasing from 1×10^1 drips/hr to 4.5×10^1 drips/hr. Event A occurs at the beginning of the 2011 wet season, which followed a wet-dry cycle of no storm passages or large rainfall (>4 inches). It may be the first overflow drip response (Arbel et al. 2010) (Table 5.1), which occurs when drip discharge capacities are exceeded and epikarst storage is completely filled and overflow. The response lag is ~ 1.5 years from Typhoon Nida. Event B is the second drip rate response associated with overflow, 109 days lag from Tropical Storm Talas (Table 4.7). Event C is the third overflow response, 140 days lag from Typhoon Haikui, and 137 days lag from Tropical Storm Kirogi. This event is the largest in magnitude (4.5×10^1 drips/hr), and occurred after two consecutive storms, 3 days apart. The drip rate then steeply decreases back to a range of <5 drips/hr from 2013 wet season. Despite multiple storm passages and varying rainfall infiltration amounts, Amidala's drip rate remained <5 drips/hr until the end of the dataset in 2015.

Amidala's wet season histogram (Figure 4.19b) has a sole frequency cluster (total 87%) between ~ 0 to 6.1 drips/hr, (-1 to 0.5σ). Majority of this season's drip rates is close to its mean, 3.8 drips/hr. The rest of the data (>6.1 drips/hr) is in the tail, skewed to the right. The dry season (Figure 4.19c) has one large frequency (71%) between 1.3 and 8. drips/hr, (-1 to 0σ), right below the mean. This season also has a tail that skews to the right. Both histograms display that Amidala's drip rates are consistently slow ($>10^0$ drips/hr), with few faster drip rates. These faster drip rates, contained in each histogram tail (and outliers beyond $+2\sigma$) are associated with the overflow responses of events A, B, and C. On all three variability vs. drip rate graphs (Figures 4.20a-c) Amidala plot in quadrant IV: slow drip rate-high variability. The wet season's variability (Figure 4.20b) is ~ 1.2 , whereas the dry season's (Figure 4.20c) is larger, ~ 1.7 , which is consistent with the station's unequal

overflow responses between seasons. There is one overflow response (Event A) in the wet season, and two responses (B and C) in the dry.

Amidala's low order of magnitude (10^0) for average drip rate associates its drip as perennial by its slow and consistent discharge despite seasonal rainfall changes (Arbel et al. 2010) (Table 5.1), and partly classified into overflow by drip rates observed in events A, B, and C. Flow type is considered as slow flow during the slow consistent discharge, and fast flow at overflow events (Sheffer et al. 2011). Percolation to Amidala's stalactite can thus be inferred as generally matrix-controlled (slow) flow (Table 4.1).

5.4 Relationship to the NGLA

Dynamics of the seven studied drip sites in Jinapsan Cave, formed in Mariana limestone and later buried by talus of a retreating Mariana cliff, provide new insights into the relationship between epikarst-vadose infiltration and groundwater recharge of the NGLA. These stations exhibited three types of percolation: (1) quick (fast), (2) intermediate (moderate/medium), or (3) slow. Drip rate patterns were characterized into types: seasonal, perennial, or overflow drips. These seasonal trends and drip rate categories help karst scientists gain insight to the vadose zone complexities on Guam. The triple-porosity observed at this cave site is only a very small representation of the larger Mariana Limestone unit. More hydrogeologic studies of caves on Guam can further our understanding of percolation through the Mariana Limestone, and potentially Guam's other limestone units. By understanding percolation patterns in the vadose zone, models can be produced to quantify recharge of the aquifer.

Figure 5.1 is a general conceptual model of a vadose zone over limestone aquifers. At the top is the weathered limestone surface; at the bottom is a cave ceiling. At the cave ceiling two drip rates, slow and fast, are discharging from stalactites. Each drip rate and drip volume is affected by the dominant storage porosities of the overlying vadose zone: (1) matrix storage or (2) fissure storage. Based on season, infiltrating rainfall amounts differ. The wet season has more rainfall, which can infiltrate through the weathered surface into fissures and storage. Dry season infiltration barely occurs since plants and root systems uptake what little rain falls on the ground surface. These varying rainfall amounts drive the two types of percolation: (1) slow percolation and (2) fast percolation.

Arbel et al.'s (2010) perennial drips and slow seasonal drips, and Sheffer et al.'s (2011) slow flow are grouped into slow percolation ($<10^2$ drips/hr) (Table 5.1), which has been observed in Amidala (perennial), Station 1 (slow seasonal), and possibly also for Stumpy in the last third of the data record (slow seasonal) (Arbel et al. 2010). Water in the matrix moves slowly from pores, out of storage, into nearby pores or fissures. After possibly months (or years) of movement through the matrix (or fissures) water is discharged slowly at a stalactite. For Amidala, this is proposed, as observed by its drip, regardless of season and rainfall amounts. For Station 1 (and Stumpy) this was observed during the dry season.

Arbel et al.'s (2010) fast seasonal drips, and Sheffer et al.'s (2011) quick flow are grouped in fast percolation ($>10^2$ drips/hr) (Table 5.1). This type of percolation has been observed as fast seasonal drips in Trinity, Flatman, Station 1, Station 2, and Stumpy's Brother, and overflow drip responses in Amidala. Rainwater saturating at the weathered surface infiltrates into the vadose zone through small fissures. The further water moves (horizontally or vertically) through the vadose, decreasing fissure density and increasing fissure apertures increases water movement rate and volume, especially at fissure

intersections. This fissure dominant storage above a dripping stalactite promotes faster dripping rates.

Arbel et al.'s (2010) post-storm drips and overflow drips (Sheffer et al.'s quick flow, 2011) is also grouped into fast percolation. Post-storm drips can only be determined by high resolution (continuous) sampling, which this study did not conduct, and thus has not observed. Overflow was observed by Amidala's three events, which detoured from its consistent perennial drip pattern. A schematic to explain the porosity pathway for Amidala's overflow drips is uncertain.

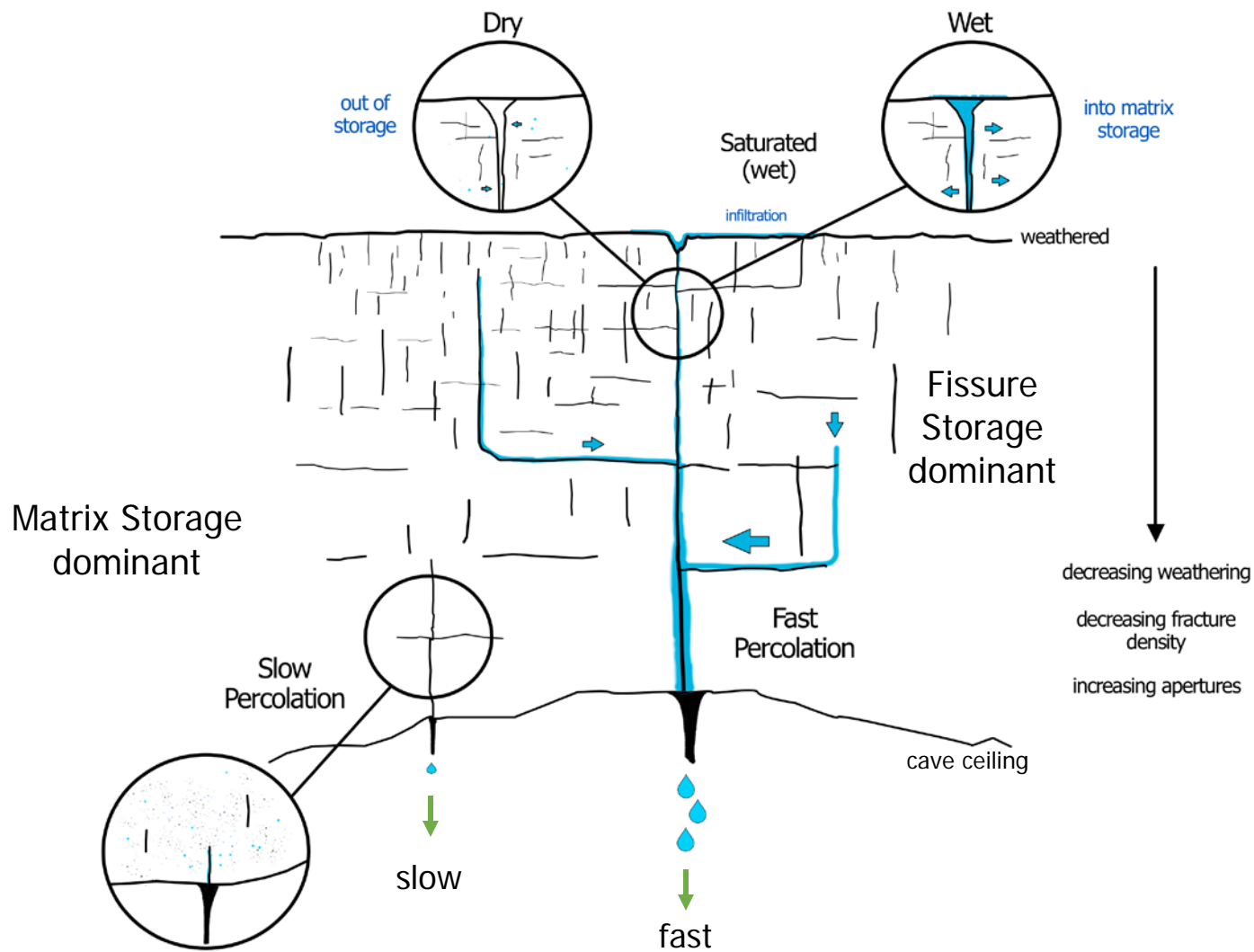


Figure 5.1 Conceptual model of vadose percolation.

SUMMARY and CONCLUSION

6.1 Summary

Ground surface and cave surveys and observations and drip rate (drips/hr) and dripwater flux (mL/day) data from seven drip stations in Jinapsan Cave, in northern Guam, were analyzed for percolation patterns (perennial, seasonal, post-storm, and overflow) to rainfall events over ~6 wet-dry season cycles. Datasets from September 2008 through September 2016 were plotted for observed (recorded) and inferred (calculated) monthly data points. Events of interest were labeled by a letter. Data determined to be suspect or spurious were also plotted and labeled. No cave visits were also marked. Graphs also show wet (Jun-Nov) and dry (Dec-May) cycles, daily rainfall (inches), and storm events that dropped significant rainfall over the island. Semi-log graphs of average drip rate and relative variation were produced to aid in categorizing stations drips into inferred hydrologic pathways: fracture (fast flow), fracture-fissure (fast flow), small fissure (medium flow), and matrix (slow flow).

6.2 Conclusion

Six stations (Trinity, Flatman, Station 1, Station 2, Stumpy's Brother, and Stumpy) exhibited seasonal drip responses to seasonal wet-dry rainfall infiltration and several responses associated with storm events. Amidala's drip displayed mostly perennial dripping, with several overflow occurrences. Inferred hydrologic pathways were: Trinity - fracture flow; Flatman – fracture-fissure flow; Station 1, Station 2, and Stumpy's Brother - fissure flow; and Stumpy and Amidala - matrix flow.

Recommendations for future analysis:

- Comparison of $d^{18}O$ rainfall and dripwater analysis with drip rate (event water vs. storage water)
- Comparison of Cl^- dripwater analysis with drip rate (typhoon sea spray washing out)
- Comparison of drip rate dynamics with calcite growth rates
- High resolution drip rate sampling (acoustic drip counters)

REFERENCES

- Arbel, Y. et al. 2008. Hydrologic classification of cave drips in a Mediterranean climate, based on hydrograph separation and flow mechanisms. *Israel Journal of Earth Sciences*, Vol. 57. DOI: 10.1560/IJES.57.3.-4.291.
- Arbel, Y. et al. 2010. Infiltration processes and flow rates in developed karst vadose zone using tracers in cave drips. *Earth Surface Processes and Landforms*, Vol. 35, 1682-1693. DOI: 10.1002/esp.2010.
- Baker, A. and C. Brundson. 2003. Non-linearities in drip water hydrology: an example from Stump Cross Caverns, Yorkshire. *Journal of Hydrology*, Vol. 277, p. 151-163. DOI: 10.1016/S0022-1694(03)00063-5.
- Baker, A., D. Genty, and I. J. Fairchild. 2000. Hydrological characterisation of stalagmite dripwaters at Grotte de Villars, Dordogne, by the analysis of inorganic species and luminescent organic matter. *Hydrology of Earth System Sciences*, 4(3), p. 439-449.
- Contractor, D. and J. W. Jenson. 2000. Simulated effects of vadose infiltration on water levels in the Northern Guam Lens Aquifer. *J. of Hydrology*, DOI: 10.1016/S0022-1694(00)00157-8.
- Dasher, G.R. 1994. *On Station*. First ed. National Speleological Society, Inc. Huntsville, Alabama. 242 p.
- Dillon, P. 1997. Groundwater pollution by sanitation on tropical islands. International Hydrological Programme of UNESCO, Paris, IHP-V Project 6-1.
- Fernandez-Cortes, A., Calaforra, J. M, and F. Sánchez-Martos. 2008. Hydrogeochemical processes as environmental indicators in drip water: Study of the Cueva del Agua (Southern Spain). *International Journal of Speleology* 31(1), p. 41-52. Bologna, Italy. ISSN: 0392-6672.
- Fetter, Charles W. 2001. *Applied hydrogeology*. Fourth ed. Prentice Hall. Upper Saddle River, NJ. 598 p.
- Ford, D. C and P. Williams. 2007. *Karst hydrogeology and geomorphology*. Second ed. John Wiley & Sons Ltd. West Sussex, England. 562 p.
- Gingerich, Stephen B. 2003. *Hydrologic Resources of Guam*. U. S. Geologic Survey Water-Resources Investigations Report 03-4126.
- Guam Waterworks Authority. 2014. *Citizen-Centric Report for Fiscal Year 2014*. Issue August 2015. Mangilao, Guam.
- Gulley, J. D. et al. 2015. Heterogeneous distributions of CO₂ may be more important for dissolution and karstification in coastal eogenetic limestone than mixing dissolution. *Earth Surf. Process. Landforms*. 15 p.
- Hong Kong Observatory 2016. *Tropical Cyclones in 2015*. Kowloon, Hong Kong. DOI: 551.515.2:551.506.1(512.317). 116 p.

- Jenson, J. W. et al. 2006. Karst of the Mariana Islands: the interaction of tectonics, glacio-eustasy, and freshwater/saltwater mixing in island carbonates. Chapter in Special Paper of the Geological Sciences of America, DOI: 10.1130/2006.2404(11).
- Jocson, J. et al. 2002. Recharge and aquifer response: Northern Guam Lens Aquifer, Guam, Mariana Islands. *Journal of Hydrology* 260. 231-254.
- Joint Typhoon Warning Center 2009. Annual Tropical Cyclone Report. Grant A. Cooper, Captain, U.S. Navy Commanding Officer. Pearl Harbor, Hawaii. 109 p.
- Joint Typhoon Warning Center 2011. Annual Tropical Cyclone Report. Michael. D. Angove, Captain, U.S. Navy Commanding Officer. Pearl Harbor, Hawaii. 108 p.
- Joint Typhoon Warning Center 2012. Annual Tropical Cyclone Report. Ashley D. Evans, Captain, U.S. Navy Commanding Officer. Pearl Harbor, Hawaii. 118 p.
- Joint Typhoon Warning Center 2013. Annual Tropical Cyclone Report. Ashley D. Evans, Captain, U.S. Navy Commanding Officer. Pearl Harbor, Hawaii. 144 p.
- Joint Typhoon Warning Center 2014. Annual Tropical Cyclone Report. Steven P. Sopko, Captain, U.S. Navy Commanding Officer. Pearl Harbor, Hawaii. 104 p.
- Jones, I. C. and J. L. Banner. 2003. Estimating recharge thresholds in tropical karst island aquifers: Barbados, Puerto Rico and Guam. *Journal of Hydrology* 278. 131-143. DOI: 10.1016/S0022-1694(03)00138-0.
- Lander, M. A. et al. 2001. Responses of well water levels on Northern Guam to variations of rainfall and sea level. Technical Report No. 94, Water and Environmental Research Institute of the Western Pacific, University of Guam, Mangilao. 42 p.
- Lander, M. A. personal communication. February 22, 2017.
- Luckman, B.H. 2013. Talus slopes. Permafrost and Periglacial Features in *Encyclopedia of Quaternary Science*. 2nd Ed. Vol. 3, pp 566-573.
- Mahmud, K. et al. 2016. Estimation of deep infiltration in unsaturated limestone environments using cave lidar and drip count data. *Hydrol. Earth Syst. Sci.*, 20, 359-373. DOI: 10.5194/hess-20-359-2016.
- McCann, S.C. 2013. Atmospheric influences on cave meteorology, Jinapsan Cave, Guam: A drip rate analysis. Master's thesis, Mississippi State University. 488 p.
- Miklavič, Blaž. 2011. Formation of geomorphic features as a response to sea-level change at Ritidian Point, Guam, Mariana. Master's thesis, Mississippi State University. 218 p.
- Mink, J.F. and Vacher, H.L. 1997. Hydrogeology of Northern Guam. In: Vacher, H.L. and Quinn, T., Eds., *Geology and Hydrogeology of Carbonate Islands*, Elsevier Science, Amsterdam, 743-761.
- Myroie, J. E. et al. 1999. Karst geology and hydrology of Guam: a preliminary report. Technical Report No. 89, Water and Environmental Research Institute of the Western Pacific, University of Guam, Mangilao. 37 p.

- Myroie, J. E. and Jenson, J. W. 2000. The carbonate island karst model applied to Guam. *Theoretical and Applied Karstology*, 13-14.pp 51-56.
- Myroie, J. R. and J. E. Myroie. 2007. Development of the carbonate island karst model. *Journal of cave and karst studies*, v. 69, no. 1, p. 59-75.
- Myroie, J. E., et al. 2001. Karst features of Guam in terms of a general model of carbonate island karst. *Journal of cave and karst studies* 63(1): 9-22.
- Myroie, J. E. et al. 2012. Unpublished Jinapsan Cave surface map and cross sections.
- Nimmo J R. (2009) Vadose Water. In: Gene E. Likens, (Editor) *Encyclopedia of Inland Waters*. Volume 1, pp. 766-777 Oxford: Elsevier.
- Osborne, R. A. L. 2002. Cave breakdown by vadose weathering. *Int. J. of Speleol.*, 31 (1/4): 37-53.
- Palmer, Arthur N. 2007. *Cave geology*. Cave Books, Dayton, OH. 454 p.
- Partin, J. W., et al. 2012. Relationship between modern rainfall variability, cave dripwater, and stalagmite geochemistry in Guam, USA, *Geochem. Geophys. Geosyst.*, 13, Q03013, DOI:10.1029/2011GC003930.
- Rotzol, K., et al. 2013. Estimating hydraulic properties from tidal attenuation in the Northern Guam Lens Aquifer, territory of Guam, USA. *Hydrogeology Journal*. 17 p. DOI:10.1007/s10040-012-0949-9.
- Sanders, D., M. Ostermann, and J. Kramers. 2009. Quarternary carbonate-rocky talus slope successions (Eastern Alps, Austria): sedimentary facies and facies architecture. *Facies*. 55: 345-373.
- Schlanger, S. O. 1964. Petrology of the limestones of Guam with a section of petrography of the insoluble residues by J. C. Hathaway and D. Carroll. U.S. Geol. Survey Prof. Paper 403-D: 52 p. & 21 plts.
- Sheffer, N. A. et al. 2011. Integrated drip monitoring for epikarst recharge estimation in a dry Mediterranean area, Sif Cave, Israel. *Hydrological Processes*. Wiley Online Library. DOI: 10.1002/hyp.8046. 9 p.
- Sinclair, D. J., et al. 2012. Magnesium and strontium systematics in tropical speleothems from the Western Pacific. *Chemical Geology*, 294-295.pp 1-17.
- Taboroši, Danko. 2004. *Field guide to caves and karst of Guam*. Bess Press: Honolulu, Hawaii. 105 p.
- Taboroši, D. et al. 2004. Karst features of Guam Mariana Islands. Technical Report No. 104, Water and Environmental Research Institute of the Western Pacific, University of Guam, Mangilao. 29 p.
- Taboroši, D. et al. 2005. Karst features of Guam, Mariana Islands. *Micronesica* 38(1): 17-46.
- Taboroši, Danko. 2006. Karst Inventory of Guam, Mariana Islands. Tech. Report 112. Water and Environmental Research Institute of the Western Pacific, University of Guam. 231 p.
- Taboroši, D. et al. 2008. Unpublished Jinapsan Cave map.

- Taboroši, Danko. 2013. Environments of Guam. First Edition. Bess Press: Honolulu, Hawaii. 145 p.
- Tooth, A. and I. J. Fairchild. 2003. Soil and karst aquifer hydrological controls on the geochemical evolution of speleothem-forming drip waters, Crag Cave, southwest Ireland. *Journal of Hydrology* 273, p. 51-68.
- Tracey, J.I., et al. 1964. General geology of Guam: U.S. Geological Survey Professional Paper 403-A, 104 p., 3 pl.
- Tribble, G. 2008. Ground water on tropical pacific islands- understanding a vital resource. U.S. Geological Survey, Circular 1312, 35 p.
- United Nations Educational, Scientific and Cultural Organization (UNESCO). 1991. Hydrology and water resources of small islands: a practical guide. Edited by A. Falkland. International Hydrological Programme, IHP-III, Project 4.6. France. 453 p.
- United States Environmental Protection Agency (USEPA). 2000. Sole Source Aquifer Designations in EPA, Region 9. Region 9 Groundwater Office (WTR-9).
- Williams, P. W. 2008. The role of epikarst in karst and cave hydrogeology: a review. *International Journal of Speleology*, 37 (1), 1-10. Bologna (Italy). ISSN 0392-6672.
- Worthington, S. R. H. 1999. A comprehensive strategy for understanding flow in carbonate aquifers. *Karst Modeling*, special publication 5, Karst Waters Institute, Charles Town, WV, pp. 30-7.

APPENDIX A.1 – Jinapsan Ground Surface and Cave Surveys

Vegetation 1 - 6/5/2014 - Kaylyn Bautista, John Jenson, John Mylroie, Joan Mylroie

KaylynThesis.DAT - Cave Editor 32

File Surveys Heading Shots Block Options Help

Select Survey | Edit Heading | Edit Survey


#	From	To	Tape	Comp	Inc	Left	Right	Up	Down	Flags	Comment
1	V1	V2	5.1m.	156.0	-3.0	0.0m.	0.0m.	0.0m.	0.0m.		V2 on boulder
2	V2	V3	5.0m.	169.0	-4.0	0.0m.	0.0m.	0.0m.	0.0m.		
3	V3	V4	5.0m.	156.5	-5.5	0.0m.	0.0m.	0.0m.	0.0m.		V3 by tree stump
4	V4	V5	5.2m.	154.5	1.5	0.0m.	0.0m.	0.0m.	0.0m.		V5 on cycad
5	V5	V6	5.0m.	171.0	-2.0	0.0m.	0.0m.	0.0m.	0.0m.		
6	V6	V7	5.0m.	155.5	3.0	0.0m.	0.0m.	0.0m.	0.0m.		
7	V7	V8	5.0m.	219.0	10.0	0.0m.	0.0m.	0.0m.	0.0m.		
8	V8	V9	5.0m.	240.0	3.0	0.0m.	0.0m.	0.0m.	0.0m.		
9	V8	V10	5.5m.	301.0	31.0	0.0m.	0.0m.	0.0m.	0.0m.		distance is along slope
10	V10	V11	5.3m.	310.0	14.0	0.0m.	0.0m.	0.0m.	0.0m.		second big boulder
11	V9	V12	5.1m.	323.0	8.0	0.0m.	0.0m.	0.0m.	0.0m.		trying to go around boulders
12	V12	V13	5.3m.	323.0	20.0	0.0m.	0.0m.	0.0m.	0.0m.		goes through gap
13	V13	V14	5.2m.	334.0	-22.0	0.0m.	0.0m.	0.0m.	0.0m.		backsite compass and inclination
14	V14	V15	5.1m.	9.5	-8.0	0.0m.	0.0m.	0.0m.	0.0m.		had to go around boulders to get within ~10 meter
15	V15	V16	5.1m.	357.0	6.0	0.0m.	0.0m.	0.0m.	0.0m.		
16	V16	V17	5.4m.	65.0	-21.0	0.0m.	0.0m.	0.0m.	0.0m.		V17 on ground; flag is on tree though
17	V17	V3	4.5m.	75.0	-7.0	0.0m.	0.0m.	0.0m.	0.0m.		closes first loop
18	V16	V18	5.0m.	3.5	1.0	0.0m.	0.0m.	0.0m.	0.0m.		V18 is close to scarp
19	V18	V19	5.1m.	336.0	15.0	0.0m.	0.0m.	0.0m.	0.0m.		V19 flag is on tree
20	V19	V20	4.9m.	65.0	-25.0	0.0m.	0.0m.	0.0m.	0.0m.		
21	V20	V1	4.9m.	70.0	-11.0	0.0m.	0.0m.	0.0m.	0.0m.		closes second loop
22	V20	V21	4.9m.	158.0	-5.0	0.0m.	0.0m.	0.0m.	0.0m.		
23	V17	V22	4.8m.	155.0	-6.0	0.0m.	0.0m.	0.0m.	0.0m.		had to raise V22 stadia rod up by 60 cm to match V17 stadia height
24	V22	V23	5.0m.	153.0	-1.0	0.0m.	0.0m.	0.0m.	0.0m.		
25	V23	V24	5.0m.	168.5	2.0	0.0m.	0.0m.	0.0m.	0.0m.		V24 will distort quad shape
26	V24	V11	7.2m.	259.0	42.0	0.0m.	0.0m.	0.0m.	0.0m.		distance of slope; measured distance is not projected length
27	V24	V10	5.6m.	204.0	43.0	0.0m.	0.0m.	0.0m.	0.0m.		distance of slope; not projected length
28											
29											

Vegetation 2 - 6/23/2014 - Kaylyn Bautista, John Joseph Bautista, Rawlin Manzanilla, Nicole Raphael

KaylynThesis.DAT - Cave Editor 32

File Surveys Heading Shots Block Options Help

Select Survey Edit Heading Edit Survey



#	From	To	Tape	Comp	Inc	Right	Up	Down	Left	Flags	Comment
1	V1	V25	5.0m.	351.0	1.0	0.0m.	0.0m.	0.0m.	0.0m.		
2	V25	V26	5.0m.	351.0	4.0	0.0m.	0.0m.	0.0m.	0.0m.		
3	V26	V27	5.2m.	356.0	12.0	0.0m.	0.0m.	0.0m.	0.0m.		
4	V27	V28	5.0m.	342.0	8.0	0.0m.	0.0m.	0.0m.	0.0m.		
5	V28	V29	5.0m.	342.0	11.0	0.0m.	0.0m.	0.0m.	0.0m.		
6	V29	V30	4.6m.	347.0	10.0	0.0m.	0.0m.	0.0m.	0.0m.		
7	V30	V31	5.0m.	250.0	23.0	0.0m.	0.0m.	0.0m.	0.0m.		
8	V31	V32	5.0m.	160.0	-17.0	0.0m.	0.0m.	0.0m.	0.0m.		Station 32 on the rock
9	V32	V29	5.1m.	58.0	-17.0	0.0m.	0.0m.	0.0m.	0.0m.		
10	V32	V33	5.0m.	162.0	-15.0	0.0m.	0.0m.	0.0m.	0.0m.		Station 33 on the rock
11	V33	V28	4.6m.	61.0	-16.0	0.0m.	0.0m.	0.0m.	0.0m.		
12	V33	V34	4.9m.	165.0	-13.0	0.0m.	0.0m.	0.0m.	0.0m.		
13	V34	V27	4.6m.	68.0	-30.0	0.0m.	0.0m.	0.0m.	0.0m.		
14	V34	V35	5.0m.	161.0	-9.0	0.0m.	0.0m.	0.0m.	0.0m.		
15	V35	V26	4.5m.	61.0	-17.0	0.0m.	0.0m.	0.0m.	0.0m.		
16	V35	V36	5.0m.	167.0	-16.0	0.0m.	0.0m.	0.0m.	0.0m.		
17	V36	V25	4.2m.	64.0	-9.0	0.0m.	0.0m.	0.0m.	0.0m.		
18	V36	V20	5.0m.	180.0	2.0	0.0m.	0.0m.	0.0m.	0.0m.		
19											
20											

Vegetation 3 - 7/7/2014 - Kaylyn Bautista, John Joseph Bautista, Nicole Raphael, Lee Ana Dela Cruz, Maria Procalla

KaylynThesis.DAT - Cave Editor 32

File Surveys Heading Shots Block Options Help

Select Survey Edit Heading Edit Survey

#	From	To	Tape	Comp	Inc	Left	Right	Up	Down	Flags	Comment
1	V14	V40	5.0m.	240.0	16.0	0.0m.	0.0m.	0.0m.	0.0m.		
2	V40	V41	5.0m.	328.0	33.0	0.0m.	0.0m.	0.0m.	0.0m.		
3	V41	V42	5.0m.	330.0	26.5	0.0m.	0.0m.	0.0m.	0.0m.		
4	V42	V43	5.0m.	329.0	17.0	0.0m.	0.0m.	0.0m.	0.0m.		
5	V43	V44	5.0m.	242.0	22.0	0.0m.	0.0m.	0.0m.	0.0m.		station is tied to a small rock
6	V44	V45	5.0m.	150.0	-16.0	0.0m.	0.0m.	0.0m.	0.0m.		
7	V45	V46	5.0m.	242.0	28.0	0.0m.	0.0m.	0.0m.	0.0m.		
8	V46	V47	5.0m.	332.0	21.0	0.0m.	0.0m.	0.0m.	0.0m.		cairn is on the side of a boulder
9	V47	V48	5.0m.	334.0	4.5	0.0m.	0.0m.	0.0m.	0.0m.		station is on top of rubble
10	V48	V49	5.0m.	332.0	17.0	0.0m.	0.0m.	0.0m.	0.0m.		
11	V49	V50	5.0m.	241.0	29.0	0.0m.	0.0m.	0.0m.	0.0m.		tree is flagged
12	V50	V51	5.0m.	331.0	23.0	0.0m.	0.0m.	0.0m.	0.0m.		station 51 is in a boulder hole
13	V51	V52	5.0m.	242.0	21.0	0.0m.	0.0m.	0.0m.	0.0m.		
14	V52	V53	5.0m.	354.0	10.0	0.0m.	0.0m.	0.0m.	0.0m.		
15	V53	V54	5.0m.	332.0	14.0	0.0m.	0.0m.	0.0m.	0.0m.		next to a wasps nest
16											
17											
18											
19											

Vegetation 4 - 7/15/2014 - Kaylyn Bautista, John Joseph Bautista, Lee Ana Dela Cruz

KaylynThesis.DAT - Cave Editor 32

File Surveys Heading Shgts Block Options Help

Select Survey | Edit Heading | Edit Survey

#	From	To	Tape	Comp	Inc	Left	Right	Up	Down	Flags	Comment
1	V1	V55	5.0m.	60.5	-7.5	0.0m.	0.0m.	0.0m.	0.0m.		
2	V55	V56	5.0m.	62.0	-9.0	0.0m.	0.0m.	0.0m.	0.0m.		
3	V56	V57	5.0m.	329.0	7.5	0.0m.	0.0m.	0.0m.	0.0m.		cairn at base of tree
4	V57	V58	5.0m.	237.5	3.0	0.0m.	0.0m.	0.0m.	0.0m.		
5	V58	V55	4.3m.	146.0	-3.0	0.0m.	0.0m.	0.0m.	0.0m.		
6	V58	V25	3.2m.	250.0	11.0	0.0m.	0.0m.	0.0m.	0.0m.		
7	V26	V59	5.0m.	60.0	-8.0	0.0m.	0.0m.	0.0m.	0.0m.		
8	V59	V58	6.2m.	184.0	-4.0	0.0m.	0.0m.	0.0m.	0.0m.		
9	V59	V60	5.0m.	61.5	-2.5	0.0m.	0.0m.	0.0m.	0.0m.		
10	V60	V57	5.7m.	188.0	-4.0	0.0m.	0.0m.	0.0m.	0.0m.		
11	V30	V61	5.0m.	70.0	-14.0	0.0m.	0.0m.	0.0m.	0.0m.		had to make a new stadia rod = 1.44 meters
12	V61	V62	5.0m.	158.5	-12.5	0.0m.	0.0m.	0.0m.	0.0m.		
13	V62	V29	5.3m.	257.0	17.0	0.0m.	0.0m.	0.0m.	0.0m.		
14	V62	V63	5.0m.	168.5	-7.5	0.0m.	0.0m.	0.0m.	0.0m.		
15	V63	V28	5.0m.	259.0	12.5	0.0m.	0.0m.	0.0m.	0.0m.		
16	V63	V64	5.0m.	159.0	-6.0	0.0m.	0.0m.	0.0m.	0.0m.		cairn at tree base
17	V64	V27	5.0m.	253.5	12.0	0.0m.	0.0m.	0.0m.	0.0m.		
18	V64	V59	4.0m.	175.5	-14.5	0.0m.	0.0m.	0.0m.	0.0m.		
19	V35	V37	5.0m.	240.0	21.0	0.0m.	0.0m.	0.0m.	0.0m.		
20	V37	V38	5.0m.	240.0	25.5	0.0m.	0.0m.	0.0m.	0.0m.		
21	V38	V39a	5.0m.	240.0	24.0	0.0m.	0.0m.	0.0m.	0.0m.		station in rock hole
22	V39a	V39b	5.0m.	240.0	23.0	0.0m.	0.0m.	0.0m.	0.0m.		station by micro station
23	V39b	V65	5.0m.	235.0	34.0	0.0m.	0.0m.	0.0m.	0.0m.		
24	V65	V66	5.0m.	243.5	27.5	0.0m.	0.0m.	0.0m.	0.0m.		
25	V66	V67	5.0m.	242.0	26.0	0.0m.	0.0m.	0.0m.	0.0m.		next to boulder
26	V67	V51	6.1m.	259.0	36.0	0.0m.	0.0m.	0.0m.	0.0m.		
27	V67	V49	3.0m.	149.0	-11.0	0.0m.	0.0m.	0.0m.	0.0m.		
28											
29											

Vegetation 5 - 7/18/2014 - Kaylyn Bautista, Holly Leon Guerrero, Nicole Raphael, Lee Ana Dela Cruz

KaylynThesis.DAT - Cave Editor 32

File Surveys Heading Shots Block Options Help

Select Survey Edit Heading Edit Survey


#	From	To	Tape	Comp	Inc	Left	Right	Up	Down	Flags	Comment
1	V2	V21	4.6m.	245.0	10.0	0.0m.	0.0m.	0.0m.	0.0m.		
2	V21	V18	4.3m.	250.0	14.0	0.0m.	0.0m.	0.0m.	0.0m.		
3	V21	V17	4.4m.	175.0	-10.5	0.0m.	0.0m.	0.0m.	0.0m.		
4	V3	V17	4.4m.	256.0	6.0	0.0m.	0.0m.	0.0m.	0.0m.		
5	V4	V22	4.5m.	255.0	6.0	0.0m.	0.0m.	0.0m.	0.0m.		
6	V5	V23	4.6m.	256.0	3.0	0.0m.	0.0m.	0.0m.	0.0m.		
7											
8											
9											
10											
11											
12											
13											
14											

Vegetation 6 - 7/25/2014 - Kaylyn Bautista, Lee Ana Dela Cruz, Kaitlyn Santos

KaylynThesis.DAT - Cave Editor 32

File Surveys Heading Shgts Block Options Help

Select Survey Edit Heading Edit Survey



#	From	To	Tape	Comp	Inc	Left	Right	Up	Down	Flags	Comment
1	V37	V68	5.0m.	330.0	15.0	0.0m.	0.0m.	0.0m.	0.0m.		base of tree
2	V68	V69	4.9m.	330.0	20.0	0.0m.	0.0m.	0.0m.	0.0m.		
3	V69	V70	5.0m.	330.0	29.0	0.0m.	0.0m.	0.0m.	0.0m.		
4	V70	V32	9.4m.	60.0	-28.0	0.0m.	0.0m.	0.0m.	0.0m.		
5	V69	V33	8.2m.	60.0	-22.0	0.0m.	0.0m.	0.0m.	0.0m.		
6	V68	V34	6.5m.	63.0	-22.0	0.0m.	0.0m.	0.0m.	0.0m.		
7	V68	V71	5.0m.	240.0	25.5	0.0m.	0.0m.	0.0m.	0.0m.		
8	V71	V38	4.8m.	150.0	-15.0	0.0m.	0.0m.	0.0m.	0.0m.		
9	V38	V72	5.0m.	150.0	-18.0	0.0m.	0.0m.	0.0m.	0.0m.		
10	V72	V73	4.5m.	60.0	-22.0	0.0m.	0.0m.	0.0m.	0.0m.		
11	V73	V36	4.6m.	70.0	-33.0	0.0m.	0.0m.	0.0m.	0.0m.		passes over cave entrance
12	V73	V19	5.6m.	194.0	2.0	0.0m.	0.0m.	0.0m.	0.0m.		
13	V73	V37	4.8m.	340.0	16.0	0.0m.	0.0m.	0.0m.	0.0m.		
14	V72	V74	5.0m.	240.0	23.0	0.0m.	0.0m.	0.0m.	0.0m.		large cairn
15	V39a	V74	5.0m.	151.0	-19.0	0.0m.	0.0m.	0.0m.	0.0m.		
16	V74	V75	5.0m.	150.0	-23.0	0.0m.	0.0m.	0.0m.	0.0m.		flag tied to tree root
17	V75	V76	4.9m.	146.0	4.0	0.0m.	0.0m.	0.0m.	0.0m.		ended day at V76
18											
19											
20											
21											
22											
23											

Vegetation 7 - 9/15/2014 - Kaylyn Bautista, John Jenson, Tim Righetti

KaylynThesis.DAT - Cave Editor 32

File Surveys Heading Shots Block Options Help

Select Survey Edit Heading Edit Survey



#	From	To	Tape	Comp	Inc	Left	Right	Up	Down	Flags	Comment
1	V70	V77	5.0m.	329.0	24.0	0.0m.	0.0m.	0.0m.	0.0m.		parallel to small dropoff
2	V77	V31	12.0m.	56.0	-29.0	0.0m.	0.0m.	0.0m.	0.0m.		extends over small cliff dropoff
3	V78	V31	5.3m.	148.0	-23.0	0.0m.	0.0m.	0.0m.	0.0m.		back sight; heading to rain collector
4	V79	V78	4.9m.	150.0	-22.0	0.0m.	0.0m.	0.0m.	0.0m.		back sight
5	V80	V79	5.4m.	150.0	-31.0	0.0m.	0.0m.	0.0m.	0.0m.		station on boulder 1 meter from ground
6	V81	V80	5.2m.	149.0	-22.0	0.0m.	0.0m.	0.0m.	0.0m.		station on boulder 70 cm from ground
7	V80	V82	5.0m.	233.0	-12.0	0.0m.	0.0m.	0.0m.	0.0m.		back sight; going along scarp on downhill side
8	V83	V82	5.0m.	349.0	14.0	0.0m.	0.0m.	0.0m.	0.0m.		base of small cliff 1 meter from ground
9	V84	V83	5.2m.	334.0	17.0	0.0m.	0.0m.	0.0m.	0.0m.		back sight
10	V77	V84	5.2m.	1.0	-3.0	0.0m.	0.0m.	0.0m.	0.0m.		back sight
11	V85	V54	5.0m.	141.0	-26.0	0.0m.	0.0m.	0.0m.	0.0m.		back sight
12	V86	V85	5.2m.	146.0	-18.0	0.0m.	0.0m.	0.0m.	0.0m.		back sight
13	V87	V86	5.0m.	148.5	-18.0	0.0m.	0.0m.	0.0m.	0.0m.		back sight
14	V88	V87	5.2m.	143.5	-20.0	0.0m.	0.0m.	0.0m.	0.0m.		back sight
15	V89	V88	5.7m.	151.5	-20.0	0.0m.	0.0m.	0.0m.	0.0m.		back sight
16	V90	V89	5.4m.	147.0	-18.0	0.0m.	0.0m.	0.0m.	0.0m.		back sight
17	V91	V90	5.2m.	139.5	-30.0	0.0m.	0.0m.	0.0m.	0.0m.		back sight
18	V91	V92	5.1m.	62.5	-38.0	0.0m.	0.0m.	0.0m.	0.0m.		descending the slope
19	V92	V93	5.0m.	63.0	-25.0	0.0m.	0.0m.	0.0m.	0.0m.		
20	V93	V94	5.4m.	44.0	-28.0	0.0m.	0.0m.	0.0m.	0.0m.		
21	V94	V95	5.1m.	55.0	-20.0	0.0m.	0.0m.	0.0m.	0.0m.		
22	V95	V96	5.0m.	53.0	-26.0	0.0m.	0.0m.	0.0m.	0.0m.		
23	V96	V97	4.7m.	63.0	-24.5	0.0m.	0.0m.	0.0m.	0.0m.		at base of boulder 2 meters high from the ground; end for the day
24											
25											
26											

Vegetation 8 - 9/29/2014 - Kaylyn Bautista, John Jenson, Tim Righetti

KaylynThesis.DAT - Cave Editor 32

File Surveys Heading Shots Block Options Help

Select Survey Edit Heading Edit Survey


#	From	To	Tape	Comp	Inc	Left	Right	Up	Down	Flags	Comment
1	V98	V82	5.3m.	63.0	-22.0	0.0m.	0.0m.	0.0m.	0.0m.		back sight
2	V99	V98	4.9m.	53.0	-25.0	0.0m.	0.0m.	0.0m.	0.0m.		back sight
3	V100	V99	5.0m.	58.5	-23.0	0.0m.	0.0m.	0.0m.	0.0m.		back sight
4	V101	V100	4.9m.	65.0	-24.0	0.0m.	0.0m.	0.0m.	0.0m.		back sight
5	V102	V101	5.0m.	53.0	-25.0	0.0m.	0.0m.	0.0m.	0.0m.		back sight
6	V103	V102	5.1m.	55.5	-27.0	0.0m.	0.0m.	0.0m.	0.0m.		back sight
7	V88	V103	6.7m.	27.8	-18.0	0.0m.	0.0m.	0.0m.	0.0m.		back sight
8	V103	V104	5.7m.	154.5	-9.5	0.0m.	0.0m.	0.0m.	0.0m.		
9	V104	V105	4.9m.	130.0	-31.0	0.0m.	0.0m.	0.0m.	0.0m.		
10	V105	V106	5.4m.	160.0	-14.0	0.0m.	0.0m.	0.0m.	0.0m.		
11	V106	V107	5.2m.	136.0	-22.0	0.0m.	0.0m.	0.0m.	0.0m.		
12	V107	V108	5.2m.	162.0	-15.0	0.0m.	0.0m.	0.0m.	0.0m.		
13	V108	V67	5.2m.	175.0	-4.0	0.0m.	0.0m.	0.0m.	0.0m.		
14	V109	V83	6.0m.	65.0	-32.0	0.0m.	0.0m.	0.0m.	0.0m.		back sight
15	V110	V109	6.2m.	58.0	-22.0	0.0m.	0.0m.	0.0m.	0.0m.		back sight
16	V111	V110	5.2m.	61.0	-27.0	0.0m.	0.0m.	0.0m.	0.0m.		back sight
17	V112	V111	5.1m.	62.5	-28.0	0.0m.	0.0m.	0.0m.	0.0m.		back sight
18	V112	V104	7.1m.	42.0	-22.0	0.0m.	0.0m.	0.0m.	0.0m.		back sight
19	V105	V113	7.3m.	61.0	-26.0	0.0m.	0.0m.	0.0m.	0.0m.		
20	V113	V114	6.7m.	63.0	-21.0	0.0m.	0.0m.	0.0m.	0.0m.		
21	V114	V115	5.2m.	81.0	-31.0	0.0m.	0.0m.	0.0m.	0.0m.		
22	V115	V77	6.6m.	88.0	-33.0	0.0m.	0.0m.	0.0m.	0.0m.		end for the day
23											
24											

Vegetation 9 - 9/30/2014 - Kaylyn Bautista, John Jenson, Xiao Wei, Brytney Miller

KaylynThesis.DAT - Cave Editor 32

File Surveys Heading Shots Block Options Help

Select Survey Edit Heading Edit Survey



#	From	To	Tape	Comp	Inc	Left	Right	Up	Down	Flags	Comment
1	V71	V116	5.0m.	335.0	15.0	0.0m.	0.0m.	0.0m.	0.0m.		flag at base of rocks/boulder
2	V116	V117	5.3m.	317.0	32.0	0.0m.	0.0m.	0.0m.	0.0m.		1m step after V116 to get to V117
3	V117	V115	7.1m.	326.5	24.0	0.0m.	0.0m.	0.0m.	0.0m.		
4	V39a	V118	6.3m.	332.0	15.0	0.0m.	0.0m.	0.0m.	0.0m.		
5	V118	V119	6.1m.	322.0	27.0	0.0m.	0.0m.	0.0m.	0.0m.		
6	V119	V120	5.1m.	324.0	24.0	0.0m.	0.0m.	0.0m.	0.0m.		
7	V120	V114	6.3m.	322.0	24.0	0.0m.	0.0m.	0.0m.	0.0m.		
8	V113	V121	5.3m.	148.0	-21.0	0.0m.	0.0m.	0.0m.	0.0m.		going slightly downhill along contour
9	V121	V122	5.1m.	143.0	-18.0	0.0m.	0.0m.	0.0m.	0.0m.		
10	V122	V123	4.7m.	148.0	-13.0	0.0m.	0.0m.	0.0m.	0.0m.		
11	V123	V124	4.7m.	138.0	-46.0	0.0m.	0.0m.	0.0m.	0.0m.		station flag tied to tree root
12	V124	V39b	4.5m.	114.0	-28.0	0.0m.	0.0m.	0.0m.	0.0m.		end day
13											
14											
15											
16											

Big Room - 1/22/2016 - Kaylyn Bautista, John Joseph Bautista, Brytney Miller

KaylynThesis.DAT - Cave Editor 32

File Surveys Heading Shots Block Options Help

Select Survey Edit Heading Edit Survey



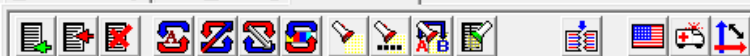
#	From	To	Tape	Comp	Inc	Left	Right	Up	Down	Flags	Comment
1	C1	C2	3.8m.	275.5	-31.0	0.0m.	0.0m.	2.4m.	0.6m.		0.00
2	C2	C3	2.6m.	210.5	-21.0	0.0m.	0.0m.	1.8m.	1.0m.		
3	C3	C4	5.3m.	252.5	-12.0	0.0m.	0.4m.	2.1m.	1.3m.		
4	C4	C5	2.6m.	191.0	0.5	0.0m.	0.3m.	0.2m.	1.0m.		
5	C5	C6	3.4m.	153.0	0.5	0.0m.	0.9m.	0.6m.	0.8m.		
6	C6	C7	3.1m.	142.5	4.0	0.0m.	1.8m.	1.5m.	0.9m.		
7	C7	C8	1.2m.	108.5	-2.0	0.0m.	1.2m.	0.9m.	0.8m.		
8	C8	C9	3.1m.	58.5	32.0	0.0m.	0.0m.	0.2m.	0.8m.		
9	C9	C10	1.0m.	87.5	14.0	0.0m.	0.0m.	0.9m.	1.2m.		
10	C10	C11	2.4m.	102.5	18.0	0.0m.	0.0m.	0.4m.	1.0m.		
11	C11	C12	4.8m.	112.0	25.0	0.0m.	0.0m.	0.9m.	0.9m.		
12	C11	C13	4.2m.	45.0	40.0	0.0m.	0.2m.	1.2m.	1.1m.		
13	C13	C14	3.7m.	83.5	24.0	0.0m.	0.0m.	2.8m.	1.0m.		
14	C14	C15	5.4m.	133.5	21.0	2.6m.	2.5m.	2.8m.	1.0m.		
15	C14	C16	6.2m.	340.5	-11.5	2.6m.	2.5m.	2.8m.	1.0m.		
16	C15	C17	6.1m.	91.0	42.5	2.1m.	1.5m.	1.9m.	1.4m.		
17	C16	C1	4.3m.	330.0	-28.0	0.0m.	0.0m.	2.8m.	2.5m.		
18	C16	C18	3.5m.	241.0	-44.0	0.0m.	0.0m.	2.8m.	2.5m.		
19	C18	C20	4.0m.	291.6	24.7	0.0m.	0.5m.	4.4m.	1.8m.		
20	C20	C3	2.7m.	281.0	-14.0	0.0m.	0.0m.	4.0m.	1.2m.		
21	C18	C19	2.5m.	244.0	-44.0	0.0m.	0.0m.	4.4m.	1.8m.		
22	C14	C19	4.1m.	304.0	-36.0	2.5m.	2.6m.	2.8m.	1.0m.		
23	C19	Trinity	5.3m.	257.5	0.5	6.6m.	5.7m.	4.2m.	1.3m.		
24	Trinity	C6	4.9m.	45.3	1.4	7.3m.	4.5m.	1.2m.	0.7m.		
25											
26											

Slide - 1/28/2016 - Kaylyn Bautista, Brytney Miller, Erin Miller

KaylynThesis.DAT - Cave Editor 32

File Surveys Heading Shots Block Options Help

Select Survey Edit Heading Edit Survey



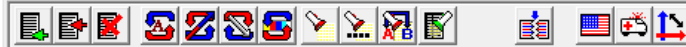
#	From	To	Tape	Comp	Inc	Left	Right	Up	Down	Flags	Comment
1	C21	C1	8.8m.	300.0	-27.0	2.3m.	2.1m.	3.5m.	0.6m.		
2	C21	C22	7.0m.	150.0	23.0	0.0m.	0.0m.	0.0m.	0.0m.		
3	C22	C23	3.3m.	98.5	34.0	3.0m.	0.5m.	3.1m.	0.9m.		
4	C23	C17	2.6m.	193.5	20.0	2.2m.	1.9m.	3.0m.	0.8m.		
5	C24	C17	3.9m.	260.0	-45.0	0.7m.	2.4m.	1.1m.	0.0m.		
6	C21	C25	3.3m.	43.0	45.0	0.0m.	0.0m.	0.0m.	0.0m.		
7	C25	Flatman	1.7m.	39.0	10.0	1.4m.	2.2m.	2.2m.	2.2m.		
8	Flatman	C26	2.6m.	320.0	23.0	5.5m.	0.4m.	4.0m.	0.6m.		
9	C26	C27	6.0m.	60.5	29.0	0.0m.	0.0m.	1.8m.	0.8m.		
10	C27	C28	2.6m.	121.0	32.0	0.6m.	1.9m.	0.9m.	0.9m.		
11	C28	C29	3.6m.	40.0	28.0	3.4m.	0.0m.	1.5m.	1.0m.		
12	C29	C30	4.3m.	187.5	-2.5	1.9m.	1.5m.	1.4m.	1.5m.		
13	C30	C31	4.6m.	47.5	7.0	0.0m.	0.9m.	1.4m.	0.9m.		
14	C30	C32	4.4m.	113.5	22.0	4.9m.	0.9m.	1.6m.	1.0m.		
15											
16											
17											
18											

Stumpy - 2/16/2016 - Kaylyn Bautista, John Joseph Bautista, Brytney Miller

KaylynThesis.DAT - Cave Editor 32

File Surveys Heading Shots Block Options Help

Select Survey Edit Heading Edit Survey




#	From	To	Tape	Comp	Inc	Left	Right	Up	Down	Flags	Comment
1	C35	Amidala	2.0m.	254.0	-21.0	1.4m.	0.5m.	0.9m.	0.8m.		
2	C35	Shakey	3.6m.	139.0	42.0	1.5m.	0.0m.	0.9m.	0.8m.		
3	Amidala	Brother	1.2m.	192.6	6.0	1.6m.	0.4m.	0.7m.	0.8m.		
4	Brother	Stumpy	0.4m.	151.0	1.0	1.9m.	0.9m.	1.1m.	0.7m.		
5	Stumpy	C36	2.8m.	92.0	55.0	1.6m.	0.7m.	1.3m.	0.8m.		
6	C36	C37	0.8m.	1.5	44.0	0.2m.	0.2m.	0.5m.	1.0m.		
7	C37	Shakey	1.8m.	63.0	10.0	0.5m.	0.6m.	0.4m.	0.8m.		
8	Shakey	S1	1.0m.	76.0	17.0	0.6m.	0.9m.	0.6m.	0.0m.		
9	C38	Shakey	3.0m.	351.0	-42.0	1.1m.	0.9m.	1.4m.	0.9m.		
10	C38	C39	3.7m.	58.0	38.0	0.0m.	0.9m.	1.4m.	0.9m.		
11	C39	C40	1.3m.	131.0	46.0	0.0m.	0.9m.	1.0m.	1.7m.		
12	C40	C41	2.5m.	210.0	32.0	0.0m.	1.6m.	3.7m.	1.7m.		
13	C41	C42	1.5m.	179.0	3.0	0.7m.	0.3m.	1.1m.	0.3m.		
14	C42	C43	3.2m.	240.0	-37.0	0.5m.	0.4m.	0.4m.	2.0m.		
15	C44	C43	1.2m.	333.0	-29.0	1.1m.	1.5m.	0.9m.	0.9m.		
16	C45	C43	2.6m.	70.0	-18.0	2.5m.	1.0m.	0.9m.	0.8m.		
17	C43	C46	2.7m.	336.0	-26.0	3.6m.	2.5m.	1.1m.	0.9m.		
18	C38	C46	2.1m.	220.0	9.0	0.4m.	1.2m.	2.3m.	0.8m.		
19	C46	C47	4.1m.	264.0	-27.0	1.6m.	1.6m.	1.4m.	0.8m.		
20	C47	C48	3.4m.	207.5	5.0	1.5m.	0.5m.	1.0m.	0.7m.		
21	C48	C49	2.6m.	197.0	10.0	2.4m.	0.5m.	1.6m.	1.4m.		
22	C50	C49	4.2m.	270.0	-27.0	1.0m.	0.8m.	1.1m.	0.9m.		
23	C50	C45	3.5m.	70.0	37.0	1.0m.	1.5m.	1.1m.	0.9m.		
24	C45	C26	4.0m.	190.0	0.0	1.0m.	2.5m.	0.9m.	0.8m.		
25	C49	C51	5.0m.	227.0	-20.0	3.1m.	1.9m.	1.1m.	1.6m.		
26	C51	C1	1.5m.	147.0	-38.0	1.2m.	0.9m.	1.0m.	0.7m.		
27											
28											

Anteroom - 2/16/2016 - Kaylyn Bautista, John Joseph Bautista, Brytney Miller

KaylynThesis.DAT - Cave Editor 32

File Surveys Heading Shots Block Options Help

Select Survey Edit Heading Edit Survey



#	From	To	Tape	Comp	Inc	Left	Right	Up	Down	Flags	Comment
1	C52	C25	4.1m.	285.0	-47.0	3.8m.	1.2m.	2.2m.	0.5m.		
2	C53	C52	4.0m.	328.0	-34.0	1.1m.	2.3m.	1.8m.	1.6m.		
3	C54	C53	3.2m.	256.0	-29.0	0.9m.	1.4m.	1.2m.	0.7m.		
4	C55	C54	3.0m.	247.0	-42.0	0.3m.	0.2m.	0.3m.	0.8m.		
5	C56	C55	2.8m.	232.5	-20.0	2.1m.	1.9m.	1.7m.	0.8m.		
6	C32	C56	1.5m.	153.0	31.0	1.6m.	0.9m.	0.7m.	0.7m.		
7	C56	C57	1.1m.	59.0	26.0	2.0m.	2.2m.	0.7m.	0.6m.		
8	C57	C58	1.8m.	73.5	45.0	2.0m.	2.5m.	0.6m.	0.5m.		
9	C58	C59	1.0m.	72.5	30.0	0.3m.	0.4m.	0.7m.	0.4m.		
10	C59	C60	1.2m.	335.0	-3.0	0.9m.	0.5m.	0.7m.	0.7m.		
11	C60	C61	1.0m.	338.0	12.0	0.4m.	1.0m.	0.7m.	0.8m.		
12	C61	C62	1.8m.	328.0	-37.0	1.4m.	0.5m.	0.8m.	0.8m.		
13	C61	Entrance	2.0m.	76.0	24.0	1.7m.	1.3m.	0.7m.	0.8m.		
14	C62	C31	4.9m.	317.0	-50.0	0.5m.	0.6m.	0.4m.	0.0m.		
15	Entrance	C63	2.6m.	146.0	42.0	0.5m.	0.7m.	0.5m.	0.4m.		
16	C63	JBoulder	2.3m.	81.5	0.3	0.0m.	0.0m.	0.0m.	1.5m.		
17	JBoulder	V2	6.8m.	153.0	3.0	0.0m.	0.0m.	0.0m.	0.5m.		
18											
19											
20											
21											

**Surface survey over Jinapsan Cave, Guam
and the relationship between the cave and the topography**

John and Joan Mylroie

Jinapsan Cave was surveyed May 21 and 22, 2012, by Joan and John Mylroie, with assistance from John Jenson. A total of 34 stations were set to accommodate 228.4 meters of linear survey (projected to 202.3 meters true horizontal cave), with a depth from the entrance to the tidal pool at the end of the cave of 24.66 m. The cave was surveyed with a Suunto® brand compass and inclinometer, with a Disto® laser range finder used for distance measurements. Sketches were made on site to scale. The data were reduced using standard latitude and departure methodology, and plotted on graph paper. The sketch detail was placed around the station grid, cross sections added, and an extended profile generated. The pencil drawing was inked, scanned, and labeled. The resulting final map is shown as Figure 1.

Even though the cave has significant internal complexity, the cave is rather short, fitting within a rectangle footprint of 26 m x 35 m. The cave slopes from the entrance downward to the west. It is a large single chamber which has been subdivided by massive flowstone walls and large stalagmites. Exposures of bedrock are rare, and are found mostly near the tidal pool and on a few ceilings where collapse has occurred to remove the stalagmitic covering. The cave origin is as a progradational collapse from a larger void at depth.

A surface survey over Jinapsan Cave was conducted April 1 and 3, 2014 by John Mylroie, Joan Mylroie, Maria Kottermair and John Jenson. A total of 23 stations were set using a Suunto compass and inclinometer and a metric fiberglass tape of 30 m length. Sketching was done in a diagrammatic manner to capture the nature of the talus slope, boulders, scree, and high cliff. The survey went from the Jinapsan Cave entrance up slope westward to the high cliff, parallel to the high cliff going north, and then downslope to the rain gauge station on its large boulder. The survey loop was closed by continuing down slope eastward to the base of the talus, and surveying south to the original station. An additional two stations were run south of the base station parallel to the slope base with an additional shot up slope (west) to make certain the surface survey contained the extent of Jinapsan Cave within the survey boundary. The data were entered in to the Compass® cave survey program for reduction and plotting, with the plot images brought into PowerPoint for map assembly.

The survey gained 43 m of elevation from the base station to a maximum height of 68 m at the base of the high cliff. The rain gauge station is at 59 m elevation, and the base of the talus slope at approximately 21 m elevation. Elevations are controlled by the 2012 Jinapsan Cave survey, which reaches sea level at a tidal pool at 25 m below the cave entrance. A total of 382.7 m of survey were shot, 357.1 m as projected horizontal length.

The plan view of the survey is shown in as a series of ever more complex images in Figures 2-4. The profile data are shown in Figure 5. Figure 6 shows a horizontal line taken from the entrance and extending west over the cave that descends beneath it, to overly the Shakey Room. The bedrock roof of the cave over the instrumentation in the Shakey Room can be no less than the distance below this line, or 20 m. The distance above this line is the greatest thickness possible for the talus slope material, at 8 m thick. Given the presence of bedrock ledges poking out from the talus slope, these 20 m and 8 m values are extreme end members, and it is more likely that the talus thickness is only a few meters, and the rest of the vertical section is bedrock down to the Shakey Room. The surface survey therefore allows some constraints to be placed on the pathway of the vadose water feeding the Shakey Room and its stalagmites and their present instrumentation.

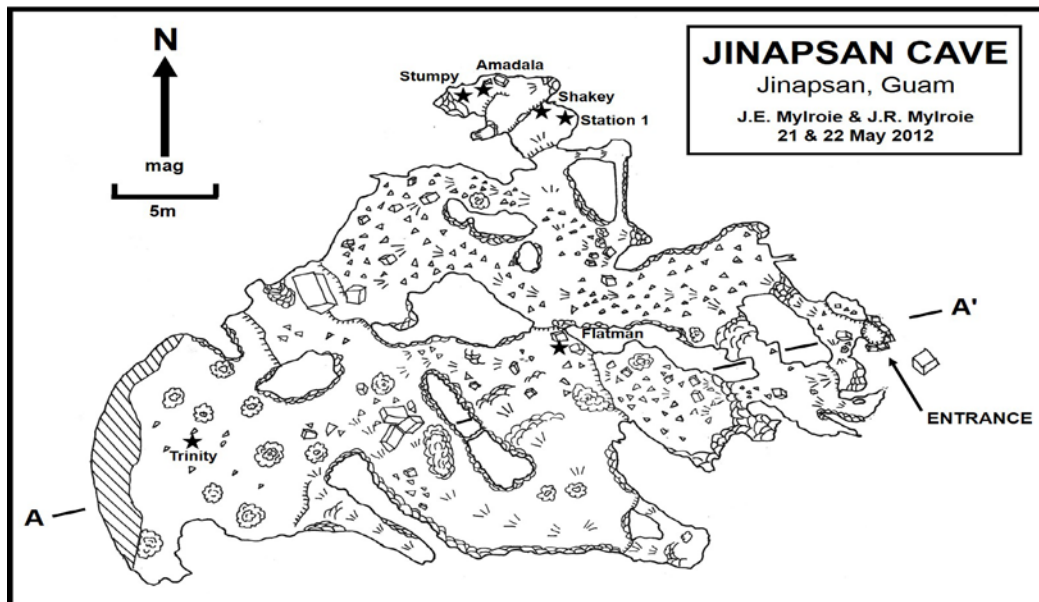


Figure 1: Map of Jinapsan Cave from May, 2012.

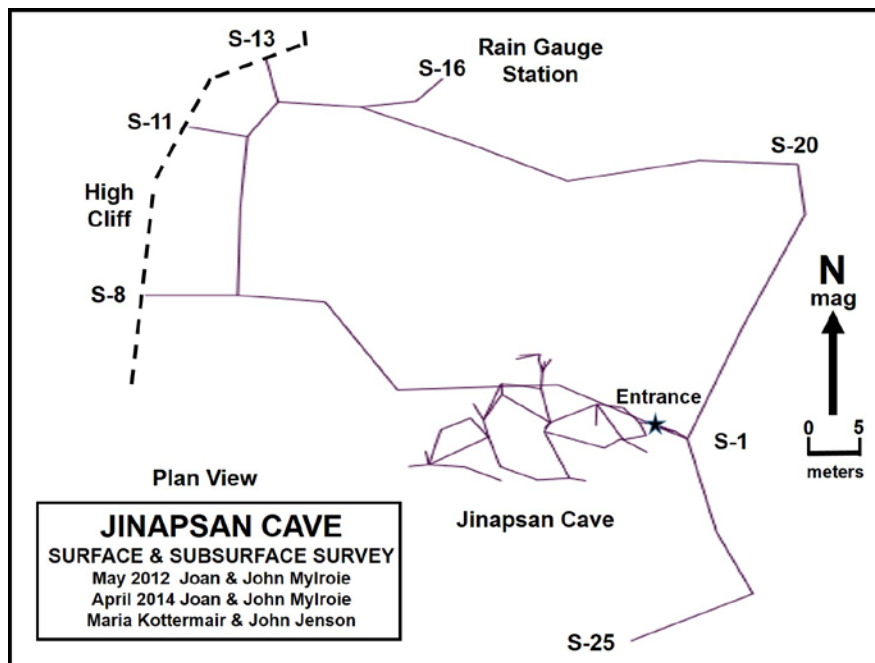


Figure 2: Plot of the surface survey, showing major features.

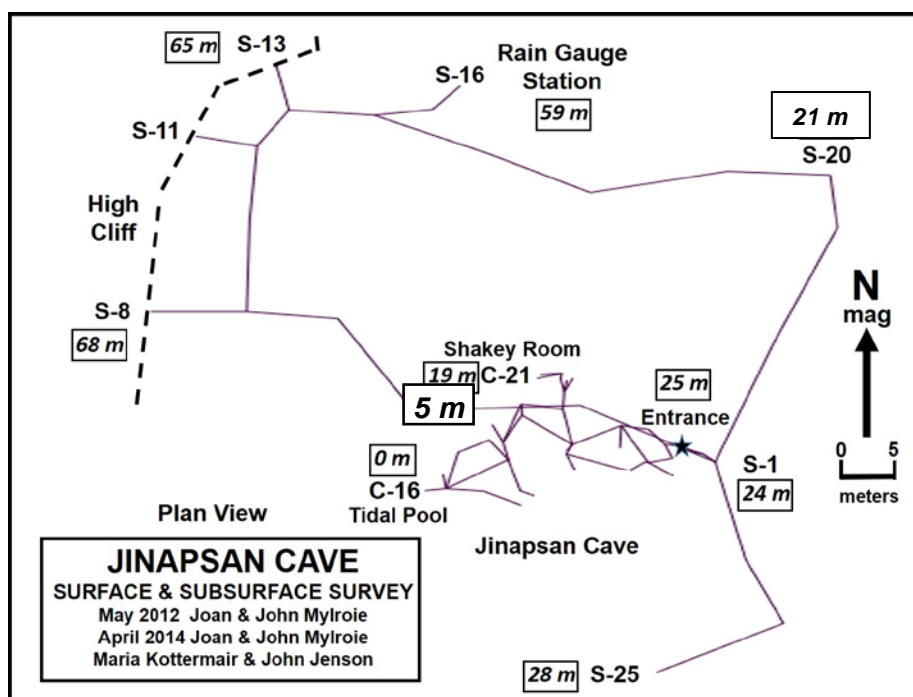


Figure 3: Plot of the surface survey, showing major features with elevations.

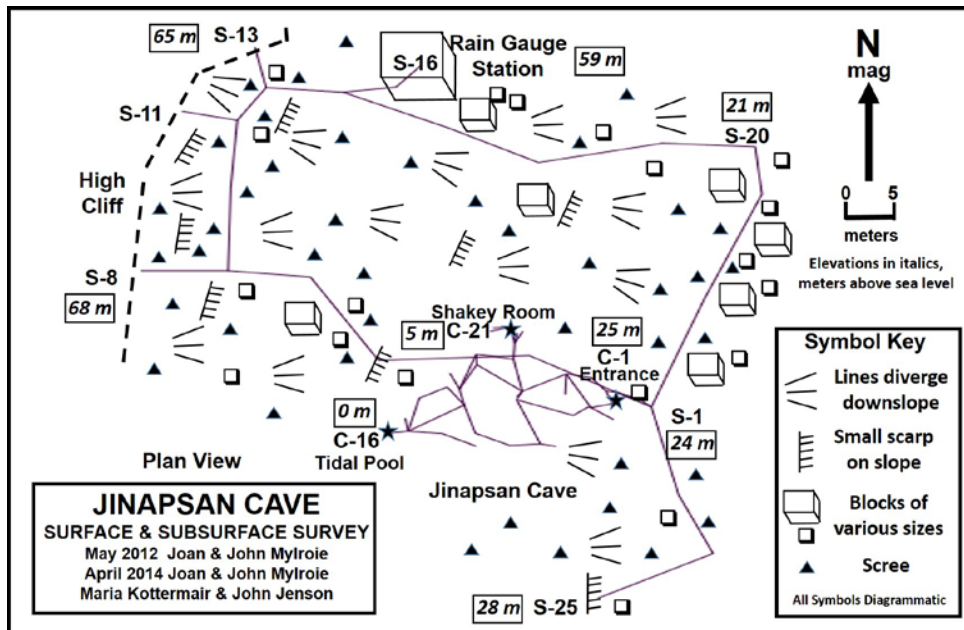


Figure 4: Plot of the surface survey, showing major features with elevations, and slope detail in a diagrammatic fashion.

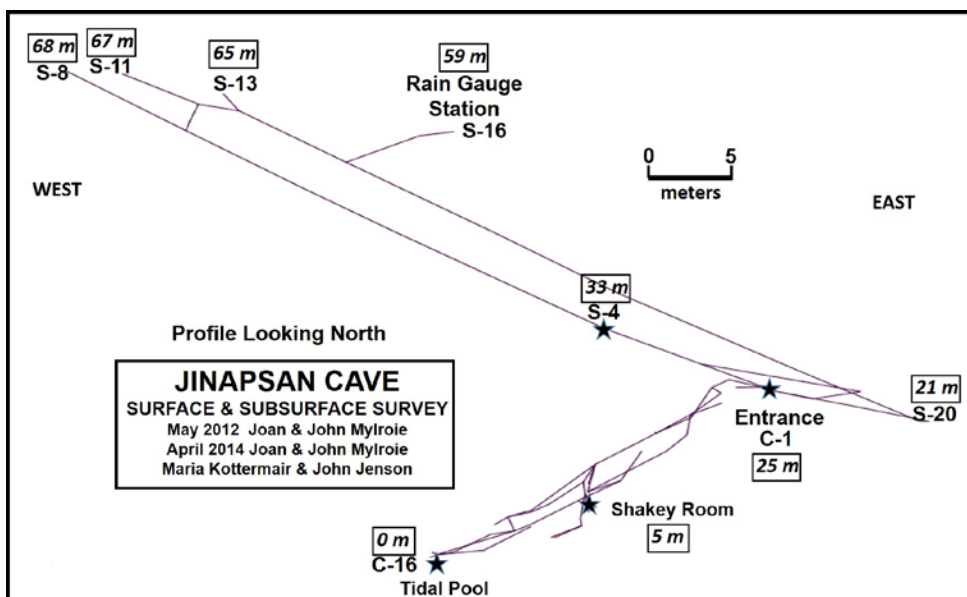


Figure 5: Plot of the surface survey, in profile view, showing major features with elevations.

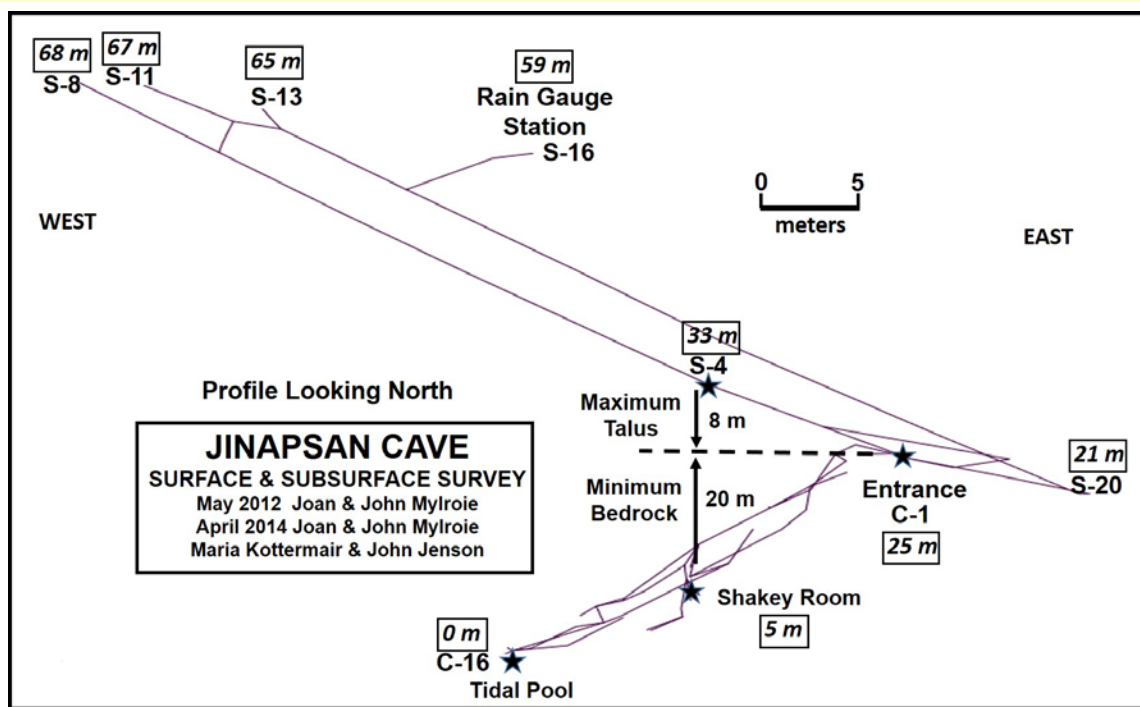


Figure 6: Plot of the surface survey, in profile view, showing major features with elevations, and vertical conditions in the Shakey Room area.

APPENDIX B – Jinapsan Cave drip-count database

Site	Date	Trip Day 1	Trip Day 2	Avg seconds/drip	Avg drips/hr	Bottle Deployment (mins)	Initial Bottle Wt (g)	Final Bottle Wt (g)	Water collected (g)	mL/drip	mL/day	Notes		
Trinity	Sep-08	9/22/2008	9/23/2008	2.6	1410	1323	102		overflowing	ERROR	ERROR			
Trinity	Oct-08	10/20/2008	10/21/2008	2.5	1450	1388	102		overflowing	ERROR	ERROR			
Trinity	Nov-08	11/17/2008	11/18/2008	2.6	1380	1452	102		overflowing	ERROR	ERROR			
Trinity	Dec-08	12/15/2008	12/16/2008	3.0	1210	1405	102		overflowing	ERROR	ERROR			
Trinity	Jan-09	1/12/2009	1/13/2009	1.2	3030	1375	102		overflowing	ERROR	ERROR			
Trinity	Feb-09	2/17/2009	2/18/2009	1.5	2470	1309	102		overflowing	ERROR	ERROR			
Trinity	Mar-09	3/16/2009	3/17/2009	1.6	2200	1421	102		overflowing	ERROR	ERROR			
Trinity	Apr-09	4/13/2009	4/14/2009	1.8	1990	1399	102		overflowing	ERROR	ERROR			
Trinity	May-09	5/12/2009	5/13/2009	1.8	1980	1560	102		overflowing	ERROR	ERROR			
Trinity	Jun-09	6/11/2009	6/12/2009	2.0	1760	1351	102		overflowing	ERROR	ERROR			
Trinity	Jul-09	7/14/2009	7/15/2009	2.3	1570	ERROR	102		overflowing	ERROR	ERROR	no bottle	up time	
Trinity	Aug-09	8/21/2009	8/22/2009	2.7	1330	1350	102		overflowing	ERROR	ERROR			
Trinity	Sep-09	9/21/2009	9/22/2009	1.3	2740	1512	102		overflowing	ERROR	ERROR			
Trinity	Oct-09	10/19/2009	10/21/2009	0.8	4670	1446	102		overflowing	ERROR	ERROR			
Trinity	Nov-09	11/23/2009	11/24/2009	0.8	4490	1482	102		overflowing	ERROR	ERROR			
Trinity	Dec-09	12/21/2009	12/22/2009	1.0	3450	63	102	385.9	283.9	0.08	6489			
Trinity	Jan-10	1/25/2010	1/26/2010	1.1	3280	1361	102		overflowing	ERROR	ERROR			
Trinity	Feb-10	Feb-10	Feb-10				102							
Trinity	Mar-10	3/1/2010	3/2/2010	1.2	3030	ERROR	102		overflowing	ERROR	ERROR	no bottle	down time	
Trinity	Apr-10	4/5/2010	4/6/2010	1.3	2840	ERROR	102		fallen bottle	ERROR	ERROR	no bottle	up time	
Trinity	May-10	5/3/2010	5/4/2010	1.3	2810	ERROR	102		overflowing	ERROR	ERROR	no bottle	down time	
Trinity	Jun-10	6/7/2010	6/8/2010	1.5	2410	ERROR	102		overflowing	ERROR	ERROR	no bottle	up time	
Trinity	Jul-10	7/12/2010	7/13/2010	1.7	2070	1348	102		overflowing	ERROR	ERROR			
Trinity	Aug-10	8/16/2010	8/17/2010	1.8	2010	ERROR	102		no bottle w	ERROR	ERROR	no bottle	up time	
Trinity	Sep-10	9/27/2010	9/28/2010	2.2	1670	1266	102		overflowing	ERROR	ERROR			
Trinity	Oct-10	10/25/2010	10/26/2010	2.5	1450	ERROR	102		overflowing	ERROR	ERROR	no bottle	up time	
Trinity	Nov-10	11/22/2010	11/23/2010	2.8	1280	57	102	193.1	91.1	0.07	2301			
Trinity	Dec-10	12/20/2010	12/21/2010	2.7	1340	42	102	171.6	69.6	0.07	2386			
Trinity	Jan-11	1/24/2011	1/25/2011	2.7	1350	57	102	192.6	90.6	0.07	2289			
Trinity	Feb-11	2/21/2011	2/22/2011	2.6	1410	41	102	178.1	76.1	0.08	2673			
Trinity	Mar-11	3/28/2011	3/29/2011	2.6	1400	26	102	154	52	0.09	2880			
Trinity	Apr-11	4/25/2011	4/26/2011	2.4	1470	11	102	122.9	20.9	0.08	2736			
Trinity	May-11	5/23/2011	5/24/2011	2.2	1650	17	102	140.5	38.5	0.08	3261			
Trinity	Jun-11	6/20/2011	6/21/2011	2.1	1710	5	102	113.4	11.4	0.08	3283			
Trinity	Jul-11	7/18/2011	7/19/2011	2.1	1690	10	102	117.9	15.9	0.06	2290			
Trinity	Aug-11	8/29/2011	8/30/2011	2.5	1430	34	102	152.9	50.9	0.06	2156			
Trinity	Sep-11	9/26/2011	9/27/2011	0.8	4337	5	91.4	118.8	27.4	0.08	7891	estimate initial weight		
Trinity	Oct-11	10/24/2011	10/25/2011	0.8	4444	15	91.4	180.4	89	0.08	8544			

Trinity	Nov-11	11/21/2011	11/22/2011	0.7	5210	20	91.4	249	157.6	0.09	11347			
Trinity	Dec-11	12/19/2011	12/20/2011	0.9	3920	20	91.4	193.7	102.3	0.08	7366			
Trinity	Jan-12	1/23/2012	1/24/2012	1.3	2860	20	91.4	181.2	89.8	0.09	6466			
Trinity	Feb-12	2/27/2012	2/28/2012	1.3	2670	20	103	173.8	70.8	0.08	5098			
Trinity	Mar-12	3/26/2012	3/27/2012	1.4	2600	20	103.4	171.8	68.4	0.08	4925			
Trinity	Apr-12	4/23/2012	4/24/2012	1.4	2520	25	103.3	185.8	82.5	0.08	4752			
Trinity	May-12	5/21/2012	5/22/2012	1.6	2320	20	103.2	164.8	61.6	0.08	4435			
Trinity	Jun-12	6/28/2012	6/29/2012	1.8	1990	20	102.6	155	52.4	0.08	3773			
Trinity	Jul-12	8/2/2012	8/3/2012	2.0	1780	20	102.4	150.7	48.3	0.08	3478			
Trinity	Aug-12	8/27/2012	8/28/2012	2.5	1450	20	102.6	140.4	37.8	0.08	2722			
Trinity	Sep-12	9/24/2012	9/25/2012	1.3	2700	20	102.6	174.5	71.9	0.08	5177			
Trinity	Oct-12	10/22/2012	10/23/2012	0.8	4490	20	102.6	233.9	131.3	0.09	9454			
Trinity	Nov-12	11/19/2012	11/20/2012	1.0	3750	20	102.6	205.7	103.1	0.08	7423			
Trinity	Dec-12	12/21/2012	12/22/2012	1.0	3460	20	102.9	196.4	93.5	0.08	6732			
Trinity	Jan-13	1/15/2013	1/16/2013	1.2	2960	20	104	180.3	76.3	0.08	5494			
Trinity	Feb-13	2/18/2013	2/19/2013	1.5	2480	20	103.4	169	65.6	0.08	4723			
Trinity	Mar-13	3/18/2013	3/19/2013	1.7	2090	20	103.5	158	54.5	0.08	3924			
Trinity	Apr-13	4/22/2013	4/23/2013	1.9	1910	20	103.4	152	48.6	0.08	3499			
Trinity	May-13	5/20/2013	5/21/2013	1.9	1860	20	103	150.4	47.4	0.08	3413			
Trinity	Jun-13	6/25/2013	6/26/2013	2.2	1650	20	103.3	144.9	41.6	0.08	2995			
Trinity	Jul-13	7/29/2013	7/30/2013	2.7	1350	20	103.2	138.4	35.2	0.08	2534			
Trinity	Aug-13	8/26/2013	8/27/2013	3.1	1160	20	103.5	132.4	28.9	0.07	2081			
Trinity	Sep-13	9/23/2013	9/24/2013	3.0	1200	20	102.9	133.3	30.4	0.08	2189			
Trinity	Oct-13	10/21/2013	10/22/2013	0.6	5840	20	104.8	286.4	181.6	0.09	13075			
Trinity	Nov-13	11/18/2013	11/19/2013	1.1	3230	20	89.8	177	87.2	0.08	6278			
Trinity	Dec-13	12/16/2013	12/17/2013	1.1	3230	20	103.9	195.7	91.8	0.09	6610			
Trinity	Jan-14	1/21/2014	1/22/2014	1.1	3170	20	103.6	191	87.4	0.08	6293			
Trinity	Feb-14	2/17/2014	2/18/2014	0.8	4630	20	102.8	225.4	122.6	0.08	8827			
Trinity	Mar-14	3/17/2014	3/18/2014	1.2	3020	20	102.5	ERROR	ERROR	ERROR	forgot to weigh			
Trinity	Apr-14	4/22/2014	4/23/2014	1.3	2740	21	103.9	177	73.1	0.08	5013			
Trinity	May-14	5/22/2014	5/23/2014	1.3	2820	20	103	177.2	74.2	0.08	5342	forgot to estimate		
Trinity	Jun-14	6/16/2014	6/17/2014	1.3	2700	20	103	172.9	69.9	0.08	5033			
Trinity	Jul-14	1-Jul	1-Jul				102							
Trinity	Aug-14	8/12/2014	8/18/2014	0.8	4520	20	103.6	217.8	114.2	0.08	8222			
Trinity	Sep-14	9/22/2014	9/23/2014	0.9	4020	20	103	213.5	110.5	0.08	7956	forgot to estimate		
Trinity	Oct-14	10/30/2014	10/31/2014	1.2	3120	20	102.5	177.7	75.2	0.07	5414			
Trinity	Nov-14	11/28/2014	11/29/2014	1.1	3170	20	102.2	187.4	85.2	0.081	6134			
Trinity	Dec-14	12/29/2014	12/30/2014	1.2	3060	20	102.3	177.2	74.9	0.07	5393		cutoff	

Site	Date	Trip Day 1	Trip Day 2	Avg seconds/drip	Avg drips/hr	Bottle Deployment (mins)	Initial Bottle Wt (g)	Final Bottle Wt (g)	Water collected (g)	mL/drip	mL/day	Notes			
Flatman	Sep-08	9/22/2008	9/23/2008	12.5	288	1335	101.7	556	454.3	0.07	490				
Flatman	Oct-08	10/20/2008	10/21/2008	16.0	225	1407	101.7	491.5	389.8	0.07	399				
Flatman	Nov-08	11/17/2008	11/18/2008	11.5	313	1419	101.7	563.6	461.9	0.06	469				
Flatman	Dec-08	12/15/2008	12/16/2008	24.5	147	1350	101.7	296.8	195.1	0.06	208				
Flatman	Jan-09	1/12/2009	1/13/2009	14.0	257	1328	101.7	462.1	360.4	0.06	391				
Flatman	Feb-09	2/17/2009	2/18/2009	15.0	240	1283	101.7	407.6	305.9	0.06	343				
Flatman	Mar-09	3/16/2009	3/17/2009	19.8	182	1401	101.7	371.1	269.4	0.06	277				
Flatman	Apr-09	4/13/2009	4/14/2009	23.7	152	1387	101.7	339.4	237.7	0.07	247				
Flatman	May-09	5/12/2009	5/13/2009	22.8	158	1641	101.7	362.6	260.9	0.06	229				
Flatman	Jun-09	6/11/2009	6/12/2009	24.3	148	1359	101.7	313.1	211.4	0.06	224				
Flatman	Jul-09	7/14/2009	7/15/2009	27.3	132	1400	101.7	298	196.3	0.06	202				
Flatman	Aug-09	8/21/2009	8/22/2009	9.8	366	1311	101.7	586.6	484.9	0.06	533				
Flatman	Sep-09	9/21/2009	9/22/2009	11.0	327	1484	101.7	478.8	377.1	0.05	366				
Flatman	Oct-09	10/19/2009	10/21/2009	11.0	327	2865	101.7	897.4	795.7	0.05	400				
Flatman	Nov-09	11/23/2009	11/24/2009	11.3	318	1452	101.7	367.8	266.1	0.03	264	error	2	should be 394	
Flatman	Dec-09	12/21/2009	12/22/2009	11.3	318	1302	101.7	311.7	210	0.03	232	error	2	should be 394	
Flatman	Jan-10	1/25/2010	1/26/2010	11.7	309	1355	101.7	311.9	210.2	0.03	223	error	2	should be 462	
Flatman	Feb-10						101.7					cave team didn't visit cave			
Flatman	Mar-10	3/1/2010	3/2/2010	11.7	309	1385	101.7	545.6	443.9	0.06	462				
Flatman	Apr-10	4/5/2010	4/6/2010	13.7	263	1424	101.7	500.2	398.5	0.06	403				
Flatman	May-10	5/3/2010	5/4/2010	17.2	210	1310	101.7	374.3	272.6	0.06	300				
Flatman	Jun-10	6/7/2010	6/8/2010	22.0	164	1349	101.7	232.5	130.8	0.04	140	error	2		
Flatman	Jul-10	7/12/2010	7/13/2010	23.7	152	1286	101.7	261.5	159.8	0.05	179	error	1	should be 247	
Flatman	Aug-10	8/16/2010	8/17/2010	24.3	148	1322	101.7	311.2	209.5	0.06	228				
Flatman	Sep-10	9/27/2010	9/28/2010	26.7	135	1175	101.7	233.8	132.1	0.05	162				
Flatman	Oct-10	10/25/2010	10/26/2010	28.5	126	1271	101.7	254.6	152.9	0.06	173				
Flatman	Nov-10	11/22/2010	11/23/2010	11.0	327	1292	101.7	528.2	426.5	0.06	475				
Flatman	Dec-10	12/20/2010	12/21/2010	13.7	263	1403	101.7	507.8	406.1	0.07	417				
Flatman	Jan-11	1/24/2011	1/25/2011	17.2	210	1489	101.7	466	364.3	0.07	352				
Flatman	Feb-11	2/21/2011	2/22/2011	15.0	240	1413	101.7	502.6	400.9	0.07	409				
Flatman	Mar-11	3/28/2011	3/29/2011	13.8	260	1459	101.7	540.8	439.1	0.07	433				
Flatman	Apr-11	4/25/2011	4/26/2011	13.0	277	1367	101.7	521.1	419.4	0.07	442				
Flatman	May-11	5/23/2011	5/24/2011	11.7	309	1467	101.7	532	430.3	0.06	422	probably user error	should be 462		
Flatman	Jun-11	6/20/2011	6/21/2011	14.3	251	1317	101.7	328.2	226.5	0.04	248				
Flatman	Jul-11	7/18/2011	7/19/2011	18.0	200	1321	101.7	373.9	272.2	0.06	297				
Flatman	Aug-11	8/29/2011	8/30/2011	11.0	327	1301	101.7	534.3	432.6	0.06	479				
Flatman	Sep-11	9/26/2011	9/27/2011	11.0	327	1341	101.7	514.9	413.2	0.06	444	probably user error	should be 479		
Flatman	Oct-11	10/24/2011	10/25/2011	10.7	338	1284	101.7	544.7	443	0.06	497				

Flatman	Nov-11	11/21/2011	11/22/2011	10.0	360	1264	101.7	564.8	463.1	0.06	528				
Flatman	Dec-11	12/19/2011	12/20/2011	11.0	327	1278	101.7	534.6	432.9	0.06	488				
Flatman	Jan-12	1/23/2012	1/24/2012	11.8	304	1360	101.7	547.8	446.1	0.06	472				
Flatman	Feb-12	2/27/2012	2/28/2012	13.0	277	1379	101.7	498.2	396.5	0.06	414				
Flatman	Mar-12	3/26/2012	3/27/2012	16.0	225	1333	101.7	401	299.3	0.06	323				
Flatman	Apr-12	4/23/2012	4/24/2012	18.5	195	1293	101.7	367.6	265.9	0.06	296				
Flatman	May-12	5/21/2012	5/22/2012	20.2	179	1401	101.7	335.4	233.7	0.06	240				
Flatman	Jun-12	6/28/2012	6/29/2012	23.7	152	1343	101.7	323.6	221.9	0.07	238				
Flatman	Jul-12	8/2/2012	8/3/2012	25.2	143	1280	101.7	290.8	189.1	0.06	213				
Flatman	Aug-12	8/27/2012	8/28/2012	15.5	232	1346	101.7	436	334.3	0.06	358				
Flatman	Sep-12	9/24/2012	9/25/2012	12.0	300	1257	101.7	512.2	410.5	0.07	470				
Flatman	Oct-12	10/22/2012	10/23/2012	11.0	327	1239	101.7	481.6	379.9	0.06	442	probably user error should be 479			
Flatman	Nov-12	11/19/2012	11/20/2012	11.0	327	1335	101.7	380.5	278.8	0.04	301	probably user error should be 479			
Flatman	Dec-12	12/21/2012	12/22/2012	12.0	300	1303	101.8	494.5	392.7	0.06	434				
Flatman	Jan-13	1/15/2013	1/16/2013	15.8	227	1280	101.7	410	308.3	0.06	347				
Flatman	Feb-13	2/18/2013	2/19/2013	18.3	196	1499	101.7	402.4	300.7	0.06	289				
Flatman	Mar-13	3/18/2013	3/19/2013	20.7	174	1393	101.8	318	216.2	0.05	223	should be ~265			
Flatman	Apr-13	4/22/2013	4/23/2013	24.0	150	1397	101.7	333.9	232.2	0.07	239				
Flatman	May-13	5/20/2013	5/21/2013	25.7	140	1433	101.8	327.7	225.9	0.07	227				
Flatman	Jun-13	6/25/2013	6/26/2013	27.2	133	1218	101.8	281.8	180	0.07	213				
Flatman	Jul-13	7/29/2013	7/30/2013	27.2	133	1454	102.4	282.7	180.3	0.06	179				
Flatman	Aug-13	8/26/2013	8/27/2013	34.7	104	1430	101.8	240	138.2	0.06	139				
Flatman	Sep-13	9/23/2013	9/24/2013	11.8	305	1422	101.7	560.1	458.4	0.06	464				
Flatman	Oct-13	10/21/2013	10/22/2013	11.0	327	1430	101.8	499.7	397.9	0.05	401	should be 479			
Flatman	Nov-13	11/18/2013	11/19/2013	12.2	295	1429	101.9	515.4	413.5	0.06	417				
Flatman	Dec-13	12/16/2013	12/17/2013	12.0	300	1423	101.8	516.9	415.1	0.06	420				
Flatman	Jan-14	1/21/2014	1/22/2014	14.3	251	1550	101.8	526.6	424.8	0.07	395				
Flatman	Feb-14	2/17/2014	2/18/2014	11.8	304	1251	101.8	522.3	420.5	0.07	484				
Flatman	Mar-14	3/17/2014	3/18/2014	11.3	318	1403	101.7	485.9	384.2	0.05	394	should be 502			
Flatman	Apr-14	4/22/2014	4/23/2014	16.3	220	1405	101.7	407	305.3	0.06	313				
Flatman	May-14	5/22/2014	5/23/2014	20.2	179	1394	101.7	358.5	256.8	0.06	265				
Flatman	Jun-14	6/16/2014	6/17/2014	23.7	152	1440	101.7	314.1	212.4	0.06	212				
Flatman	Jul-14						101.7					3 storms in this month			
Flatman	Aug-14	8/12/2014	8/13/2014	11.8	304	1382	101.8	ERROR	ERROR			no final weight			
Flatman	Sep-14	9/22/2014	9/23/2014	11.8	304	1416	101.8	579.8	478	0.07	486				
Flatman	Oct-14	10/30/2014	10/31/2014	12.0	300	1355	101.7	553	451.3	0.07	480				
Flatman	Nov-14	11/28/2014	11/29/2014	10.8	332	1381	101.8	587.6	485.8	0.06	507				
Flatman	Dec-14	12/29/2014	12/30/2014	11.3	318	1324	102	563.6	461.6	0.07	502			cutoff	

Date	Trip Day 1	Trip Day 2	Avg seconds/drip	Avg drips/hr	Bottle Deployment (mins)	Initial Bottle Wt (g)	Final Bottle Wt (g)	Water collected (g)	mL/drip	mL/day	estimate mL/day for E>5 min/drip	Notes		
Sep-08	9/22/2008	9/23/2008	44.8	80	1363	35.8	159	123.2	0.07	130.2				
Oct-08	10/20/2008	10/21/2008	41.8	86	1407	35.8	173.3	137.5	0.07	140.7				
Nov-08	11/17/2008	11/18/2008	42.5	85	1444	35.8	184.8	149	0.07	148.6				
Dec-08	12/15/2008	12/16/2008	58.3	62	1401	35.8	153.6	117.8	0.08	121.1				
Jan-09	1/12/2009	1/13/2009	292.0	12	1392	35.8	70.9	35.1	0.12	36.3	slower Day 2 drip rate dramatically			
Feb-09	2/17/2009	2/18/2009	267.7	13.4	1346	35.8	72	36.2	0.12	38.73	38.73	drip rate>5 min;		
Mar-09	3/16/2009	3/17/2009	70.0	51	ERROR	35.8	ERROR	ERROR	ERROR	ERROR	bottle fell			
Apr-09	4/13/2009	4/14/2009	97.0	37	1397	35.8	103.2	67.4	0.08	69.5				
May-09	5/12/2009	5/13/2009	70.8	51	1573	35.8	134.8	99	0.07	90.6				
Jun-09	6/11/2009	6/12/2009	115.3	31	1350	35.8	79.3	43.5	0.06	46.4				
Jul-09	7/14/2009	7/15/2009	120.8	30	1470	35.8	86.3	50.5	0.07	49.5				
Aug-09	8/21/2009	8/22/2009	61.7	58	1342	35.8	146.4	110.6	0.08	118.7				
Sep-09	9/21/2009	9/22/2009	30.2	119	1510	35.8	263	227.2	0.08	216.7				
Oct-09	10/19/2009	10/21/2009	36.8	98	2889	35.8	overflowing	ERROR	ERROR	ERROR	overflowing			
Nov-09	11/23/2009	11/24/2009	37.2	97	1493	35.8	206.7	170.9	0.07	164.8				
Dec-09	12/21/2009	12/22/2009	31.7	114	1326	35.8	219.5	183.7	0.07	199.5				
Jan-10	1/25/2010	1/26/2010	37.0	97	1395	35.8	201.7	165.9	0.07	171.3				
Feb-10						35.8								
Mar-10	3/1/2010	3/2/2010	46.4	78	1398	35.8	156	120.2	0.07	123.8				
Apr-10	4/5/2010	4/6/2010	ERROR	ERROR	1465	35.8	ERROR	ERROR	ERROR	ERROR	forgot to weigh no drip count taken			
May-10	5/3/2010	5/4/2010	127.0	28	1386	35.8	85.2	49.4	0.075	51.3				
Jun-10	6/7/2010	6/8/2010	155.8	23	1375	35.8	96.79	61.0	0.115	63.9	Day 2 faster drip rate			
Jul-10	7/12/2010	7/13/2010	110.3	33	1319	35.8	88.3	52.5	0.073	57.3	Day 2 slower drip rate			
Aug-10	8/16/2010	8/17/2010	106.2	34	1355	35.8	93.2	57.4	0.075	61.0				
Sep-10	9/27/2010	9/28/2010	156.2	23	1252	35.8	65.7	29.9	0.062	34.4				
Oct-10	10/25/2010	10/26/2010	46.8	77	1214	35.8	151.8	116.0	0.075	137.6				
Nov-10	11/22/2010	11/23/2010	39.5	91	1362	35.8	197	161.2	0.078	170.4				
Dec-10	12/20/2010	12/21/2010	44.7	81	1394	35.8	194	158.2	0.084	163.4				
Jan-11	1/24/2011	1/25/2011	130.5	28	1408	35.8	82.3	46.5	0.072	47.6				
Feb-11	2/21/2011	2/22/2011	38.7	93	1360	35.8	196.3	160.5	0.076	169.9				
Mar-11	3/28/2011	3/29/2011	65.0	55	1381	35.8	151.9	116.1	0.091	121.1	Day 2 faster drip rate			
Apr-11	4/25/2011	4/26/2011	244.8	15	1324	35.8	108.8	73.0	0.225	79.4	Day 2 faster drip rate			
May-11	5/23/2011	5/24/2011	57.7	62	1375	35.8	158.4	122.6	0.086	128.4				
Jun-11	6/20/2011	6/21/2011	111.3	32	1313	35.8	99.9	64.1	0.091	70.3	slower Day 2 drip rate			
Jul-11	7/18/2011	7/19/2011	102.8	35	1322	35.8	102.2	66.4	0.086	72.3				
Aug-11	8/29/2011	8/30/2011	28.8	125	1306	35.8	238.3	202.5	0.075	223.3				
Sep-11	9/26/2011	9/27/2011	19.5	185	1391	35.8	overflowing	ERROR	ERROR	ERROR	overflowing			
Oct-11	10/24/2011	10/25/2011	44.2	82	1289	35.8	154.9	119.1	0.068	133.1				

Nov-11	11/21/2011	11/22/2011	76.7	47	1265	35.8	107.9	72.1	0.073	82.1				
Dec-11	12/19/2011	12/20/2011	44.7	81	1292	35.8	178.6	142.8	0.082	159.2				
Jan-12	1/23/2012	1/24/2012	46.8	77	1346	35.8	174.9	139.1	0.081	148.8				
Feb-12	2/27/2012	2/28/2012	76.5	47	1364	35.8	139	103.2	0.096	109.0				
Mar-12	3/26/2012	3/27/2012	981.5	4	1379	35.8	49.1	13.3	0.158	13.9				
Apr-12	4/23/2012	4/24/2012	23005.7	0.2	1342	35.8	36.5	0.7	0.200	0.751	0.751	drip rate > 5 mins		
May-12	5/21/2012	5/22/2012	506.9	7.1	1339	35.8	67.5	31.7	0.200	34.09	34.091	drip rate > 5 mins		
Jun-12	6/28/2012	6/29/2012	40230.0	0.1	1341	35.8	36.3	0.5	0.250	0.537	0.537	drip rate > 5 mins; no sample		
Jul-12	8/2/2012	8/3/2012	1471.2	2.4	1335	35.8	45.6	9.8	0.180	10.571	10.571	drip rate > 5 mins; no sample		
Aug-12	8/27/2012	8/28/2012	47.2	76	1325	35.8	171	135.2	0.080	146.9				
Sep-12	9/24/2012	9/25/2012	50.2	72	1281	35.8	167.4	131.6	0.086	147.9				
Oct-12	10/22/2012	10/23/2012	52.8	68	1279	35.8	148.3	112.5	0.077	126.7				
Nov-12	11/19/2012	11/20/2012	84.2	43	1356	35.8	111.3	75.5	0.078	80.2				
Dec-12	12/21/2012	12/22/2012	128.7	28	1350	35.8	88.2	52.4	0.083	55.9				
Jan-13	1/15/2013	1/16/2013	2048.9	1.8	1312	35.8	43.1	7.3	0.190	8.0	8.01	drip rate > 5 mins		
Feb-13	2/18/2013	2/19/2013	2204.0	1.6	1450	35.8	43.3	7.5	0.190	7.45	7.45	drip rate > 5 mins		
Mar-13	3/18/2013	3/19/2013	920.7	3.9	1477	35.9	51.3	15.4	0.160	15.0	15.01	drip rate > 5 mins		
Apr-13	4/22/2013	4/23/2013	2437.6	1.5	1410	35.8	41.7	5.9	0.170	6.03	6.03	drip rate > 5 mins		
May-13	5/20/2013	5/21/2013	1441.0	2.5	1441	35.9	46.7	10.8	0.180	10.79	10.79	drip rate > 5 mins		
Jun-13	6/25/2013	6/26/2013	589.6	6.1	1225	35.8	54.5	18.7	0.150	21.98	21.98	drip rate > 5 mins		
Jul-13	7/29/2013	7/30/2013	735.8	4.9	1447	35.8	53.5	17.7	0.150	17.6	17.61	drip rate > 5 mins		
Aug-13	8/26/2013	8/27/2013	4788.0	0.8	1444	35.8	39.6	3.8	0.210	3.79	3.79	drip rate > 5 mins		
Sep-13	9/23/2013	9/24/2013	61.0	59	1417	35.8	146.4	110.6	0.079	112.4				
Oct-13	10/21/2013	10/22/2013	41.6	87	1406	35.8	188.9	153.1	0.075	156.8				
Nov-13	11/18/2013	11/19/2013	42.2	85	1419	35	188.9	153.9	0.076	156.2				
Dec-13	12/16/2013	12/17/2013	83.7	43	1388	35.9	109.9	74	0.074	76.8				
Jan-14	1/21/2014	1/22/2014	105.7	34	1534	35.9	76.6	40.7	0.047	38.2	error	should be 61		
Feb-14	2/17/2014	2/18/2014	101.2	36	1335	35.8	96	60.2	0.076	64.9				
Mar-14	3/17/2014	3/18/2014	112.3	32	1418	35.7	100.08	64.38	0.085	65.4				
Apr-14	4/22/2014	4/23/2014	446.0	8	1402	35.7	50.1	14.4	0.076	14.8				
May-14	5/22/2014	5/23/2014	12411.0	0.3	1379	35.9	37.3	1.4	0.210	1.46	1.46	drip rate > 5 mins		
Jun-14	6/16/2014	6/17/2014	1431.7	2.5	1445	35.8	46.7	10.9	0.180	10.86	10.86	drip rate > 5 mins		
Jul-14						35.8								
Aug-14	8/12/2014	8/18/2014	59.8	60	8760	35.8	332 overflowing	ERROR				overflowing		
Sep-14	9/22/2014	9/23/2014	69.0	52	1432	35.8	134.5	98.7	0.079	99.3				
Oct-14	10/30/2014	10/31/2014	58.7	61	1388	35.8	136.5	100.7	0.071	104.5				
Nov-14	11/28/2014	11/29/2014	93.7	38	1342	35.8	92.3	56.5	0.066	60.6				
Dec-14	12/29/2014	12/30/2014	86.2	42	1434	35.85	96.9	61.05	0.061	61.3		cutoff		

Site	Date	Trip Day 1	Trip Day 2	Avg seconds/drip	Avg drips/hr	Bottle Deployment (mins)	Initial Bottle Wt (g)	Final Bottle Wt (g)	Water collected (mL)	mL/drip	mL/day	Notes		
Station 2	Sep-08	9/22/2008	9/23/2008	30	122	1364	58.1	250	191.9	0.07	203			
Station 2	Oct-08	10/20/2008	10/21/2008	33	109	1407	58.1	218.4	160.3	0.06	164			
Station 2	Nov-08	11/17/2008	11/18/2008	40	89	1445	58.1	203.8	145.7	0.07	145			
Station 2	Dec-08	12/15/2008	12/16/2008	44	83	1401	58.1	191	132.9	0.07	137			
Station 2	Jan-09	1/12/2009	1/13/2009	49	73	1375	58.1	176.1	118	0.07	124			
Station 2	Feb-09	2/17/2009	2/18/2009	52	69	1347	58.1	168	109.9	0.07	117			
Station 2	Mar-09	3/16/2009	3/17/2009	56	65	1433	58.1	167.2	109.1	0.07	110			
Station 2	Apr-09	4/13/2009	4/14/2009	73	49	103	58.1	63.7	5.6	0.07	78			
Station 2	May-09	5/12/2009	5/13/2009	79	46	1579	58.1	142.9	84.8	0.07	77			
Station 2	Jun-09	6/11/2009	6/12/2009	82	44	1352	58.1	128.7	70.6	0.07	75			
Station 2	Jul-09	7/14/2009	7/15/2009	80	45	1470	58.1	137	78.9	0.07	77			
Station 2	Aug-09	8/21/2009	8/22/2009	62	58	1341	58.1	131.5	73.4	0.06	79	prob error		
Station 2	Sep-09	9/21/2009	9/22/2009	45	79	1516	58.1	200.7	142.6	0.07	135			
Station 2	Oct-09	10/19/2009	10/21/2009	50	72	2897	58.1	306.9	248.8	0.07	124			
Station 2	Nov-09	11/23/2009	11/24/2009	57	63	1487	58.1	170.2	112.1	0.07	109			
Station 2	Dec-09	12/21/2009	12/22/2009	59	61	1326	58.1	154.3	96.2	0.07	104			
Station 2	Jan-10	1/25/2010	1/26/2010	62	58	1355	58.1	83.9	25.8	0.02	27	prob error		
Station 2	Feb-10	Feb-10	Feb-10				58.1							
Station 2	Mar-10	3/1/2010	3/2/2010	71	51	1400	58.1	143.2	85.1	0.07	88			
Station 2	Apr-10	4/5/2010	4/6/2010	80	45	1396	58.1	133	74.9	0.07	77			
Station 2	May-10	5/3/2010	5/4/2010	81	45	1389	58.1	133.6	75.5	0.07	78			
Station 2	Jun-10	6/7/2010	6/8/2010	84	43	1374	58.1	131.5	73.4	0.07	77			
Station 2	Jul-10	7/12/2010	7/13/2010	83	43	1319	58.1	126	67.9	0.07	74			
Station 2	Aug-10	8/16/2010	8/17/2010	86	42	1353	58.1	127.1	69	0.07	73			
Station 2	Sep-10	9/27/2010	9/28/2010	89	40	1220	58.1	116.6	58.5	0.07	69			
Station 2	Oct-10	10/25/2010	10/26/2010	90	40	1215	58.1	116.1	58	0.07	69			
Station 2	Nov-10	11/22/2010	11/23/2010	89	41	1354	58.1	157.9	99.8	0.11	106	Day 2 increase		
Station 2	Dec-10	12/20/2010	12/21/2010	66	55	1393	58.1	149.1	91	0.07	94			
Station 2	Jan-11	1/24/2011	1/25/2011	81	45	1401	58.1	133	74.9	0.07	77			
Station 2	Feb-11	2/21/2011	2/22/2011	75	48	1341	58.1	138.5	80.4	0.07	86			
Station 2	Mar-11	3/28/2011	3/29/2011	72	50	1381	58.1	141.1	83	0.07	87			
Station 2	Apr-11	4/25/2011	4/26/2011	81	45	1322	58.1	114.4	56.3	0.06	61	prob error		
Station 2	May-11	5/23/2011	5/24/2011	77	47	1376	58.1	137.2	79.1	0.07	83			
Station 2	Jun-11	6/20/2011	6/21/2011	85	42	1314	58.1	127.8	69.7	0.08	76			
Station 2	Jul-11	7/18/2011	7/19/2011	88	41	1320	58.1	124.4	66.3	0.07	72			
Station 2	Aug-11	8/29/2011	8/30/2011	68	53	1306	58.1	143.5	85.4	0.07	94			
Station 2	Sep-11	9/26/2011	9/27/2011	66	55	1324	58.1	148.4	90.3	0.08	98			
Station 2	Oct-11	10/24/2011	10/25/2011	68	53	1288	58.1	59.6	1.5	0.001	2	barely collected drip water		

Station 2	Nov-11	11/21/2011	11/22/2011	69	52	137	58.1		4	0.03	42 Misplaced bottle		
Station 2	Dec-11	12/19/2011	12/20/2011	80	45	1290	58.1	131	72.9	0.08	81		
Station 2	Jan-12	1/23/2012	1/24/2012	82	44	1345	58.1	131.4	73.3	0.07	78		
Station 2	Feb-12	2/27/2012	2/28/2012	84	43	1367	58.1	131.6	73.5	0.08	77		
Station 2	Mar-12	3/26/2012	3/27/2012	95	38	1382	58.1	122.2	64.1	0.07	67		
Station 2	Apr-12	4/23/2012	4/24/2012	98	37	1344	58.1	120	61.9	0.08	66		
Station 2	May-12	5/21/2012	5/22/2012	107	34	1323	58	113.6	55.6	0.07	61		
Station 2	Jun-12	6/28/2012	6/29/2012	115	31	1348	58	120.8	62.8	0.09	67		
Station 2	Jul-12	8/2/2012	8/3/2012	124	29	1333	58	105.2	47.2	0.07	51		
Station 2	Aug-12	8/27/2012	8/28/2012	93	39	1308	58	120.9	62.9	0.07	69		
Station 2	Sep-12	9/24/2012	9/25/2012	86	42	1279	58	124.9	66.9	0.08	75		
Station 2	Oct-12	10/22/2012	10/23/2012	80	45	1283	58	130.1	72.1	0.07	81		
Station 2	Nov-12	11/19/2012	11/20/2012	97	37	1359	58	119.8	61.8	0.07	65		
Station 2	Dec-12	12/21/2012	12/22/2012	104	35	1349	58	114.6	56.6	0.07	60		
Station 2	Jan-13	1/15/2013	1/16/2013	113	32	1305	58	109.4	51.4	0.07	57		
Station 2	Feb-13	2/18/2013	2/19/2013	116	31	1450	58	112.2	54.2	0.07	54		
Station 2	Mar-13	3/18/2013	3/19/2013	124	29	1476	58.1	110	51.9	0.07	51		
Station 2	Apr-13	4/22/2013	4/23/2013	133	27	1407	58.1	104.3	46.2	0.07	47		
Station 2	May-13	5/20/2013	5/21/2013	134	27	1441	58.1	104.3	46.2	0.07	46		
Station 2	Jun-13	6/25/2013	6/26/2013	135	27	1223	58.1	97.1	39	0.07	46		
Station 2	Jul-13	7/29/2013	7/30/2013	135	27	1447	58.1	104.8	46.7	0.07	46		
Station 2	Aug-13	8/26/2013	8/27/2013	136	26	1443	58.2	103.4	45.2	0.07	45		
Station 2	Sep-13	9/23/2013	9/24/2013	133	27	1417	58.1	103.4	45.3	0.07	46		
Station 2	Oct-13	10/21/2013	10/22/2013	81	45	1409	58.1	134.8	76.7	0.07	78		
Station 2	Nov-13	11/18/2013	11/19/2013	77	47	1422	58.1	137.6	79.5	0.07	81		
Station 2	Dec-13	12/16/2013	12/17/2013	91	40	1387	58.2	124.6	66.4	0.07	69		
Station 2	Jan-14	1/21/2014	1/22/2014	96	38	1536	58.1	126.4	68.3	0.07	64		
Station 2	Feb-14	2/17/2014	2/18/2014	81	44	1339	58	123.7	65.7	0.07	71		
Station 2	Mar-14	3/17/2014	3/18/2014	93	39	1502	58	61.1	3.1	0.003	3 barely collected drip water		
Station 2	Apr-14	4/22/2014	4/23/2014	108	33	1400	57.8	110.2	52.4	0.07	54		
Station 2	May-14	5/22/2014	5/23/2014	112	32	1392	57.7	95.2	37.5	0.05	39 error		
Station 2	Jun-14	6/16/2014	6/17/2014	113	32	1432	57.8	106.6	48.8	0.06	49		
Station 2	Jul-14	1-Jul	1-Jul				57.9						
Station 2	Aug-14	8/12/2014	8/18/2014	84	43	8789	57.8	489.3	431.5	0.07	71		
Station 2	Sep-14	9/22/2014	9/23/2014	93	39	1431	57.8	122.3	64.5	0.07	65		
Station 2	Oct-14	10/30/2014	10/31/2014	98	37 ERROR		58	117.1	59.1 ERROR	ERROR			
Station 2	Nov-14	11/28/2014	11/29/2014	101	36	1354	57.8	112.5	54.7	0.07	58		
Station 2	Dec-14	12/29/2014	12/30/2014	111	33 ERROR		57.8	111.6	53.8 ERROR	ERROR	no bottle down time cutoff		

Site	Date	Trip Day 1	Trip Day 2	Avg seconds/drip	Avg drips/hr	Bottle Deployment (mins)	Initial Bottle Wt (g)	Final Bottle Wt (g)	Water collected (g)	mL/drip	mL/day	Notes			
Brother	Sep-08	9/22/2008	9/23/2008	0	0	0	0	0	0	0	0	0 not collecting data			
Brother	Oct-08	10/20/2008	10/21/2008	0	0	0	0	0	0	0	0	0 not collecting data			
Brother	Nov-08	11/17/2008	11/18/2008	0	0	0	0	0	0	0	0	0 not collecting data			
Brother	Dec-08	12/15/2008	12/16/2008	0	0	0	0	0	0	0	0	0 not collecting data			
Brother	Jan-09	1/12/2009	1/13/2009	0	0	0	0	0	0	0	0	0 not collecting data			
Brother	Feb-09	2/17/2009	2/18/2009	0	0	0	0	0	0	0	0	0 not collecting data			
Brother	Mar-09	3/16/2009	3/17/2009	0	0	0	0	0	0	0	0	0 not collecting data			
Brother	Apr-09	4/13/2009	4/14/2009	0	0	0	0	0	0	0	0	0 not collecting data			
Brother	May-09	5/12/2009	5/13/2009	85	43	1531	67.8	141.6	73.8	0.07	69.4				
Brother	Jun-09	6/11/2009	6/12/2009	92	39	1338	67.8	123.8	56	0.06	60.3				
Brother	Jul-09	7/14/2009	7/15/2009	91	40	1556	67.8	70.3	2.5	0.002	2.3	fell over			
Brother	Aug-09	8/21/2009	8/22/2009	76	48	1355	67.8	145.7	77.9	0.07	82.8				
Brother	Sep-09	9/21/2009	9/22/2009	71	51	1527	67.8	162	94.2	0.07	88.8				
Brother	Oct-09	10/19/2009	10/21/2009	72	50	2910	67.8	80.2	12.4	0.01	6.1	probably user error			
Brother	Nov-09	11/23/2009	11/24/2009	75	48	1605	67.8	77.6	9.8	0.01	8.8	fell over			
Brother	Dec-09	12/21/2009	12/22/2009	75	48	1342	67.8	145.6	77.8	0.07	83.5				
Brother	Jan-10	1/25/2010	1/26/2010	75	48	1412	67.8	150.3	82.5	0.07	84.1				
Brother	Feb-10	Feb-10	Feb-10				67.8					cave team didn't visit cave			
Brother	Mar-10	3/1/2010	3/2/2010	76	47	1415	67.8	149.4	81.6	0.07	83.0				
Brother	Apr-10	4/5/2010	4/6/2010	79	46	1456	67.8	141.2	73.4	0.07	72.6	slower Day 2		should be 81	
Brother	May-10	5/3/2010	5/4/2010	81	44	1366	67.8	141	73.2	0.07	77.2				
Brother	Jun-10	6/7/2010	6/8/2010	91	40	1408	67.8	138.5	70.7	0.08	72.3				
Brother	Jul-10	7/12/2010	7/13/2010	92	39	1343	67.8	132.4	64.6	0.07	69.3				
Brother	Aug-10	8/16/2010	8/17/2010	88	41	1391	67.8	132.5	64.7	0.07	67.0	Day 2 increase drip rate		should be 75	
Brother	Sep-10	9/27/2010	9/28/2010	99	36	1234	67.8	122.9	55.1	0.07	64.3				
Brother	Oct-10	10/25/2010	10/26/2010	87	42	1287	67.8	126.4	58.6	0.07	65.6				
Brother	Nov-10	11/22/2010	11/23/2010	78	46	1388	67.8	117	49.2	0.05	51.0	probably user error		should be ~81	
Brother	Dec-10	12/20/2010	12/21/2010	78	46	1389	67.8	148.9	81.1	0.08	84.1				
Brother	Jan-11	1/24/2011	1/25/2011	83	43	1423	67.8	140.5	72.7	0.07	73.6				
Brother	Feb-11	2/21/2011	2/22/2011	79	46	1366	67.8	145.4	77.6	0.07	81.8				
Brother	Mar-11	3/28/2011	3/29/2011	83	44	1392	67.8	139.8	72	0.07	74.5				
Brother	Apr-11	4/25/2011	4/26/2011	84	43	1329	67.8	137.9	70.1	0.07	76.0				
Brother	May-11	5/23/2011	5/24/2011	83	44	1382	67.8	142.3	74.5	0.07	77.6				
Brother	Jun-11	6/20/2011	6/21/2011	87	41	1323	67.8	91.8	24	0.03	26.1	probably user error		should be 75	
Brother	Jul-11	7/18/2011	7/19/2011	90	40	1321	67.8	132.7	64.9	0.07	70.7				
Brother	Aug-11	8/29/2011	8/30/2011	79	46	1302	67.8	141.1	73.3	0.07	81.1				
Brother	Sep-11	9/26/2011	9/27/2011	82	44	1330	67.8	102.5	34.7	0.04	37.6			should be ~77	
Brother	Oct-11	10/24/2011	10/25/2011	85	42	1292	67.8	128.1	60.3	0.07	67.2				

Brother	Nov-11	11/21/2011	11/22/2011	78	46	1267	67.8	138.7	70.9	0.07	80.6				
Brother	Dec-11	12/19/2011	12/20/2011	83	44	1297	67.8	139.2	71.4	0.08	79.3				
Brother	Jan-12	1/23/2012	1/24/2012	86	42	1355	67.8	139.3	71.5	0.08	76.0				
Brother	Feb-12	2/27/2012	2/28/2012	87	42	1354	67.8	138.7	70.9	0.08	75.4				
Brother	Mar-12	3/26/2012	3/27/2012	85	43	1373	67.8	70.1	2.3	0.002	2.4	probably user error	should be ~76		
Brother	Apr-12	4/23/2012	4/24/2012	91	39	1337	67.8	132.3	64.5	0.07	69.5				
Brother	May-12	5/21/2012	5/22/2012	97	37	1333	68.1	129.8	61.7	0.07	66.7				
Brother	Jun-12	6/28/2012	6/29/2012	100	36	1332	68.1	59.1	-9	-0.01	-9.7	no sample			
Brother	Jul-12	8/2/2012	8/3/2012	98	37	1310	68.1	124.5	56.4	0.07	62.0		should be ~67		
Brother	Aug-12	8/27/2012	8/28/2012	89	40	1345	68.1	137.4	69.3	0.08	74.2				
Brother	Sep-12	9/24/2012	9/25/2012	87	42	1287	68.1	138.6	70.5	0.08	78.9				
Brother	Oct-12	10/22/2012	10/23/2012	84	43	1261	68.1	138.8	70.7	0.08	80.7				
Brother	Nov-12	11/19/2012	11/20/2012	82	44	1361	68.1	142.5	74.4	0.07	78.7				
Brother	Dec-12	12/21/2012	12/22/2012	87	41	1341	68.1	137.3	69.2	0.07	74.3				
Brother	Jan-13	1/15/2013	1/16/2013	88	41	1312	68.1	131.9	63.8	0.07	70.0	prob error	should be 74		
Brother	Feb-13	2/18/2013	2/19/2013	102	35	1498	68.3	118.75	50.45	0.06	48.5	prob error	should be 61		
Brother	Mar-13	3/18/2013	3/19/2013	107	34	1449	68.2	129.6	61.4	0.08	61.0				
Brother	Apr-13	4/22/2013	4/23/2013	108	33	1374	68	125.5	57.5	0.07	60.3				
Brother	May-13	5/20/2013	5/21/2013	105	34	1411	68.1	128.8	60.7	0.08	61.9				
Brother	Jun-13	6/25/2013	6/26/2013	102	35	1213	68.1	119.5	51.4	0.07	61.0				
Brother	Jul-13	7/29/2013	7/30/2013	103	35	1445	68.2	129.7	61.5	0.07	61.3				
Brother	Aug-13	8/26/2013	8/27/2013	105	34	1409	68	125.9	57.9	0.07	59.2				
Brother	Sep-13	9/23/2013	9/24/2013	105	34	1413	68.1	124.9	56.8	0.07	57.9				
Brother	Oct-13	10/21/2013	10/22/2013	81	45	1425	68	145.5	77.5	0.07	78.3				
Brother	Nov-13	11/18/2013	11/19/2013	79	45	1400	68.1	142.7	74.6	0.07	76.7				
Brother	Dec-13	12/16/2013	12/17/2013	82	44	1421	68.1	142.8	74.7	0.07	75.7				
Brother	Jan-14	1/21/2014	1/22/2014	86	42	1536	68.3	142.8	74.5	0.07	69.8		should be 74		
Brother	Feb-14	2/17/2014	2/18/2014	84	43	1392	68	141.1	73.1	0.07	75.6				
Brother	Mar-14	3/17/2014	3/18/2014	86	42	1408	68.1	140.4	72.3	0.07	73.9				
Brother	Apr-14	4/22/2014	4/23/2014	87	41	1396	68	135.4	67.4	0.07	69.5				
Brother	May-14	5/22/2014	5/23/2014	98	37	1402	68	130.6	62.6	0.07	64.3				
Brother	Jun-14	6/16/2014	6/17/2014	105	34	1420	68.2	125.9	57.7	0.07	58.5				
Brother	Jul-14	1-Jul	1-Jul				67.8								
Brother	Aug-14	8/12/2014	8/18/2014	84	43	8745	68.1	496.9	428.8	0.07	70.6		should be ~76		
Brother	Sep-14	9/22/2014	9/23/2014	82	44	1426	68.1	142.4	74.3	0.07	75.0				
Brother	Oct-14	10/30/2014	10/31/2014	85	43	1368	68.1	135.9	67.8	0.07	71.4				
Brother	Nov-14	11/28/2014	11/29/2014	87	42	1386	68.1	132.8	64.7	0.07	67.2		should be ~74		
Brother	Dec-14	12/29/2014	12/30/2014	89	40	1377	68.1	132.8	64.7	0.07	67.7		cutoff		

Site	Date	Trip Day 1	Trip Day 2	Avg seconds/drip	Avg drips/hr	Bottle Deployment (mins)	Initial Bottle Wt (g)	Final Bottle Wt (g)	Water collected (g)	mL/drip	mL/day	estimate mL/day for E>5 min/drip	Notes			
Stumpy	Sep-08	9/22/2008	9/23/2008	0	0	0	102	120	0	0	0		not collecting data			
Stumpy	Oct-08	10/20/2008	10/21/2008	0	0	0	102	119.8	0	0	0		not collecting data			
Stumpy	Nov-08	11/17/2008	11/18/2008	0	0	0	102	113.1	0	0	0		not collecting data			
Stumpy	Dec-08	12/15/2008	12/16/2008	0	0	0	0	0	0	0	0		not collecting data			
Stumpy	Jan-09	1/12/2009	1/13/2009	0	0	0	102	112.8	10.8	0	0		not collecting data			
Stumpy	Feb-09	2/17/2009	2/18/2009	0	0	1326	102	112.6	10.6				only collected weight and water			
Stumpy	Mar-09	3/16/2009	3/17/2009	0	0	1436	102	114.1	12.1				only collected weight and water			
Stumpy	Apr-09	4/13/2009	4/14/2009	0	0	1403	102	113.8	11.8				only collected weight and water			
Stumpy	May-09	5/12/2009	5/13/2009	140	25.7	1539	102	141.6	39.6	0.060	37.1	37.1	drip rate > 5 mins			
Stumpy	Jun-09	6/11/2009	6/12/2009	528	6.8	1337	102	114	12	0.079	12.9	12.9	drip rate > 5 mins			
Stumpy	Jul-09	7/14/2009	7/15/2009	301	11.9	1452	102	123.1	21.1	0.073	20.9	20.9	drip rate > 5 mins			
Stumpy	Aug-09	8/21/2009	8/22/2009	294	12.2	1356	102	122.2	20.2	0.073	21.5	21.5	no bottle down time; drip rate > 5 mins			
Stumpy	Sep-09	9/21/2009	9/22/2009	261	13.8	1520	102	126.8	24.8	0.071	23.5	23.5	drip rate > 5 mins			
Stumpy	Oct-09	10/19/2009	10/21/2009	489	7.4	2907	102	127.3	25.3	0.071	12.5	12.5	drip rate > 5 mins			
Stumpy	Nov-09	11/23/2009	11/24/2009	307	11.7	1506	102	123.5	21.5	0.073	20.6	20.6	drip rate > 5 mins			
Stumpy	Dec-09	12/21/2009	12/22/2009	670	5.4	1346	102	112	10	0.083	10.7	10.7	drip rate > 5 mins			
Stumpy	Jan-10	1/25/2010	1/26/2010	336	10.7	1410	102	120.9	18.9	0.075	19.3	19.3	drip rate > 5 mins			
Stumpy	Feb-10	Feb-10	Feb-10										cave team didn't visit cave			
Stumpy	Mar-10	3/1/2010	3/2/2010	780	4.6	1425	102	111.1	9.1	0.083	9.20	9.2	drip rate > 5 mins			
Stumpy	Apr-10	4/5/2010	4/6/2010	396	9.1	1454	102	118.1	16.1	0.073	15.9	15.9	drip rate > 5 mins			
Stumpy	May-10	5/3/2010	5/4/2010	1676	2.1	1380	102	106.2	4.2	0.085	4.4	4.4	drip rate > 5 mins			
Stumpy	Jun-10	6/7/2010	6/8/2010	1149	3.1	1409	102	108.4	6.4	0.087	6.5	6.5	drip rate > 5 mins			
Stumpy	Jul-10	7/12/2010	7/13/2010	3820	0.9	1344	102	103.9	1.9	0.090	2.0	2.0	drip rate > 5 mins			
Stumpy	Aug-10	8/16/2010	8/17/2010	525	6.9	1391	102	114.4	12.4	0.078	12.8	12.8	drip rate > 5 mins			
Stumpy	Sep-10	9/27/2010	9/28/2010	3176	1.1	1235	102	104.1	2.1	0.090	2.4	2.4	drip rate > 5 mins			
Stumpy	Oct-10	10/25/2010	10/26/2010	6009	0.6	1224	102	103.1	1.1	0.090	1.3	1.3	drip rate > 5 mins			
Stumpy	Nov-10	11/22/2010	11/23/2010	300	12	1389	102	0	0 ERROR				bottle not centered under drip; no water			
Stumpy	Dec-10	12/20/2010	12/21/2010	662	5.4	1458	102	112.7	10.7	0.081	10.6	10.6	drip rate > 5 mins			
Stumpy	Jan-11	1/24/2011	1/25/2011	10977	0.3	1423	102	102.7	0.7	0.090	0.7	0.7	drip rate > 5 mins			
Stumpy	Feb-11	2/21/2011	2/22/2011	363	9.9	1367	102	118.5	16.5	0.073	17.4	17.4	drip rate > 5 mins			
Stumpy	Mar-11	3/28/2011	3/29/2011	3268	1.1	1392	102	104.3	2.3	0.090	2.4	2.4	drip rate > 5 mins			
Stumpy	Apr-11	4/25/2011	4/26/2011	7980	0.5	1330	102	102.9	0.9	0.090	1.0	1.0	drip rate > 5 mins			
Stumpy	May-11	5/23/2011	5/24/2011	7468	0.5	1383	102	103	1	0.090	1.0	1.0	drip rate > 5 mins			
Stumpy	Jun-11	6/20/2011	6/21/2011	10214	0.4	1324	102	102.7	0.7	0.090	0.8	0.8	drip rate > 5 mins			
Stumpy	Jul-11	7/18/2011	7/19/2011	10198	0.4	1322	102	102.7	0.7	0.090	0.8	0.8	drip rate > 5 mins			
Stumpy	Aug-11	8/29/2011	8/30/2011	4687	0.8	1302	102	103.5	1.5	0.090	1.7	1.7	drip rate > 5 mins			
Stumpy	Sep-11	9/26/2011	9/27/2011	598	6.0	1391	102	113.3	11.3	0.081	11.7	11.7	drip rate > 5 mins			
Stumpy	Oct-11	10/24/2011	10/25/2011	1243	2.9	1292	102	107.3	5.3	0.085	5.9	5.9	drip rate > 5 mins			

Stumpy	Nov-11	11/21/2011	11/22/2011	648	5.6	1267	102	111.5	9.5	0.081	10.8					
Stumpy	Dec-11	12/19/2011	12/20/2011	544	6.6	1298	102	113.3	11.3	0.079	12.5	12.5	drip rate > 5 mins			
Stumpy	Jan-12	1/23/2012	1/24/2012	24354	0.1	1353	102	102.3	0.3	0.090	0.3	0.3	no sample water			
Stumpy	Feb-12	2/27/2012	2/28/2012	962	3.7	1352	102	109	7	0.083	7.5	7.5	drip rate > 5 mins			
Stumpy	Mar-12	3/26/2012	3/27/2012	7409	0.5	1372	102	103	1	0.090	1.0	1.0	no sample water			
Stumpy	Apr-12	4/23/2012	4/24/2012	675	5.3	1320	102	111.5	9.5	0.081	10.4	10.4	drip rate > 5 mins			
Stumpy	May-12	5/21/2012	5/22/2012	1444	2.5	1331	102.3	107	4.7	0.085	5.1	5.1	drip rate > 5 mins			
Stumpy	Jun-12	6/28/2012	6/29/2012	3316	1.1	1334	102.3	104.4	2.1	0.087	2.3	2.3	no sample water			
Stumpy	Jul-12	8/2/2012	8/3/2012	1060	3.4	1310	102.3	108.6	6.3	0.085	6.9	6.9	no sample water			
Stumpy	Aug-12	8/27/2012	8/28/2012	349	10.3	1345	102.3	119.2	16.9	0.073	18.1	18.1	drip rate > 5 mins			
Stumpy	Sep-12	9/24/2012	9/25/2012	455	7.9	1287	102.3	115.2	12.9	0.076	14.4	14.4	drip rate > 5 mins			
Stumpy	Oct-12	10/22/2012	10/23/2012	407	8.8	1267	102.3	116.3	14	0.075	15.9	15.9	drip rate > 5 mins			
Stumpy	Nov-12	11/19/2012	11/20/2012	434	8.3	1362	102.3	117	14.7	0.078	15.5	15.5	drip rate > 5 mins			
Stumpy	Dec-12	12/21/2012	12/22/2012	448	8.0	1341	102.4	116.4	14	0.078	15.0	15.0	drip rate > 5 mins			
Stumpy	Jan-13	1/15/2013	1/16/2013	6264	0.6	1305	102.3	103.3	1	0.080	1.1	1.1	barely any water			
Stumpy	Feb-13	2/18/2013	2/19/2013	166	21.7	1462	102.3	135.15	32.85	0.062	32.4	32.4	drip rate > 5 mins			
Stumpy	Mar-13	3/18/2013	3/19/2013	382	9.4	1446	102.5	119.1	16.6	0.073	16.5	16.5	drip rate > 5 mins			
Stumpy	Apr-13	4/22/2013	4/23/2013	405	8.9	1376	102.3	117.6	15.3	0.075	16.0	16.0	drip rate > 5 mins			
Stumpy	May-13	5/20/2013	5/21/2013	384	9.4	1411	102.4	118.5	16.1	0.073	16.4	16.4	drip rate > 5 mins			
Stumpy	Jun-13	6/25/2013	6/26/2013	358	10.0	1211	102.3	116.9	14.6	0.072	17.4	17.4	drip rate > 5 mins			
Stumpy	Jul-13	7/29/2013	7/30/2013	381	9.5	1443	102.3	118.9	16.6	0.073	16.6	16.6	drip rate > 5 mins			
Stumpy	Aug-13	8/26/2013	8/27/2013	394	9.1	1412	102.2	117.9	15.7	0.073	16.0	16.0	drip rate > 5 mins			
Stumpy	Sep-13	9/23/2013	9/24/2013	701	5.1	1411	102.3	112.2	9.9	0.082	10.1	10.1	drip rate > 5 mins			
Stumpy	Oct-13	10/21/2013	10/22/2013	345	10.4	1420	102.2	120.5	18.3	0.074	18.6	18.6	drip rate > 5 mins			
Stumpy	Nov-13	11/18/2013	11/19/2013	343	10.5	1400	102.3	120.4	18.1	0.074	18.6	18.6	drip rate > 5 mins			
Stumpy	Dec-13	12/16/2013	12/17/2013	347	10.4	1429	102.3	120.6	18.3	0.074	18.4	18.4	drip rate > 5 mins			
Stumpy	Jan-14	1/21/2014	1/22/2014	387	9.3	1536	102.5	119.9	17.4	0.073	16.3	16.3	drip rate > 5 mins			
Stumpy	Feb-14	2/17/2014	2/18/2014	318	11.3	1396	102.3	121.5	19.2	0.073	19.8	19.8	drip rate > 5 mins			
Stumpy	Mar-14	3/17/2014	3/18/2014	284	12.7	1411	102.3	123.8	21.5	0.072	21.9	21.9	drip rate > 5 mins			
Stumpy	Apr-14	4/22/2014	4/23/2014	380	9.5	1394	102.1	118.4	16.3	0.074	16.8	16.8	drip rate > 5 mins			
Stumpy	May-14	5/22/2014	5/23/2014	435	8.3	1403	102.2	117.3	15.1	0.078	15.5	15.5	drip rate > 5 mins			
Stumpy	Jun-14	6/16/2014	6/17/2014	490	7.4	1420	102.3	115.7	13.4	0.077	13.6	13.6	drip rate > 5 mins			
Stumpy	Jul-14	1-Jul	1-Jul										3 storms in one month; cave team didn't visit cave			
Stumpy	Aug-14	8/12/2014	8/18/2014	307	11.7	8742	102.2	226.9	124.7	0.073	20.5	20.5	drip rate > 5 mins			
Stumpy	Sep-14	9/22/2014	9/23/2014	366	9.8	1426	102.25	119.3	17.05	0.073	17.2	17.2	drip rate > 5 mins			
Stumpy	Oct-14	10/30/2014	10/31/2014	399	9.0	1368	102.2	117.2	15	0.073	15.8	15.8	drip rate > 5 mins			
Stumpy	Nov-14	11/28/2014	11/29/2014	444	8.1	1382	102.2	116.4	14.2	0.076	14.8	14.8	drip rate > 5 mins			
Stumpy	Dec-14	12/29/2014	12/30/2014	418	8.6	1385	67.3	82.2	14.9	0.075	15.5	15.5	used wrong bottle			

Site	Date	Trip Day 1	Trip Day 2	Avg seconds/drip	Avg drips/hr	Bottle Deployment (mins)	Initial Bottle Wt (g)	Final Bottle Wt (g)	Water collected (g)	mL/drip	mL/day	estimate mL/day for E>5 min/drip	Notes	
Amidala	Sep-08	9/22/2008	9/23/2008	0	0	0	0	0	0	0	0		not collecting data	
Amidala	Oct-08	10/20/2008	10/21/2008	0	0	0	0	0	0	0	0		not collecting data	
Amidala	Nov-08	11/17/2008	11/18/2008	0	0	0	0	0	0	0	0		not collecting data	
Amidala	Dec-08	12/15/2008	12/16/2008	0	0	0	0	0	0	0	0		not collecting data	
Amidala	Jan-09	1/12/2009	1/13/2009	0	0	0	0	0	0	0	0		not collecting data	
Amidala	Feb-09	2/17/2009	2/18/2009	0	0	0	0	0	0	0	0		not collecting data	
Amidala	Mar-09	3/16/2009	3/17/2009	0	0	0	0	0	0	0	0		not collecting data	
Amidala	Apr-09	4/13/2009	4/14/2009	0	0	0	0	0	0	0	0		not collecting data	
Amidala	May-09	5/12/2009	5/13/2009	847	4.3	1528	67.08	75.2	8.12	0.075	7.7	7.7		
Amidala	Jun-09	6/11/2009	6/12/2009	1870	1.9	1338	67.08	70.3	3.22	0.075	3.5	3.5		
Amidala	Jul-09	7/14/2009	7/15/2009	2843	1.3	1453	67.1	69.4	2.3	0.075	2.3	2.3		
Amidala	Aug-09	8/21/2009	8/22/2009	ERROR			67.1	bottle fell Day 2						
Amidala	Sep-09	9/21/2009	9/22/2009	2143	1.7	1524	67.1	70.3	3.2	0.075	3.0	3.0		
Amidala	Oct-09	10/19/2009	10/21/2009	1636	2.2	2909	67.1	75.1	8	0.075	4.0	4.0		
Amidala	Nov-09	11/23/2009	11/24/2009	1181	3.0	105	67.1	67.5	0.4	0.075	5.5	5.5	fell over	
Amidala	Dec-09	12/21/2009	12/22/2009	1965	1.8	1354	67.1	70.2	3.1	0.075	3.3	3.3		
Amidala	Jan-10	1/25/2010	1/26/2010	2538	1.4	1410	67.1	69.6	2.5	0.075	2.6	2.6		
Amidala	Feb-10	Feb-10	Feb-10				67.1							
Amidala	Mar-10	3/1/2010	3/2/2010	1328	2.7	1415	67.1	72.6	5.5	0.086	5.6	5.6		
Amidala	Apr-10	4/5/2010	4/6/2010	2183	1.6	1455	67.1	70.1	3	0.075	3.0	3.0		
Amidala	May-10	5/3/2010	5/4/2010	2669	1.3	1364	67.1	69.4	2.3	0.075	2.4	2.4		
Amidala	Jun-10	6/7/2010	6/8/2010	2437	1.5	1408	67.1	69.7	2.6	0.075	2.7	2.7		
Amidala	Jul-10	7/12/2010	7/13/2010	3360	1.1	1344	67.1	68.9	1.8	0.075	1.9	1.9		
Amidala	Aug-10	8/16/2010	8/17/2010	3297	1.1	1392	67.1	69	1.9	0.075	2.0	2.0		
Amidala	Sep-10	9/27/2010	9/28/2010	3269	1.1	1235	67.1	68.8	1.7	0.075	2.0	2.0		
Amidala	Oct-10	10/25/2010	10/26/2010	3243	1.1	1225	67.1	68.8	1.7	0.075	2.0	2.0		
Amidala	Nov-10	11/22/2010	11/23/2010	1785	2.0	1396	67.08	70.6	3.52	0.075	3.6	3.6		
Amidala	Dec-10	12/20/2010	12/21/2010	2707	1.3	1456	67.08	69.5	2.42	0.075	2.4	2.4		
Amidala	Jan-11	1/24/2011	1/25/2011	4269	0.8	1423	67.1	68.6	1.5	0.075	1.5	1.5		
Amidala	Feb-11	2/21/2011	2/22/2011	878	4.1	1366	67.1	74.1	7	0.075	7.4	7.4		
Amidala	Mar-11	3/28/2011	3/29/2011	1842	2.0	1392	67.1	70.5	3.4	0.075	3.5	3.5		
Amidala	Apr-11	4/25/2011	4/26/2011	2213	1.6	1328	67.1	69.8	2.7	0.075	2.9	2.9		
Amidala	May-11	5/23/2011	5/24/2011	2591	1.4	1382	67.1	69.5	2.4	0.075	2.5	2.5		
Amidala	Jun-11	6/20/2011	6/21/2011	302	11.9	1322	67.1	86.8	19.7	0.075	21.5	21.5		
Amidala	Jul-11	7/18/2011	7/19/2011	613	5.9	1322	67.1	76.8	9.7	0.075	10.6	10.6		
Amidala	Aug-11	8/29/2011	8/30/2011	518	6.9	1302	67.1	78.4	11.3	0.075	12.5	12.5		
Amidala	Sep-11	9/26/2011	9/27/2011	711	5.1	1391	67.1	75.9	8.8	0.075	9.1	9.1		
Amidala	Oct-11	10/24/2011	10/25/2011	684	5.3	1292	67.1	75.6	8.5	0.075	9.5	9.5		

Amidala	Nov-11	11/21/2011	11/22/2011	1424	3	1267	67.1	71.7	4.6	0.086	5.2	5.2		
Amidala	Dec-11	12/19/2011	12/20/2011	121	29.6	1296	67.1	119.6	52.5	0.082	58.3	58.3		
Amidala	Jan-12	1/23/2012	1/24/2012	484	7.4	1355	67.1	79.7	12.6	0.075	13.4	13.4		
Amidala	Feb-12	2/27/2012	2/28/2012	1793	2.0	1355	67.1	70.5	3.4	0.075	3.6	3.6		
Amidala	Mar-12	3/26/2012	3/27/2012	1817	2.0	1373	67.1	70.5	3.4	0.075	3.6	3.6		
Amidala	Apr-12	4/23/2012	4/24/2012	2405	1.5	1336	67.1	69.6	2.5	0.075	2.7	2.7		
Amidala	May-12	5/21/2012	5/22/2012	542	6.6	1330	67.5	78.55	11.05	0.075	12.0	12.0		
Amidala	Jun-12	6/28/2012	6/29/2012	914	3.9	1331	67.5	75.1	7.6	0.087	8.2	8.2		
Amidala	Jul-12	8/2/2012	8/3/2012	2354	1.5	1308	67.5	70	2.5	0.075	2.8	2.8		
Amidala	Aug-12	8/27/2012	8/28/2012	611	5.9	1345	67.5	77.4	9.9	0.075	10.6	10.6		
Amidala	Sep-12	9/24/2012	9/25/2012	1608	2.2	1286	67.5	71.1	3.6	0.075	4.0	4.0		
Amidala	Oct-12	10/22/2012	10/23/2012	424	8.5	1263	67.5	80.9	13.4	0.075	15.3	15.3		
Amidala	Nov-12	11/19/2012	11/20/2012	144	25.0	1361	67.5	114	46.5	0.082	49.2	49.2		
Amidala	Dec-12	12/21/2012	12/22/2012	74	49.0	1340	67.5	148.4	80.9	0.074	86.9	86.9		
Amidala	Jan-13	1/15/2013	1/16/2013	76	47	1313	67.5	133.4	65.9	0.064	72.3	72.3	user error	
Amidala	Feb-13	2/18/2013	2/19/2013	82	44	1483	67.4	146.9	79.5	0.074	77.2	77.2		
Amidala	Mar-13	3/18/2013	3/19/2013	164	22	1450	67.5	111.1	43.6	0.082	43.3	43.3		
Amidala	Apr-13	4/22/2013	4/23/2013	243	15	1382	67.4	94.2	26.8	0.079	27.9	27.9		
Amidala	May-13	5/20/2013	5/21/2013	496	7.26	1410	67.5	80.3	12.8	0.075	13.1	13.1		
Amidala	Jun-13	6/25/2013	6/26/2013	692	5.21	1214	67.5	75.4	7.9	0.075	9.4	9.4		
Amidala	Jul-13	7/29/2013	7/30/2013	845	4.26	1446	67.4	75.1	7.7	0.075	7.7	7.7		
Amidala	Aug-13	8/26/2013	8/27/2013	1908	1.89	1399	67.3	70.6	3.3	0.075	3.4	3.4		
Amidala	Sep-13	9/23/2013	9/24/2013	1927	1.87	1413	67.3	70.6	3.3	0.075	3.4	3.4		
Amidala	Oct-13	10/21/2013	10/22/2013	1642	2.19	1423	67.3	71.2	3.9	0.075	3.9	3.9		
Amidala	Nov-13	11/18/2013	11/19/2013	1415	2.54	1399	67.3	72.4	5.1	0.086	5.2	5.2		
Amidala	Dec-13	12/16/2013	12/17/2013	1421	2.53	1421	67.4	71.9	4.5	0.075	4.6	4.6		
Amidala	Jan-14	1/21/2014	1/22/2014	1051	3.42	1542	67.6	74.2	6.6	0.075	6.2	6.2		
Amidala	Feb-14	2/17/2014	2/18/2014	1604	2.24	1390	67.5	71.4	3.9	0.075	4.0	4.0		
Amidala	Mar-14	3/17/2014	3/18/2014	1654	2.18	1397	67.4	71.2	3.8	0.075	3.9	3.9		
Amidala	Apr-14	4/22/2014	4/23/2014	1460	2.47	1398	67.2	72.1	4.9	0.086	5.1	5.1		
Amidala	May-14	5/22/2014	5/23/2014	2745	1.31	1403	67.3	69.6	2.3	0.075	2.4	2.4		
Amidala	Jun-14	6/16/2014	6/17/2014	4915	0.73	1420	67.3	68.6	1.3	0.075	1.3	1.3		
Amidala	Jul-14	1-Jul	1-Jul											
Amidala	Aug-14	8/12/2014	8/18/2014	2204	1.63	8742	67.5	86.3	18.8	0.079	3.1	3.1		
Amidala	Sep-14	9/22/2014	9/23/2014	2069	1.74	1425	67.4	70.5	3.1	0.075	3.1	3.1		
Amidala	Oct-14	10/30/2014	10/31/2014	1721	2.09	1377	67.3	70.9	3.6	0.075	3.8	3.8		
Amidala	Nov-14	11/28/2014	11/29/2014	2574	1.40	1373	67.3	69.7	2.4	0.075	2.5	2.5		
Amidala	Dec-14	12/29/2014	12/30/2014	3430	1.05	1372	102.5	104.3	1.8	0.075	1.9	1.9	cutoff	